Advanced Drug Delivery Systems - a Synthetic and Biological Applied Evaluation

Bjerg, Lise Nørkjær

Publication date:
2013

Document Version
Publisher's PDF, also known as Version of record

Advanced Drug Delivery Systems - a Synthetic and Biological Applied Evaluation

PhD Thesis

Lise Nørkjær Bjerg

January 2013

Department of Micro- and Nanotechnology
Technical University of Denmark
DTU Nanotech, Building 423
DK-2800 Kongens Lyngby
Denmark

Advanced Drug Delivery Systems - a Synthetic and Biological Applied Evaluation

PhD Thesis

Lise Nørkjær Bjerg

January 2013

Department of Micro- and Nanotechnology
Technical University of Denmark
DTU Nanotech, Building 423
DK-2800 Kongens Lyngby
Denmark

This thesis is submitted as a partial fulfilment for obtaining the Ph.D. degree at the Technical University of Denmark.

Supervisor: Professor Thomas L. Andresen

Preface and acknowledgments

The work presented in this thesis was conducted during the last three years as a Ph.D. student at DTU Nanotech, Department of Micro- and Nanotechnology, Technical University of Denmark, under the supervision of Professor Thomas L. Andresen. The work has been focused on developing functionalized liposomes, which have practical *in vivo* applications in especially cancer treatment.

Many people made this work possible. I would like to thank my supervisor Professor Thomas L. Andresen for giving me the opportunity to work in his group. His understanding of this field and his tireless work ethic has been an immense inspiration. The fact that his door was always open and his encouraging guidance helped this thesis greatly along the way.

Thanks to all the people I had productive collaborations with; Postdoc Rasmus I. Jølck for his help with the synthesis of TATE-derivatives; Postdoc Pramod Kumar Ek for his work on polymeric nanoparticles; Assistant Professor Jonas R. Henriksen for his collaboration on phospholipid membranes; Postdoc Anncatrine Luisa Petersen for her work on the ^{64}Cu-liposomes and great help in interpreting the results.

A very special thanks goes to my many fantastic colleagues in the 'Colloids and Biological Interfaces' group for daily scientific discussions and great fun at the lunch table. Researcher Fredrik Melander and Ph.D. student Jonas Bruun for their fruitful guidance in the cell-lab and with flow cytometry experiments. Postdoc Rikke Vicky Benjaminsen for helping me with the confocal imaging and output of this thesis. Postdoc Maria Ahlm Mattebjerg and Postdoc Anncatrine Luisa Petersen for their help in putting the thesis together and their help with proofreading it. Ph.D. student Thomas Christopher Bogh Klauber and Ph.D. student Chiara Tassone for inspiring and enjoyable conversations.

Finally I would like to thank my family for their support and encouragement during these years. Especially, my husband Kasper for his endless patience and for making my life wonderful.

Summary

Specific delivery of drugs to diseased sites in the body is a major topic in the development of drug delivery system today. Especially, the field of cancer treatment needs improved drug delivery systems as the strong dose-limiting side effects of chemotherapy today often present a barrier for an effective cure.

Liposomes have attracted much attention since they were first proposed as potential drug carrier agents in the 1970s. Chapter one gives an introduction to the strategies used in liposomal drug delivery today. The important issues as enhanced specific uptake in diseased tissue and effective unloading of the encapsulated drug have been tried optimized in a variety of ways. Many propose the use of small molecules, such as vitamins and peptides, for active targeting of the liposomes to overexpressed receptors on the cancerous tissue. Once located close to the diseased site a trigger mechanism for releasing the drug from the liposome interior is often needed. Several approaches have been suggested to work as release mechanisms such a pH changes, the presence of enzymes or external applied stimulus as heat or light.

Chapter two deals with the synthesis of the functionalized phospholipids, which function as the targeting moiety on the surface of the liposomes. Several examples of synthetic procedures known from the literature are presented. The chapter is completed with a study covering the conjugation efficiencies of a variety of chemical functionalities. Large differences are revealed between the conjugation efficiency in solution and directly on the surface of the pre-formed liposomes.

In chapter three the efficiency of the targeted liposomes is investigated. *In vitro* experiments using fluorescent phospholipids and *in vivo* experiments using radiolabeled liposomes and a PET imaging technique. The results were encouraging and proved the large potential of radiolabeled liposomes as candidates for revealing the biodistribution of drug delivery systems.

Chapter four deals with one of the large dilemmas, when using liposomes as drug delivery agents. The presence of a shielding polymer layer on the surface of the liposome is important in order for it to circulate in the blood stream. However, the presence of the polymer obstructs the uptake pattern of the liposomes, limiting the therapeutic efficacy of the liposomes. We developed liposomal formulations which present a targeting moiety on the surface to guide the uptake, in addition to an enzymatically cleavable peptide sequence, whose cleavage would result in removal of the polymer layer as well as uncovering cationic charges on the liposomal surface. These systems were shown to have superior drug efficacy *in vitro*.

Dansk resumé

Specifik levering af lægemidler til sygdomsramte steder i kroppen spiller en stor rolle i udvikling af nye drug delivery systemer i dag. Især indenfor kræft behandlingen er der brug for forbedringer, da de dosis-afhængige bivirkningerne i kemoterapien i dag ofte forhindrer en effektiv helbredelse.

Liposomer har tiltrukket sig meget opmærksomhed, siden det i 1970'erne blev foreslået, at de havde potentiale som drug delivery system. Kapitel et giver en introduktion til de strategier, der anvendes i liposomal drug delivery i dag. De vigtige emner, som øget specifikt optag i sygdomsramt væv og den effektive frigivelse af det indkapslede lægemiddel, har været forsøgt optimeret på utallige måder. Mange foreslår anvendelsen af små molekyler, såsom vitaminer og peptider, som en aktiv metode til at styre liposomerne hen imod overudtrykte receptorer på kræftvæv. Når liposomet er fremme ved det sygdomsramte sted er der ofte brug for en trigger mekanisme for at frigive lægemidlet. Utallige fremgangsmåder er blevet foreslået som frigivelsesmekanisme såsom ændringer i pH, tilstedeværelsen af enzymer eller udfrakomne stimulus såsom varme eller lys.

Kapitel to omhandler fremstillingen af funktionelle phospholipider, der sidder på overfladen af liposomet og leder det hen til de sygdomsramte celler. Adskellige eksempler på syntese procedurer kendt fra litteraturen præsenteres. Dette kapitel er afsluttet med et studie som omhandler effektiviteten af konjugeringsreaktioner mellem forskelige kemiske funktionaliteter. Det viste sig, at der var store forskelle mellem effektiviteten for konjugeringer udført i opløsning og konjugeringer udført direkte på liposomets overflade.

I kapitel tre undersøges effektiviteten af de targeterede liposomer. *In vitro* eksperimenter, hvor der blev anvendt fluoriserende phospholipider samt *in vivo* eksperimenter, hvor der blev anvendt radioaktiv mærket liposomer og PET billeddannelse. Resultaterne var opløftende og beviste de radioaktiv mærkede liposomes' store potentiale til at afdække biodistributionen af drug delivery systemer.

Kapitel fire omhandler ét af de store dilemmaer, når det kommer til brugen af liposomer som drug delivery agenter. Tilstedeværelsen af en skærmende polymer på overfladen af liposomet er vigtigt for, at den kan cirkulere i blodbanen. Men tilstedeværelsen forstyrer optagelsesmønstret af liposomerne og begrænser derved deres terapeutiske effect. Vi har udviklet liposome formuleringer, som præsenterer en targetering del på overfladen af liposomet for at guide dets optag, samt en enzymatisk spaltbar peptide sekvens, hvis spaltning vil resultere i fjernelse af polymer laget såvel som afdække kationiske ladninger på liposomets overflade. Disse systemer viste sig at have give en høj effektivitet af lægemidlet *in vitro*.

Abbreviations

DSPC	1,2-distearoyl-*sn*-glycero-3-phosphocholine
($sPLA_2$)	Secretory phospholipase A_2
% ID	Percent injected dose
AcOH	Acetic acid
ADC	Antibody-drug conjugate
Bq	Becquerel
CPP	Cell-penetrating peptide
cryoTEM	Cryogenic transmission electron microscopy
CT	Computed tomography
CuAAC	Copper-catalyzed azide-alkyne cycloaddition
DLS	Dynamic light scattering
DMF	N,N-dimethylformamide
DOPE	Diacylphosphatidylethanolamine
DOTA	1,4,7,10-tetra-azacyclododecane-1,4,7,10-tetraacetic acid
DP-MCP-PEG	Dipalmitoyl-metalloproteinase cleavable peptide-PEGylated
DPPC	1,2-dipalmitoyl-*sn*-glycero-3-phosphocholine
DSPE-NBD	1,2-distearoyl-*sn*-glycero-3-phosphoethanolamine-N-(7-nitro-2-1,3-benzoxadiazol-4-yl)
$DSPE\text{-}PEG_{2000}$	1,2-distearoyl-*sn*-glycero-3-phosphoethanolamine-*N*-[methoxy(polyethylene glycol)-2000]
DTT	Dithiothreitol
ECM	Extracellular matrix
EDC	1-ethyl-3-(3-dimethylaminopropyl) carbodiimide
ELAM	Endothelial-leukocyte adhersion molecule-1
EPR	Enhanced permeability and retention
Fab´	Antigen-binding fragment
Fc	Fragment crystallizable
Fmoc	9-fluorenylmethyloxycarbonyl
FR	Folate receptor
GRD	Glycine-arginine-aspartic acid
GPCR	G protein-coupled receptor
HA2	Influenza hemagglutinin
HATU	*O*-(7-azabenzotriazol-1-yl)-N,N,N′,N′-tetramethyluroniumhexafluorophosphate
HEPES	4-(2-hydroxyethyl)-1-piperazineethanesulfonic acid
HER2	Human epidermal growth factor 2
HPLC	High-performance liquid chromatography
ICAM	Intercellular adhersion molecule-1
ICP-AES	Inductively coupled plasma atomic emission spectroscopy

i.v.	Intravenous
LUV	Large unilamellar vesicle
mAb	Monoclonal antibody
MALDI TOF MS	Matrix assisted laser desorption/ionization time-of-flight mass spectroscopy
MFI	Mean fluorescence intensity
MLV	Multi-lamellar vesicle
MMP	Matrix metalloproteinase
MRI	Magnetic resonance imaging
MSC	Mesenchymal stem cell
MTS	3-(4,5-dimethylthiazol-2-yl)-5-(3-carboxymethoxyphenyl)-2-(4-sulfophenyl) 2H-tetrazolium salt
NGR	Asparagine-glycine-arginine
OA	Oleic acid
PBS	Phosphate-buffered saline
PC	Phosphatidylcholine
PDP	N-[3-(2-pyridyldithio)propionate]
PE	Phosphatidylethanolamine
PEG	Poly(ethyleneglycol)
PET	Positron emission tomography
p.i.	Post injection
PMS	Phenazine methosulfate
RES	Reticuloendothelial system
RGD	Arginine-glycine-aspartic acid
SAR	Structure-activity relationship
scFv	Single chain variable fragment
SEC	Size exclusion chromatography
SPECT	Single-photon emission computed tomography
SST	Somatostatin
SSTR	Somatostatin receptor
T½	Half-life
TATE	[Tyr^3,Thr^8]-octreotate
TFA	Trifluoroacetic acid
TFE	2,2,2-trifluoroethanol
TIS	Triisopropylsilane
VCAM	Vascular cell adhersion molecule-1
V_H	Variable region heavy chain
V_L	Variable region light chain

Table of contents

Chapter 1

Liposomes as drug delivery agents

Despite a major effort in the search for more effective cancer treatments this devastating disease still causes the death of more than 7.5 million people worldwide every year (www.iarc.fr). The pharmaceutical industry continues to successfully develop cytotoxic drugs which can serve as potential candidates for the treatment of cancers; however upon administration these are often broadly distributed within the whole body resulting in toxicity to normal tissues, limited tumor accumulation and severe dose-limiting side effects, which are reducing their clinical application.

Cancer originates from the accumulation of numerous critical somatic mutations of healthy cells. This results in malignant cancer cells being identical to healthy cells in most aspects. Consequently, finding selective drugs; toxic to malignant cells and non-toxic to healthy cells can be rather challenging. The use of drug loaded nanocarriers which can deliver their payload at specific tumor sites in a clinical relevant dose could prove to be a superior strategy in the fight against cancer. In an attempt to improve tumor accumulation and specificity of the drug unloading site new methodologies of drug delivery is finding its use.

1.1 Liposomes

Since their discovery in 1965 by Bangham and co-workers [Bangham, 1965] the liposomes have been a subject of increasing interest. These nanoparticles were suggested to hold potential as drug carriers in 1974 by Gregoriadis [Gregoriadis, 1971; Gregoriadis,

1974] as their composition of natural phospholipids makes them highly biocompatible and biodegradable with low intrinsic toxicity as well as low immunogenicity. They can encapsulate drugs of different lipophilicities in either their hydrophilic lumen or hydrophobic bilayer [Gulati, 1998].

Broad biodistribution to non-diseased tissue and low inefficient accumulation of drug at the actual tumor site, are two key problems, which liposomes can help overcome. When cytotoxic drugs are loaded into liposomes these are no longer dictated by their own pharmacokinetic and pharmacodynamic profile, but instead controlled by the properties of the liposome. Liposomes protect the encapsulated drug while assisting it in reaching its target site by passive accumulation (*vide infra*).

In general three basic requirements are needed for the liposomes to be considered as a successful drug delivery agent in chemotherapy: (I) long, stable blood circulation, (II) high tumor accumulation and (III) effective release of the encapsulated drug once at tumor site.

Intensive research during the last decade has generated liposomes optimized for *in vivo* use and a few have entered the clinic such as Doxil®, Myocet® and DaunoXome®.

1.1.1 Stealth liposomes

Early formulations of liposomes were challenged by their fast blood clearance by the phagocytic cells of the reticuloendothelial system (RES). It was discovered that their physiochemical properties such as size, surface charge [Juliano, 1975] and lipid composition [Gabizon 1988] correlated with the types of proteins binding to them and thereby their clearance. In general, large liposomes are cleared faster than small ones, and those composed of unsaturated lipid are cleared faster than those composed of saturated lipid [Senior, 1982]. The incorporation of cholesterol further stabilizes the liposomes *in vivo* [Damen, 1981]. Negatively charged liposomes are cleared faster than neutral charged ones, while a positive surface charge leads to toxic liposomes which are quickly removed from the blood circulation. Despite combining this knowledge when formulating the liposomes, they could not fully avoid binding with serum proteins and the uptake by RES was too significant for them to be efficient drug carriers.

This issue was solved by coating the liposomes with polymers which would suppress protein absorption and opsonisation, especially the hydrophilic polymer poly(ethyleneglycol) (PEG) is now used for this purpose [Woddle, 1992; Klibanov, 1990]. The polymer provides steric hindrance by occupying the space just adjacent to the

liposome surface with its flexible chain, which tend to limit the binding of serum opsonins and reduce the RES uptake rate [Drummond, 1999].

The incorporation of PEG results in long-circulating stabilized liposomes, also known as sterically stabilized liposomes or Stealth. This longer circulation lifetime provides the liposomes a greater chance for accumulation in the tumor tissue.

1.2 Passive accumulation in tumors

The longer blood circulation of the liposomes also lead to an improvement in the second requirement for this drug delivery system since long circulating liposomes were found to have increased accumulation in tumor tissue over healthy tissue [Gabizon, 1994]. A phenomenon later described as the enhanced permeability and retention (EPR) effect.

Characteristic of many malignant tumors are their fast growth and need to form new blood vessels (angiogenesis). These newly formed blood vessels are often abnormal in their form and architecture with large fenestrations varying from 100-1200 nm [Yuan, 1995; Hobbs, 1998; Jang, 2003], a pore size much larger than the ones found in normal vessels (around 6 nm [Drummond, 1999]). This leakiness combined with an ineffective lymphatic drainage make liposomes passively accumulate in tumor tissue [Maeda, 2000]. A large distribution of liposomes in the interstitium surrounding the tumor cells is hindered due to a high interstitial pressure and a large interstitial space compared with healthy tissue [Jain, 1990]. Consequently, not all solid tumors are suitable for treatment with passive accumulating liposomes, as the tumor vasculature is highly heterogeneous in terms of density and distribution of vessels, depending on the size of the tumor as well as their location inside the tumor [Rubin, 1966]. Generally, peripheral regions have a higher vessel density than central parts, and the central parts have a higher interstitial pressure than the periphery. This leads to an irregular drug distribution throughout the solid tumor, resulting in larger tumors being more difficult to treat than smaller ones.

1.3 Active tumor targeting

A way to maintain the liposomes in the interstitial space of the tumor is to take advantage of specific surface receptors and antigens that are overexpressed on cancer cells [Ruoslahti, 2002; Peer, 2007] or on endothelial cells in the angiogenic blood vessels [Folkman, 1995; Ruoslahti, 2010]. The targeted liposomes concentrate in the tumor site by the EPR effect like for the non-targeted liposomes, but once there, they can actively be

taken up by the tumor cells after binding to their target receptor or antigen [Allen, 2002]. This is commonly referred to as active targeting (Figure 1).

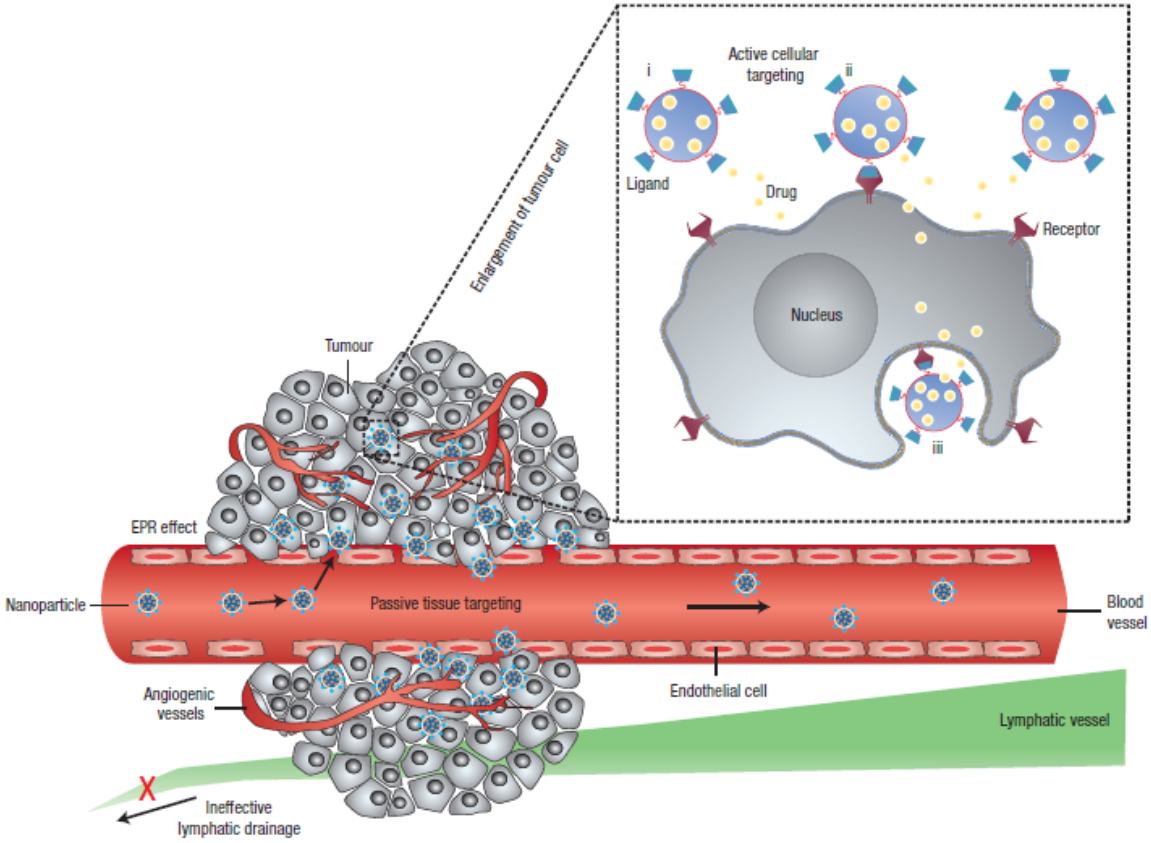

Figure 1: Schematic presentation showing passive and active targeting strategies of liposomes. Liposomes are concentrated in the tumor interstitium by extravasation of the fenestrated tumor vessels and are retained due to ineffective lymphatic drainage (EPR effect). The passive accumulation of liposomes results in a local release of the drug near the cancer cells, while the active targeted liposomes can release their drug load extracellular before or after binding to the surface of the cells, or the liposomes can be endocytosed and drug released intracellular [Peer, 2007].

Targeting of endothelial cells in angiogenic blood vessels is generally considered to be advantageous over tumor cell targeting as endothelial cells are generitically stable and the risk of developing drug resistance is reduced [Lila, 2009]. They are highly accessible for circulating liposomes, and damage to a few tumor blood vessels may result in a strong growth inhibition of the surrounding tumor cells, which are depending on nutrients and oxygen supply from these vessels. The special characteristics of proliferating endothelial cells in tumors are shared between a variety of tumor types which can be beneficial when trying to develop a wide-ranging chemotherapeutic formulation. Strategies, which target both tumor vasculature as well as tumor cells, have proved to be more effective than targeting of the two tissues individually [Koning, 2004].

Different approaches have been tested for attachment of the targeting ligand to the liposome surface. Targeting ligands have been conjugated directly to the phospholipid headgroups of non-PEGylated liposomes. However, these liposomes suffered from rapid blood clearance. A similar conjugation approach was used on PEGylated liposomes, resulting in longer circulating liposomes, but these liposomes showed reduced targeting properties due to steric hindrance from the PEG chains [Torchilin, 1992]. To minimize shielding of the targeting ligand by the PEG chains, the targeting ligand was moved to the end of the PEG chain, giving it opportunity to extend beyond the PEG coating and maximize its exposure to the targeted receptor [Maruyama, 2002].

A great number of different targeting ligands have been conjugated to the liposome surface including vitamins, peptides and antibodies using a variety of chemical methods [Jølck, 2010].

1.3.1 Antibodies as targeting ligands

Antibodies are proteins used by the immune system to identify foreign objects in the body and they represent one of the most versatile ligands that can be attached to liposomes. However, the antibody functionalization of liposomes is generally challenging, where region specificity and degree and conversions are the main problems. One of the key reasons for this is that antibodies can only be attached to liposomes by post-functionalization, i.e. the liposomes are formed prior to attachment and the conjugation chemistry therefore has to work well in aqueous buffer. Antibodies can be attached as whole monoclonal antibodies (mAb) or as fragments thereof (Figure 2).

Full antibodies have stability advantages over small fragments such as Fab´ and scFv, but can trigger compliment activation [Moghimi, 2010] and induce antibody-dependent cytotoxicity [Sapra, 2003]. Furthermore, the Fc fragment is known to accelerate clearance of the immunoliposomes by RES and thus decrease the blood circulation time of the liposomes [Allen, 1995]. This undesired clearance can be minimized by using just Fab´ or scFv [Baxter, 1994].

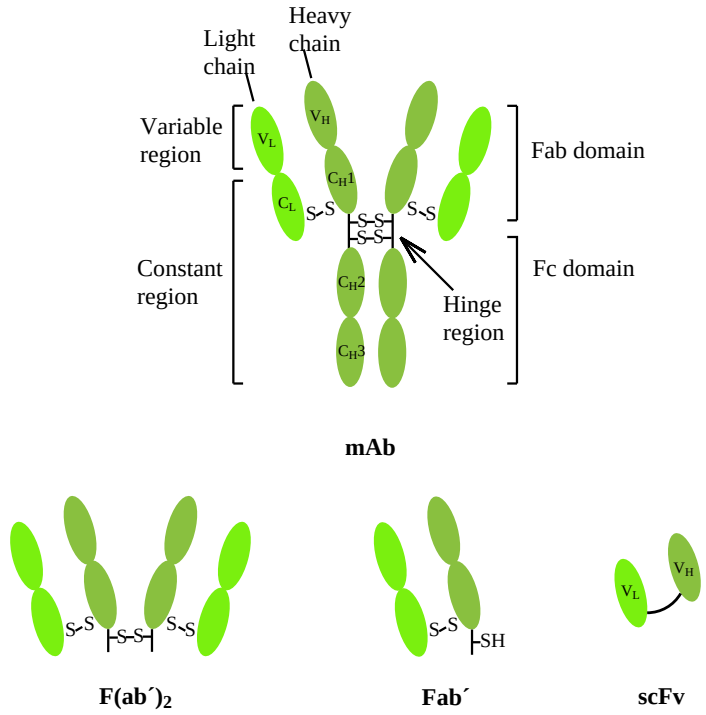

Figure 2. Schematic representation of various antibody constructs: Monoclonal antibody (mAb); F(ab´)$_2$ generated by pepsin digestion of the Fc domain of mAb; Fab´ from reduction of the disulfide bond in the hinge region of F(ab´)$_2$; scFv of recombinant V_L and V_H regions linked by a short peptide sequence.

Antibodies against the human epidermal growth factor 2 (HER2) have been widely used in combination with liposomal drug delivery systems. This antigen is frequently overexpressed on cancer cells and only weakly expressed in normal tissue [Martin, 1982]. Another popular targeting site using antibodies is the adhesion molecules expressed in endothelial cells such as endothelial-leukocyte adhesion molecule-1 (ELAM), intercellular adhesion molecule-1 (ICAM) and vascular cell adhesion molecule-1 (VCAM) [Gunawan, 2010].

Generally, immunoliposomes show a superior anticancer efficacy over non-targeted liposomes, though several studies have proved this efficacy to be caused by increased cancer cell uptake and internalization and not due to a change in biodistribution or increased tumor accumulation [Kirpotin, 2006; Hatakeyama, 2007].

1.3.2 Peptides as targeting ligands

The use of peptide-targeted liposomes as therapeutics has become highly interesting with the increasing knowledge of specific peptide sequences of proteins involved in cell-cell interactions as well as the improvement in synthesis of synthetic peptides that closely resemble the human ones. The peptide-targeted liposomes can increase the delivery of

drug to cancer cells by targeting overexpressed receptors or by using unspecific cell penetrating peptides.

G protein-coupled receptors (GPCR) are a diverse family of transmembrane proteins responsible for interacting with extracellular molecules and thus regulate various functions in the cell. A large number of GPCRs with known binding peptides are found to be overexpressed on the surface of cancer cells, including the somatostatin receptor [Volante, 2008], the neurotensin receptor [Myers, 2009] and cholecystokinin receptor [Miyasaka, 2003].

Cell-penetrating peptides (CPP) are a class of peptides which typically contain a large portion of highly charged amino acids such as arginine or lysine. The first one identified was transactivator of transcription (TAT) from the HIV-1 TAT peptide [Frankel, 1988]. Later a variety of peptides which share TAT's ability to carry a drug across the hydrophobic cell membrane into the cytoplasm of cells have been identified, as penetratin [Dupont, 2011] and synthetic polyarginines. When applying these sorts of peptide sequences, it is critical to have the right ratio between cell-penetrating peptide and a shielding PEG layer on the surface of the liposome. PEG needs to ensure long enough blood circulation time for the liposome to accumulate in the target site by the EPR effect and hinder that the cell-penetrating peptide has too much unspecific binding to healthy cells encountered on its way. However, PEG must not shield the cell-penetrating peptide too much, making it unable to interact with the target cell membrane.

Peptides targeting the endothelial cells and mimic local bioadhesion have attracted much attention in the peptide targeting field. The integrins, especially, which are a receptor family that mediates the attachment of cells to their surrounding extracellular matrix, such as vitronectin, fibronectin and collagen. Integrins play a major role in tumor progression and metastasis [Desgrosellier, 2010] and is highly upregulated in both solid tumors as well as tumor vasculature. The small tripeptide RGD (Arginine-Glycine-Aspartic acid) found in many of the extracellular matrix proteins bind strongly to the integrin receptors and have been broadly used in liposomal peptide-targeted drug delivery [Meerovitch, 2003]. The NGR (Asparagine-Glycine-Arginine) sequence binds to an endothelium associated aminopeptidase-N form, found upregulated in angiogenesis and tumor growth [Corti, 2008]. Good tumor accumulation and therapeutic efficacy have been shown for both these targeting peptides [Murphy, 2008; Pastorino, 2003].

1.3.3 Folic acid as targeting ligand

Liposomes functionalized with the vitamin, folic acid, have attracted much attention as the folate receptors are highly overexpressed in a number of cancers. The vitamin is internalized to a large extent in proliferating cells as folic acid is essential in the biosynthesis of nucleotides; consequently fast dividing malignant cells are in great need of this nutrient. Normally, the folate receptors are expressed at the apical side of epithelial cells and not accessible to drug in the blood circulation. However, when the epithelial cell becomes malignant, the membrane loses its polarity and the folate receptor can be located at the basal surface of the membrane as well [Lu, 2002].

An interesting feature of folate-targeted liposomes is that they have shown an ability to bypass the P-glycoprotein efflux pump. This is often involved in multi-drug resistance mechanisms and considered to be a major complication in cancer therapy. It is found that the ability is coupled to folate-liposomes being taken up by receptor-mediated endocytosis [Goren, 2000].

Although the active targeting strategies can seem promising, obstacles still exist. Unfortunately, the use of targeted liposomes does not necessary results in increased tumor accumulation and even if an increased accumulation is achieved, this does not guarantee an improved therapeutic outcome. Attaching a targeting ligand on the surface of a liposome naturally decreases its blood circulation time as the ligand will increase unspecific binding to healthy cells and may trigger enhanced opsonisation and removal by RES. When liposomes with strong binding ligands bind to the first cancerous cells they meet, there is a risk that they will block the extravasation of more liposomes to the tumor interstitial space [Barenholz, 2001]. Moreover, their fast binding will prevent their diffusion through the tumor tissue and they will mainly be located in the blood vessel region. This is known as the binding-site barrier. Another challenge of active targeting via receptor-mediated uptake is release of the encapsulated drug once the liposomes have been internationalized. The harsh environment found in endosomes and especially lysosomes can degrade the encapsulated drug, if it does not succeed in escaping these vesicles [Sapra, 2003].

1.4 Triggered release of drug content

The third requirement for liposomes to be good drug delivery agents is dependent upon their ability to release the encapsulated drug once at target site. Drug release may take

place extracellular in close proximity to the cell followed by cell uptake of the drug, or the intact drug loaded liposomes can be internalized and release their drug intracellular (Figure 1).

High accumulation of drug loaded liposomes in the tumor site does not necessarily result in high therapeutic effect. This limited therapeutic effect can partly be due to degradation of the drug in the endosomes/lysosomes, before it has a chance to carry out its effect. Several specific drug release mechanisms have been investigated in order to optimize the therapeutic efficacy of the delivered liposomes. The strategies involve exploiting tumor microenvironment such as pH changes or the presence of enzymes [Andresen, 2010], applying external stimulus such as heat [Manzoor, 2012], light [Leung, 2012], ultrasound [Barenholz, 2009] or simple physio-chemical characteristics of the encapsulated drug [Barenholz, 2001].

1.4.1 pH sensitive liposomes

The pH of the tumor microenvironment is lower than in healthy tissues, though often not much lower than 6.5. This small difference from normal tissue pH makes it very challenging to design liposomes which are stable through circulation, but becomes ruptured in the tumor. A better strategy is to utilize the low pH in the endosomes and lysosomes, where pH can be lower than 5 [Benjaminsen, 2011].

Four classes of pH sensitive liposomes have been describers [Drummond, 2000]. The first class applies liposomes formulated with a combination of an unsaturated phospholipid as diacylphosphatidylethanolamine (DOPE) and an acidic amphiphile as oleic acid (OA). As DOPE cannot form a stable bilayer structure on its own the OA is added as a stabilizer. Once the OA becomes protonated in the acidic endosome/lysosome the membrane will be destabilized and non-bilayer structures important for fusiogenic events are created [Chernomordik, 1996].

The second class of liposomes includes specially engineered phospholipid components that contain chemical bonds which can be hydrolyzed in an acidic environment and thus increase the presence of membrane destabilizing phospholipid. This has been done with a head-modified DOPE-maleyl that would release the stabilizing group at low pH leaving the unmodified DOPE [Drummond, 1995]. Another example is removal of the stabilizing PEG chains by using an acid-labile vinyl ether PEG lipid, resulting in unmodified DOPE and destabilization of the liposomal membrane [Shin, 2003].

The third class involves the incorporation of pH-sensitive peptides into the liposomal membrane to promote fusion between the liposomes and the endosomal/lysosomal membrane [Etzerodt, 2012]. The most studied pH-sensitive peptides are GALA and the influenza hemagglutinin-derived (HA2) peptides, which have both shown increased contents leakage from liposomes [Parente, 1990; Ishiguro, 1996].

The final class of pH sensitive liposome formulations contains pH-titratable polymers. An advantage with the use of synthetic polymers is their large structure flexibility, large-scale synthesis and low immunogenicity. The polymer is normally a polycation (weak base) or a polyanion (weak acid) and its mechanism of destabilization of the membrane depends on these properties [Uster, 1985; Zignani, 2000].

1.4.2 Heat and light sensitive liposomes

Liposomes sensitive to light and heat are interesting strategies for triggered release. However, a shortcoming for these two methods is that the tumor localization needs to be known [Kong, 1999]. Unfortunately, patients often die from metastatic cancer and not the primary tumor itself.

One rational behind using hyperthermia and liposomes together is that the local elevation of temperature can increase extravasation of the liposomes into the tumor site due to vasodilation, while at the same time the heating can trigger the liposomes to release their content [Gaber, 1996].

Liposomes sensitive to heat are formulated with phospholipids showing a narrow main phase transition temperature just above body temperature. This has been achieved by using a blend of the saturated phospholipids DPPC and DSPC which released their content at 42 °C [Gaber, 1996]. By formulating the liposomes from DPPC, DSPE-PEG_{2000} and a lysolipid instead the content was released at 39-40 °C [Needham, 2013].

Strategies using a light source to trigger release from liposomes can broadly be categorized as photochemical or photophysical strategies. Photochemical strategies include photopolymerization, photoisomerization and photocleavage, while strategies including the use of molecular dyes and gold nanoparticles belong in the photophysical field [Leung, 2012].

Applications of the photochemical methods often require synthesis of a molecule which contains the desired light-responsive properties as well as a moiety that can be stably incorporated into the liposomal membrane. Release using photoisomerization often depend upon the molecule changing its conformational shape by illumination and hence

destabilizes the membrane. The photocleavable strategy involves amphiphiles molecules which upon illumination triggers separation of the polar and nonpolar moieties and causes destabilization of the membrane [Anderson, 1992], while the photopolymerization strategy utilizes the formation of phospholipid domains and hence destabilization of the membrane by cross-linking polymerizable phospholipids in the presence of non-polymerizable phospholipids [O'Brien, 1998]. However, since the need for relatively high energies is involved in photochemistry, UV light is often used, which leads to concerns regarding UV radiation toxicity and the formation of reactive oxygen species.

Liposomes can be sensitized to light using dyes or gold nanoparticles embedded in their lumen, their membrane or surrounding them. This photophysical strategy takes advantage of the photothermal heating via molecular absorbers or metallic nanoparticles which can lead to controlled release from liposomes [Khoobene, 1990]. Especially the use of plasmon resonance from metallic nanoparticles is interesting, as their optical properties can be tuned from the visible to the near-infrared range just by varying their shape and size [Troutman, 2008]. This tunability makes it possible to apply wavelengths that are safe and still able to penetrate the tissue to a relevant depth.

1.4.3 Enzymatic sensitive liposomes

Enzymes of particular interest in the tumor tissue are those that catalyze the degradation of phospholipids such as secretory phospholipase A_2 ($sPLA_2$) or enzymes that are secreted in high concentrations into the tumor interstitium as the matrix metalloproteinases (MMP), where the liposomes accumulate.

The $sPLA_2$ catalyzes the hydrolysis of phospholipids in their *sn*-2 position yielding free fatty acids and lysolipids which acts as detergents and destabilizes the membrane [Henriksen, 2010]. The enzyme is found overexpressed in the environment surrounding malignant tumors and has been linked to increased aggressiveness of the cancer [Dong, 2010]. $sPLA_2$ demonstrates an enhanced activity towards aggregated phospholipids such as liposomes over monomeric phospholipids. This enhanced activity is found to be influenced by the surface charge of the liposome and phospholipid composition. Healthy mammalian cells are characterized by a neutral phospholipid composition in their outer leaflet and are poor substrates for the $sPLA_2$ in order to keep them safe, when the enzyme is upregulated. Experimentally, it has been confirmed that $sPLA_2$ is more active towards PEGylated phospholipids and other negatively charged membranes [Jørgensen, 2002; Leidy, 2006]. The steric barrier induced by PEGylation of the liposomes does not hinder

the $sPLA_2$ enzyme from reaching the liposomal surface where hydrolysis takes place. However, the practical application of using $sPLA_2$ as a trigger system in chemotherapy with encapsulated drugs is limited, as $sPLA_2$ is inactive towards membranes containing significant amounts of cholesterol. Cholesterol increases the ability of liposomes to retain their drug load and is an important component in e.g. Stealth formulations [Drummond, 1999].

The matrix metalloproteinase family consists of multiple subtypes, all being zinc-containing endopeptidase, where MMP-2 and MMP-9 are the most studied ones, as they are found highly upregulated in cancers. Their function in breaking down the extracellular matrix (ECM), assist cancerous cells in their invasion, angiogenesis and metastatic spread [Rundhaug, 2003]. The MMPs have been applied in triggered drug release aspects; although the strategy is less straightforward as for utilizing the sPLA2 strategies. A synthetic lipid component has to be constructed, showing a specific cleavage site for the enzyme in mind. Despite this synthetic need, several strategies have been applied using MMP enzymes. MMP-9 degradable lipopeptides have been incorporated into liposomes, resulting in destabilization of the membrane and drug release [Sarkar, 2004]; MMP-2 unmasking of the PEG layer on a liposome surface resulting in the exposure of a galactosylated liposome for macrophage targeting [Terada, 2006]; and lipid-peptide-PEG conjugates incorporated in liposomes showed an enhanced transfection efficiency of a HT1080 cell line after MMP removal of the PEG layer [Hatakeyama, 2007].

Despite being larger than the $sPLA_2$ enzyme (14 kDa) the MMPs (MMP-2 72 kDa; MMP-9 92 kDa) have shown no difficulties in reaching the hydrolytic site below the shielding PEG layer.

Though, $sPLA_2$ and MMP are the two most studied enzymes for triggered drug release from liposomes, others have been suggested, such as elastase [Meers, 2001], alkaline phosphatase [Davis, 1998] and phospholipase C [Villar, 2001].

These strategies selectively target the cancerous tissue over healthy by using targeting ligands on the surface of liposomes. To have the liposomes release their content in a location relevant to treatment of the tumor, appear promising in the search for more efficacious chemotherapeutic treatments.

Chapter 2

Engineering liposomes for biological targeting

There is an increasing demand for delivery systems that specifically transport drug to cancerous tissue and improve the therapeutic index of the encapsulated drug by triggered release. In an attempt to fulfil this demand liposomes have been coated with a variety of targeting ligands aimed at selectively or overexpressed receptors in cancerous tissues. Liposomes with targeting ligands as drug delivery vehicles are superior to e.g. antibody-drug conjugates (ADC) as only few targeting ligands are required for the liposomes to deliver thousands of drug molecules.

However, surface functionalization of liposomes with targeting ligands is not a trivial process and care has to be taken in evaluating the degree of functionalization. Often the conjugation of a ligand to a pre-formed liposome does not proceed as well on the liposome surface as it does in solution. Many times this evaluation is not performed which can pose a problem, as many of the utilized chemistries are far from quantitative. This has resulted in a strong motivation for improving the synthetic approaches towards these promising functionalized nanomaterials.

2.1 Functionalized liposomes

Generally three different methods are used for the surface functionalization of liposomes.

The first one is often applied for small ligands, such as peptides [Elegbede, 2008; Espuelas, 2005], vitamins [Lee, 1995; Saul, 2003] and saccharides [Shimada, 1997; Zhu, 2007] which are conjugated to a lipid (e.g. DSPE-PEG, cholesterol or fatty acids) in an

organic solvent and purified afterwards. This results in a functionalized lipid which can be mixed with natural phospholipids and thus incorporated into the liposomal membrane in the hydration step. A disadvantage of this process is that a significant amount of the ligand is need, and roughly half of the functionalized lipid will be facing the lumen of the liposome and being unable to interact with target receptors. However, a major advantage of this strategy is that the amount of functionalized lipid added can be accurately controlled.

The second approach to functionalize liposomes is the post-insertion approach [Ishida, 1999]. This is usually used for ligands which are expensive such as antibodies [Pan, 2007; ElBayoumi, 2009] and proteins [Chiu, 2006]. Lipids with a reactive functional group on the distal end of e.g. DSPE-PEG are formed in a micelle and the ligand reacted onto the surface. Alternative the lipid-ligand conjugate can be prepared as above and self-assembled in a micelle. The micelles are mixed with pre-formed liposomes and in a time and temperature dependent manner the functionalized lipids from the micelle will transfer to the outer membrane of the liposomes. The advantage with this method is that no functionality is lost to the inside of the liposomes, while a disadvantage is that a quantification of the amount of functionality on the final liposome preparation will have to be carried out.

The third strategy is the post-functionalization. Pre-formed liposomes displaying a reactive group in their headgroup can be conjugated with the desired targeting ligand. This method is usually applied for large ligands like antibodies and proteins. A challenge using this method is that the reaction has to perform well in aqueous buffer and the degree of functionalization will have to be quantified. The advantage is that no ligand is lost to the interior of the liposome and that the pre-formed liposomes can be loaded with drug under stronger conditions (e.g. heat) without having to protect the ligand.

A wide variety of coupling methods have been developed and to ensure correct orientation of the targeting ligand, bioorthogonal and site-specific reactions are required. Preferably, the conjugation method chosen should be able to proceed under mild conditions; it should be fast, reproducible and result in non-toxic and non-immunogenic chemical bonds. A few of these conjugation strategies are presented below.

2.1.1 Conjugation of ligands to amino-functionalized liposomes

This functionalization approach is based on naturally occurring phospholipids and can be used without prior functionalization of these. Torchilin was one of the first ones to

describe the use of this method by conjugating an antigen to the surface of the liposome using a homobifunctional amine-amine crosslinker [Torchilin, 1978]. However, the use of crosslinkers can result in uncontrolled polymerization and liposome aggregation. Furthermore, an antibody or peptide often contains more than one amine functionality and specificity of the reaction can be lost.

2.1.2 Conjugation of ligands to carboxylic acid functionalized liposomes

Conjugation to carboxylic acids on the surface of liposomes [Yagi, 2000; Bendas, 2003] can be achieved by either reacting phosphatidylethanolamine (PE lipids) with an anhydride [Kung, 1986] or by using commercial available phospholipids and activating them with 1-ethyl-3-(3-dimethylaminopropyl) carbodiimide (EDC). This activated ester can react with amines with efficiencies depending on the spacer length between the liposome surface and carboxylic acid functionality. If the carboxylic acid is attached to the distal end of a PEG chain instead of directly on the liposome surface, no real effect of spacer length is seen [Maruyama, 1995]. Often many amine functionalities are present in antibodies and peptides; hence a random attachment and altered binding affinity towards the receptor can be the consequence.

2.1.3 Conjugation of ligands to thiol-functionalized liposomes

Often the thiol functionality is introduced on the liposome surface as disulfide protected in the form of N-[3-(2-pyridyldithio) propionate] (PDP). This group is removed by reduction *in situ* with dithiothreitol (DTT) [Allen, 1995] and the free thiol can be reacted with a thiol or maleimide functionalized ligand [Muñoz, 1998; Mercadal, 1999]. The shortcoming of this method is the risk of forming intermolecular disulfide bonds leading to crosslinking of the reactive ligands or liposomes.

2.1.4 Conjugation of ligands to maleimide-functionalized liposomes

A very frequently used approach to functionalize liposomes is by the Michael Addition. A thioether bond is formed between a maleimide-functionalized phospholipid and a thiol-containing ligand [Fleiner, 2001; Park, 2001; Gradauer, 2012]. Often the maleimide moiety is attached to the distal end of PEG, but a direct surface functionalization can be obtained by using N-(4-(p-Maleimidophenyl)butyryl)-phosphatidylethanolamine. The Michael Addition has been used for attaching proteins like Annexin-A5 [Garnier, 2009], antibodies [Béduneau, 2007] and small peptides as cRGD [Janssen, 2003]. This method is straightforward without any need for prior activation or catalysts to support the

reaction, it takes place close to neutral pH and for smaller ligands it can be expected to be quantitative. However, the maleimide derivatives have been shown to be immunogenic [Peeters, 1989; Boeckler, 1996].

2.1.5 Conjugation of ligands to alkyne-functionalized liposomes

Meldal and Sharpless were the first to show the application of Cu(I) to catalyze the azide-alkyne Huisgen 1,3-dipolar cycloaddition (CuAAC) [Tornøe 2001; Tornøe 2002; Sharpless, 2002], generally referred to as the Click Reaction. Based on this work liposomes have been functionalized with a variety of ligands; e.g. an azido-modified mannose ligand [Hassane, 2006] and an azido-NBD ligand [Cavalli, 2006]. The reaction is highly orthogonal to other chemical functionalities and site-specific conjugation is possible as azides and alkynes are not naturally found in biomolecules. One limiting factor is the mandatory use of catalytic copper. As the reaction requires a catalytic amount of copper(II)sulphate and sodium ascorbate to generate Cu(I) *in situ*, this will need to be completely removed before the liposomes can be used for *in vitro* or *in vivo* applications, as copper is considered toxic. Furthermore, the copper catalyzed reaction is only applicable for saturated liposomes as unsaturated phospholipids are prone to oxidation by the copper ions [Gal, 2003].

Copper-free Click Reactions are reported, which relies on the use of strain-promoted cycloalkynes [Bostic, 2012]. Their use decreases the activation energy of the reaction, enabling it to be carried out without the presence of a copper catalyst [Shea, 1992]. The reaction is fast and results often in almost quantitative yields of the triazole formation. No toxicity has been observed from the use of cyclooctynes [Chang, 2010].

2.1.6 Conjugation of ligands to aldehyde-functionalized liposomes

The conjugation between an aldehyde and a hydrazide occur spontaneously without the need of a catalyst. The aldehyde functionality can be anchored into the liposome membrane as described by Bonnet *et al.* using the ether lipid di-*O*-hexadecyl-*rac*-glyceraldehyde [Bourel-Bonnet, 2005]. For the coupling of peptides to the liposome surface a hydrazide moiety can easily be introduced to the peptide during its on resin synthesis, in the form of *N,N,N*-(tri(*tert*-butyloxycarbonyl)hydrazinoacetic acid, which is fully compatible with solid-phase peptide synthesis (SPPS) [Bonnet, 2003].

2.1.7 Conjugation of ligands to hydrazide-functionalized liposomes

For the conjugation of antibodies to the liposome surface the inverted position of the functional groups is widely applied [Hansen, 1995; Lopes de Menezes, 1998]. The hydrazide group can be introduced to the liposome membrane in the form of lauric acid hydrazide [Chua, 1984] or by attaching it to the distal end of DSPE-PEG [Zalipsky, 1993]. The carbohydrate groups on the constant region of the antibody's heavy chain can be mildly oxidized by e.g. sodium periodate resulting in the formation of an aldehyde [Koning, 1999; Harding, 1997], which can be coupled to the hydrazide liposomes.

2.2 Objective

In order to address the problems touched upon in the introduction to this chapter such as non-quantitative conjugation reactions on the surface of liposomes, low reproducibility and highly varying yields compared to reactions performed in solution, a systematic study was done. This study investigated PEGylated liposomes functionalized with a neuroendocrine tumor targeting peptide, Octreotate; synthesized with several functionalities that have been used for surface conjugation of nanoparticles. The reaction kinetics and overall yield was quantified by high-performance liquid chromatography (HPLC). Reactions were conducted in solution as well as by post-functionalization of liposomes in order to study the effects of steric hindrance and possible affinity between the peptide and liposome surface.

Furthermore, we present a new highly efficient and chemoselective liposome functionalization method based on oxime bond formation between a hydroxylamine and an aldehyde modified phospholipid component.

2.2.1 Octreotate as model peptide

Targeted liposomes that recognize overexpressed receptors or antigens on diseased cells have great potential in therapeutic and diagnostic applications; hence an analogue of the Somatostatin peptide was applied as model peptide in this study.

The regulatory hormone Somatostatin (SST) was discovered in 1973 by Brazeau *et al.* [Brazeau, 1973]. They discovered the SST-14 member from the Somatostatin family, while the other important member of this family, the SST-28, was discovered by Pradayrol in 1980 [Pradayrol, 1980]. Somatostatin is secreted in the form of a precursor molecule which enzymatically is processed to yield the active forms. In the case of

Somatostatin the processing of the 92-amino acid long promolecule results in the two active segments SST-14 and SST-28 (Figure 3) [Shen, 1982].

SST-28: Ser^{1}-Ala^{2}-Asn^{3}-Ser^{4}-Asn^{5}-Pro^{6}-Ala^{7}-Met^{8}-Ala^{9}-Pro^{10}-Arg^{11}-Glu^{12}-Arg^{13}-Lys^{14}-Ala^{15}-Gly^{16}-Cys^{17}-Lys^{18}-Asn^{19}-Phe^{20}-Phe^{21}-Trp^{22}-Lys^{23}-Thr^{24}-Phe^{25}-Thr^{26}-Ser^{27}-Cys^{28}.

SST-14: Ala^{1}-Gly^{2}-Cys^{3}-Lys^{4}-Asn^{5}-Phe^{6}-Phe^{7}-Trp^{8}-Lys^{9}-Thr^{10}-Phe^{11}-Thr^{12}-Ser^{13}-Cys^{14}.

Figure 3: SST-28 has 28 amino acids and SST-14 has 14 amino acids. As can be seem from the sequences the SST-14 is derived from SST-28 by cleavage between Lys^{14} and Ala^{15}.

These two peptides bind to five different forms of the G protein-coupled receptors ($SSTR_{1-5}$) expressed in various tissues, and often in more than one form in a single cell. The SST-14 and SST-28 are somewhat selective for the receptors, where $SSTR_{1-4}$ bind SST-14 with higher affinity than SST-28, and $SSTR_5$ predominantly binds SST-28 [Patel, 1995].

The biological role of the hormone Somatostatin is to regulate the endocrine system. The peptide is naturally produced by neurons in the hypothalamus - and other parts of the brain - and is transported through the median eminence to the anterior pituitary where it inhibits the synthesis and secretion of growth hormone and thyroid-stimulating-hormone. Somatostatin is classified as an inhibitory hormone, and in addition to these two hormone regulations it has a regulating effect on the secretion of insulin, glucagon, gastrointestinal hormones; it can reduce gastric emptying as well as blood flow in the intestine, and smooth muscle contraction [Widmaier, 2004]. By Somatostatin's inhibition of growth hormone the protein synthesis as well as carbohydrate and lipid metabolism are effected throughout the body.

The secretion of Somatostatin is controlled by a negative feedback mechanism which can be exploited in a number of diseases, where the amount of secretion of Somatostatin has gone wrong. Many tumor cell lines have been found to overexpress Somatostatin receptors; hence Somatostatin analogues can be administrated, affecting mainly cancerous cells over healthy cells.

Many hormones have a minimum sequence that fulfils the requirements for a complete biological function. Hence, peptide analogues for these hormone receptors have

often been modified extensively and it can be difficult to find the relation to the natural occurring hormone. To determine which sequence that is important for a full biological activity one can systematically modify each amino acid, either deleting it or substituting it for an alanine or glycine residue - called an ala or gly scan [Morrison, 2001]. Once these single modifications have been carried out and a minimum bioactive sequence determined, it can be convenient to search for a certain required secondary structure. This is mainly done by substituting $_D$-amino acids for the natural found $_L$-amino acid. Adding a $_D$-amino acid in a hormone analogue can be advantageous as peptides containing these, generally are found to have a longer half-live *in vivo* due to reduced susceptibility to enzymatic degradation. For cyclic peptides, as Somatostatin, an optimization of the ring size can be utilized as well.

Mainly the SST-14 has been inspiration to many Somatostatin analogues. These have been developed by systematic studies and have resulted in analogues with a reduced ring size as well. Structure-activity relationship (SAR) studies done on a large number of Somatostatin analogues have shown that the sequence Phe^7-Trp^8-Lys^9-Thr^{10} is critical for biological recognition [Melacini, 1997]. These amino acids will form a β turn which is necessary for biological activity. Trp^8 and Lys^9 are essential, while Phe^7 and Thr^{10} can undergo minor substitutions such as from Phe^7 to Tyr^7, or Thr^{10} to Ser^{10} or Val^{10} [Veber, 1984].

One analogue which has received much attention is Octreotate (Figure 4). It consists of only eight amino acids compared to the 14 amino acids in SST-14 and consequently, the ring size of this analogue is smaller than the natural hormone. This analogue binds primarily to the $SSTR_2$ subtype, which most Somatostatin receptor-positive tumors express [Reubi, 2000].

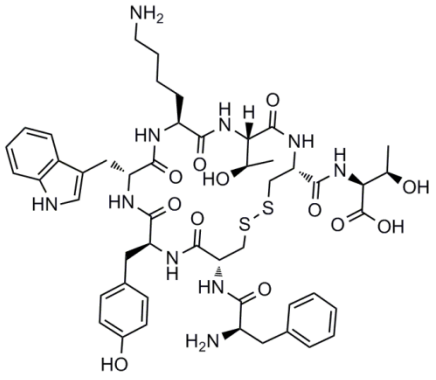

Figure 4. The cyclic Somatostatin analogue Octreotate (TATE): NH_2-$_D$-Phe-Cys-Tyr-$_D$-Trp-Lys-Thr-Cys-Thr-OH used as a model peptide for surface functionalization of liposomes.

This Somatostatin analogue was used as a model peptide for the surface functionalization of liposomes testing the conjugation competence of matching chemical functionalities.

2.3 Materials and methods

Full experimental details and characterizations are available in Appendix II.

2.3.1 Synthesis of functionalized TATE peptides

The model peptides **1a-e** for somatostatin receptor targeting, were prepared using a SPPS strategy as shown in Figure 5. The N-terminal functionalized TATE peptides **1a-e** were synthesized by SPPS on H-Thr(*t*Bu)-OH preloaded Wang Resin by standard Fmoc methodology. Each coupling was performed by activating the Fmoc protected amino acid with *O*-(7-azabenzotriazol-1-yl)-*N,N,N′,N′*-tetramethyluronium hexafluorophosphate (HATU) in the presence of 2,4,6-collidine in DMF. Cleavage of the Fmoc group was carried out using piperidine in DMF (Figure 5). Completion of each coupling and deprotection step was monitored by the Kaiser test. HATU was used to ensure high conversion with minimum epimerization.

After assembly of the resin immobilized octapeptide, NH_2-$_D$-Phe-Cys(Acm)-Tyr(*t*Bu)-$_D$-Trp-(Boc)-Lys(Boc)-Thr(*t*Bu)-Cys(Acm)-Thr(*t*Bu)-resin, the linear peptide was treated with $Tl(CF_3COO)_3$, which in a single step removed the two Acm-protection groups present on the cysteine residues and formed the intramolecular disulfide bond. The reaction was followed by cleavage of a small amount of peptide from the resin with TFA and analyzing the crude peptide by MALDI-TOF MS. Complete Acm-removal and disulfide formation were observed after 75 min with no sign of dimerization.

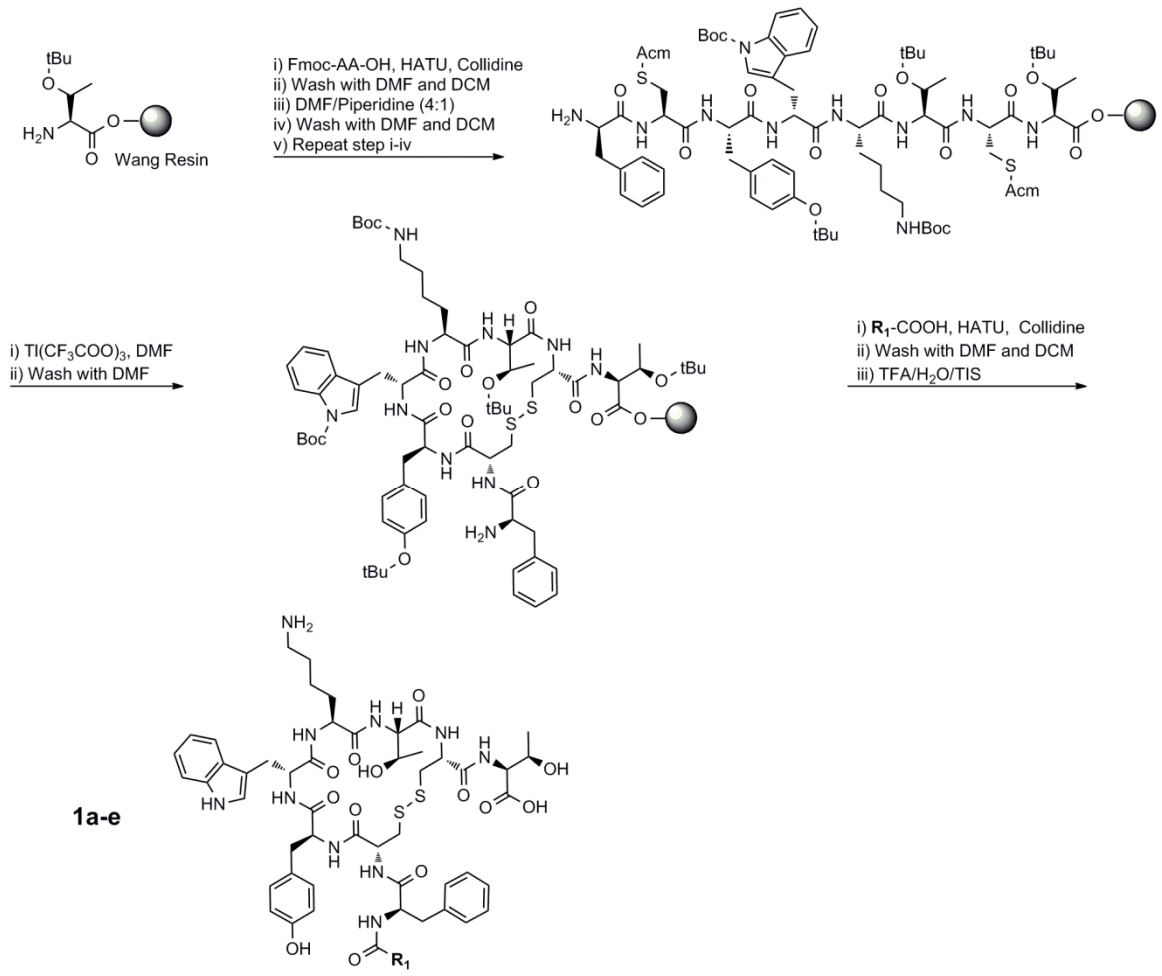

Figure 5. Synthesis of TATE derivatives **1a-e** using solid phase peptide synthesis.

After extensive washing of the resin, the N-terminal of the resin bound peptide was acylated with either 4-maleimidobutyric acid (**1a**), 3-(tritylthio)-propionic acid (**1b**), 5-azidopentanoic acid (**1c**), 4-pentynoic acid (**1d**) or bis-Boc-amino-oxyacetic acid (**1e**), before being cleaved from the solid support by treatment with a mixture of TFA/H_2O/TIS (95:2.5:2.5) to give the maleimide-, thiol-, azide-, alkyne- or hydroxylamine-modified TATE peptides (Table 1).

Table 1. Chemical structure of R-COOH used for synthesis of TATE derivatives **1a-e** and corresponding characterization by MALDI TOF MS.

Compound #	R_1	MS $(M+Na)^+$ (cald.)	MS $(M+Na)^+$ (found)
1a	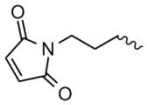	1236.35	1236.39
1b		1159.33	1159.57
1c		1196.33	1196.60
1d	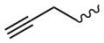	1129.31	1129.47
1e	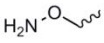	1144.25	1144.41

Final purification of the peptides was accomplished by HPLC.

2.3.2 Synthesis of DSPE-PEG_{2000} functionalized phospholipids

In order to formulate liposomes exposing the appropriate chemical functionalities at the distal end of the PEG-corona, PEGylated phospholipids with the desired functionalities were synthesized in a single step from DSPE-PEG_{2000}-NH_2 by acylation of the amino group with the desired functionality in the presence of either HATU or EDC·HCl (Figure 6) or by reduction of the DSPE-PEG_{2000}-PDP to yield the free thiol moiety (Figure 7).

PEGylated phospholipids exposing a terminal alkyne, a cyclic alkyne, an aldehyde, or an azide functionality at the distal end of the polymer (**2a-d**) were synthesized by acylating DSPE-PEG_{2000}-NH_2 with 4-pentynoic acid (**2a**), 1-fluorocyclooct-2-ynecarboxylic acid (**2b**), 4-carboxybenzaldehyde (**2c**), or 5-azidopentanoic acid (**2d**), respectively. 1-Fluorocyclooct-2-ynecarboxylic acid was synthesized as described elsewhere [Schultz, 2010]. DSPE-PEG_{2000}-SH (**3**) was synthesized in a single step from DSPE-PEG_{2000}-PDP by reduction of the pyridyldithiopropionate (PDP) group by DTT applying standard conditions [Cleland, 1964] which resulted in the desired free thiol (**3**). The DSPE-PEG_{2000}-maleimide (**4**) functionalized phospholipid was purchased from Avanti Polar Lipids, Inc., Alabama.

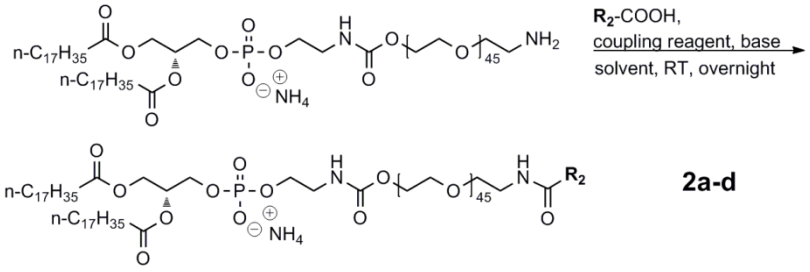

Compound #	R_2	Coupling reagent	Base	Solvent
2a	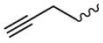	EDC·HCl	DMAP	CH_2Cl_2
2b	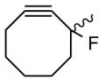	HATU	Et_3N	DMF
2c	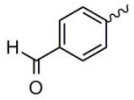	HATU	Et_3N	DMF
2d		HATU	Et_3N	DMF

Figure 6. Synthesis of functionalized DSPE-PEG_{2000}-NH_2 phospholipid conjugates **2a-d** and their corresponding reaction conditions.

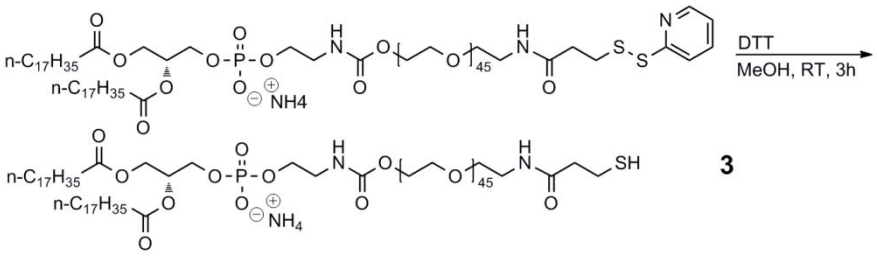

Figure 7. Synthesis of DSPE-PEG_{2000}-SH phospholipid conjugate **3**.

2.3.3 Liposome formulation

In order to evaluate the efficiency of the different coupling strategies and make a valid comparison, a standardized protocol was used to minimize the influence of other parameters.

Functionalized liposomes composed of DSPC/DSPE-PEG_{2000}/DSPE-PEG_{2000}-R (95:4:1) (R = alkyne (**2a**), cycloalkyne (**2b**), aldehyde (**2c**), azide (**2d**), thiol (**3**), or maleimide (**4**)) were prepared by the method described by Bangham *et al*. [Bangham, 1964]. Lipids were dissolved in CH_3Cl/MeOH (9:1) and mixed in the ratio (95:4:1)

DSPC/DSPE-PEG_{2000}/DSPE-PEG_{2000}-R. The solvent was removed under a stream of nitrogen to form a lipid film. The lipid films were placed under vacuum overnight to remove remaining traces of organic solvent. The obtained lipid films were hydrated in a HEPES buffer, (10 mM HEPES, pH 6.5, 145 mM NaCl) at 65 °C for 1 h; followed by 10 freeze-thaw cycles and extrusion at 65 °C through a 100 nm polycarbonate filter using an Avanti Polar Lipids mini-extruder.

The size distribution of the liposomes was analyzed using dynamic light scattering (DLS), as well as their zeta potential using a Brookhaven Zeta PALS analyzer. All liposomes had a diameter of approximately 100 nm and slightly negative ζ-potential due to the presence of the DSPE-PEG_{2000} lipids (approximately -5 mV).

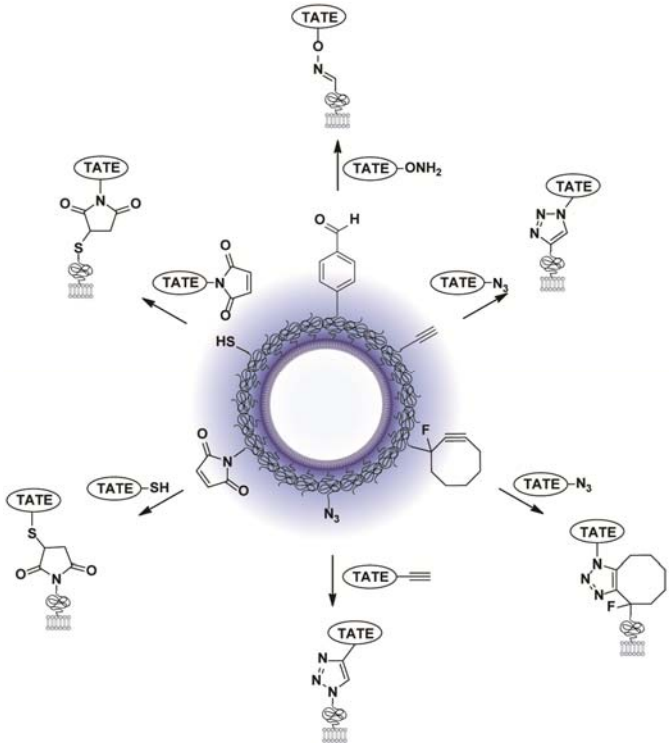

Figure 8. Schematic presentation of a liposome presenting functional moieties and their matching reactive counterparts, as well as final product. Figure kindly provided by Rasmus I. Jølck.

2.3.4 Conjugation in solution

For the conjugation reactions in solution DSPE-PEG_{2000} functionalized lipid (0.2 mM, 0.55 mL, 1.1 equiv.) was dissolved in MeOH and mixed with the corresponding functionalized TATE in MeOH (0.2 mM, 0.50 mL, 1.0 equiv.). The reaction was stirred at room temperature and aliquots (50 μL) were removed at the indicated times and analyzed by analytical HPLC. A linear gradient was used from 100% A (aqueous solution containing 5% MeCN and 0.1% TFA) to 100% B (MeCN containing 0.1% TFA) over 15 min with a flow rate of 1 mL/min and AUC for the free TATE was measured relative to

AUC for the coupled product at 280 nm. For the reaction between the maleimide and thiol functionalities Et_3N (50 mM, 6.0 μL, 3.0 equiv.) was added to facilitate the coupling, while for the copper catalyzed click reactions $CuSO_4 \cdot 5H_2O$ (1.0 M, 2.5 μL, 25 equiv.) and sodium ascorbate (1.0 M, 5.0 μL, 50 equiv.) were added.

Before injecting the aliquots from the copper catalyzed click reactions onto the analytical HPLC column 20 μL of a 10% NH_4OH solution was added to ensure the copper ions were in solution and not interfering with the HPLC signals [Sharpless, 2005].

2.3.5 Conjugation by post-functionalization of liposomes.

Pre-formed functionalized liposomes ((25 mM, 0.50 mL, 1.1 equiv.) - normalized according to a 45:55 distribution ratio between the inner- and outer liposomal membrane) were mixed with the corresponding TATE peptide (4.2 mM, 15 μL, 1.0 equiv.) dissolved in MeOH. The reactions were shaken (not stirred; to avoid foaming) at room temperature and aliquots (40 μL) removed for analysis by analytical HPLC. A linear gradient was used from 100% A (aqueous solution containing 5% MeCN and 0.1% TFA) to 100% B (MeCN containing 0.1% TFA) over 15 min with a flow rate of 1 mL/min. The AUC for the free TATE was calculated relative to the AUC of the phospholipid coupled product at 280 nm to monitor the conjugation efficiency. For the copper catalyzed click reactions $CuSO_4 \cdot 5H_2O$ (1.0 M, 1.6 μL, 25 equiv.) and sodium ascorbate (1.0 M, 3.1 μL, 50 equiv.) were added. As for the conjugations done in solution 20 μL of a 10% NH_4OH solution was added to the copper catalyzed click aliquots prior to HPLC analysis.

Triplicates of all reactions were carried out to ensure reproducibility and elucidate the heterogeneity of liposomal post-functionalization. The amount of functionalized TATE added in the two conjugation approaches was carefully controlled by measuring the concentration of the peptide stock solution by UV-vis, thus ensuring exactly the same peptide concentration in all reactions.

To ensure the same total concentration of phospholipids in all reactions, phosphorus content measurement was carried out by inductive coupled plasma atomic emission spectroscopy (ICP-AES). All reactions were monitored for 24 hours by HPLC using UV-detection (λ = 280 nm), and up to 72 hours in selected cases, by removing small aliquots from the reaction vial, and the conjugation efficiency was calculated based on the area under the curve (AUC) for the free peptide and the DSPE-PEG_{2000}-TATE conjugate, respectively (Figure 9). MALDI-TOF MS was used to verify that an excess of the

functionalized phospholipids reagent existed in all reactions that did not go to completion within 72 hours.

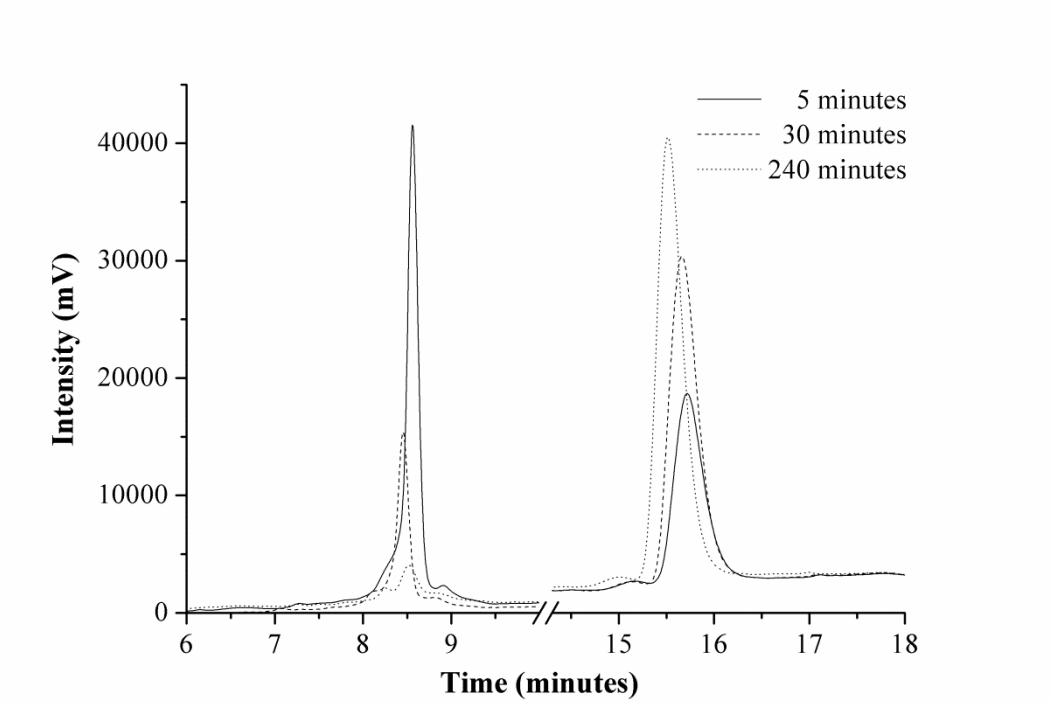

Figure 9. Example of monitoring a conjugation reaction by HPLC over time at 280 nm. The decreasing peak at 8.5 min belongs to the free TATE-maleimide (**1a**), while the peak increasing at 15.6 min is the product from the Michael Addition between TATE-maleimide (**1a**) and DSPE-PEG_{2000}-SH (**3**).

2.4 Results and discussion

2.4.1 Conjugation of TATE and DSPE-PEG_{2000} by oxime formation

This method, which has not previously been reported for the surface functionalization of liposomes, is chemoselective and bioorthogonal to functional groups in most natural occurring ligands and could serve as an excellent alternative to existing liposome post-functionalization methods [Richard, 2005]. TATE-hydroxylamine (**1e**) and DSPE-PEG_{2000}-benzaldehyde (**2c**) were conjugated, both in solution and on the liposome surface, by simply mixing the two components without any additives.

Oxime bond formation in solution was found to be quantitative within one hour, whereas eight hours of incubation was needed once performed directly on the liposome surface (Figure 10). Both procedures resulted in complete conversion to the phospholipid coupled TATE within 24 hours under mild conditions.

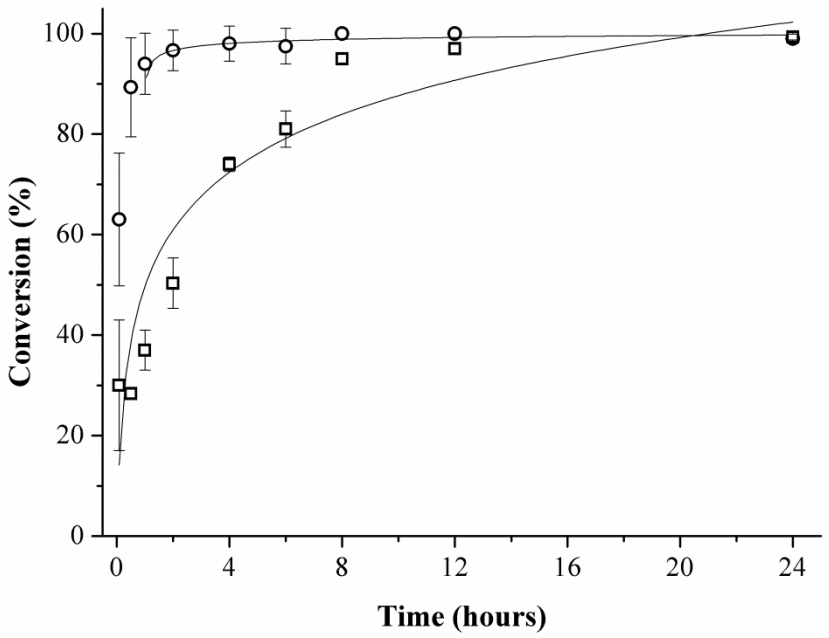

Figure 10. Conjugation of DSPE-PEG_{2000} and TATE by oxime bond formation. Reactions carried out in solution and directly on the liposome surface. TATE-hydroxylamine (**1e**) + DSPE-PEG_{2000}-benzaldehyde (**2c**) in solution (○), TATE-hydroxylamine (**1e**) +DSPE-PEG_{2000}-benzaldehyde (**2c**) on liposomes (□). All values are means ± SEM (n = 3).

Oxime bond formation is known to be accelerated by the presence of aniline [Dirksen, 2008], acetic acid [Gustafsson, 2001] or Lewis acids [Sridhar, 2011]. In order to verify this, acetic acid (0.1% v/v) was added to a liposome batch containing TATE-hydroxylamine (**1e**). Under these conditions, the conjugation yield reached 78% within 5 minutes. Without the presence of the catalyst, 30% conversion was observed within the same time frame. The oxime bond formation is a reversible process; however, HPLC and MALDI TOF MS did not show any reversible formation of the starting materials within one week in aqueous medium, which supports the reporting of oxime bonds to be more hydrolytically stable than, e.g., its analogous hydrazine bond at physiologically relevant pH [Rose, 1996].

The position of these two functional groups is not interchangeable, as placing the aldehyde functionality on TATE will induce the risk of intramolecular imine formation.

2.4.2 Conjugation of TATE and DSPE-PEG_{2000} by CuAAC

Conjugation of TATE and DSPE-PEG_{2000} by the CuAAC reaction was carried out using sodium ascorbate to generate Cu(I) from $CuSO_4 \cdot 5H_2O$ *in situ* [Tornøe, 2002; Rostovtsev 2002]. Reactions were carried out with the azide present on the TATE peptide, the alkyne

at the PEG terminal of DSPE-PEG_{2000}, and vice versa. The relative position of the functional moieties was found to have no significant effect on the reaction efficacy under the solution conditions, as both orientations result in approximately 98% yield after 12 hours (Figure 11). A different result was obtained when monitoring the post-functionalization reaction on the liposome surface.

The cycloaddition between the azide-functionalized TATE (**1c**) and the alkyne-modified phospholipid (**2a**) resulted in about 75% yield after 2 hours, while the opposite position having the azide functionality present on the liposomes and the alkyne at the N-terminal of the peptides levelled out at 43%.

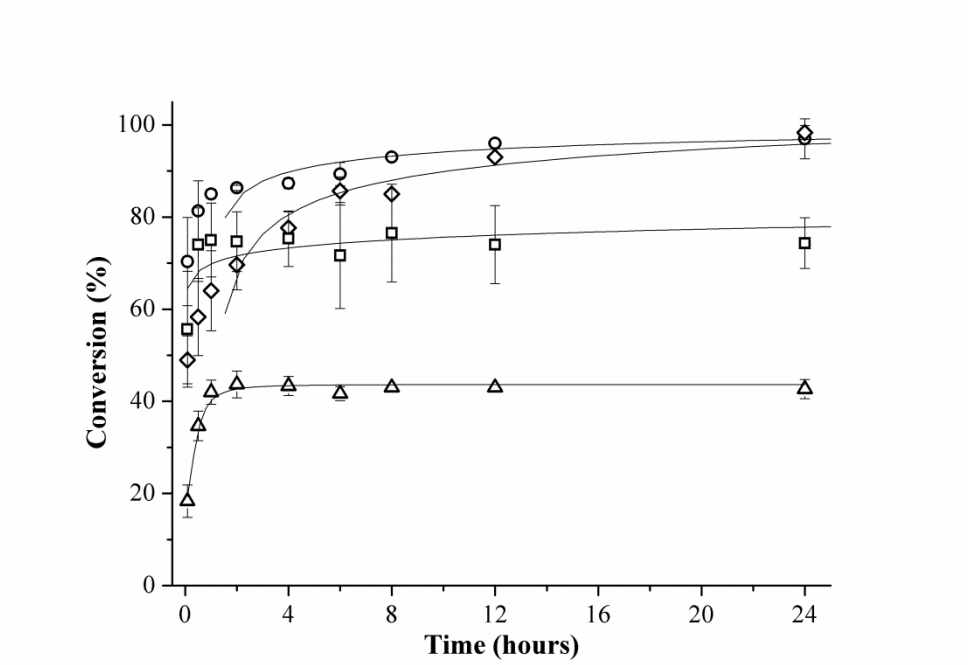

Figure 11. Conjugation of DSPE-PEG_{2000} and TATE by the CuAAC reaction. Reactions carried out in solution and directly on the liposome surface. TATE-azide (**1c**) + DSPE-PEG_{2000}-alkyne (**2a**) in solution (○), TATE-azide (**1c**) + DSPE-PEG_{2000}-alkyne (**2a**) on liposomes (□), TATE-alkyne (**1d**) + DSPE-PEG_{2000}-azide (**2d**) in solution (◊), TATE-alkyne (**1d**) + DSPE-PEG_{2000}-azide (**2d**) on liposomes (Δ). All values are means ± SEM (n = 3).

Functionalization of azide-modified liposomes by the CuAAC reaction has not previously been reported elsewhere to our knowledge. Functionalization of liposomes by the CuAAC reaction has consistently been carried out with alkyne-modified liposomes and azide-functionalized ligands; thus, these reports have not observed the clear negative trend observed here with the azide-functionalized liposomes. Furthermore, removing the copper fully from the final product to avoid copper induced cytotoxicity can be challenging, which to some degree reduces the usability of this reaction for biological purposes.

2.4.3 Conjugation of TATE and DSPE-PEG$_{2000}$ by Cu-free click chemistry

A method to avoid addition of toxic copper salts as catalyst in the triazole formation is to use strained or electron-deficient alkynes [Agard, 2004; Li, 2004]. This strategy was studied using the DSPE-PEG$_{2000}$-cyclooctyne (**2b**) and azide-functionalized TATE (**1c**). In solution, the conjugation was remarkably slow, yet highly reliable and reproducible with no form of decomposition or side product formation. As the reaction was terminated after 50 days, a product yield of 86% was obtained without reaching a plateau. Applying the post-functionalization protocol resulted in a remarkably faster initial reaction (Figure 12), and a level of 84% yield was reached after 72 hours.

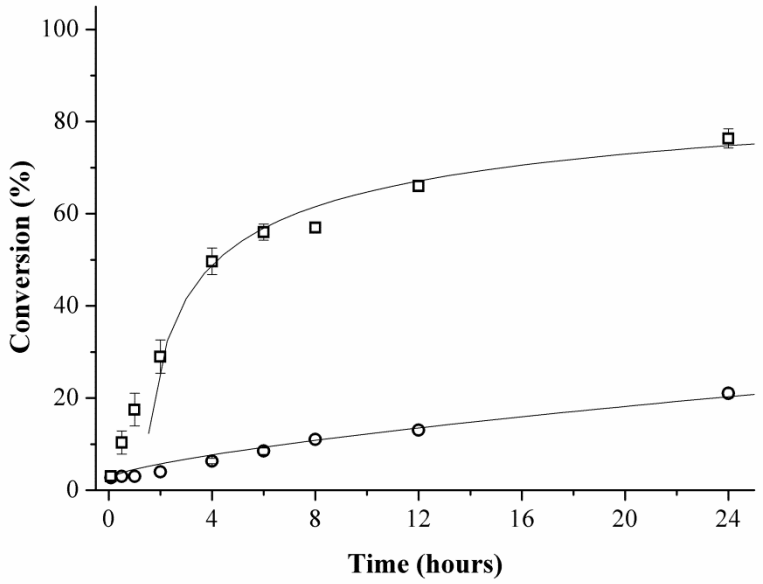

Figure 12. Conjugation of DSPE-PEG$_{2000}$ and TATE by strain-promoted Click reaction. Reactions were carried out in solution and directly on the liposome surface. TATE-azide (**1c**) + DSPE-PEG$_{2000}$-cyclooctyne (**2b**) in solution (○), TATE-azide (**1c**) + DSPE-PEG$_{2000}$-cyclooctyne (**2b**) on liposomes (□). All values are means ± SEM (n = 3).

Interestingly, triazole formation was significantly faster when performed on liposome surfaces compared to the reaction in solution. This is presumably due to favourable interactions between the liposome surface and TATE-azide (**1c**). As TATE-azide (**1c**) is not highly soluble in the buffer, it prefers to bind to the PEG layer, bringing it closer to the reaction sites on the surface, which leads to a faster reaction.

Choosing a more reactive cyclooctyne could not only increase the reaction rate in solution, but also increase the risk of side product formation [Chenoweth, 2009; Codelli, 2008]. However, a relatively long synthetic procedure to obtain the cyclooctyne moiety

limits the use of this type of copper-free click reaction. Furthermore, it has been shown that thiols can add spontaneously to cyclooctynes limiting the bioorthogonality, as some degree of nonspecific reactions can occur [Fairbanks, 2010].

2.4.4 Conjugation of TATE and DSPE-PEG$_{2000}$ by Michael Addition

The final approach tested to conjugate TATE and DSPE-PEG$_{2000}$ was using the Michael Addition procedure. In general, the Michael Addition proceeded rapidly within the first four hours until reaching a plateau, and reactions carried out in solution were slightly faster compared to the liposomal counterpart. The orientation of the maleimide and the thiol was found to have a decisive impact on the conjugation efficiency. Michael addition in solution between DSPE-PEG$_{2000}$-SH (**3**) and TATE-maleimide (**1a**) resulted in 97% conversion, whereas when performed on the liposome surface, 92% conversion was observed. The opposite orientation of functionalities expressed in the form of DSPE-PEG$_{2000}$-maleimide (**4**) and TATE-thiol (**1b**) only resulted in 53% product formation when performed in solution and 40% for the postfunctionalization of liposomes (Figure 13), which was surprising.

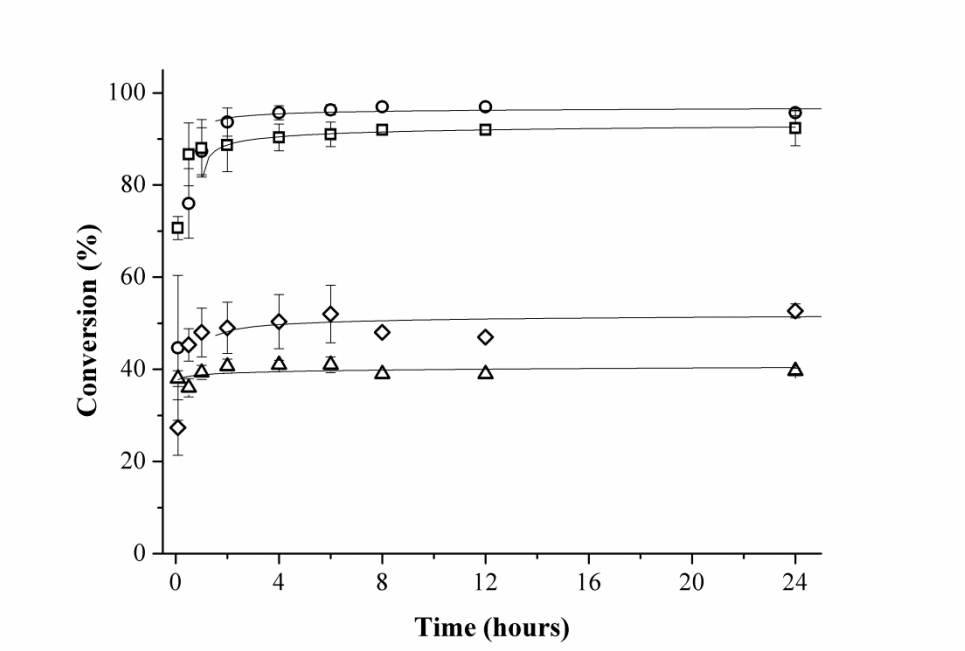

Figure 13. Conjugation of DSPE-PEG$_{2000}$ and TATE by Michael addition. Reactions carried out in solution and directly on the liposome surface. TATE-maleimide (**1a**) + DSPE-PEG$_{2000}$-SH (**3**) in solution (○), TATE-maleimide (**1a**) + DSPE-PEG$_{2000}$-SH (**3**) on liposomes (□), TATE-thiol (**1b**) + DSPE-PEG$_{2000}$-maleimide (**4**) in solution (◊), TATE-thiol (**1b**) + DSPE-PEG$_{2000}$-maleimide (**4**) on liposomes (Δ). All values are means ± SEM (n = 3).

The origin for this observation is not clear, however; multiple factors could have caused this drop in conversion. Hydrolysis of the maleimide moiety to the nonreactive maleamic acid at pH > 8.5 has been reported in the literature [Gregory, 1955], but at pH 6.5 where our reactions are carried out, this should be minimized [Barradas, 1976; Matsui, 1978]. This was confirmed by MALDI-TOF MS where intact DSPE-PEG_{2000}-maleimide as well as unreacted TATE-SH was observed. However, a minor amount of methoxysubstituted maleimide was also observed by MALDI-TOF MS indicating that the oxa-Michael Addition is a competing side reaction [Finnegan, 1965].

As poor conversion was observed for the reaction carried out in solution as well as on the surface, we speculated that the TATE-thiol (**1b**) peptide was the limiting factor in this reaction. TATE-thiol (**1b**) is highly prone to oxidation resulting in nonreactive TATE-dimers; however, dimerization was not observed by HPLC or by MALDI-TOF MS.

As a positive control of the reactivity of the commercial DSPE-PEG_{2000}-maleimide (**4**), a test reaction using 2-mercaptoethanol was conducted. Using this small and highly reactive thiol, complete product formation was observed within two hours as confirmed by MALDI-TOF MS, confirming excellent reactivity of DSPE-PEG_{2000}-maleimide (**4**). Hence, the reason for the low coupling efficiency between DSPE-PEG_{2000}-maleimide (**4**) and TATE-SH (**1b**) is not clear.

2.5 Concluding remarks

These studies demonstrate the importance of choosing the correct chemistry in order to obtain a quantitative surface functionalization of liposomes.

A novel highly effective method to functionalize liposomes by post-functionalization as well as under solution conditions has been introduced in the form of an oxime bond formation between an aldehyde and a hydroxylamine. This conjugation is chemoselective and bioorthogonal to functional groups in most naturally occurring relevant ligands, and based on our investigations, it could serve as an excellent alternative to existing liposome post-functionalization methods.

In addition, a systematic study has been conducted to elucidate the optimal postfunctionalization chemistry with focus on the relative position of the reactive functionalities. In general, the reactions carried out directly on the surface of the functionalized liposomes were slower than the solution phase counterpart, except for the strain-promoted click reaction, which surprisingly showed the opposite trend. Despite of

possible heterogeneities of liposomal formulations, surface conjugation reactions were, in general, highly reproducible.

The relative position of the reactive functionalities was found to have a significant impact on the degree of conversion for the Michael Addition and the CuAAC reaction. The Michael Addition was found to be most effective when the nucleophilic thiol was present at the distal end of the PEG polymer compared to the N-terminal of TATE. A similar observation was observed for the CuAAC reaction. The relative positions of the azide and the alkyne did not influence the degree of conversion in solution; however, once performed on the liposome surface it had a decisive impact. Having the alkyne functionality present at the liposome surface resulted in 75% conversion, whereas the azide functionalized liposomes only resulted in 43% product formation.

The findings described above will be useful for future postfunctionalization designs and clearly illustrate that care should be taken to select the most appropriate chemistry for the desired chemical manipulation. Furthermore, it is also evident that post-functionalized nanoparticles in general should always be analyzed in order to ensure the desired composition of the nanoparticle constructs.

Chapter 3

Targeted liposomes as radiopharmaceuticals

Cancer management requires reliable diagnosis and fast identification of the primary tumor as well as metastases, as the cure rate in cancer patients is strongly dependent on the stage of the cancer, when it is diagnosed. Early detection remains a key issue and radiopharmaceuticals have played a major role in this aspect. Imaging by the use of radiopharmaceuticals is usually one of the first steps in cancer diagnostics.

Positron emission tomography (PET) is one of the fastest growing imaging techniques as it allows for the tracking of organ function at the molecular level, unlike other imaging modalities such as magnetic resonance imaging (MRI), computed tomography (CT) and x-ray. The combination of PET and CT or MRI imaging - called hybrid imaging techniques - complements each other by combining the metabolic sensitivity of PET with the spatial resolution of CT or MRI. This provides quantitative and accurate pictures of abnormalities characteristic in cancer [Fass, 2008].

Nuclear imaging techniques such as PET and single photon emission computed tomography (SPECT) involve the injection of a radionuclide, followed by imaging after a suitable time giving the radionuclide time to reach its target. Several approaches have been investigated using liposomes as nanocarriers of the radionuclide, either by utilizing the EPR effect or by using targeted liposomes [Phillips, 2008].

3.1 PET as imaging technique

In the early 1970s the first PET camera for clinical studies was build and ^{11}C-glucose, ^{15}O-water and ^{13}N-ammonia were applied as radiotracers to demonstrate its potential clinical application [Phelps, 1975]. Compared to SPECT, PET has a higher detection sensitivity, which makes it possible to visualize radiotracer concentrations as low as 10^{-12} M [Gambhir, 2000; Gambhir, 2002; Phelps, 1975].

PET imaging utilizes positron-emitting radionuclides such as ^{18}F, ^{11}C, ^{64}Cu, ^{15}O and ^{124}Y. When a positron is released, it will travel a few millimetres (1-3 mm) before collision and annihilation with an electron, emitting a pair of γ-rays with the energy of 511 keV each at almost 180 degrees [Bailey, 2005] (Figure 14).

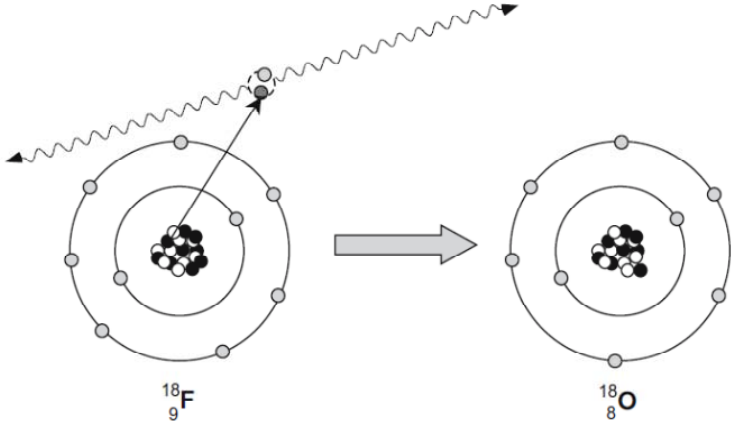

Figure 14. A positron is being ejected from the unstable atomic nuclei and travels a finite distance, before annihilation with an electron giving rise to two anticolinear high-energy photons [Bailey, 2005].

Currently, most PET cancer imaging agents are based on [^{18}F]-2-fluoro-D-deoxyglucose (^{18}FDG), an analogue of glucose, because of its high uptake in metabolically active tumors as the rate of glycolysis is far greater in neoplastic tissue compared to normal tissue [Larson, 1999]. However, not all cancers are well imaged with ^{18}FDG e.g. prostatic cancer has a limited uptake of ^{18}FDG, while normal brain tissue have a high uptake of ^{18}FDG giving rise to a high background, when trying to image brain tumors [Salminen, 2002]. Sensitivity and specificity is compromised as inflamed and infected tissues will have a high uptake of this radiotracer as well.

New radiotracers for PET are attracting much interest as the ability to monitor trace amounts of radiolabeled ligands without affecting biochemical processes *in vivo* are important for the staging of cancer and monitoring of chemotherapy efficacy. PET makes it possible to determine drug biodistribution and concentration in tumor versus healthy

tissue, and a variety of targeting ligands have been attached to radionuclides such as antibodies [Collingridge, 2002] and peptide sequences [Kwekkeboom, 2010].

3.1.1 Radionuclides used in PET

The most commonly used radionuclides for PET imaging have relatively short half-lives, such as ^{18}F ($t_{½}$ = 110 min), ^{11}C ($t_{½}$ = 20 min), ^{13}N ($t_{½}$ = 10 min), ^{15}O ($t_{½}$ = 2 min). Since the energy for the annihilation process for photons is the same for all positron emitters (511 keV) the selection of radionuclide is mainly based on the biochemical event that needs imaging.

Radionuclides with long half-lives, such as ^{64}Cu ($t_{½}$ = 12.7 hours) and ^{124}I ($t_{½}$ = 101 hours) may be preferred for tracking longer circulating formulations as liposomes [Phillips, 2008; Petersen 2012].

Copper has several positron emitting radioisotopes; ^{60}Cu, ^{61}Cu, ^{62}Cu, ^{64}Cu and ^{67}Cu with half-lives ranging from 10 minutes to 62 hours. The most applied copper isotopes are ^{62}Cu ($t_{½}$ = 9.7 min) and ^{64}Cu ($t_{½}$ = 12.7 hours), which are used for different purposes. ^{62}Cu has a higher sensitivity than ^{64}Cu, but because of its short half-life it is only suitable for studying fast kinetics, whereas the longer imaging time for ^{64}Cu can compensate for the lower sensitivity, due to a better spatial resolution [Williams, 2005].

3.1.2 The use of liposomes for PET imaging

Liposomes are one of the more popular systems when it comes to the delivery of radionuclides *in vivo*. Their ability to deliver molecules with a high variety of physiochemical properties, in addition to their particular accumulation in tumor and metastatic tissue, give them a central position in diagnostics [Maede, 2000]. The combination of this specific tissue targeting and the radionuclides encapsulated in the liposome aqueous core or conjugated to the liposome surface, makes it possible to obtain PET images with lower radionuclide concentrations.

The first use of radiolabeled liposomes was done in 1970s [Neerunjun, 1977; Richardson, 1977]. Tumor bearing rats were injected with ^{99m}Tc labeled liposomes for SPECT imaging. The radioactivity distribution in the whole rat was visualized by a γ-camera-computer system, and the radioactivity in each organ was measured quantitatively after the rat was sacrificed. Since then much progress have been made; in regard to technology as well as in regard to radiolabeling techniques.

As the radionuclides typically used for PET imaging are relatively short-lived the radiolabeling of liposomes should be carried out just prior to the beginning of an experiment. Ideally, pre-manufactured stock liposomes should be utilized together with a remote loading technique. This technique has generally been achieved by the use of different lipophilic chelators to carry the radionuclide across the phospholipid bilayer membrane. Already encapsulated in the liposome core is a hydrophilic agent for which the radionuclide has a high affinity. Hence, the radionuclide will bind stronger to the agent inside than to the lipophilic chelator and stay inside of the liposome. This method typically provides high loading efficiencies (>90%) in addition to good *in vivo* stability as the radionuclide is protected inside the liposome [Phillips, 1999; Petersen 2012].

Other radiolabeling methods exist, however these are shown to be less effective and not as widely applied. Liposomes can be labeled in their bilayer membrane. This can be accomplished by embedding the radionuclide into the bilayer membrane during liposome formation [Espinola, 1979], by attaching the radionuclide to the liposome surface via basic electrostatic interactions [Phillips, 1999] or by binding the radionuclide to a surface anchored chelator [Hnatowich, 1981; Seo, 2011]. These methods are generally less applied, as the radionuclide is not covalently bound to the surface or the bilayer, and the risk of release of the radionuclide under *in vivo* conditions is high.

The aqueous lumen in the liposome can hold radionuclides as well. These can be passively loaded into the hydrophilic lumen in the hydration step of the liposomes [McDougall, 1974; Oku, 1993]. This passive accumulation is less practical as it is limited by the interior volume of the liposome and often provides low encapsulation - liposomes of 100 nm give < 10% encapsulation efficiency [Petersen, 2012].

For *in vivo* purposes it is important that the radiolabeled liposomes are stable and able to retain their radionuclide as release of the radionuclide during or after injection can lead to incorrect interpretation of biodistribution results. From a traditional drug delivery point of view a long blood circulation time is considered advantageous, however when considering radioactive labeled liposomes a too slow clearance could be a limiting factor, as un-accumulated liposomes will add to the background signal, resulting in deteriorating the image quality. Hence, a compromise has to be made between desired tumor accumulation and blood circulation time.

3.2 cRGD as targeting ligand

As for drug delivery purposes radioactive labeled liposomes can be aimed at specific tissues by the use of targeting ligands. A ligand that has attracted much attention since its discovery more than 25 years ago is the RGD (Arginine-Glycine-Aspartic acid) peptide [Pierschbacher, 1984]. This tripeptide sequence is naturally found in proteins of the extracellular matrix (ECM) such as fibronectin, vitronectin and fibrinogen, where integrins link the intracellular cytoskeleton of cells to the ECM by recognizing the RGD sequence [Ruoslahti, 1996]. Cells that are unable to attach to the extracellular matrix will generally undergo apoptosis; consequently, RGD containing conjugates have the ability to inhibit cell attachment and accordingly induce apoptosis [Saiki, 1990].

Cell adhesion molecules such as the integrins play a major role in angiogenesis and metastasis. The integrin family includes at least 24 heterodimers assembled from 18 alpha and 8 beta subunits. Integrin heterodimers contain binding sites for divalent magnesium and calcium ions that facilitate their binding of ligands. Several integrins recognise the RGD sequence; all five α_v integrins ($\alpha_v\beta_1$, $\alpha_v\beta_3$, $\alpha_v\beta_5$, $\alpha_v\beta_6$ and $\alpha_v\beta_8$), two β_1 integrins ($\alpha_5\beta_1$ and $\alpha_8\beta_1$), and $\alpha IIb\beta_3$ [Humphries, 2006]. Studies have shown that especially $\alpha_v\beta_3$ and $\alpha_v\beta_5$ integrins are upregulated in endothelial cells of angiogenic blood vessels supplying tumor tissues as well as many types of malignant tumor cells. These integrins are not widely detected in healthy tissues and can thus serve as a valuable biomarker for neovascularisation [Friedlander, 1996]. Clinical studies have correlated the expression of $\alpha_v\beta_3$ integrins with tumor grade and aggressiveness [Schnell, 2008] and the capability to detect upregulated $\alpha_v\beta_3$ integrin expression could lead to better characterization and staging of cancers.

A large variety of RGD analogues which serve as integrin inhibitors have been developed, and a few have been evaluated in clinical trials as anti-angiogenic treatments [Mas-Moruno, 2010]. Pioneering studies by Pierschbacher and Ruoslahti [Pierschbacher, 1984] described the tetrapeptide sequence RGDS (Arginine-Glycine-Aspartic acid-Serine) as the minimal sequence for binding of fibronectin with its surface receptor. However, later studies revealed that the serine residue could be replaced with other amino acids without loss of biological function, while the first three were essential for activity.

Linear peptides have a great number of conformations in solution, which can lead to poor binding affinity and receptor selectivity. A useful way to reduce this number is by cyclization of the linear peptide, and all selective RGD ligands are cyclic. A cyclic

conformation has furthermore proved to be less susceptible to degradation [Bogdanowich-Knipp, 1999]. One last modification to introduce stability and high receptor specificity of the RGD peptide is the introduction of a hydrophobic D-amino acid in position 4. Often the amino acid in position 5 is a lysine residue, which makes an ideal building block for further chemical conjugation reactions (Figure 15).

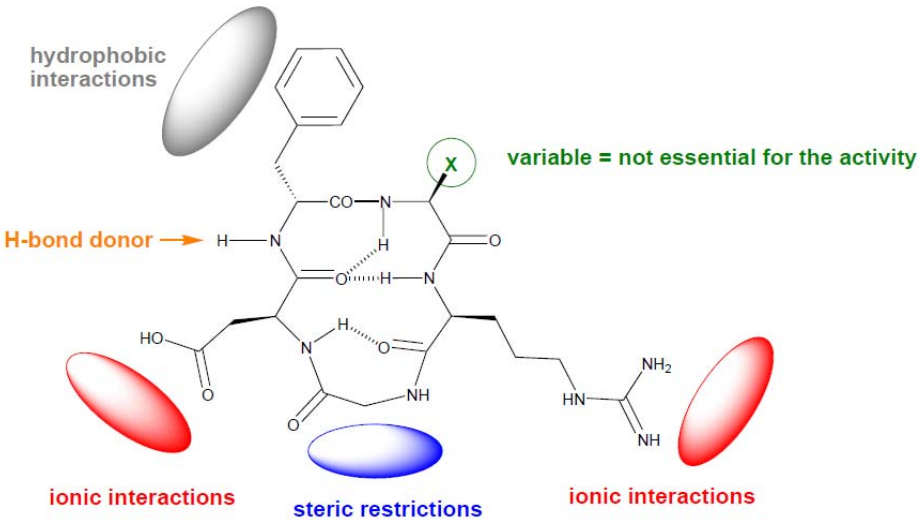

Figure 15. The Arg in position 1 and Asp in position 3 promote ionic interactions with the receptor. Gly in position 2 could enforce steric restrictions, while the amino acid in position 4 should be a hydrophobic D-amino acid in order to provide optimal interaction with the receptor. Position 5 can be chosen freely without significant impact on the biological activity [Mas-Monuro, 2010].

Crystal structures of integrins complexed with RGD ligands have revealed that the peptide binds at an interface between the α and β subunits. The arginine fits into a cleft in the α-subunit, while the aspartic acid coordinates to a cation bound in the β-subunit [Xiong, 2002].

Multimeric cRGD analogues have superior biological activity compared to monomeric analogues in targeting the integrin receptors [Ye, 2006; Liu, 2007]. When attached to a nanocarrier system, such as a liposome, the chance of longer blood circulation time as well as increased chances for receptor-mediated internalization is often larger than for single peptide constructs [Boturyn, 2004].

3.3 Objective

The integrins $\alpha_v\beta_3$ and $\alpha_v\beta_5$ are cell adhesion molecules known to play a critical role in tumor angiogenesis and metastasis. The ability to visualize and quantify the uptake of liposomes targeted towards $\alpha_v\beta_3$ and $\alpha_v\beta_5$ integrins on a whole body basis could provide

an excellent tool for the development of targeted liposome drug delivery systems. This allows for direct assessment of integrin expression *in vivo* and efficacy of anti-angiogenic treatment.

This study investigated the *in vitro* and *in vivo* characteristics of tumor-targeting liposomes presenting a cRGD peptide sequence and liposomes presenting a non-active cGRD peptide sequence on the surface.

In vitro uptake experiments were performed using fluorescent phospholipids in the liposomal membrane and flow cytrometry, while *in vivo* biodistribution was quantified using ^{64}Cu-loaded liposomes and a combined PET/CT system.

3.4 Materials and methods

Full experimental details and characterizations are available in Appendix III.

3.4.1 Synthesis of propargyl functionalized cRGD and cGRD peptides

The click reaction was chosen as conjugation method for the attachment of cRGD and cGRD peptides to DSPE-PEG_{2000} phospholipids. Consequently, the alkyne functionality needed to be introduced to the peptide sequence. This was achieved by the commercial available amino acid derivative Fmoc-propargyl-Gly-OH.

The two peptides were prepared using a SPPS strategy. The linear peptides were synthesized on a 2-chlorotrityl chloride resin using standard Fmoc methodology. The coupling of each amino acid was carried out by pre-activation of the Fmoc protected amino acid with HATU in the presence of 2,4,6-collidine in DMF. Cleavage of the Fmoc group was done using piperidine in DMF and the completion of each coupling was monitored by the Kaiser test. The 2-chlorotrityl chloride resin is highly acid labile and the fully protected linear peptides NH_2-Asp(O*t*Bu)-$_D$-Phe-Propargyl-Arg(Pbf)-Gly-OH and NH_2-Asp(O*t*Bu)-$_D$-Phe-Propargyl-Gly-Arg(Pbf)-OH were cleaved from the solid support by use of a mixture of AcOH:TFE:CH_2Cl_2 (10:20:70).

Cyclization was performed in solution between the N-terminal of the aspartic acid and the free carboxylic acid on either glycine (cRGD) or arginine (cGRD) using diphenyl phosphoryl azide to give the desired propargyl functionalized cyclic peptides **5** and **6** (Figure 16). Final purification of the peptides was accomplished by HPLC.

3.4.2 Synthesis of DSPE-PEG$_{2000}$-cRGD and DSPE-PEG$_{2000}$-cGRD phospholipids

Synthesis of the azide functionalized DSPE-PEG$_{2000}$ (**2d**) was carried out as described in section 2.3.2.

For the conjugation between DSPE-PEG$_{2000}$-N$_3$ and the propargyl functionalized peptides general CuAAC conditions were applied (Figure 16). Sodium ascorbate was used to generate the catalytic amount of Cu(I) from copper(II)sulphate pentahydrate resulting in formation of a triazole ring between the azide and alkyne moieties.

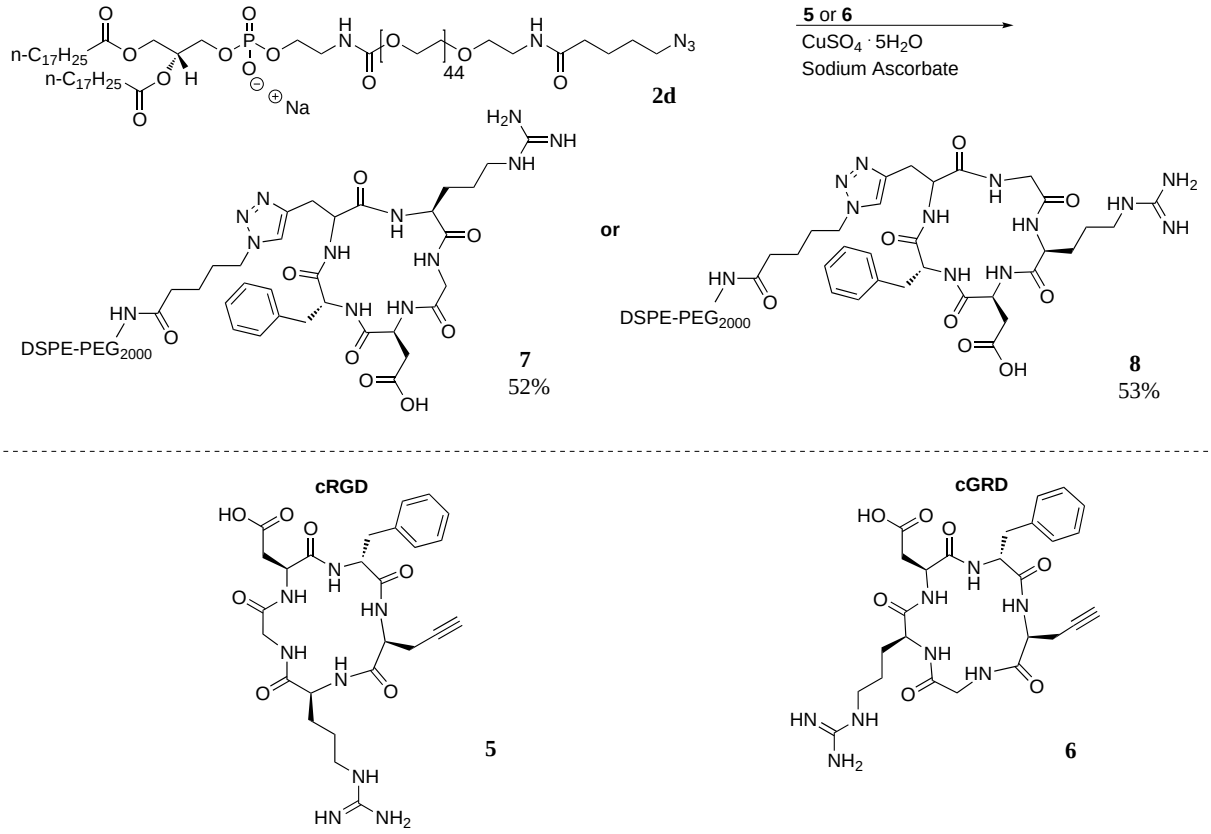

Figure 16. CuAAC coupling conditions for DSPE-PEG$_{2000}$-N$_3$ (**2d**) and cRGDfPropargyl (**5**) or cGRDfPropargyl (**6**) resulting in peptide functionalized phospholipids **7** and **8**.

The coupled products were purified by HPLC and characterized by MALDI-TOF MS.

3.4.3 Preparation of liposomes for *in vitro* studies

Liposomes composed of DSPC/DSPE-PEG$_{2000}$/DSPE-NBD/DSPE-PEG$_{2000}$-cRGD or DSPE-PEG$_{2000}$-cGRD (94.5:4:0.5:1) as well as control liposomes composed of DSPC/DSPE-PEG$_{2000}$/DSPE-NBD (94.5:5:0.5) were prepared by the method described by Bangham *et al.* [Bangham, 1964]. The phospholipids were dissolved in CH_3Cl/MeOH

(9:1), the solvent was removed under a stream of nitrogen resulting in a lipid film which was placed under vacuum overnight to remove trace amounts of organic solvent.

The obtained lipid films were hydrated in a sterile PBS buffer for 1 hour at 65 °C, followed by freeze-thaw cycles and extrusion at 65 °C through 100 nm polycarbonate filters using an Avanti Polar Lipids mini-extruder. The formed liposomes were characterized by DLS and zeta potential measurements (Zeta PALS, Brookhaven Instruments).

3.4.4 Preparation of ^{64}Cu-liposomes for *in vivo* studies

Liposomes composed of DSPC/cholesterol/DSPE-PEG_{2000}/DSPE-PEG_{2000}-cRGD (55:40:4:1) or DSPE-PEG_{2000}-cGRD (55:40:4:1) as well as control liposomes composed of DSPC/cholesterol/DSPE-PEG_{2000} (55:40:5) were prepared by the method described by Bangham *et al.* [Bangham, 1964]. The phospholipids were dissolved in CH_3Cl/MeOH (9:1), the solvent removed under a stream of nitrogen resulting in a lipid film which was placed under vacuum overnight to remove trace amounts of organic solvent.

The obtained lipid films were hydrated in a HEPES buffer containing the hydrophilic copper chelating agent DOTA for 1 hour at 65 °C, followed by extrusion at 65 °C through a 100 nm polycarbonate filer using an Avanti Polar Lipids mini-extruder. Un-encapsulated DOTA was removed from the outside of the formed liposomes by filtration, exchanging the external DOTA containing buffer with a HEPES buffer.

The purified DOTA containing liposomes were added to a vial containing radioactive ^{64}Cu and incubated 1 hour at 50-55 °C resulting in a loading efficiency of <95%.

3.4.5 Flow cytometry

To obtain a quantitative picture of the internalization of cRGD-liposomes, cGRD-liposomes and control PEG-liposomes flow cytometry was performed. The human glioblastoma cell line U87MG has a high expression of integrins and were used to evaluate receptor-mediated uptake [Fueyo, 2003]. Cells were incubated with NBD-fluorescent liposomes for 5 hours, washed with PBS, trypsinated and washed again before analysis using by flow cytometry on a Gallios system. The NBD-fluorescent cells were measured with a blue laser (488 nm) for excitation and emission passfilter of 525 ± 10 nm. 10,000 events were collected for each sample and non-treated cells were used as reference and the gates adjusted from those.

3.4.6 Confocal microscopy

The uptake of cRGD-liposomes, cGRD-liposomes and control PEG-liposomes were visualized using confocal microscopy. U87MG cells were grown on top of glass slides, incubated with the NBD-labeled liposomes for 24 hours, washed with PBS as well as PBS containing Heparin and two times with PBS again. They were fixated in 4% paraformaldehyde in PBS for 3 minutes, followed by washing with PBS. The plates were allowed to dry, before being mounted onto a microscopy slide using Vectashield® HardSet Mounting Medium. Imaging was performed with a Leica confocal microscope using an excitation wavelength of $\lambda = 476$ nm and an emission bandwidth range of 485-600 nm.

3.4.7 Peptide-targeted ^{64}Cu liposomes *in vivo*

For quantification of the biodistribution of ^{64}Cu labeled liposomes, U87MG cells were inoculated in the flank of nude female mice and allowed to grow for four weeks. ^{64}Cu cRGD-liposomes, cGRD-liposomes and control PEG-liposomes were intravenous injected through the tail vein. PET scans were acquired at times 1 hour, 18 hours and 45 hours, and for the anatomical localization of radioactivity CT images were acquired at the same time point.

At the 45 hours time point the animals were sacrificed and the level of radioactivity was measured in selected tissues using a gamma-counter.

3.5 Results and discussion

3.5.1 *In vitro* studies

To visualize internalization of cRGD-liposomes, cGRD-liposomes and control PEG-liposomes (Table 2) confocal microscopy was used.

Table 2. Mol% composition of liposome formulations used for uptake studies in the human glioblastoma U87MG cell line.

Type of liposome	DSPC	DSPE-PEG	DSPE-NBD	DSPE-PEG-cRGD (**7**)	DSPE-PEG-cGRD (**8**)
a - PEG-liposomes	94.5	5	0.5	0	0
b - cGRD-liposomes	94.5	4	0.5	0	1
c - cRGD-liposomes	94.5	4	0.5	1	0

The human glioblastoma cell line U87MG commonly known to have a high expression of integrins was used for this purpose. Cells were incubated for 24 hours with liposomes, washed thoroughly with PBS buffer containing Heparin to release surface-bound particles, before being imaged with a confocal microscope (Figure 17).

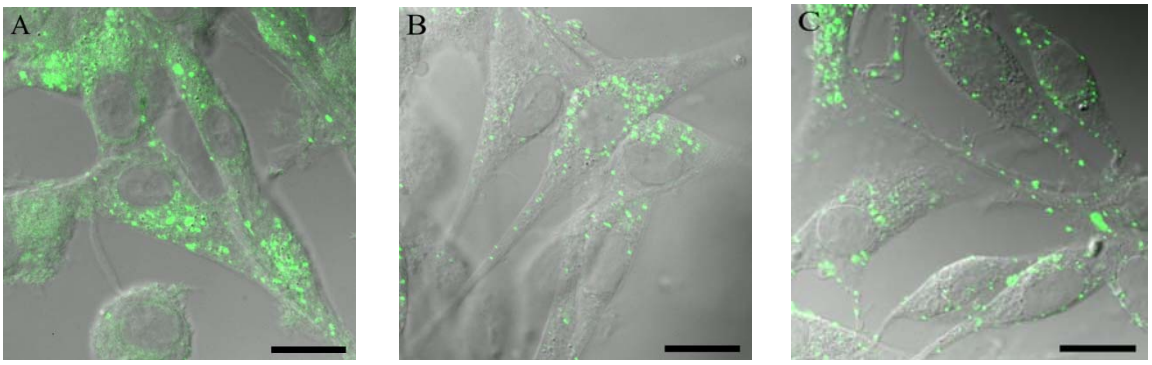

Figure 17. Representative confocal microscope images showing U87MG cells with internalized NBD-liposomes. (A) cRGD-liposomes (**c**). (B) cGRD-liposomes (**b**). (C) control PEG-liposomes (**a**). Scale bar 15 μm.

By the use of flow cytometry a quantitative uptake of cRGD- (**c**), cGRD- (**b**), and control PEG-liposomes (**a**) could be determined. Cells were incubated for 5 hours with peptide-labeled liposomes (**b** or **c**) or control PEG-liposomes (**a**), before their uptake was quantified (Figure 18).

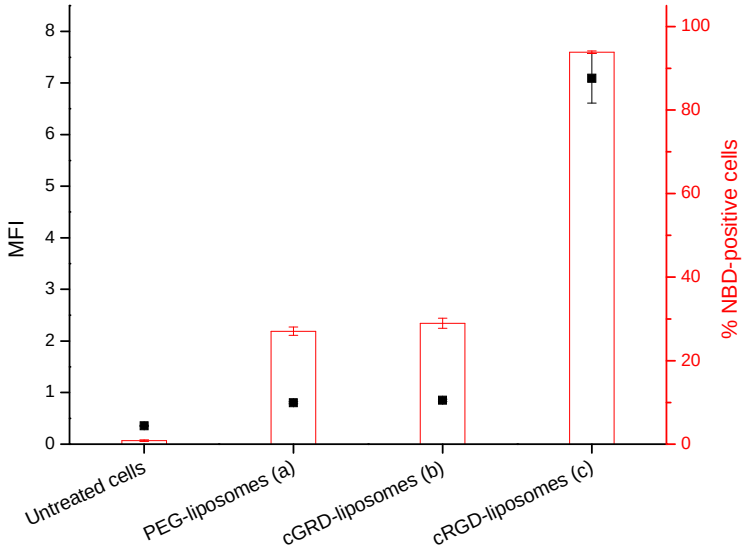

Figure 18. Uptake in U87MG cells, reported as mean fluorescence intensity (MFI) and percentage of cells with internalized NBD-labeled liposomes relative to the total amount of cells measured. All values are means ± SEM (n = 2).

cRGD-liposomes (**c**) had by far the highest internalization in U87MG cells compared to cGRD-liposomes (**b**) and control PEG-liposomes (**a**). cGRD-liposomes (**b**) as well as PEG-liposomes (**a**) were nearly identical and a small amount of unspecific uptake could be observed for these two formulations. To estimate possible background fluorescence, values for untreated cells are reported.

As uptake of positively charged liposomes are often more significant than for negative or neutral charged ones [Miller, 1998], the surface charge of the three different liposome compositions (Table 2) were measured (Table 3).

Table 3. Size and surface charge of liposomes used for uptake studies in the human glioblastoma U87MG cell line.

Type of liposome	DLS (nm)	PDI	Zeta (mV)	Std. error (mV)
a - PEG-liposomes	72.4	0.040	- 1.28	± 1.19
b - cRGD-liposomes	75.4	0.006	- 1.70	± 1.89
c - cGRD-liposomes	92.7	0.005	- 0.36	± 2.74

Since all the liposome formulations evaluated exposed approximately the same surface charge, it is believed that their difference in uptake is largely due to specific integrin receptor uptake of the cRGD-targeted liposomes.

In order to further confirm the presence of integrin receptors on the human glioblastoma cell line U87MG, we conducted an inhibition study using free peptide. Cells were incubated with free cRGD peptide or free cGRD peptide for 15 minutes followed by addition of cRGD-liposomes (**c**) or control PEG-liposomes (**a**) (Figure 19).

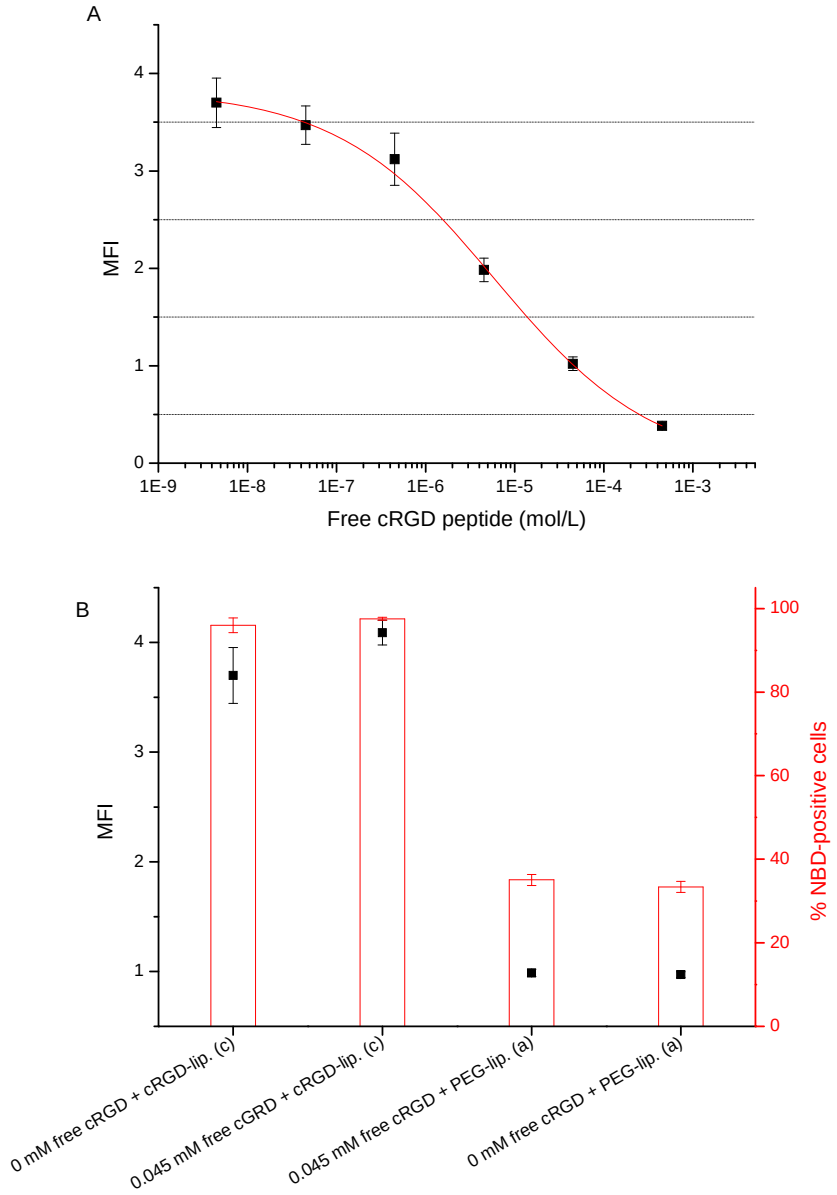

Figure 19. Inhibition of liposomal uptake using free cRGD and free cGRD peptide in U87MG cells. (A) Incubation with increasing concentrations of free cRGD peptide leads to decrease in the uptake of cRGD-liposomes (**c**). (B) Incubation with free scrambled cGRD peptide followed by addition of cRGD-liposomes (**c**), or incubation with free cRGD peptide followed by addition of PEG-liposomes (**a**). All values are means ± SEM (n = 2).

The addition of increasing concentrations of free cRGD peptide led to a reduction in the uptake of cRGD-liposomes (**c**) presumably by inhibition of the integrins receptors (Figure 19 A). To ensure that it was not the sole presence of any peptide that led to decreased liposome uptake, cells were incubated with free cGRD peptide in the highest possible concentration, before addition of cRGD-liposomes (**c**). The presence of free cGRD peptide had no influence on the uptake of cRGD-liposomes (**c**) as this was approximately equal to conditions with no free peptide added (Figure 19 B). To confirm that the free

cRGD peptide would only influence uptake through the integrin receptors, cells were incubated with and without free cRGD peptide followed by addition of control PEG-liposomes (**a**). The uptake of PEG-liposomes (**a**) was identical under both conditions (Figure 19 B).

These uptake studies supported the existence of integrin receptors on the U87MG cell line and their important function in the superior uptake of cRGD-targeted liposomes (**c**) over scrambled cGRD-liposomes (**b**) and control PEG-liposomes (**a**).

3.5.2 *In vivo* studies

Existing studies often report inconsistent results, when it comes to the difference between active targeted and passive accumulation of drug delivery systems *in vivo*. Positive results are commonly obtained *in vitro*, while *in vivo* results are more conflicting [Kirpotin, 2006; Bartlett, 2007]. In order to compare the *in vivo* biodistribution of cRGD-liposomes and its scrambled analogue cGRD-liposomes to the *in vitro* results, liposomes were loaded with radioactive ^{64}Cu and accumulation in mice xenograft models were measured by PET/CT.

Table 4. Mol% composition of liposome formulations used in a tumor-bearing (glioblastoma U87MG) mouse xenograft model.

Type of liposome	DSPC	DSPE-PEG	Cholesterol	DSPE-PEG-cRGD	DSPE-PEG-cGRD
d - PEG-liposomes	55	5	40	0	0
e - cGRD-liposomes	55	4	40	0	1
f - cRGD-liposomes	55	4	40	1	0

Postdoc Anncatrine Luisa Petersen (DTU Nanotech) and Postdoc Tina Binderup (University of Copenhagen) prepared and injected ^{64}Cu-liposomes (Table 4) into U87MG tumor bearing mice. The mice were scanned in a micro-PET/CT scanner allowing for direct determination of organ and tumor distribution (Figure 20).

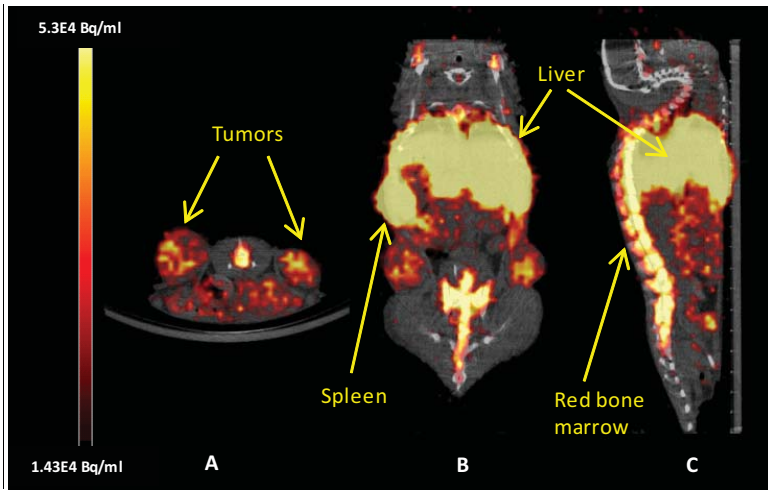

Figure 20. Biodistribution of ^{64}Cu-cRGD-liposomes (**f**) in a tumor-bearing (glioblastoma U87MG) mouse xenograft model. PET/CT images 45 hours post-injection. (A) Axial PET/CT image; tumor marked with arrows. (B) Coronal PET/CT image; spleen and liver marked with arrows. (C) Sagittal PET/CT image; liver and red bone marrow marked with arrows. Figure kindly provided by Anncatrine Luisa Petersen and Tina Binderup.

The biodistribution was visualized and quantified for ^{64}Cu-containing cRGD- (**f**), cGRD- (**e**), and control PEG-liposomes (**d**) (Figure 20 and 21). Figure 20 shows ^{64}Cu-cRGD-liposomes (**f**) 45 hours post-injection. A high accumulation can be visualized in the spleen and liver as expected, while an accumulation within the red bone marrow was surprisingly. The satisfactorily accumulation within the tumors was also visualized (Figure 20), and measured (Figure 21).

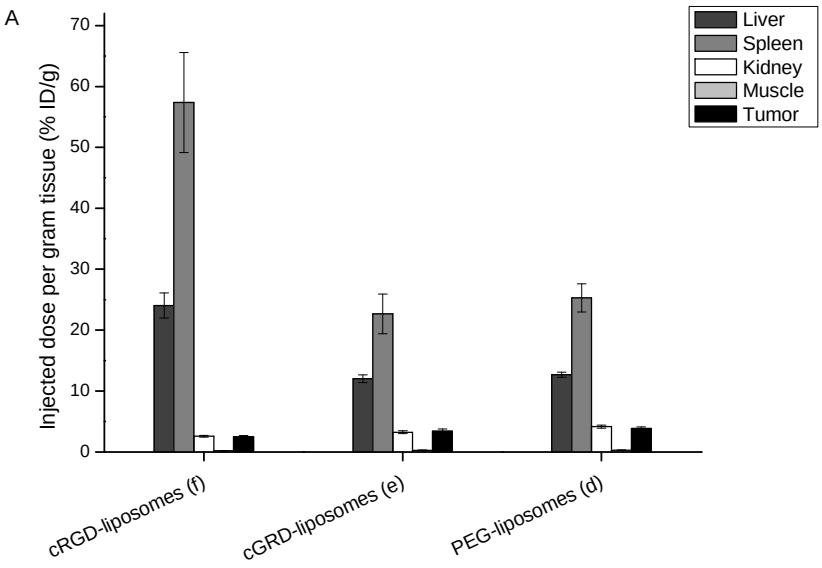

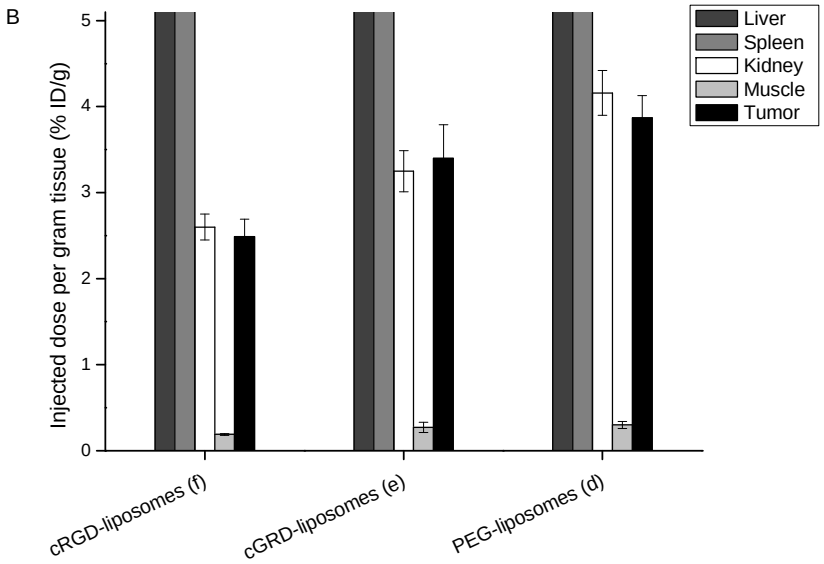

Figure 21. *In vivo* biodistribution of ^{64}Cu-cRGD-liposomes (**f**), ^{64}Cu-cGRD-liposomes (**e**), ^{64}Cu-PEG-liposomes (**d**). Accumulation in liver, spleen, kidney, muscle and tumor expressed as percent injected dose per organ (% ID/g). (A) Full graphic picture of the biodistribution; (B) zoom of graph A.

The majority of all three liposome formulations were detected in the spleen and liver, as expected, as these organs participate in the extraction of liposomes from the blood circulation by the RES (Figure 21). ^{64}Cu-cRGD-liposomes (**f**) showed a much higher accumulation in the spleen and liver, than both ^{64}Cu-cGRD-liposomes (**e**) and ^{64}Cu-PEG-liposomes (**d**), indicating that these organs were responsible for a larger clearance of the ^{64}Cu-cRGD-liposomes (**f**). Particularly, the spleen accumulation were significant larger than normally observed for liposomes [Petersen, 2012]. This enhanced accumulation could probably be explained by the expression of both $\alpha_v\beta_1$ and $\alpha_5\beta_1$ in especially the red pulp, but also the white pulp of the spleen [Liakka, 1994].

The tumor accumulation for ^{64}Cu-cRGD-liposomes (**f**) was 2.49 % ID/g, while ^{64}Cu-cGRD-liposomes (**e**) and ^{64}Cu-PEG-liposomes (**d**) showed a higher value of 3.40 % ID/g and 3.87 % ID/g, respectively, at 45 hours post-injection. They all show high tumor-to-muscle ratios. In order to identify a tumor on a medical image, the tumor needs to contain activity sufficiently larger than the background. Often muscle tissue represents the background. Generally, a tumor-to-muscle ratio of at least 1.5 to 2 is required to identify a tumor and at the same time provide diagnostically significant images [Philips, 1999]. The tumor-to-muscle ratios for the three formulations are shown in Table 5.

Table 5. Tumor-to-muscle ratio for ^{64}Cu containing liposomes in a tumor-bearing (glioblastoma U87MG) mouse xenograft model.

Type of liposome	Tumor-to-muscle ratio	Std. dev.
d - ^{64}Cu-PEG-liposomes	13.7	± 4.2
e - ^{64}Cu-cGRD-liposomes	14.6	± 8.0
f - ^{64}Cu-cRGD-liposomes	13.3	± 3.0

The tumor-to-muscle ratios were very similar (Table 5), despite the more pronounced clearance of ^{64}Cu-cRGD-liposomes (**f**) compared to ^{64}Cu-cGRD-liposomes (**e**) and ^{64}Cu-PEG-liposomes (**d**), indicating a targeting effect of the cRGD peptide sequence.

Interestingly, an accumulation could be detected in the red bone marrow for the ^{64}Cu-cRGD-liposomes (**f**) (Figure 20), whereas none were detected for either ^{64}Cu-cGRD-liposomes (**e**) or ^{64}Cu-PEG-liposomes (**d**) (data not shown). The increased accumulation of ^{64}Cu-cRGD-liposomes (**f**) could possibly be explained by the high expression of $\alpha_5\beta_1$ on undifferentiated adult mesenchymal stem cells (MSC) from bone marrow and adipose tissue [Goessler, 2008].

3.6 Concluding remarks

Hybrid imaging techniques such as PET/CT are used in all phases of cancer management. Early detection and correct treatment of cancer can be a major contributor to a reduction in mortality and these techniques are able to supply complementary information for improved staging and therapy planning. Targeted therapies are developing into being an important part of modern cancer treatment and the integrins are interesting targets in this aspect.

This study aimed to visualize and quantify the uptake and biodistribution of integrin targeted liposomes opposed to non-targeted formulations *in vitro* as well as *in vivo*. *In vitro* results demonstrated the superior uptake of cRGD-liposomes in a human glioblastoma cell line (U87MG). This uptake was assigned to receptor-mediated uptake, as studies showed inhibition of the uptake, in the presence of free cRGD peptide. The presence of free scrambled cGRD had no impact on the uptake, and the unspecific uptake of control PEG-liposomes was not affected by the presence of free cRGD peptide.

Encouraged by these results the biodistribution of the liposomal formulations were tested in a xenograft mouse model bearing an integrin expressing tumor cell line (U87MG). Three different formulations of ^{64}Cu-liposomes were prepared and their

accumulation in organs and tumors evaluated. The ^{64}Cu-cRGD-liposomes showed large accumulation in spleen, liver and red bone marrow. The accumulation in spleen and liver could be attributed to their function in clearance of nanoparticles from the blood circulation. However, the extremely high accumulation - even for nanoparticles - in the spleen could also be influenced by the presence of integrins in this organ. The accumulation in the red bone marrow was unexpected, but can potentially be explained by the high expression of integrins on undifferentiated adult mesenchymal stem cells. However, the profound uptake of ^{64}Cu-cRGD-liposomes in the spleen and liver may hamper the imaging of abdominal tumors and could limit the safely administrated active dose.

The scrambled ^{64}Cu-cGRD-liposomes and control ^{64}Cu-PEG-liposomes showed very similar biodistribution indicating the targeting potential of ^{64}Cu-cRGD-liposomes. ^{64}Cu-cGRD-liposomes and ^{64}Cu-PET-liposomes demonstrated a higher accumulation in the tumors than the ^{64}Cu-cRGD-liposomes; however, when looking at their tumor-to-muscle ratios these were practically identical, despite the extensive clearance of ^{64}Cu-cRGD-liposomes in the spleen.

Future studies with targeted ^{64}Cu-liposomes could provide a great insight into the actual biodistribution of various targeted drug delivery systems and illustrate their potentials.

Chapter 4

Cationic liposomes and the PEGylation dilemma

Cationic liposomes have been applied for drug delivery as the positively charged liposomes bind to negatively charged cell membranes as a cause of electrostatic attraction and an enhanced uptake can be expected. However, cationic liposomes have been reported to bind serum proteins, which can lead to aggregation and rapid clearance from the blood circulation. In addition, unspecific binding to healthy cells is difficult to avoid under *in vivo* conditions and the positive charged particles thus leads to higher cytotoxicity. Currently, the strategy to avoid unspecific binding and fast blood clearance is to use PEG chains to sterically shield the liposomes from blood components [Torchilin, 1994]. Although the enhanced circulation time of PEGylated liposomes allows for enhanced accumulation in tumors, the influence of PEG on cell uptake and intracellular trafficking can compromise the drug efficiency [Harvie, 2000; Hyvönen, 2004].

To solve this PEG-associated issue, multiple examples are reported, where the PEG chains have been attempted removed once at target site. The dissociation of PEG from the rest of the liposomes can be accomplished by the use of breakable bonds such thiol reducible bonds [McNeeley, 2009; Ishida, 2001], esterase-catalyzed cleavable bonds [Xu, 2008], or by choosing the correct length of the lipid anchor, which in a time dependent manner would exchange out of the membrane [Wheeler, 1999]. The shedding of PEG can occur before or after cellular uptake (Figure 22).

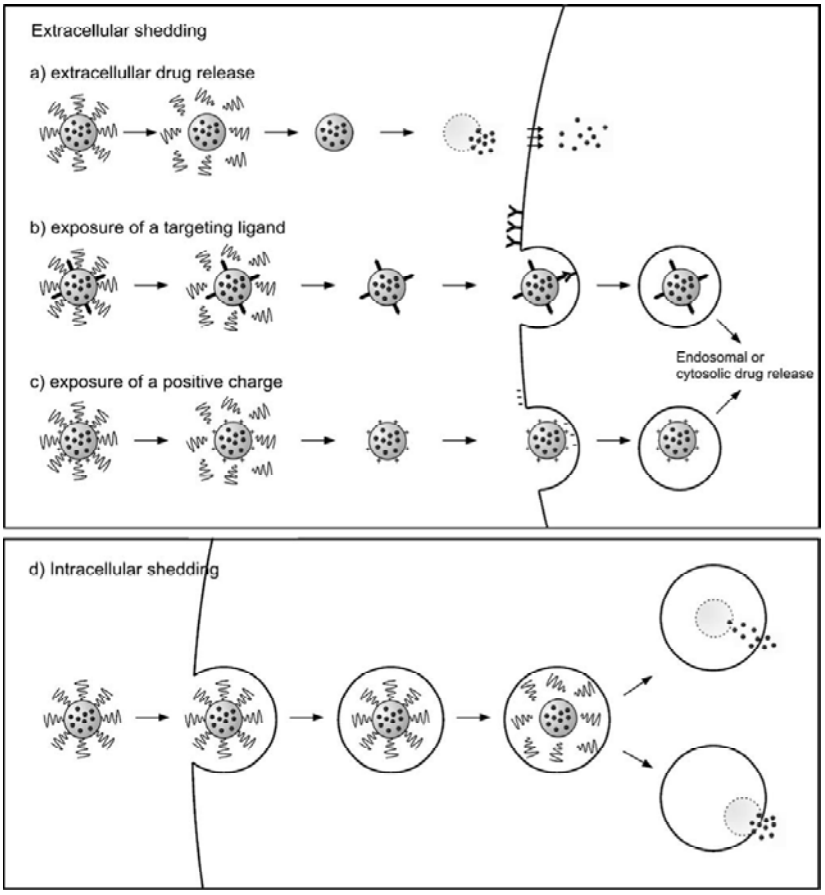

Figure 22. Schematic representation of dissociation of PEG from the liposome. Top panel shows the extracellular removal of PEG. (a) PEG is removed, drug released and taken up by the cell; (b) removal of PEG leads to exposure of a targeting moiety and receptor-mediated uptake; (c) removal of PEG leads to exposure of a hidden cationic charge. Lower panel shows the removal of PEG after internalization in the cell [Romberg, 2008].

The removal of the hydrophilic PEG coating can lead to destabilization of the liposomal membrane resulting in release of encapsulated content [Ishida, 2001; Shin, 2003], exposure of a hidden targeting ligand [McNeeley, 2009; Hatakeyama, 2009] or exposure of a positive charge leading to stronger interaction with the cell membrane [Miller, 1998].

4.1 Removal of PEG using matrix metalloproteinase enzymes

An applied method to remove PEG from the surface of liposomes once accumulated at target site has been to take advantage of the high secretion of MMPs from tumors into the extracellular space. MMP is involved in many aspects of the tumor growth and spread such as angiogenesis, invasion and metastasis by its ability to degrade extracellular matrix. MMPs are secreted as inactive zymogens (proMMPs) and they need to be activated to carry out their function. Their expression is low in normal cells [Coussens, 2002]; hence they can potentially be used for site specific removal of PEG chains.

Terada *et al.* have developed a functionalized liposomal system consisting of PEG-peptide-DOPE in combination with galactose moieties as targeting ligands. The special synthesized peptide contained a MMP-2 cleavable sequence which is degraded in proximity to the tumor cells due to their enhanced excretion of MMPs. The removal of PEG would uncover the galactose ligands on the surface of the liposomes, resulting in enhanced specific uptake in HepG2 cells [Terada, 2006]. A similar approach was used by Harakeyama *et al.* were MMP-2 cleavage of a PEG-peptide-DOPE led to removal of PEG. They observed a higher interaction with the MMP secreting cell lines (HT1080, MG-63 and HOS) and enhanced transfection efficiency within these [Harakeyama, 2007].

Inspired by the work above, a special lipo-peptide was designed for embedding into positive charged liposomal membranes. It consisted of two dipalmitoyl acyl chains connected to a cleavable peptide sequence followed by a PEG_{2000}. The peptide would be sensitive towards MMP-2 and MMP-9 enzymatic cleavage and by this process release the shielding PEG layer as well as four negatively charged amino acid residues. This results in liposomes exposing a positive surface charge due to the lipids formulated in the liposome, allowing for high interaction with the cell membrane. In addition, the PEG layer could also be removed after internalization into the endosomes, where MMP enzymes can be found; e.g. MMP-14 which function as a potent activator of proMMP-2 [Messarltou, 2009] (Figure 23).

By additional targeting of the cancer tissue by the use of a targeting moiety the intracellular MMP activation in the endosomes could be particular useful.

Whether the liposomal membrane would be destabilized by the removal of PEG and release its content outside the cells or it would be internalized in the endosome before release remains to be revealed.

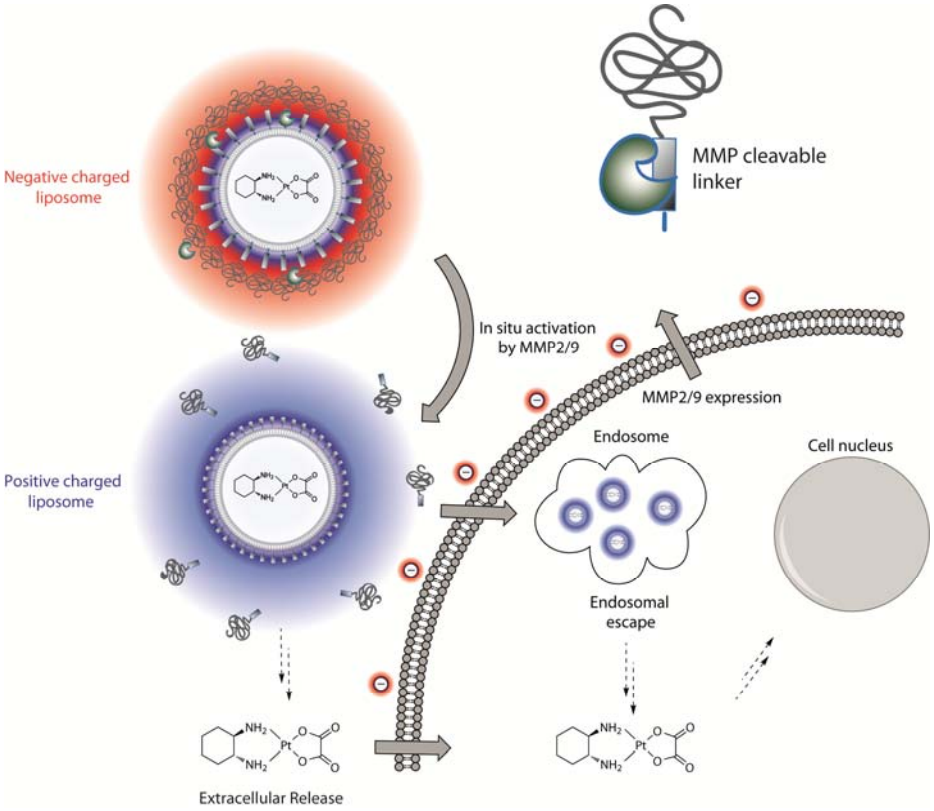

Figure 23. Negatively charged liposome exposed to secreted MMP-2 and MMP-9 in the extracellular space of tumor cells. Enzymatic cleavage removes the shielding PEG layer along with four negative charged amino acid residues. The positive charged liposome can release its content before internalization in the cell or after uptake in the endosomes, where the PEG layer can also be removed. Figure kindly provide by Jonas R. Henriksen.

4.2 Objective

The positive charged liposomes are important potential candidates in drug delivery. However, their unspecificity is a major challenge which needs to be addressed.

The goal of these studies was to elucidate, if the combination of a targeting ligand and a cleavable PEG lipo-peptide could enhance uptake and cytotoxicity of oxaliplatin loaded liposomes *in vitro*. The liposomes were formulated with the cationic lipid DOTAP that should stay hidden underneath the shielding PEG layer until the encounter with MMPs. The removal of PEG will expose the cationic charge which should facilitate interactions with cell membranes as well as the release of cytotoxic oxaliplatin. The results will be validated using flow cytometry methods and cytotoxic colorimetric assays.

The ability to both tune the release of encapsulated drug in addition to an improvement in the specific delivery in one single formulation would be a great advantage in future drug delivery systems.

4.3 Materials and methods

Full experimental is available in Appendix IV.

4.3.1 Synthesis of dipalmitoyl-metalloproteinase cleavable peptide-PEGylated

A special lipo-peptide needed to be synthesized in order to address the PEG dilemma. This peptide contained a recognition site for MMP-2 and MMP-9, flanked by two palmitoyl chains for insertion into the liposomal membrane on one side, and four glutamic acid residues connected to a PEG_{2000} chain on the other site (Figure 24).

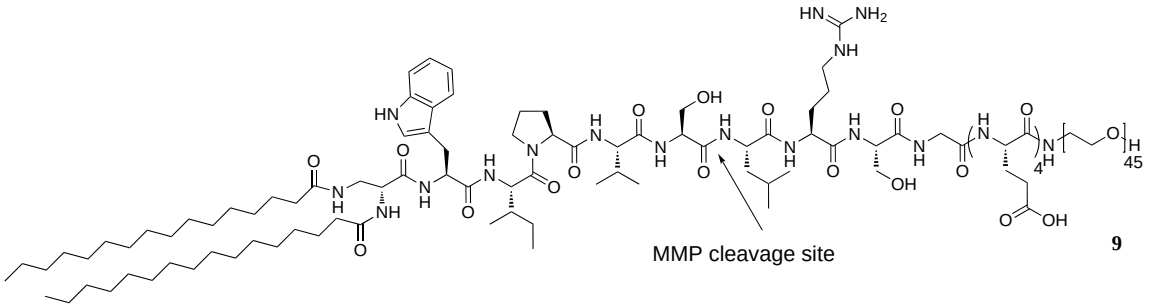

Figure 24. Chemical structure of dipalmitoyl-metalloproteinase cleavable peptide-PEGylated (DP-MCP-PEG) (**9**).

The linear peptide was synthesized using a SPPS strategy on a TentaGEL PAP_{2000} resin with standard Fmoc methodology. The coupling of each amino acid was carried out by pre-activation of the Fmoc protected amino acid with HATU in the presence of 2,4,6-collidine in DMF. Cleavage of the Fmoc group was done using piperidine in DMF and the completion of each coupling was monitored by the Kaiser test. The fully deprotected peptide dipalmitoyl-Dap-Trp-Ile-Pro-Val-Ser-Leu-Arg-Ser-Gly-Glu-Glu-Glu-Glu-PEG_{2000} was cleaved from the resin using a mixture of TFA: H_2O:TIS (95:2.5:2.5). The lipo-peptide was purified by HPLC and characterized by MALDI-TOF MS.

4.3.2 Synthesis of DSPE-PEG_{2000}-cRGD phospholipid

This phospholipid conjugate was prepared as described in section 3.4.2

4.3.3 Synthesis of DSPE-PEG_{2000}-Folate phospholipid

The commercial available DSPE-PEG_{2000}-NH_2 was functionalized with folic acid. The folic acid was pre-activated with HATU in the presence of triethylamine and product formation was followed and characterized by MALDI-TOF MS (Figure 25). The folate modified phospholipid was purified before use by HPLC.

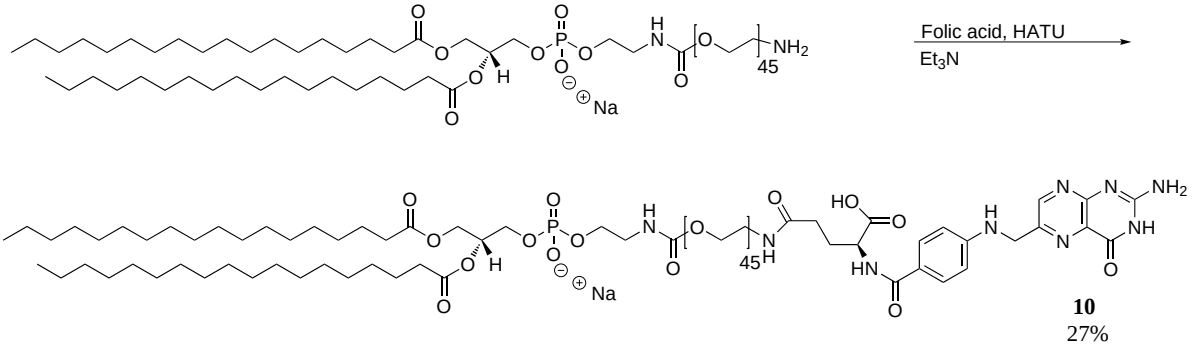

Figure 25. Coupling conditions for DSPE-PEG_{2000}-NH_2 and folic acid resulting in the γ-folate functionalized phospholipid (**10**).

4.3.4 Synthesis of DSPE-PEG_{2000}-Octaarginine phospholipid

The highly positively charged octaarginine sequence was synthesized on a TentaGEL resin using SPPS strategy and a standard Fmoc methodology. The coupling of each amino acid was carried out by pre-activation of the Fmoc protected amino acid with HATU in the presence of 2,4,6-collidine in DMF. Cleavage of the Fmoc group was done using piperidine in DMF and the completion of each coupling was monitored by the Kaiser test. The peptide hydroxylamine-$(Arg)_8$-NH_2 (**11**) was cleaved from the resin and simultaneously deprotected using a mixture of TFA:H_2O:TIS (95:2.5:2.5). The crude peptide was purified by HPLC.

DSPE-PEG_{2000} aldehyde functionalized phospholipid (**2c**) was prepared as described in section 2.3.2.

The hydroxylamine-octaarginine (**11**) and DSPE-PEG_{2000}-aldehyde (**2c**) were dissolved in a solvent mixture of methanol and water, and the conjugation reaction took place without further addition of additives (Figure 26). The octaarginine modified phospholipid was purified by HPLC.

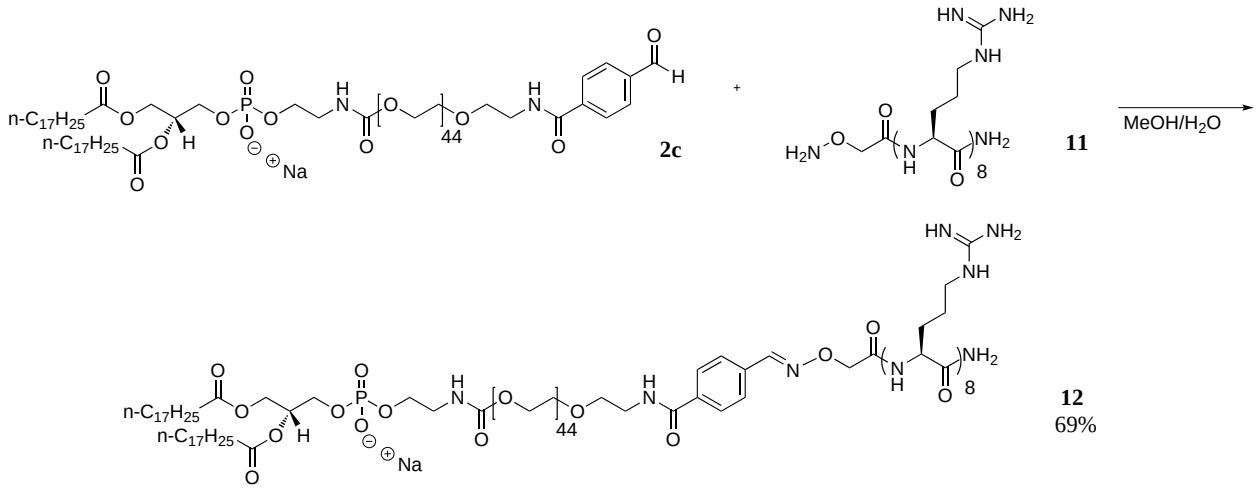

Figure 26. Coupling conditions for DSPE-PEG_{2000}-aldehyde (**2c**) and hydroxylamine-octaarginine (**11**) resulting in the octaarginine functionalized phospholipid (**12**).

4.3.5 Preparation of liposomes for uptake studies

Liposomes were in general composed of DSPC/DOPE-RhoB/cholesterol and total of 5% DSPE-PEG_{2000} lipid - either as pure DSPE-PEG_{2000} phospholipid or as a mixture with functionalized DSPE-PEG_{2000} phospholipids. The functionalized DSPE-PEG_{2000} phospholipids used were DSPE-PEG_{2000}-Octaarginine, DSPE-PEG_{2000}-cRGD and DSPE-PEG_{2000}-Folate as well as the lipo-peptide DP-MCP-PEG. DOTAP was excluded or used in an amount of 7.5%. Hence, liposomes formulated without DOTAP had the composition DSPC/DOPE-RhoB/cholesterol/DSPE-PEG_{2000} (54.5:0.5:40:5), while liposomes containing DOTAP had the composition DSPC/DOPE-RhoB/cholesterol/DSPE-PEG_{2000}/DOTAP (47:0.5:40:5:7.5). In a few studies the DSPC phospholipid was replaced with a POPC phospholipid; however the use of matrix phospholipid will be pointed out.

The phospholipids were dissolved in CH_3Cl/MeOH (9:1), the solvent removed under a stream of nitrogen and the lipid film placed under vacuum overnight to remove trace amounts of organic solvent. The obtained lipid films were hydrated in a HEPES/sucrose buffer for 1 hour at 65 °C, followed by freeze-thaw cycles and extrusion at 65 °C through 100 nm polycarbonate filters using an Avanti Polar Lipids mini-extruder. The formed liposomes were characterized by DLS and zeta potential measurements (Zeta PALS, Brookhaven Instruments).

4.3.6 Preparation of oxaliplatin loaded liposomes for cytotoxicity studies

Liposomes had identical compositions as described above only excluding the fluorescent DOPE-RhoB phospholipid.

As described above, the phospholipids were dissolved in CH_3Cl/MeOH (9:1), the solvent removed under a stream of nitrogen and the lipid film placed under vacuum overnight to remove trace amounts of organic solvent. The obtained lipid films were hydrated in a HEPES/sucrose buffer containing oxaliplatin (~15 mg/mL) for 1 hour at 70 °C, followed by extrusion at 70 °C through 100 nm polycarbonate filters using an Avanti Polar Lipids mini-extruder. To remove un-encapsulated oxaliplatin from the outside of the liposomes, they were transferred to dialysis cassettes and dialyzed 3 days, exchanging the external oxaliplatin containing buffer with a HEPES/sucrose buffer.

Encapsulation efficiency of oxaliplatin and leakiness of the liposomes were measured by ICP-AES.

4.3.7 Cell lines

HT1080, a human fibrosarcoma cell line was used in most of the experiments. This cell line has a high secretion of MMP-2 and MMP-9 enzymes [Roomi, 2009], which corresponds well with the idea of the DP-MCP-PEG peptide. Two other cell lines used were expressing receptors to cRGD and folate, respectively. The human glioblastoma cell line U87MG [Fueyo, 2003] for cRGD targeted experiments, and the human nasopharyngeal epidermal carcinoma cell line KB [Weitman, 1992] for folate targeted experiments.

4.3.8 Flow cytometry

To obtain a quantitative measure of the internalization of mono- and dual-functionalized liposomes as well as control PEG-liposomes flow cytometry was performed. Cells were incubated with RhoB-fluorescent liposomes for 2 hours (KB and HT1080 cell lines) or 5 hours (U87MG and HT1080 cell lines), washed with PBS, trypsinated and washed again before analysis by flow cytometry on a Gallios system using a blue laser (488 nm) for excitation and a filter of 575 ± 10 nm for emission. 10,000 events were collected for each sample and non-treated cells were used as reference and the gates adjusted from those.

4.3.9 Confocal microscopy

The uptake of mono-functionalized, dual-functionalized and control PEG-liposomes were visualized using confocal microscopy. Cells were grown on top of glass slides, incubated

with the RhoB-labeled liposomes for 24 hours, washed with PBS as well as PBS containing Heparin and two times with PBS again. They were fixated in 4% paraformaldehyde in PBS for 3 minutes, followed by washing with PBS. The plates were allowed to dry, before being mounted onto a microscopy slide using Vectashield® HardSet Mounting Medium. Imaging was performed with a Leica confocal microscope using an excitation wavelength of λ = 561 nm and an emission bandwidth range of 568-711 nm.

4.3.10 Cytotoxicity assay

The cytotoxicity of oxaliplatin loaded liposomes was evaluated using a colorimetric method for determining the number of viable cells. This assay uses the tetrazolium compound 3-(4,5-dimethylthiazol-2-yl)-5-(3-carboxymethoxyphenyl)-2-(4-sulfophenyl)-2H-tetrazolium salt (MTS) and phenazine methosulphate (PMS). MTS is reduced by metabolically active cells into a formazan product. The quantity of formazan product measured at 490 nm absorbance is directly proportional to the number of living cells.

Cells were seed in 96-well plates and incubated overnight, before the addition of oxaliplatin liposomes in concentrations from 0.3 μM to 50 μM oxaliplatin. After incubation for 24 hours, the liposome containing medium was replaced with fresh, and the plates incubated for another three days. Medium was replaced with MTS/PMS containing medium and the plates incubated 2 hours before the absorbance was measured using a micro plate reader (Perkin Elmer).

4.3.11 Cryogenic transmission electron microscopy

Specimens for cryoTEM were prepared on freshly glow-discharged carbon copper grids covered with formvar (300 mesh). The concentrations of phospholipids were in the range of 10 mM and 4 μl were applied to each grid surface. The grids were blotted for excess liquid and plunge-frozen in liquid ethane using a Vitrobot (FEI Company). Frozen grids were transferred to a cryoholder and visualized in a Tecnai G20 electron microscope (FEI Company) at 200 kV accelerating voltage.

4.4 Results and discussion

4.4.1 Cationic liposomes

Liposomes were formulated with octaarginine and their internalization was compared to control PEG-liposomes (Table 6) in HT1080 cells.

Table 6. Mol% composition of liposome formulations used for uptake studies in the human fibrosarcoma HT1080 cell line.

Type of liposome	POPC	DSPE-PEG	DOPE-RhoB	Cholesterol	DOTAP	DSPE-PEG-Octaarginine(**12**)
g - PEG-liposomes	47	5	0.5	40	7.5	0
h - Octaarginine-liposomes	47	4	0.5	40	7.5	1

When liposomes were formulated with 1% octaarginine functionalized DSPE-PEG_{2000} phospholipid (**h**) the zeta potential would become highly positive (Table 7).

Table 7. Size and surface charge of liposomes used for uptake studies in the human fibrosarcoma HT1080 cell line.

Type of liposome	DLS (nm)	PDI	Zeta (mV)	Std. error (mV)
g - PEG-liposomes	143.0	0.026	7.30	± 0.84
h - Octaarginine-liposomes	126.4	0.069	16.89	± 1.60

Human fibrosarcoma HT1080 were treated for 5 hours with octaarginine-liposomes (**h**) or control PEG-liposomes (**g**), before their internalization were measured by flow cytometry (Figure 27).

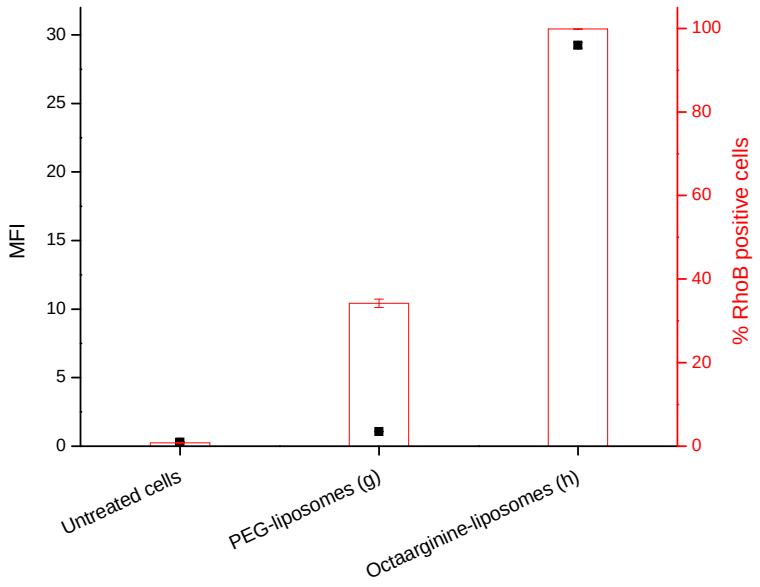

Figure 27. Uptake in HT1080 cells, reported as mean fluorescence intensity (MFI) and percentage of cells with internalized RhoB-labeled liposomes relative to the total amount of cells measured. All values are means ± SEM (n = 2).

The liposomes functionalized with octaarginine (**h**) showed increased uptake compared to control PEG-liposomes (**g**). It could be seen from the high MFI value that numerous cells had taken up a large amount of liposomes. To validate if this high internalization had any enhanced cytotoxic effect, liposomes containing oxaliplatin were made.

Oxaliplatin is a platinum-based anticancer drug approved for colorectal cancer treatment. The precise mechanism by which oxaliplatin kills cancer cells are not clear, but broadly speaking the platinum-based drugs reacts with DNA bases and disrupt essential processes such as DNA replication and transcription, leading to apoptosis [Di Francesco, 2002]. In order for oxaliplatin to reach the DNA it has to escape the liposome. To investigate if this escape was possible with the described liposomes formulations, cells were incubated with oxaliplatin containing liposomes (Figure 28).

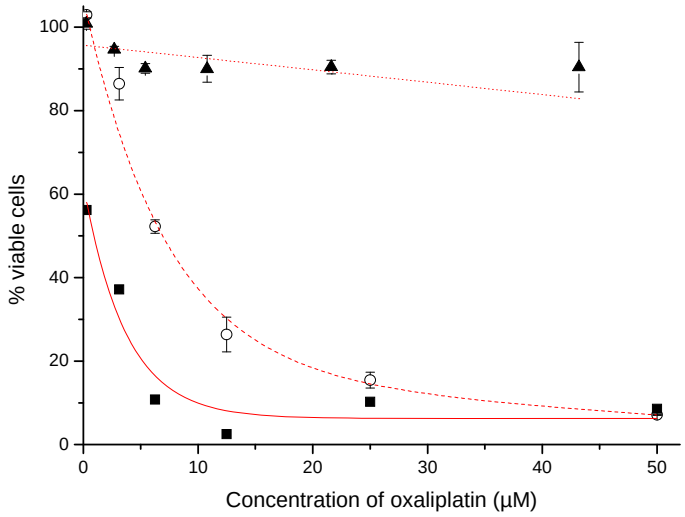

Figure 28. HT1080 cells treated with oxaliplatin loaded liposomes as well as free oxaliplatin. ▲ PEG-liposomes; ■ Octaarginine-liposomes; ○ free oxaliplatin. The liposome formulations were as described in Table 6 only substituting DOPE-RhoB with POPC. All values are means ± SEM (n = 2).

Control PEG-liposomes showed very low cytotoxic effect on the HT1080 cells, while octaarginine-liposomes were more toxic than free oxaliplatin. The enhanced internalization of octaarginine liposomes compared to control PEG-liposomes is likely to be caused by the high interaction between the negatively charged cell surface and the positive charged liposomes [Zabner, 1995]. The enhanced cytotoxic effect seen for only octaarginine-liposomes could be due to the ability of the cationic liposomes to fuse with the anionic endosomal/lysosomal membranes and release the encapsulated oxaliplatin into the cytoplasm [Dominska, 2010]. If the liposomes stay too long in the

endosomes/lysosomes the risk is that they and their encapsulated content will be degraded of the harsh environment existing in these vesicles. Another explanation to the difference observed in cytotoxicity between the two formulations could be a higher exocytosis degree of the PEG-control liposomes compared to octaarginine-liposomes. However, initial studies have shown that longer incubation times leads to higher internalization of the liposomes. Indicating that no significant exocytosis of the liposomes are taken place within a 24 hour timeframe (data not shown).

It could seem like the octaarginine-liposomes would serve as great drug delivery agents, however an *in vivo* use of these particles would be completely unacceptable as they would not interact specifically with cancerous cells, but with all cell membranes, likely to result in large side effects.

If the charge could be shielded beneath a PEG layer and a targeting moiety could direct the way to diseased cells, this could provide an opportunity of creating an effective and specific drug delivery system. Promising uptake results from cRGD-liposomes were illustrated in Chapter Three; hence the efficiency of this targeting moiety was tested with and without positive surface charge *in vitro* (Table 8).

Table 8. Mol% composition of liposome formulations used for uptake studies in the human fibrosarcoma HT1080 cell line and human glioblastoma U87MG cell line.

Type of liposome	DSPC	DSPE-PEG	DOPE-RhoB	Cholesterol	DOTAP	DSPE-PEG-cRGD(**7**)
i - cRGD-liposomes	54.5	4	0.5	40	0	0.5
j - cRGD/ DOTAP-liposomes	47	4	0.5	40	7.5	0.5

cRGD-liposomes were formulated with or without the presence of the cationic phospholipid DOTAP (Table 8) and characterized (Table 9).

Table 9. Size and surface charge of liposomes used for uptake studies in the human fibrosarcoma HT1080 cell line and human glioblastoma U87MG cell line.

Type of liposome	DLS (nm)	PDI	Zeta (mV)	Std. error (mV)
i - cRGD-liposomes	176.8	0.122	- 12.57	± 1.44
j - cRGD / DOTAP-liposomes	174.7	0.119	4.89	± 1.30

The internalization of these formulations was tested in two different cell lines HT1080 and U87MG (Figure 29).

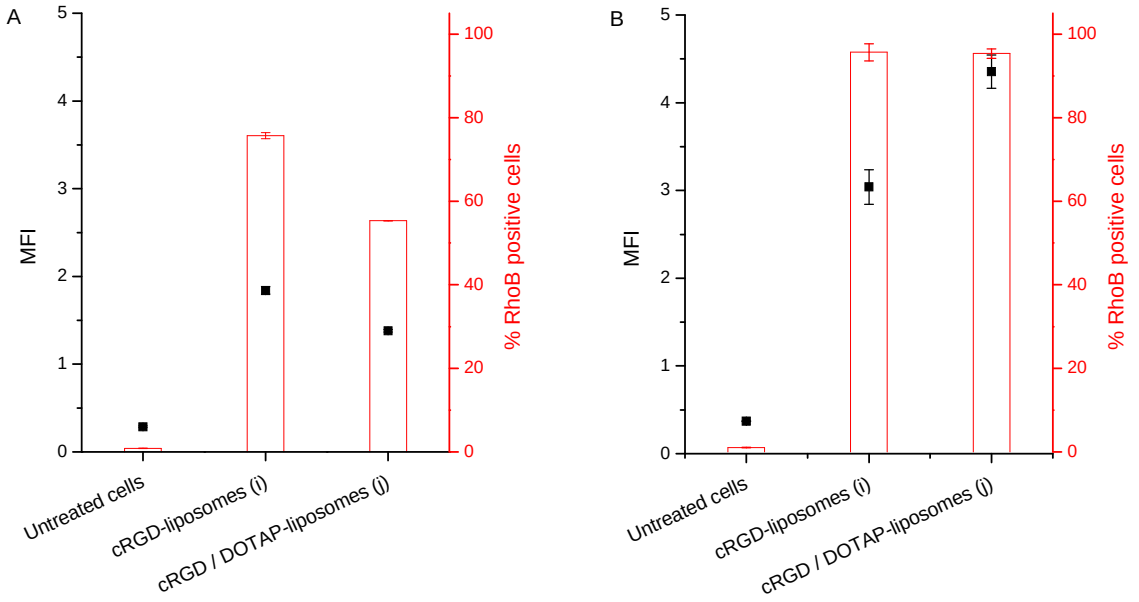

Figure 29. Uptake in HT1080 cells (A) and U87MG cells (B) reported as mean fluorescence intensity (MFI) and percentage of cells with internalized RhoB-labeled liposomes relative to the total amount of cells measured. All values are means ± SEM (n = 2).

Since both cell lines express integrin receptors [Conforti, 1994; Fueyo, 2003] the receptor-mediated internalization is not widely affected by the presence of DOTAP. They both (**i** and **j**) show a high degree of uptake compared to control PEG-liposomes (**g**) (Figure 27), however the uptake in either of the two cell lines do not compare to the high uptake of octaarginine liposomes, when examining the MFI values (Figure 27). This is expected, as the surface charge of octaarginine-liposomes (**h**) is significant more positive than for cRGD-liposomes (**i**, **j**). Eventhough the surface charge of PEG-liposomes (**g**) is slightly more positive, than for cRGD-liposomes with DOTAP (**j**) (Table 7 and Table 9), the uptake is still higher for the latter. This indicates that receptor-mediated uptake is playing a role as well, and not sole surface-surface charge interactions are responsible for the uptake.

The cytotoxic effect of oxaliplatin liposomes - targeted, and with and without the presence of DOTAP - was evaluated (Figure 30).

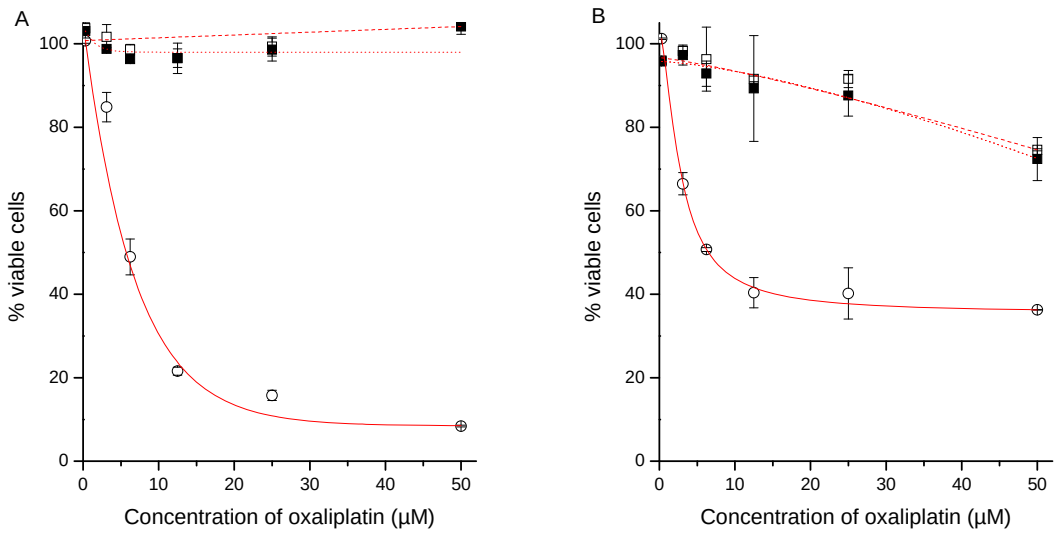

Figure 30. HT1080 (A) and U87MG (B) cells treated with oxaliplatin loaded liposomes as well as free oxaliplatin. □ cRGD-liposomes; ■ cRGD/DOTAP-liposomes; ○ free oxaliplatin. The liposome formulations were as described in Table 8 only substituting DOPE-RhoB with DSPC. All values are means ± SEM (n = 2).

None of the two targeted formulations showed any cytotoxic effect. This confirms that the positive charge coming from DOTAP has limited influence on the fate of the liposomes. The positive charge on the liposomes is not large enough to interact with the endosomal/lysosomal membranes and they do not escape or release their content before degradation, hence the toxic effect of oxaliplatin is lacking. Receptor-mediated uptake seem to be the major cause for increased uptake and not surface charge interactions, as also concluded from Figure 29. From the curve ascribed to free oxaliplatin is can be seen that the HT1080 cells are more sensitive to oxaliplatin than U87MG. For the HT1080 cells ~10 % are alive after treatment with 50 µM oxaliplatin, while for the U87MG cells this number is ~40%.

The positive charge from DOTAP is situated directly on the surface of the liposome likely to be fully covered by the surrounding PEG layer, while the charge coming from the octaarginine peptide is extending beyond the PEG layer of the liposome, being free to interact with the cell membranes. The DP-MCP-PEG peptide was designed to overcome this limitation by removing the PEG layer and allowing for more direct interaction between DOTAP and the cell membranes.

4.4.2 cRGD and DP-MCP-PEG functionalized liposomes

As the DP-MCP-PEG contains four negatively charged residues (glutamic acid) exposed just beneath the PEG layer these should preferably keep the liposomes negatively charged while in circulation, despite the presence of DOTAP. When the PEG layer along with the four negative charges are removed by the MMPs, the DOTAP charge is exposed, being able to interact strongly with the cell membrane. The combination with the targeting cRGD peptide should give the liposomes a possibility to undergo receptor-mediated endocytosis once accumulated in the ECM by the EPR effect.

The zinc-dependent endopeptidase thermolysin was selected as a convenient model enzyme for the MMP enzymes, since their catalytic domains as well as their substrate selectivity are similar [Pelmenschikov, 2002]. The MMP enzymes have a tendency to undergo self-hydrolysis which can be problematic, when performing an experimental setup [Sakar, 2008].

Liposomes were formulated with the targeting peptide cRGD and DP-MCP-PEG with and without the presence of DOTAP (Table 10). Their size (Table 11) and zeta potential (Table 12) were characterized.

Table 10. Mol% composition of liposome formulations used for uptake studies in the human fibrosarcoma HT1080 cell line and human glioblastoma U87MG cell line as well as for MALDI-TOF MS analysis.

Type of liposome	DSPC	DSPE-PEG	DOPE-RhoB	Cholesterol	DOTAP	DSPE-PEG-cRGD(**7**)	DP-MCP-PEG(**9**)
k - DP-MCP-PEG-lipo.	54.5	0.5	0.5	40	0	0	4.5
l - DP-MCP-PEG / DOTAP-lipo.	47	0.5	0.5	40	7.5	0	4.5
m - cRGD / DP-MCP-PEG-lipo.	54.5	0	0.5	40	0	0.5	4.5
n - cRGD / DP-MCP-PEG / DOTAP-lipo.	47	0	0.5	40	7.5	0.5	4.5

Table 11. Size of liposomes used for uptake studies in the human fibrosarcoma HT1080 cell line and glioblastoma U87MG cell line.

Type of liposome	Without DOTAP		With DOTAP	
	DLS (nm)	PDI	DLS (nm)	PDI
cRGD / DP-MCP-PEG-liposome (**m**, **n**)	179.9	0.037	177.2	0.146
DP-MCP-PEG-liposome (**k**, **l**)	140.2	0.109	167.0	0.080

Table 12. Surface charge of liposomes used for uptake studies in the human fibrosarcoma HT1080 cell line and glioblastoma U87MG cell line.

Type of liposome	Without DOTAP		With DOTAP	
	Zeta (mV)	Std. error (mV)	Zeta (mV)	Std. error (mV)
cRGD / DP-MCP-PEG- liposome (**m**, **n**)	- 9.98	± 1.15	- 8.28	± 1.54
DP-MCP-PEG-liposome (**k**, **l**)	- 23.42	± 2.42	- 7.51	± 1.03

The surface charge of the liposomes changed, when DOTAP was incorporated in the formulation. Especially, the mono-functionalized DP-MCP-PEG-liposomes (**k** versus **l**) had a large change, while the dual-functionalized were more moderate (**m** versus **n**). However, they did not show positive charges as observed for the cRGD-liposomes (**j**) (Table 9) due to shielding of the positive DOTAP by the negative charges carried by DP-MCP-PEG.

As a proof-of-concept, liposomes containing DP-MCP-PEG and DOTAP were incubated in the presence of thermolysin (Table 13 and Figure 31). The negative surface charge of the DP-MCP-PEG/DOTAP liposomes (**l**) changed to positive, when exposed to thermolysin.

Table 13. Surface charge of liposomes incubated with or without thermolysin.

Type of liposome	Without thermolysin		With thermolysin	
	Zeta (mV)	Std. error (mV)	Zeta (mV)	Std. error (mV)
l - DP-MCP-PEG / DOTAP-liposomes	- 8.85	± 1.17	2.86	± 0.968

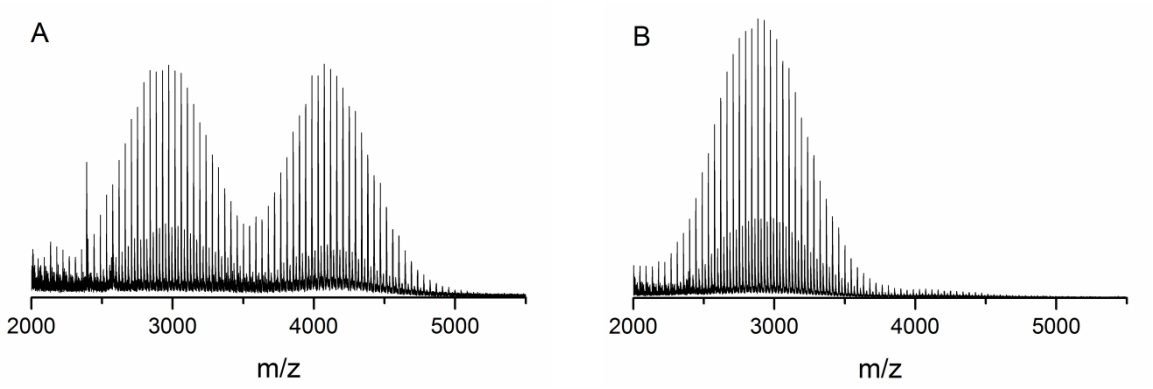

Figure 31. MALDI-TOF MS showing the DP-MCP-PEG liposomes (**l**) after exposure to thermolysin. (A) not fully cleaved DP-MCP-PEG; (B) fully cleaved DP-MCP-PEG.

MALDI-TOF MS analysis confirmed that the DP-MCP-PEG peptide was cleaved by thermolysin.

In order to evaluate if the presence of the MMP cleavable lipo-peptide would change the uptake pattern of the liposomes, their uptake was investigated in the MMP secreting cell line HT1080, as well as the integrin presenting cell U87MG (Figure 32).

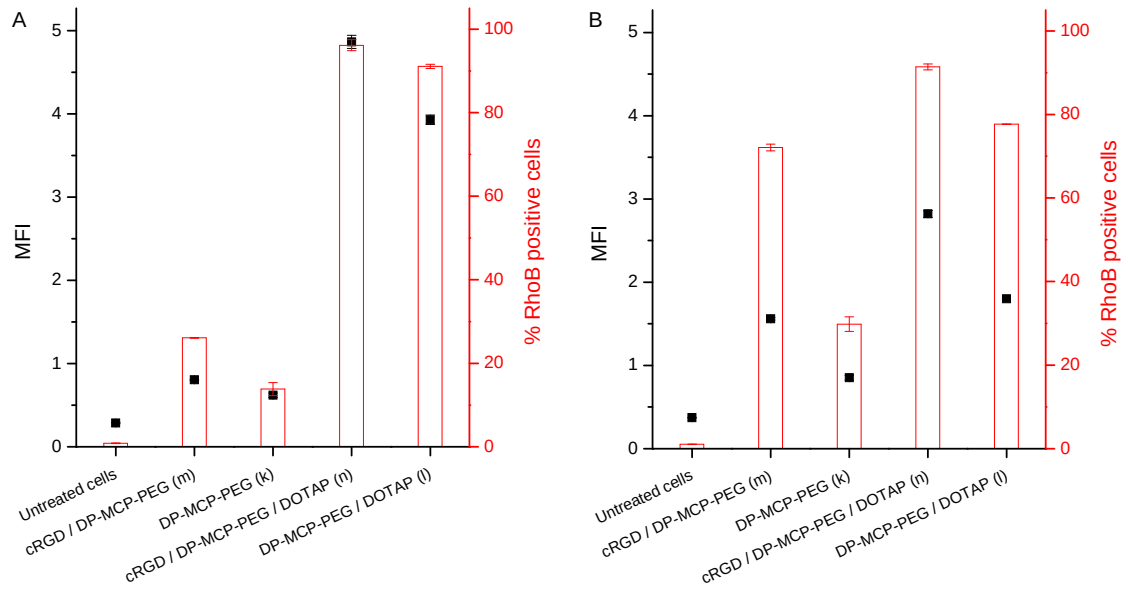

Figure 32. Uptake in HT1080 cells (A) and U87MG cells (B) reported as mean fluorescence intensity (MFI) and percentage of cells with internalized RhoB-labeled liposomes relative to the total amount of cells measured. All values are means ± SEM (n = 2).

For the internalization in the HT1080 cell line the DOTAP containing liposomes (**l**, **n**) were superior (Figure 32 A). The combination of the targeting cRGD moiety and the MMP cleavable DP-MCP-PEG part (**n**) showed enhance uptake over the both the mono-functionalized cRGD/DOTAP-liposomes (**j**) (Figure 29) and the DP-MCP-PEG/DOTAP-liposomes (**l**) (Figure 32). More or less the same picture is seen in the uptake pattern for the U87MG cell line (Figure 32 B). However, in this cell line the cRGD-targeting has a higher effect on the uptake. The uptake of dual-functionalized cRGD/DP-MCP-PEG-liposomes (**m**) is comparable with mono-functionalized DP-MCP-PEG/DOTAP-liposomes (**l**).

The quantitative flow cytometry measurements were supported by confocal imaging using the human glioblastoma cell line U87MG (Figure 33).

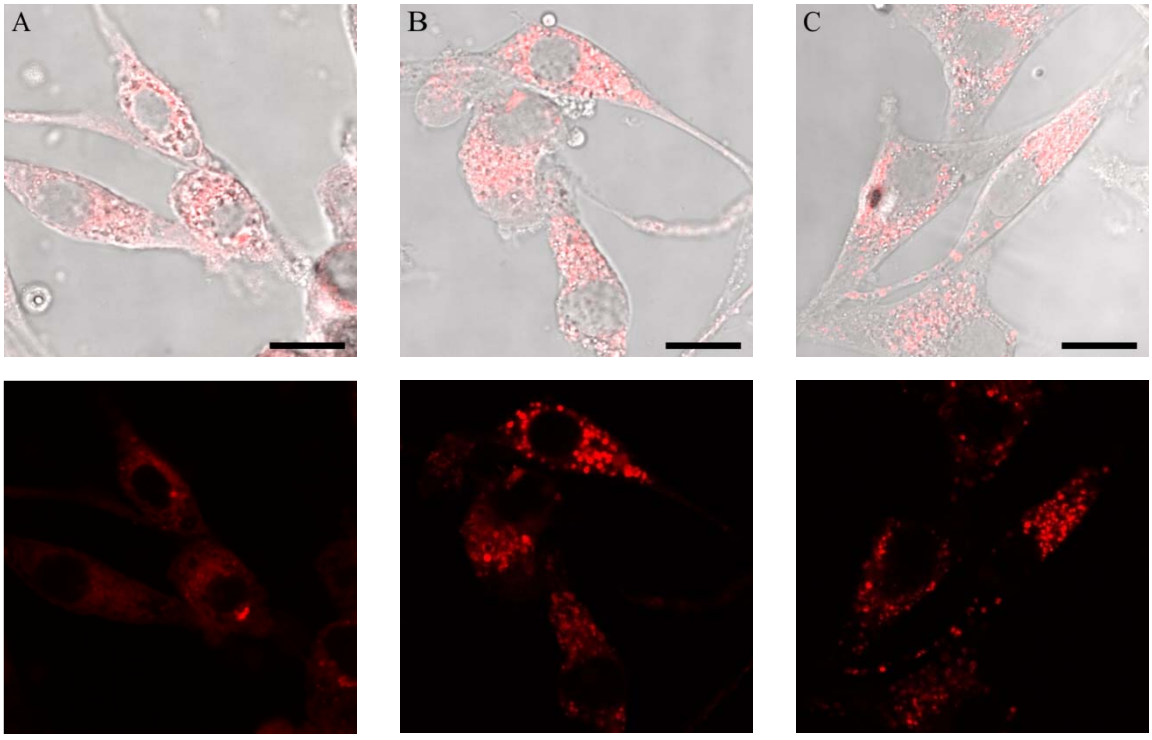

Figure 33. Representative confocal microscope images showing U87MG cells with internalized RhoB-liposomes. (A) cRGD/DOTAP-liposomes (**j**). (B) cRGD/DP-MCP-PEG/DOTAP-liposomes (**n**). (C) DP-MCP-PEG/DOTAP-liposomes (**l**). Scale bar 15 μm.

From the confocal images it is difficult to distinguish any real difference in the internalization of fluorescent liposomes between the three formulations (Figure 33). However, the images proved that internalization was indeed occurring and indicated that different uptake mechanisms could be taking place. For the mono-functionalized cRGD/DOTAP-liposomes (**j**) it seemed like most of the cytoplasma was fluorescent,

while for the mono-functionalized DP-MCP-PEG/DOTAP-liposomes (**l**) the fluorescence showed up in spots. However, due to time constrains this was not investigated further.

To decide which strategy - dual-functionalization or mono-functionalization combined with a positive charge - would give a greater therapeutic efficacy the uptake pattern was compared to the cytotoxic profile of the liposomes containing encapsulated oxaliplatin (Figure 34).

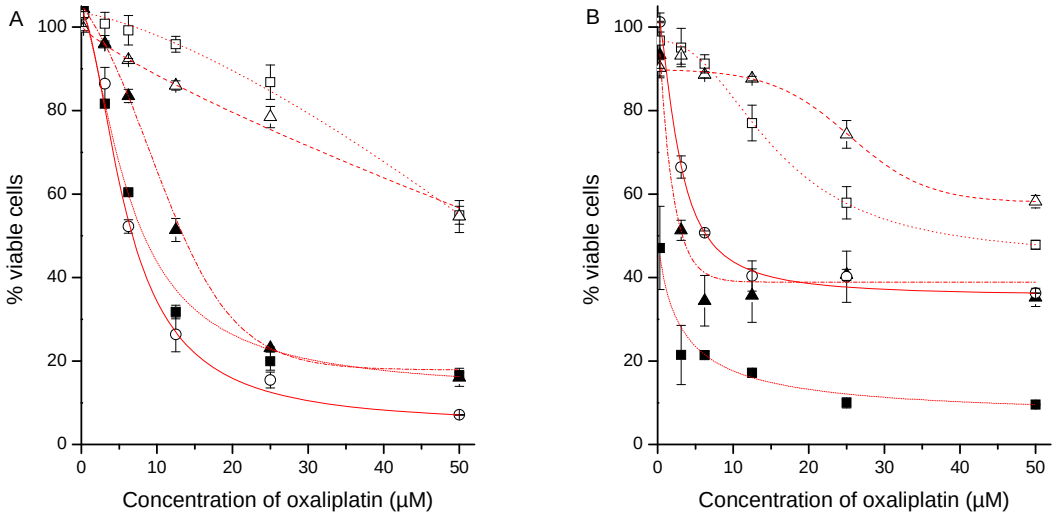

Figure 34. HT1080 (A) and U87MG (B) cells treated with oxaliplatin loaded liposomes as well as free oxaliplatin. □ cRGD/DP-MCP-PEG-liposomes; Δ DP-MCP-PEG-liposomes; ▲ cRGD/DP-MCP-PEG/DOTAP-liposomes; ■ DP-MCP-PEG/DOTAP-liposomes; ○ free oxaliplatin. The liposome formulations were as described in Table 10 only substituting DOPE-RhoB with DSPC. All values are means ± SEM (n = 2).

In both cell lines; HT1080 (Figure 34 A) and U87MG (Figure 34 B), the dual-functionalized DOTAP liposomes (**n**) turned out to be the most toxic ones. A minor cytotoxic effect was seen at the highest concentrations for liposomes without DOTAP (**k**, **m**) compared to the cRGD-liposomes (**i**, **j**) (Figure 30). Free oxaliplatin and the two DOTAP containing liposomes (**l**, **n**) showed similar cytotoxic profiles in the HT1080 cell line (Figure 34 A). In the U87MG cell line an increased cytotoxic effect was seen from the DOTAP containing liposomes (**l**, **n**), with the mono-functionalized DP-MCP-PEG/DOTAP-liposomes (**l**) showing the highest cytotoxicity, while the dual-functionalized cRGD/DP-MCP-PEG/DOTAP-liposomes (**n**) would lie in the range of free oxaliplatin (Figure 34 B).

From the cytotoxic effect on especially the U87MG cells, it can be concluded that a high uptake not necessarily leads to a high toxicity. In Figure 32 B the dual-

functionalized-cRGD/DP-MCP-PEG-liposomes (**m**) and mono-functionalized DP-MCP-PEG/DOTAP-liposomes (**l**) showed almost identical uptake, but only the DOTAP formulation showed significant cytotoxicity. This emphasizes the importance of the liposomes to be able to escape the endosomes/lysosomes in order to release their content and provide a cytotoxic response [Dominska, 2010].

From these cytotoxic profiles it did not seem like the extracellular secretory MMP enzymes from HT1080 had a large effect on the cytotoxicity pattern. This is likely to be caused by the relative short incubation time, where the HT1080 have a chance to secrete the MMP enzymes. The situation would possibly look different in an *in vivo* situation, due to the difference in MMP enzyme concentration. Typically 5 x 10^4 cells were cultured in 1 mL of medium; comparing this to an *in vivo* situation where 1 g of tissue consist of 1 x 10^9 cells surrounded by approximately 200 µl of extracellular space, the MMP enzymes would be largely diluted in the *in vitro* situation [Tsuji, 1983].

The outcome of dual-functionalization together with a hidden cationic charge had proved to be rather effective and to examine, if this effect was a general trend, a different targeting ligand was investigated.

4.4.3 Folate and DP-MCP-PEG functionalized liposomes

The folate receptor has been found overexpressed in a variety of cancers such as cervical, ovarian, breast and colorectal carcinomas [Mathias, 1998], while being limited in most normal tissues [Weitman, 1992]. The high affinity of folic acid for folate receptors provides a unique opportunity to use folic acid as a targeting ligand on the surface of liposomes to delivery therapeutic agents to cancer cells.

To validate the expression of folate receptors on the human nasopharyngeal epidermal carcinoma cell line KB an inhibition study was carried out (Table 14 and Figure 35).

Table 14. Mol% composition of liposome formulations used for uptake studies in the human fibrosarcoma HT1080 cell line and human nasopharyngeal epidermal carcinoma KB cell line.

Type of liposome	DSPC	DSPE -PEG	DOPE -RhoB	Cholesterol	DOTAP	DSPE-PEG-Folate(**10**)	DP-MCP-PEG(**9**)
o - Folate-lipo.	47	4.5	0.5	40	7.5	0.5	0
p - Folate / DP-MCP-PEG-liposome	47	0	0.5	40	7.5	0.5	4.5
q - DP-MCP-PEG-liposome	47	0.5	0.5	40	7.5	0	4.5
r - PEG-liposome	47	5	0.5	40	7.5	0	0

All formulations used contained DOTAP.

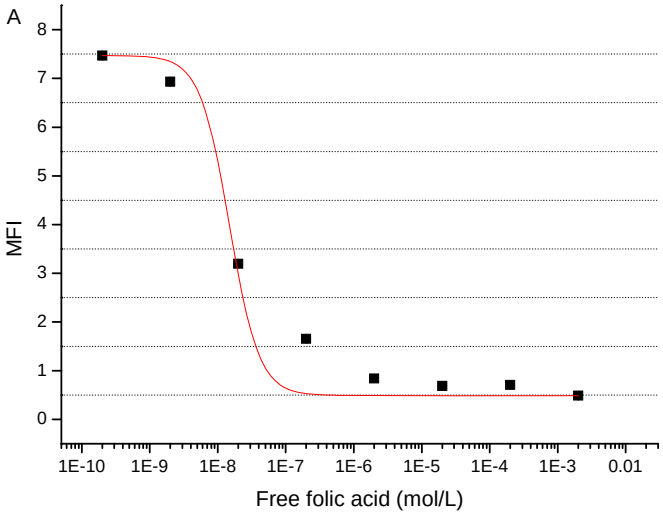

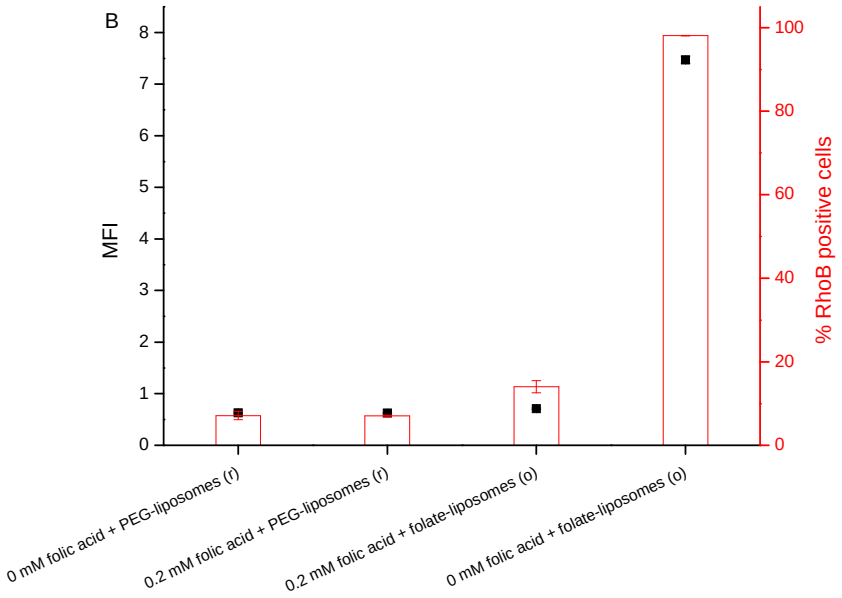

Figure 35. Inhibition of liposomal uptake using free folic acid. (A) Incubation with increasing concentrations of free folic acid leads to a decrease in the uptake of folate-liposomes (**o**). (B) Incubation with free folic acid followed by addition of control PEG-liposomes (**r**) or folate-liposomes (**o**). All values are means ± SEM (n = 2).

Increasing amounts of free folic acid inhibited the uptake of folate-liposomes (**o**) (Figure 35 A), indicating the presence of folate receptors. In order to test that the free folic acid would not inhibit all uptake, the KB cells were treated with free folic acid followed by addition of control PEG-liposomes (**r**). The uptake of control PEG-liposomes (**r**) were unaffected by the presence of free folic acid. As a comparison, data are shown for KB cells with or without treatment with free folic acid followed by addition of folate-liposomes (**o**) (Figure 35 B).

The HT1080 cell line are known as folate receptor negative [Moon, 2003]; however they were used along with the KB cell line in order to validate, if their MMP secretion would have an impact on the fate of the liposomes (Figure 36).

Table 15. Size and surface charge of liposomes used for uptake studies in the human fibrosarcoma HT1080 cell line and human nasopharyngeal epidermal carcinoma KB cell line.

Type of liposome	DLS (nm)	PDI	Zeta (mV)	Std. error (mV)
o - folate-liposomes	95.0	0.199	- 6.26	± 1.05
p - folate / DP-MCP-PEG-liposomes	93.0	0.005	- 10.91	± 0.82
q - DP-MCP-PEG-liposomes	97.0	0.005	- 11.26	± 0.94

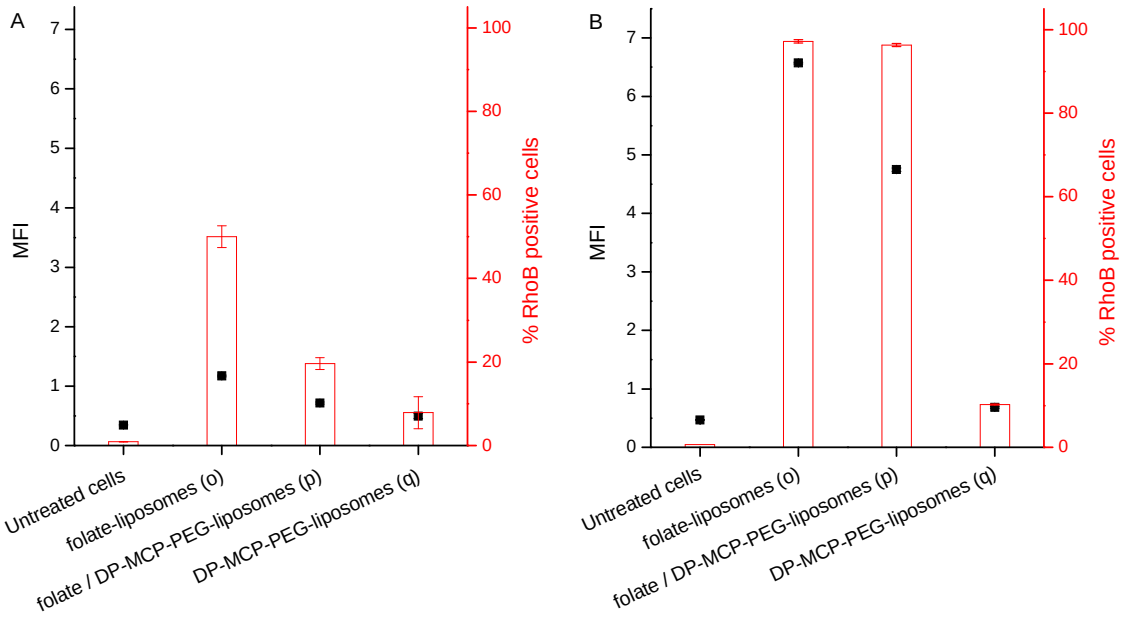

Figure 36. Uptake in HT1080 cells (A) and KB cells (B) reported as mean fluorescence intensity (MFI) and percentage of cells with internalized RhoB-labeled liposomes relative to the total amount of cells measured. All values are means ± SEM (n = 2).

Even though the HT1080 cell line should be folate receptor negative [Moon, 2003], the highest uptake in this cell line was the folate-functionalized liposomes. However, the internalization was not very high as can be seen from the low MFI values for all the liposome formulations (Figure 36 A). For the folate expressing cell line KB both liposome formulations containing folate (**o**, **p**) gave rise to roughly 100 percent positive cells within the 2 hours incubation time. Nevertheless, the mono-functionalized folate-liposomes (**o**) had the highest internalization degree seen from the MFI point of view.

This internalization degree was confirmed by confocal microscopy using the human nasopharyngeal epidermal carcinoma KB cell line (Figure 37).

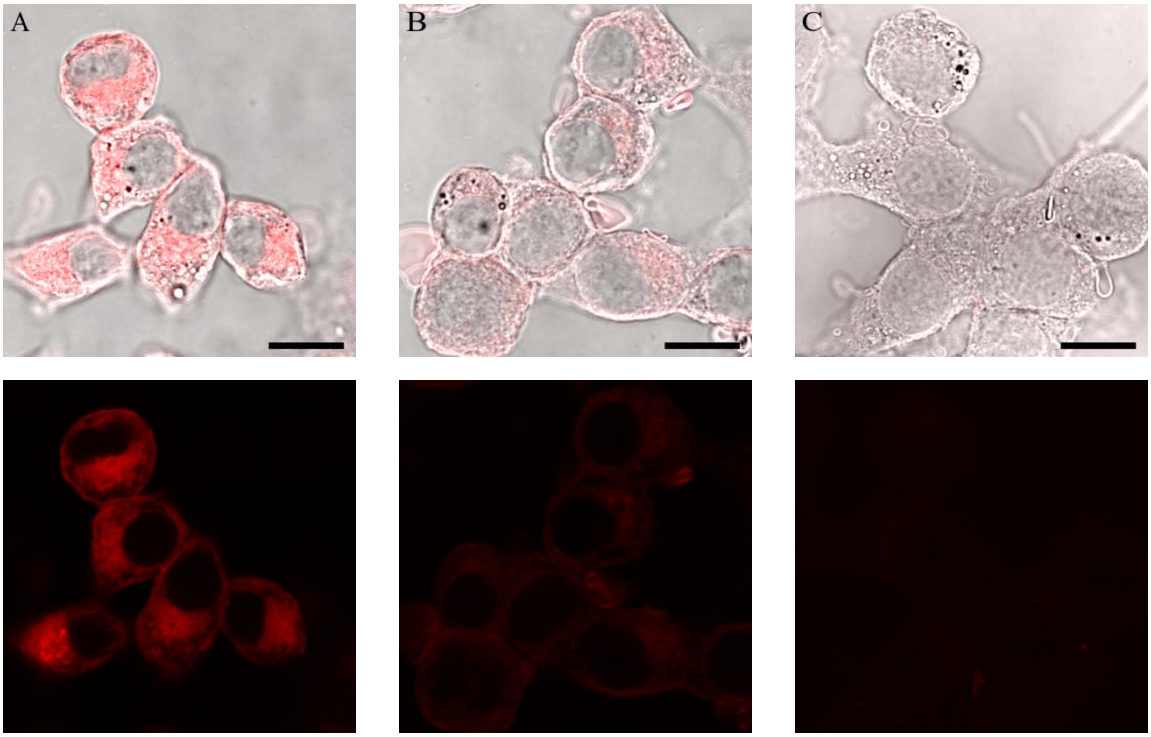

Figure 37. Representative confocal microscope images showing KB cells with internalized RhoB-liposomes. (A) folate-liposomes (**o**). (B) folate/DP-MCP-PEG-liposomes (**p**). (C) DP-MCP-PEG-liposomes (**q**). Scale bar 15 µm.

The confocal images clearly show higher amount of fluorophore internalized in the mono-functionalized folate-liposomes (**o**) compared to both dual-functionalized folate/DP-MCP-PEG-liposomes (**p**) and mono-functionalized DP-MCP-PEG-liposomes (**q**); as indicated by the MFI values (Figure 36 B). For the mono-functionalized folate-liposomes (**o**) the fluorescence seemed to be located in all cytoplasm as visualized in the case of mono-functionalized cRGD-liposomes (**j**) too (Figure 33 A).

To validate if the different degrees of internalization would affect the cytotoxicity of the liposomes, identical formulated oxaliplatin liposomes were made and their cytotoxic potential was evaluated (Figure 38).

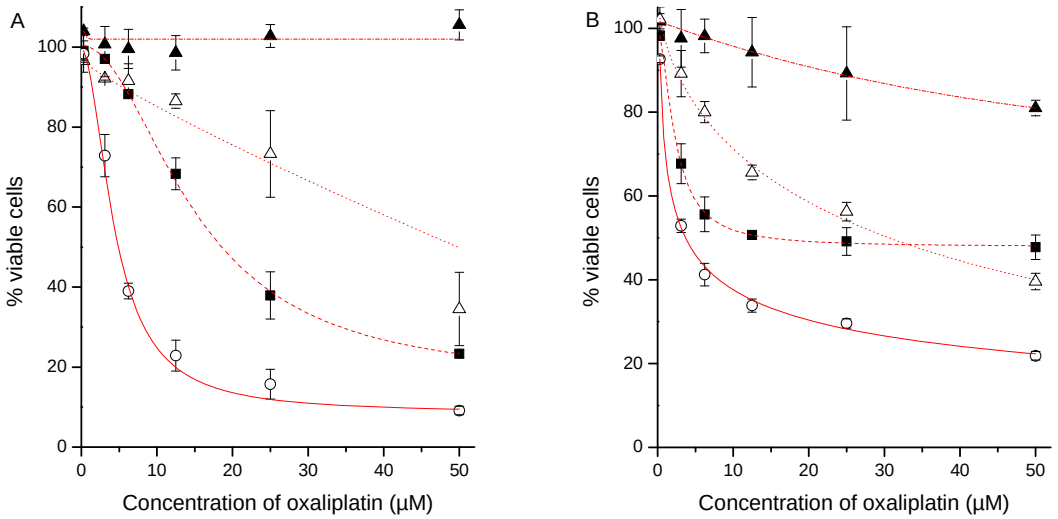

Figure 38. HT1080 (A) and KB (B) cells treated with oxaliplatin loaded liposomes as well as free oxaliplatin. ▲ folate-liposomes; Δ DP-MCP-PEG-liposomes; ■ folate/DP-MCP-PEG-liposomes; ○ free oxaliplatin. The liposome formulations were as described in Table 14 only substituting DOPE-RhoB with DSPC. All values are means ± SEM (n = 2).

Again it is interesting to notice that the high uptake of liposomes not necessary leads to a high cytotoxicity. For the mono-functionalized DP-MCP-PEG-liposomes that hardly had any uptake in either of the two cell lines tested, a minor cytotoxic effect can be seen, while for the mono-functionalized folate-liposomes that showed a major uptake no cytotoxicity is observed. The combination of the targeting folate ligand and the cleavable lipo-peptide demonstrated the highest cytotoxic effect on both cell lines of the liposomes tested (Figure 38), demonstrating that escape from the endosomes/lysosomes is a vital process in order to obtain any effect of the encapsulated drug.

4.4.4 Saturated and unsaturated phospholipids

The matrix phospholipid mainly used in these experiments was the saturated DSPC. It was demonstrated by Senior and Gregoriadis [Senior, 1982] that liposomes composed of phosphatidylcholine (PC) with saturated fatty acyl chains - as DSPC - were more stable in blood than liposomes composed of PC with unsaturated fatty acyl chains - as POPC. In addition the saturated DSPC liposomes were less permeable than their unsaturated counterparts and retain their drug load more efficient. Nevertheless, they have also shown to be rapid cleared from the bloodstream, as their inflexible membranes can result in packing defects [Kirby, 1980]. The incorporation of cholesterol was found to be the

solution to this problem, as cholesterol increases the fluidity of the membrane as well as the packing of phospholipid molecules [Demel, 1976].

Hence, for all encapsulation experiments the saturated DSPC system was utilized. However, unsaturated POPC formulations (Table 16) were characterized (Table 17) and tested as well, showing comparable encapsulation efficiency of oxaliplatin as DSPC (data not shown).

Table 16. Mol% composition of liposome formulations used for uptake studies in the human glioblastoma U87MG cell line and human nasopharyngeal epidermal carcinoma KB cell line.

Type of liposome	POPC	DSPE -PEG	cholesterol	DOTAP	DSPE-PEG -cRGD(**7**)	DSPE-PEG -Folate(**10**)	DP-MCP -PEG(**9**)
s - cRGD-liposome	47.5	4.5	40	7.5	0.5	0	0
t - cRGD / DP-MCP-PEG-liposome	47.5	0	40	7.5	0.5	0	4.5
u - DP-MCP-PEG-liposome	47.5	0.5	40	7.5	0	0	4.5
v - folate-liposome	47.5	4.5	40	7.5	0	0.5	0
w - folate / DP-MCP-PEG-liposome	47.5	0	40	7.5	0	0.5	4.5

Table 17. Size and surface charge of oxaliplatin containing liposomes used for uptake studies in the human glioblastoma U87MG cell line and human nasopharyngeal epidermal carcinoma KB cell line. The matrix phospholipid was POPC.

Type of liposome	DLS (nm)	PDI	Zeta (mV)	Std. error (mV)
s - cRGD-liposomes	135.5	0.005	9.31	± 1.67
t - cRGD / DP-MCP-PEG-liposomes	156.2	0.191	1.28	± 1.52
u - DP-MCP-PEG-liposomes	161.3	0.144	0.49	± 1.71
v - folate-liposomes	135.4	0.015	11.75	± 1.49
w - folate / DP-MCP-PEG-liposomes	168.7	0.161	0.10	± 1.49

When performing cytotoxicity experiments with the POPC matrix phospholipid systems similar cytotoxic profiles were obtained (Figure 39).

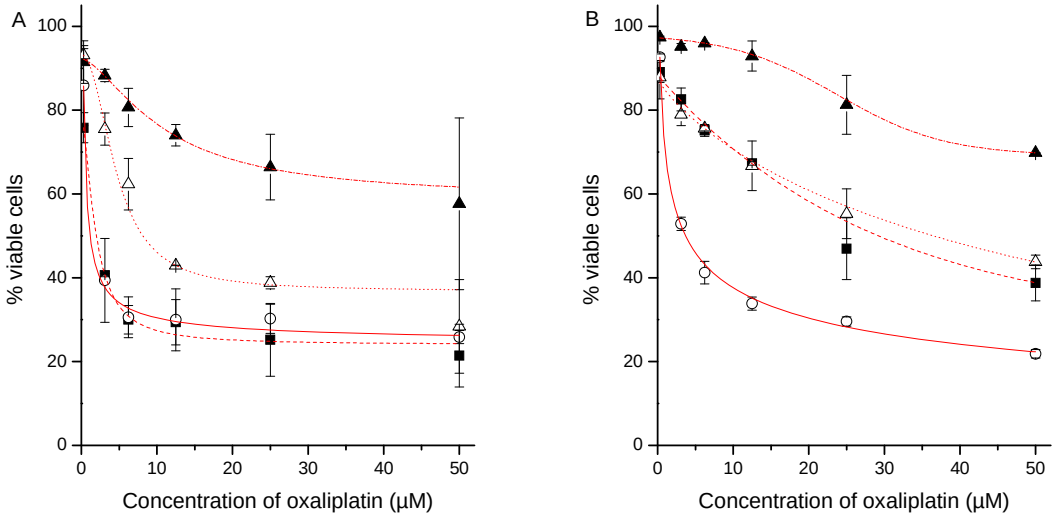

Figure 39. (A) U87MG cells treated with oxaliplatin loaded liposomes as well as free oxaliplatin. ▲ cRGD-liposomes (**s**); Δ DP-MCP-PEG-liposomes (**u**); ■ cRGD/DP-MCP-PEG-liposomes (**t**); ○ free oxaliplatin. (B) KB cells treated with oxaliplatin loaded liposomes as well as free oxaliplatin. ▲ folate-liposomes (**v**); Δ DP-MCP-PEG-liposomes (**u**); ■ folate/DP-MCP-PEG-liposomes (**w**); ○ free oxaliplatin. The liposome formulations were as described in Table 16. All values are means ± SEM (n = 2).

The cytotoxicity of the POPC based liposomal formulations was comparable to the DSPC formulations (Figure 30B, 34B and 38B).

When studying the morphology of the liposomes using cryogenic transmission electron microscopy (cryoTEM) a difference was observed between the DSPC and POPC liposomal systems (Figure 40).

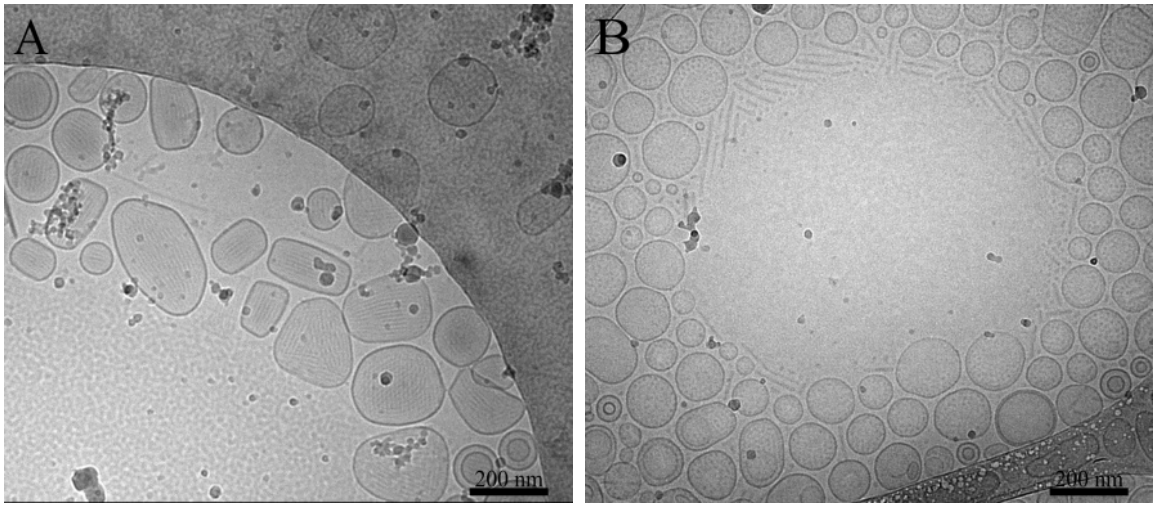

Figure 40. Representative cryoTEM images of DP-MCP-PEG containing liposomes with different matrix phospholipids. (A) DSPC-liposomes (**l** / **q**); (B) POPC-liposomes (**u**).

The cryoTEM image of DSPC-liposomes (Figure 40 A) shows a striped morphology of the liposomes most possibly caused by the presence of the lipo-peptide DP-MCP-PEG. Striped domains have been reported as indicating a proximity to a miscibility critical point [Keller, 1999]. It was first reported in lipid monolayers [McConnell, 1989], but has later been observed in multicomponent lipid bilayers [Honerkamp-Smith, 2008] and lipid/protein mixtures [Lipp, 1997]. The direction of the stripes seems to direct the form of the liposomes and consequently they are less spherical than usually observed for liposomes. The POPC-liposomes are without stripes and shows a much more spherical form (Figure 40 B). Outside the liposomes small stripes can be observed, which can be assigned to free lipo-peptide not embedded in the phospholipid membrane. We have previously observed this trend, when using lipo-peptides (Andersen, 2011). A cryoTEM image gives an idea of the morphology of the studied systems; however, more quantitative methods should be applied to determine the amount of lipo-peptide embedded in the membrane relative to free lipo-peptide.

4.5 Concluding remarks

The aim of this study was to investigate, if the combination of a tumor targeting ligand and a special designed cleavable PEG peptide could enhance the uptake and cytotoxicity of liposomes.

We showed by the use of a highly positive liposome formulation expressing octaarginine on the surface, that this charge resulted in high uptake by cells *in vitro* and a high degree of cytotoxicity. As this kind of formulation is not relevant for *in vivo* purposes we investigated other means of achieving the enhanced uptake and cytotoxicity observed in the octaarginine formulation.

Liposomes with the targeting ligand cRGD was produced and tested in human glioblastoma and human fibrosarcoma cell lines. A large uptake was observed after just five hours of incubation with the liposomes as characterized by flow cytometry. However, the high uptake did not correlate to cytotoxicity as these liposomes showed no cytotoxic effect on either cell lines; despite the presence of the positive charged lipid DOTAP.

Dual-functionalized liposomes were made expressing both the targeting moiety cRGD in addition to a special designed lipo-peptide with an enzyme sensitive part. By the use of thermolysin as model enzyme, we showed enzymatic cleavage of the peptide would result in removal of PEG chains and negatively charged amino residues, resulting in exposure of the positive charged lipids below the PEG layer. These formulations

showed high uptake as for the mono-functionalized cRGD-liposomes. Additionally they also showed high cytotoxic effect on the cells. This led us to believe that the dual-functionalized liposomes could circumvent the PEG dilemma. The liposomal encapsulated content would escape the endosomes/lysosomes before degradation; by interacting strongly with the endosomal/lysosomal membranes after removal of the PEG chains and negatively charged residues.

In addition to these studies we tested if the cleavable lipo-peptide would provide similar results with a different targeting ligand than cRGD or, when embedded into a mono-unsaturated phospholipid membrane. The folate receptor targeting ligand was utilized as targeting agent and tested with and without the lipo-peptide present in the liposomes, on a human fibrosarcoma cell line and a human nasopharyngeal epidermal carcinoma cell line. Both the mono- and dual-functionalized liposomes showed a high uptake, but as in the previous experiments only the dual-functionalized formulation resulted in cytotoxicity.

The mono- and dual-functionalized liposomes formulated from the unsaturated phospholipid POPC showed cytotoxic curves very alike to the ones observed when using a saturated phospholipid as matrix phospholipid. However, their morphology visualized in cryoTEM was quite different and emphasized the importance of utilizing multiple characterizations methods.

These studies have shown that by removing the protective PEG layer from the liposome surface, uncovering positively charged lipids an enhanced effect of encapsulated drugs can be achieved. The targeting moieties have proved to be important in order to improve cytotoxicity, but their real potential can not be established, before going *in vivo*, where their ability to increase specific drug delivery to cancerous tissue can be elucidated.

Chapter 5

Concluding remarks and perspective

An immense amount of research is invested in the drug delivery field today. Especially, the cancer research field is attracting much attention, as this devastating disease is the second leading cause of death every year. Since the liposomes were suggested as drug carrier candidates, these have been intensively investigated and many attempts have been made to optimize the use of these for chemotherapeutic treatments. Their ability to hold cytotoxic drugs in their lumen in addition to their potential to passively accumulate in diseased tissues makes them highly interesting. With some degree of success active targeting of liposomes has been investigated as a route to improve specificity and accumulation in selective tissues.

This thesis covered three different aspects of the use of liposomes as targeted drug delivery systems.

The first part included the actual synthetic approaches to obtain targeted liposomes. Many methods have been applied over the years. Several important things need to be considered, when designing a targeted liposomal system for *in vivo* use. Preferably, the synthetic approach chosen should be able to proceed under mild conditions; it should be fast, reproducible and result in non-toxic and non-immunogenic chemical bonds. It should be considered how to determine the degree of functionalization as not all reported methods are quantitative. We introduced in this section a new conjugation method which utilized the binding forming ability between a hydroxylamine and an aldehyde. This

resulted in fast and quantitative reactions when performed in solution as well as on the surface of pre-formed liposomes.

It is important to continue the development of new synthetic procedures, which perform well in aqueous buffers without toxic additives, as for instance metallic catalysts.

The second part of this thesis aimed to elucidate the *in vitro* and *in vivo* efficiency of active targeting. *In vitro*, this was done by the use of fluorescent liposomes, whose uptake in cells could be monitored visually by confocal microscopy and quantitatively by flow cytometry. Targeted liposomes showed a clear superior uptake compared to two different formulations of control liposomes. For *in vivo* studies a remote loading technique was applied to manufacture radioactive labeled liposomes, which could be tracked *in vivo* by the use of positron emission tomography. These results were greatly interesting as a different profile could clearly be visualized for the targeted liposomes compared to the two formulations of control liposomes; both in regard to accumulation profile and clearance profile. Despite, higher clearance of the targeted liposomes by the spleen and liver, an equivalent uptake in tumor tissue was observed.

We believe that the radiolabeled liposomes will be a valuable tool for investigating the biodistribution of targeted drug delivery, as this technique can provide a quantitative image of the actual effect of the targeting moiety.

The third and last part of this thesis covered the combination of two functionalities on the surface of liposomes. One functionality should target the liposomes to diseased tissue, while the other functionality should function as a combined enhancer of internalization and drug escape. It became clear in this section that a high uptake is not enough to obtain efficacy of the drug containing liposomal system. Despite the presence of cationic charges on the surface of the applied liposomes, these did not show sufficient interaction with the endosomal/lysosomal membranes to induce any drug release and cytotoxic effect. To obtain sufficient interaction the shielding PEG layer needed to be removed; which was facilitated by a special synthesized lipo-peptide. Greater cytotoxicity was observed for two different targeting moieties, each in combination with the removable PEG moiety, than for mono-functionalized systems expressing targeting moieties or removable PEG lipo-peptide on their own.

Future studies in this field should investigate the *in vivo* biodistribution and cytotoxic effect of this dual-functionalized system; e.g. by application of the radiolabeled technique described above.

Overall the work presented in this thesis emphasize the importance of acquiring knowledge at more than one level - synthetic and biological - before being able to design novel efficient targeted drug delivery systems.

References

Agard NJ, Prescher JA, Bertozzi CR (2004). A strain-promoted [3+2] azide-alkyne cycloaddition for covalent modification of biomolecules in living systems. *J. Am. Chem. Soc.* 126:15046-15047.

Allen TM (2002). Ligand-targeted therapeutics in anticancer therapy. *Nat. Rev. Cancer* 2:750-765.

Allen TM, Brandeis E, Hansen CB, Kao GY, Zalipsky S (1995). A new strategy for attachment of antibodies to sterically stabilized liposomes resulting in efficient targeting to cancer cells. *Biochim. Biophys. Acta* 1237:99-108.

Andersen S (2011). Synthesis and characterisation of lipid derivatives for incorporation in matrix metalloproteinase sensitive drug delivery systems. PhD Thesis, DTU Nanotech.

Anderson VC, Thompson DH (1992). Triggered release of hydrophilic agents from plasmalogen liposomes using visible light or acid. *Biochim. Biophys. Acta* 1109:33-42.

Andresen TL, Thompson DH, Kaasgaard T (2010). Enzyme-triggered nanomedicine: Drug release strategies in cancer therapy. *Mol. Membr. Biol.* 27:353-363.

Arap W, Pasqualini R, Ruoslahti E (1998). Cancer treatment by targeted drug delivery to tumor vasculature in a mouse model. *Science* 279:377-380.

Bailey DL, Townsend DW, Valk PE, Maisey MN (2005). Positron emission tomography. London, UK: Basic Science, Springer -Verlag.

Bangham AD, Horne RW (1964). Negative staining of phospholipids and their structural modification by surface-active agents as observed in the electron microscope. *J. Mol. Biol.* 8:660-668.

Bangham AD, Standish MM, Watkins JC (1965). Diffusion of univalent ions across lamellae of swollen phospholipids. *J. Mol. Biol.* 13:238-258.

Barenholz Y (2001). Liposome application: Problems and prospects. *Curr. Opin. Colloid Interfase Sci.* 6:66-77.

Barradas RG, Fletcher S, Porter JD (1976). The hydrolysis of maleimide in alkaline solution. *Can. J. Chem.* 54:1400-1404.

Bartlett DW, Su H, Hildebrandt IJ, Weber WA, Davis ME (2007). Impact of tumor-specific targeting on the biodistribution and efficacy of siRNA nanoparticles measured by multimodality *in vivo* imaging. *Proc. Natl. Acad. Sci. U.S.A.* 104:15549-15554.

Baxter LT, Zhu H, Mackensen DG, Jain RK (1994). Physiologically based pharmacokinetic model for specific and nonspecific monoclonal antibodies and fragments in normal tissues and human tumor xenografts in nude mice. *Cancer Res.* 54:1517-1528.

Béduneau A, Saulnier P, Hindré F, Clavreul A, Leroux J-C, Benoit J-P (2007). Design of targeted lipid nanocapsules by conjugation of whole antibodies and antibody Fab' fragments. *Biomaterials* 28:4978-4990.

Bendas G, Rothe U, Scherphof GL, Kamps JAAM (2003). The influence of repeated injections on pharmocokinetics and biodistribution of different types of sterically stabilized immunoliposomes. *Biochim. Biophys. Acta* 1609:63-70.

Benjaminsen RV, Sun H, Henriksen JR, Christensen NM, Almdal K, Andresen TL (2011). Evaluating nanoparticle sensor design for intracellular pH measurements. *ASC Nano* 5:5864-5873.

Boeckler C, Frisch B, Muller S, Schuber F (1996). Immunogenicity of new heterobifunctional cross-linking reagents used in the conjugation of synthetic peptides to liposomes. *J. Immunol. Methods* 191:1-10.

Bogdanowich-Knipp, Chakrabarti S, Williams TD, Dillman RK, Siahaan TJ (1999). Solution stability of linear vs. cyclic RGD peptides. *J. Pept. Res.* 53:530-541.

Bonnet D, Grandjean C, Rousselot-Pailley P, Joly P, Bourel-Bonnet L, Santraine V, Gras-Masse H, Melnyk O (2003). Solid-phase functionalization pf peptides by an α-hydrazinoacetyl group. *J. Org. Chem.* 68:7033-7040.

Bostic HE, Smith MD, Poloukhtine AA, Popik VV, Best MD (2012). Membrane labeling and immobilization via copper-free click chemistry. *Chem. Commun.* 48:1431-1433.

Boturyn D, Col J-L, Garanger E, Favrot M-C, Dumy P (2004). Template assembled cyclopeptides as multimeric system for integrin targeting and endocytosis. *J. Am. Chem. Soc.* 126:5730-5739.

Bourel-Bonnet L, Pécheur E-I, Grandjean C, Blanpain A, Baust T, Melnyk O, Hoflack B, Gras-Masse H (2005). Anchorage of synthetic peptides onto liposomes via hydrazone and α-oxo hydrazone bonds. Preliminary functional investigations. *Bioconjugate Chem.* 16:450-457.

Brazeau P, Vale W, Burgus R, Ling N, Butcher M, Rivier J, Guillemin R (1973). Hypothalamic polypeptide that inhibits the secretion of immunoreactive pituitary growth hormone. *Science* 179:77-79.

Cavalli S, Tipton AR, Overhand M, Kros A (2006). The chemical modification of liposome surfaces via a copper-mediated [3+2] azide-alkyne cycloaddition monitored by a colorimetric assay. *Chem. Commun.* 30:3193-3195.

Chang PV, Prescher JA, Sletten EM, Baskin JM, Miller IA, Agard NJ, Lo A, Bertozzi CR (2010). Copper-free click chemistry in living animals. *Proc. Natl. Acad. Sci. U.S.A.* 107:1821-1826.

Chenoweth K, Chenoweth D, Goddard III WA (2009). Cyclooctyne-based reagents for uncatalyzed click chemistry: A computational survey. *Org. Biomol. Chem.* 7:5255-5258.

Chernomordik L (1996). Non-bilayer lipids and biological fusion intermediates. *Chem. Phys. Lipids* 81:203-213.

Chiu S-J, Liu S, Perrotti D, Marcucci G, Lee RJ (2006). Efficient delivery of a Bcl-2-specific antisense oligodeoxyribonucleotide (G3139) via transferrin receptor-targeted liposomes. *J. Controlled Release* 112:199-207.

Chua MM, Fan ST, Karush F (1984). Attachment of immunoglobulin to liposomal membrane via protein carbohydrate. *Biochim. Biophys. Acta* 800:291-300.

Cleland WW (1964). Dithiothreitol, a new protective reagent for SH groups. *Biochemistry* 3:480-482.

Codelli JA, Baskin JM, Agard NJ, Bertozzi CR (2008). Second-generation difluorinated cyclooctynes for copper-free click chemistry. *J. Am. Chem. Soc.* 130:11486-11493.

Collingridge DR, Carroll VA, Glaser M, Aboagye EO, Osman S, Hutchinson OC, Barthel H, Luthra SK, Brady F, Bicknell R, Price P, Harris AL (2002). The development of [124I]Iodinated-VG76e: A novel tracer for imaging vascular endothelial growth factor *in vivo* using positron emission tomography. *Cancer Res.* 62:5912-5919.

Conforti G, Calza M, Beltrán-Nuñez A (1994). V5 integrin is localized at focal contact by HT-1080 fibrosarcoma cells and human skin fibroblasts attached to vitronectin. *Cell adhersion and Communication* 1:279-293.

Corti A, Curnis F, Arap W, Pasqualini R (2008). The neovasculature homing motif NGR: More than meets the eye. *Blood* 112:2628-2635.

Coussens LM, Fingleton B, Matrisian LM (2002). Matrix metalloproteinase inhibitors and cancer: Trials and tribulations. *Science* 295:2387-2392.

Damen J, Regts J, Scherphpf G (1981). Transfer and exchange of phospholipid between small unilamellar liposomes and rat plasma high density lipoproteins. *Biochim. Biophys. Acta* 665:538-545.

Davis SC, Szoka FS (1998). Cholesterol phosphate derivatives: Synthesis and incorporation into a phosphatese and calcium-sensitive triggered release liposome. *Bioconjugate Chem.* 9:783-792.

Demel RA, de Kruyff B (1976). The function of sterols in membranes. *Biochim. Biophys. Acta.* 457:109-132.

Desgrosellier JS, Cheresh DA (2010). Integrins in cancer: Biological implications and therapeutic opportunities. *Nat. Rev. Cancer* 10:9-22.

Di Francesco AM, Ruggiero A, Riccardi R (2002). Drugs of the future: Cellular and molecular aspects of drugs of the future: Oxaliplatin. *Cell. Mol. Life Sci.* 59:1914-1927.

Dirksen A, Dawson PE (2008). Rapid oxime and hydrazone ligations with aromatic aldehydes for biomolecular labeling. *Bioconjugate Chem.* 19:2543-2548.

Dominska M, Dykxhoorn DM (2010). Breaking down the barriers: siRNA delivery and endosome escape. *J. Cell Sci.* 123:1183-1189.

Dong Z, Liu Y, Scott KF, Levin L, Gaitonde K, Bracken RB, Burke B, Zhai QJ, Wang J, Oleksowicz L, Lu S (2010). Secretory phospholipase A2-IIa is involved in prostate cancer progression and may potentially serve as a biomarker for prostate cancer. *Carcinogenesis* 31:1948-1955.

Drummond DC, Daleke DL (1995). Synthesis and characterization of N-acylated, pH-sensitive 'caged' aminophospholipids. *Chem. Phys. Lipids* 75:27-41.

Drummond DC, Meyer O, Hong K, Kirpotin DB, Papahadjopoulos D (1999). *Pharmacol. Rev.* 51:692-743.

Drummond DC, Zignani M, Leroux J-C (2000). Current status of pH-sensitive liposomes in drug delivery. *Prog. Lipid Res.* 39:409-460.

Dupont E, Prochiantz A, Joliot A (2011). Penetratin story: An overview. *Methods Mol. Biol.* 683:21-29.

ElBayoumi TA, Torchilin VP (2009). Tumor-specific anti-nucleosome antibody improves therapeutic efficacy of doxorubicin-loaded long-circulating liposomes against primary and metastatic tumor in mice. *Mol. Pharmaceutics* 6:246-254.

Elegbede AI, Banerjee J, Hanson AJ, Tobwala S, Ganguli B, Wang R, Lu X, Srivastava DK, Mallik S (2008). Mechanistic studies of the triggered release of liposomal contents by matrix metalloproteinase-9. *J. Am. Chem. Soc.* 130:10633-10642.

Espinola LG, Beaucaire J, Gottschalk A, Caride VJ (1979). Radiolabeled liposomes as metabolic and scanning tracers in mice. II. In-111 oxine compared with TC-99m DTPA, entrapped in multilamellar lipid vesicles. *J. Nucl. Med.* 20:434-440.

Espuelas S, Roth A, Thumann C, Frisch B, Schuber F (2005). Effect of synthetic lipopeptides formulated in liposomes on the maturation of human dendritic cells. *Mol. Immunol.* 42:721-729.

Etzerodt TP, Trier S, Henriksen JR, Andresen TL (2012). A GALA lipopeptide mediates pH- and membrane charge dependent fusion with stable giant unilamellar vesicles. *Soft Matter* 8:5933-5939.

Fairbanks BD, Sims EA, Anseth KS, Bowman CN (2010). Reaction rates and mechanisms for radical, photoinitated addition of thiols to alkynes, and implications for thiol-yne photopolymerizations and click reactions. *Macromolecules* 43:4114-4119.

Fass L (2008). Imaging and cancer: A review. *Molecular Oncology* 2:115-152.

Finnegan RA, Mueller WH (1965). Base-catalyzed addition and solvolysis reactions of N-phenylmaleimide in methanol. *J. Pharm. Sci.* 54:1257-1260.

Fleiner M, Benzinger P, Fichert T, Massing U (2001). Studies on protein-liposome coupling using novel thiol-reactive coupling lipids: Influence of spacer lenght and polarity. *Bioconjugate Chem.* 12:470-475.

Folkman J (1995). Angiogenesis in cancer, vascular, rheumatoid and other disease. *Nat. Med.* 1:27-31.

Frankel AD, Pabo CO (1988). Cellular uptake of the tat protein from human immunodeficiency virus. *Cell* 6:1189-1193.

Friedlander M, Theesfeld CL, Sugita M, Fruttiger M, Thomas MA, Chang S, Cheresh DA (1996). Involvement of integrins $\alpha_v\beta_3$ and $\alpha_v\beta_5$ in ocular neovascular diseases. *Proc. Natl. Acad. Sci. U.S.A.* 93:9764-9769

Fueyo J, Alemany R, Gomez-Manzano C, Fuller GN, Khan A, Conrad CA, Liu T-J, Jiang H, Lemoine MG, Suzuki K, Sawaya R, Curiel DT, Yung WKA, Lang FF (2003). Preclinical characterization of the antiglioma activity of tropism-enhanced adenovirus targeted to the retinoblastoma pathway. *J. Nat. Cancer Inst*. 95:652-660.

Gaber MH, Wu NZ, Hong K, Huang SK, Dewhirst M, Papahadjopoulos D (1996). Thermosensitive liposomes: Extravasation and release of contents in tumor microvascular networks. *Int. J. Radiat. Oncol. Biol. Phys.* 36:1177-1187.

Gabizon A, Catane R, Uziely B, Kaufman B, Safra T, Cohen R, Martin F, Huang A, Barenholz Y (1994). Prolonged circulation time and enhanced accumulation in malignant exudates of doxorubicin encapsulated in polyethylene-glycol coated liposomes. *Cancer Res.* 54:987-992.

Gabizon A, Papahadjopoulos D (1988). *Proc. Natl. Acad. Sci. U.S.A.* 85:6949-6953.

Gal S, Pinchuk I, Lichtenberg D (2003). Peroxidation of liposomal palmitoyllinoleoylphosphatidylcholine (PLPC), effect of the surface charge on the oxidizability and the potency of antioxidants. *Chem. Phys. Lipids* 126: 95-110.

Gambhir SS, Herschman HR, Cherry SR, Barrio JR, Satyamurthy N, Toyokuni T, Phelps ME, Larson SM, Balatoni J, Finn R, Sadelain M, Tjuvajev J, Blasberg R (2000). Imaging transgene expression with radionuclide imaging technologies. *Neoplasia* 2:118-138.

Gambhir SS (2002). Molecular imaging of cancer with positron emission tomography. *Nat. Rev. Cancer* 2:683-693.

Garnier B, Bouter A, Gounou C, Petry KG, Brisson AR (2009). Annexin A5-functionalized liposomes for targeting phosphatidylserine-exposing membranes. *Bioconjugate Chem.* 20:2114-2122.

Goessler UR, Bugert P, Bieback K, Stern-Straeter J, Bran G, Hörmann K, Riedel F (2008). Integrin expression in stem cells from bone marrow and adipose tissue during chondrogenic differentiation. *Int. J. Mol. Med.* 21:271-279.

Goren D, Horowitz AT, Tzemach D, Tarshish M, Zalipsky S, Gabizon A (2000). Nuclear delivery of doxorubicin via folate-targeted liposomes with bypass of multidrug-resistance efflux pump. *Clin. Cancer Res.* 6:1949-1957.

Gradauer K, Dünnhaupt S, Vonach C, Szöllösi H, Pali-Schöll I, Mangge H, Jensen-Jarolim E, Bernkop-Schnürch A, Prassl R. (2012). Thiomer-coated liposomes harbor permeation enhancing and efflux pump inhibitory properties. *J. Controlled Release* http://dx.doi.org/10.1016/j.jconrel.2012.12.001.

Gregoriadis G, Ryman BE (1971). Liposomes as carriers of enzymes or drugs - new approach to treatment of storage diseases. *Biochem. J.* 124:P58

Gregoriadis G, Wills EJ, Swain CP, Tavill AS (1974). Drug-carrier potential of liposomes in cancer chemotherapy. *Lancet* 1:1313-1316.

Gregory JD (1955). The stability of N-ethylmaleimide and its reaction with sulfhydryl groups. *J. Am. Chem. Soc.* 77:3922-3923.

Gulati M, Grover M, Singh S, Singh M (1998). Lipophilic drug derivatives in liposomes. *Int. J. Pharm.* 165:129-168.

Gunawan RC, Auguste DT (2010). The role of antibody synergy and membrane fluidity in the vascular targeting of immunoliposomes. *Biomaterials* 31:900-907.

Gustafsson M, Olsson R, Andersson C-M (2001). General combinatorial synthesis of tertiary amines on solid support. A novel conditional release strategy based on traceless linking at nitrogen. *Tetrahedron Lett.* 42:133-136.

Hansen CB, Kao GY, Moase EH, Zalipsky S, Allen TM (1995). Attachment of antibodies to sterically stabilized liposomes: Evaluation, comparison and optimization of coupling procedures. *Biochim. Biophys. Acta* 1239:133-144.

Harding JA, Engbers CM, Newman MS, Goldstein NI, Zalipsky S (1997). Immunogenicity and pharmacokinetic attributes of poly(ethylene glycol)-grafted immunoliposomes. *Biochem. Biophys. Acta* 1327:181-192.

Harvie P, Wong FMP, Bally MB (2000). Use of poly(ethylene glycol)-lipid conjugates to regulate the surface attributes and transfection activity of lipid-DNA particles. *J. Pharm. Sci.* 89:652-663.

Hassane FS, Frisch B, Schuber F (2006). Targeted liposomes: Convenient coupling of ligands to preformed vesicles using "Click Chemistry". *Bioconjugate Chem.* 17:849-854.

Hatakeyama H, Akita H, Ishida E, Hashimoto K, Kobayashi H, Aoki T, Yasuda J, Obata K, Kikuchi H, Ishida T, Kiwada H, Harashima H (2007). Tumor targeting of doxorubicin by anti-MT1-MMP antibody-modified PEG liposomes. *Int. J. Pharm.* 342:194-200.

Hatakeyama H, Akita H, Kogure K, Oishi M, Nagasaki Y, Kihita Y, Ueno M, Kobayashi H, Kikuchi H, Harashima H (2007). Development of a novel systemic gene delivery system for cancer therapy with a tumor-specific cleavable PEG-lipid. *Gene Therapy* 14:68-77.

Hatakeyama H, Ito E, Akita H, Oishi M, Nagasaki Y, Futaki S, Harashima H (2009). A pH-sensitive fusogenic peptide facilitates endosomal escape and greatly enhances the gene silencing of siRNA-containing nanoparticles *in vitro* and *in vivo*. *J. Controlled Release* 139:127-132.

Haubner R, Weber WA, Beer AJ, Vabuliene E, Reim D, Sarbia M, Becker KF, Goebel M, Hein R, Wester HJ, Kessler H, Schwaiger M (2005). Noninvasive visualization of the activated $alpha_v beta_3$ integrin in cancer patients by positron emission tomography and [(18)F]Galacto-RGD. *PLoS Med.* 2:244-252.

Henriksen JH. Andresen TL, Feldborg LN, Duelund L, Ipsen JH (2010). Understanding detergent effects on lipid membranes: A model study of lysolipids. *Biophys. J.* 98:2199-2205.

Hnatowich DJ, Friedman B, Clancy B, Novak M (1981). Labeling of preformed liposomes with Ga-67 and Tc-99m by chelation. *J. Nucl. Med.* 22:810-814.

Hobbs SK, Monsky WL, Yuan F, Roberts WG, Griffith L, Torchilin VP and Jain RK (1998). Regulation of transport pathways in tumor vessels: Role of tumor type and microenvironment. *Proc. Natl. Acad. Sci. U.S.A.* 95:4607-4612.

Honerkamp-Smith AR, Cicuta P, Collins MD, Veatch SL, den Nijs M, Schick M, Keller SL (2008). Line tensions, correlation lenghts, and critical exponents in lipid membranes near critical points. *Biophys. J.* 95:236-246.

Humphries JD, Byron A, Humphries MJ (2006). Integrin ligands at a glance. *J. Cell Sci.* 119:3901-3903.

Hyvönen Z, Rönkkö S, Toppinen M-R, Jääskeläinen I, Plotniece A, Urtti A (2004). Dioleoyl phosphatidylethanolamine and PEG-lipid conjugates modify DNA delivery mediated by 1,4-dihydropyridine amphiphiles. *J. Controlled Release* 99:177-190.

IAEA (2006). Advances in medical radiation imaging for cancer diagnosis and treatment. *Nucl. Technol. Rev.* 110-127.

Ishida T, Iden DL, Allen TM (1999). A combinatorial approach to producing sterically stabilized (Stealth) immunoliposomal drugs. *FEBS Lett.* 460:129-133.

Ishida T, Kirchmeier MJ, Moase EH, Zalipsky S, Allen TM (2001). Targeted delivery and triggered release of liposomal doxorubicin enhances cytotoxicity against human B lymphoma cells. *Biochim. Biophys. Acta.* 1515:144-158.

Ishiguro R, Matsumoto M, Takahashi S (1996). Interaction of fusiogenic synthetic peptide with phospholipid bilayers: Orientation of the peptide α-helix and binding isotherm. *Biochemistry* 35:4976-4983.

Jain RK (1988). Determinants of tumor blood flow: A review. *Cancer Res.* 48:2641-2658.

Jain RK (1990). Physiological barriers to delivery of monoclonal antibodies and other macromolecules in tumors. *Cancer Res. (Suppl:)* 50:814s-819s.

Jang SH, Wientjes MG, Lu D, Au JLS (2003). *Pharm. Res.* 20:1337-1350.

Janssen APCA, Schiffelers RM, ten Hagen TLM, Koning GA, Schraa AJ, Kok RJ, Storm G, Molema G (2003). Peptide-targeted PEG-liposomes in anti-angiogenic therapy. *Int. J. Pharm.* 254:55-58.

Jølck RI, Feldborg LN, Andersen S, Moghimi SM, Andresen TL (2010). Engineering liposomes and naoparticles for biological targeting. *Adv. Biochem. Engin./Biotechnol.* 125:251-280.

Jørgensen K, Davidsen J, Mouritsen OG (2002). Biophysical mechanisms of phospholipase A2 activation and their use in liposome-based drug delivery. *FEBS Lett.* 1:23-27.

Juliano RL, Stamp D (1975). The effect of particle size and charge on the clearance rate of liposomes and liposome encapsulated drugs. *Biochem. Biophys. Res. Commun.* 63:651-658.

Keller SL, McConnell HM (1999). Stripe phases in lipid monolayers near a miscibility critical point. *Phys. Rev. Lett.* 82:1602-1605.

Khoobeni B, Char CA, Peyman GA, Schuele KM (1990). Study of the mechanisms of laser-induced release of liposome-encapsulated dye. *Lasers Surg. Med.* 10:303-309.

Kirby C, Clarke J, Gregoriadis G (1980). Effect of the cholesterol content of small unilamellar liposomes on their stability *in vivo* and *in vitro*. *Biochem. J.* 186:591-598.

Kirpotin DB, Drummond DC, Shao Y, Shalaby MR, Hong K, Nielsen UB, Marks JD, Benz CC, Park JW (2006). Antibody targeting of long-circulation lipidic nanoparticles does not increase tumor localization, but does increase internalization in animal models. *Cancer Res.* 66:6732-6740.

Klibanov AL, Maruyama K, Torchilin VP, Huang L (1990). Amphipathic polyethyleneglycols effectively prolong the circulation time of liposomes. *FEBS Lett.* 268:235-237.

Kong G, Dewhirst MW (1999). Review: Hyperthermia and liposomes. *Int. J. Hyperthermia* 15:345-370.

Koning GA, Fretz MM, Woroniecka U, Storm G, Krijger GC (2004). Targeting liposomes to tumor endothelial cells for neutrin capture therapy. *Appl. Radiat. Isot.* 61:963-967.

Koning GA, Morselt HWM, Velinova MJ, Donga J, Gorter A, Allen TM, Zalipsky S, Kamps JAAM, Scherphof GL (1999). Selective transfer of a lipophilic prodrug of 5-fluorodeoxyuridine from immunoliposomes to colon cancer cells. *Biochem. Biophys. Acta* 1420:153-167.

Kung VT, Redemann CT (1986). Synthesis of carboxyacyl derivatives of phosphatidylethanolamine and use as an efficient method for conjugation of protein to liposomes. *Biochim. Biophys. Acta* 862:435-439.

Kwekkeboom DJ, Kam BL, van Essen M, Teunissen JJM, van Eijck CHJ, Valkema R, de Jong M, de Herder WW, Krenning EP (2010). Somatostatin receptor-based imaging and therapy of gastroenteropancreatic neuroendocrine tumors. *Endocrine-Related Cancer* 17:R53-R73.

Larson SM, Erdi Y, Akhurst T, Mazumdar M, Macapinlac HA, Finn RD, Casilla C, Fazzari M, Srivastava N, Yeung HWD, Humm JL, Guillem J, Downey R, Karpeh M, Cohen AE, Ginsberg R (1999). The visual response score and the change in total lesion glycolysis. *Clinical Positron Imaging* 2:159-171.

Lee RJ, Low PS (1995). Folate-mediated tumor cell targeting of liposome-entraped doxorubicin *in vitro*. *Biochim. Biophys. Acta* 1233:134-144.

Leidy C, Linderoth L, Andresen TL, Mouritsen OG, Jørgensen K, Peters GH (2006). Domain-induced activation of human phospholipase A_2 type IIA: Local versus global lipid composition. *Biophys. J.* 90:3165-3175.

Leung SJ, Romanowski M (2012). Light-activated content release from liposomes. *Theranostics* 2:1020-1036.

Li Z, Seo TS, Ju J (2004). 1,3-dipolar cycloaddition of azides with electron-deficient alkynes under mild condition in water. *Tetrahedron Lett.* 45:3143-3146.

Liakka KA (1994). The integrin subunits α2, α3, α4, α5, α6, αv, β1, β3 in fetal, infant and adult human spleen as detected by immunohistochemistry. *Differentiation* 56:183-190.

Lila AAS, Ishida T, Kiwada H (2009). Recent advances in tumor vasculature targeting using liposomal drug delivery systems. *Expert Opin. Drug Delivery* 6:1297-1309.

Lipp MM, Lee KYC, Waring A, Zasadzinski JA (1997). Fluorescence, polarized fluorescence, and brewster angle microscopy of palmitic acid and lung surfactant protein B monolayers. *Biophys. J.* 72:2783-2804.

Liu S, Hsieh W-Y, Jiang Y, Kim Y-S, Sreerama SG, Chen X, Jia B, Wang F (2007). Evaluation of a ^{99m}Tc-labeled cyclic RGD tetramer for noninvasive imaging integrin $\alpha_v\beta_3$-positive breast cancer. *Bioconjugate Chem.* 18:438-446.

Lopes de Menezes DE, Pilarski LM, Allen TM (1998). *In vitro* and *in vivo* targeting of immunoliposomal doxorubicin to human B-cell lymphoma. *Cancer Res.* 58:3320-3330.

Lu Y, Low PS (2002). Folate-mediated delivery of macromolecular antocancer therapeutic agents. *Adv. Drug Delivery Rev.* 54:675-693.

Maeda H, Wu J, Sawa T, Matsumura Y, Hori K (2000). Tumor vascular permeability and the EPR effect in macromolecular therapeutics: A review. *J. Controlled Release* 65:271-284.

Martin FJ, Papahadjopoulos D (1982). Irreversible coupling of immunoglobulin fragments to preformed vesicles. *J. Biol. Chem.* 257:286-288.

Maruyama K (2002). PEG-Immunoliposome. *Biosci. Rep.* 22:251-266.

Maruyama K, Takizawa T, Yuda T, Kennel SJ, Huang L, Iwatsuru M (1995). Targetability of novel immunoliposomes modified with amphipathic poly(ethylene glycol)s conjugated at their distal terminals to monoclonal antibodies. *Biochim. Biophys. Acta* 1234:74-80.

Mas-Moruno C, Rechenmacher F, Kessler H (2010). Cilengitide: The first anti-angiogenic small molecule drug candidate. Design, synthesis and clinical evaluation. *Anti-cancer Agents in Med. Chem.* 10:753-768.

Mathias CJ, Wang S, Waters DJ, Turek JJ, Low PS, Green MA (1998). Indium-111-DTPA-folate as a potential folate-receptor-targeted radiopharmaceutical. *J. Nucl. Med.* 39:1579-1585.

Matsui S, Aida H (1978). Hydrolysis of some N-alkylmaleimides. *J. Chem. Soc. Perkin Trans 2* 1277-1280.

McConnell HM (1989). Theory of hecagonal and stripe phases in monolayers. *Proc. Natl. Acad. Sci. U.S.A.* 86:3452-3455.

McDougall IR, Dunnick JK, McNamee MG, Kriss JP (1974). Distribution and fate of synthetic lipid vesicles in the mouse: A combined radionuclide and spin label study. *Proc. Natl. Acad. Sci. U.S.A.* 71:3487-2491.

McNeeley KM, Karathanasis E, Annapragada AV, Bellamkonda RV (2009). Masking and triggered unmasking of targeting ligands to improve drug delivery to brain tumors. *Biomaterials* 30:3986-3995.

Meerovitch K, Bergeron F, Leblond L, Grouix B, Poirier C, Bubenik M, Chan L, Gourdeau H, Bowlin T, Attardo G (2003). A novel RGD antagonist that targets both $\alpha_v\beta_3$ and $\alpha_5\beta_1$ induces apoptosis of angiogenic endothelial cells on type I collagen. *Vasc. Pharmacol.* 40:77-89.

Meers P (2001). Enzyme-activated targeting of liposomes. *Adv. Drug Delivery Rev.* 53:265-272.

Melacini G, Zhu Q, Ösapay G, Goodman M (1997). A refined model for the somatostatin pharmacophore: Conformational analysis of lanthionine-sandostatin analogs. *J. Med. Chem.* 40:2252-2258.

Mercadal M, Domingo JC, Petriz J, Garcia J, de Madariaga MA (1999). A novel strategy affords high-yield coupling of antibody to extremities of liposomal surface-grafted PEG chains. *Biochim. Biophys. Acta* 1418:232-238.

Messarltou G, East L, Roghl C, Isacke CL, Yarwood H (2009). Membrane type-1 matrix metalloproteinase activity is regulated by the endocytic collagen receptor Endo180. *J. Cell Sci.* 122, 4042-4048.

Miller CR, Bondurant B, McLean SD, McGovern KA, O'Brian DF (1998). Liposome-cell interactions *in vitro*: Effect of liposome surface charge on the binding and endocytosis of conventional and sterically stabilized liposomes. *Biochemistry* 37:12875-12883.

Miyasaka K, Funakosho A (2003). Cholecystokinin and cholecystokinin receptors. *J. Gastroenterol.* 38:1-13.

Moghimi SM, Andersen AJ, Hashemi SH, Lettiero B, Ahmadvand D, Hunter AC, Andresen TL, Hamad I, Szebeni J (2010). Complement activation cascade triggered by PEG-PL engineered nanomedicines and carbon nanotubes: The challenges ahead. *J. Controlled Release* 146:175-181.

Monzoor A, Lindner LH, Landon CD, Park JY, Simnick AJ, Dreher MR, Das S, Hanna G, Park W, Chilkoti A, Koning GA, ten Hagen TLM, Needham D, Dewhirst MW (2012). Overcoming limitations in nanoparticle drug delivery: Triggered, intravascular release to improve drug penetration into tumors. *Cancer Res.* doi:10.1158/0008-5472.CAN-12-1683.

Moon WK, Lin Y, O'Loughlin T, Tang Y, Kim D-E, Weissleder R, Tung C-H (2003). Enhanced tumor detection using a folate receptor-targeted near-infrared fluorochrome conjugate. *Bioconjugate Chem.* 14:539-545.

Morrison KL, Weiss GA (2001). Combinatorial alanine-scanning. *Curr. Opin. Chem. Biol.* 5:302-307.

Muñoz M, García M, Reig F, Alsina MA, Haro I (1998). Physico-chemical characterization of liposomes with covalently attached hepatitis A VP3(101-121) synthetic peptide. *Analyst* 123:2223-2228.

Murphy EA, Majeti BK, Barnes LA, Makale M, Weis SM, Lutu-Fuga K, Wrasidlo W, Cheresh DA (2008). Nanoparticle-mediated drug delivery to tumor vasculature suppresses metastasis. *Proc. Natl. Acad. Sci. U.S.A.* 105:9343-9348.
Myers RM, Shearman JW, Kitching MO, Ramos-Montoya A, Neal DE, Ley SV (2009). Cancer, chemistry, and the cell: Molecules that interact with the neurotensin receptors. *ACS Chem. Biol.* 4:503-525.

Needham D, Park J-Y, Wright AM, Tong J (2013). Materials characterization of the low temperature sensitive liposome (LTSL): Effects of the lipid composition (lysolipid and DSPE-PEG_{2000}) on the thermal transition and release of doxorubicin. *Faraday Discuss.* DOI: 10.1039/C2FD20111A .

Neerunjun ED, Hunt R, Gregoriadis (1977). Fate of a liposome-associated agent injected into normal and tumor-bearing rodents: Attempts to improve localization in tumour tissues. *Biochem. Soc. Trans.* 5:1380-1383.

O'Brien DF, Armitage B, Benedicto A, Bennett DE, Lamparski HG, Lee Y-S, Srisiri W, Sisson TM (1998). Polymerization of preformed self-organized assemblies. *Acc. Chem. Res.* 31:861-868.

Oku N, Namba Y, Takeda A, Okada S (1993). Tumor imaging with technetium-99m-DTPA encapsulated in RES-avoiding liposomes. *Nucl. Med. Biol.* 20:407-412.

Pan X, Wu G, Yang W, Barth RF, Tjarks W, Lee RJ (2007). Synthesis of cetuximab-immunoliposomes via a cholesterol-based membrane anchor for targeting of EGFR. *Bioconjugate Chem.* 18:101-108.

Parente RA, Nir S, Szoka FC (1990). Mechanism of leakage of phospholipid vesicle contents induced by the peptide GALA. *Biochemistry* 29:8720-8728.

Park JW, Kirpotin DB, Hong K, Shalaby R, Shao Y, Nielsen UB, Marks JD, Papahadjopoulos D, Benz CC (2001). Tumor targeting using anti-her2 immunoliposomes. *J. Controlled Release* 74:95-113.

Pastorino F, Brignole C, Marimpietri D, Cilli M, Gambino C, Ribatti D, Longhi R, Allen TM, Corti A, Ponzoni M (2003). Vascular damage and anti-angiogenic effects of tumor vessel-targeted liposomal chemotherapy. *Cancer Res.* 63:7400-7409.

Patel YC, Greenwood MT, Panetta R, Demchyshyn L, Niznik H, Srikant CB (1995). The somatostatin receptor family. *Life Science* 75:1249-1265.

Peer D, Karp JM, Hong S, Farokhzad OC, Margalit R, Langer R (2007). Nanocarriers as an emerging platform for cancer therapy. *Nat. Nanotechnol.* 2:751-760.

Peeters JM, Hazendonk TG, Beuvery EC, Tesser GI (1989). Comparison of four bifunctional reagents for coupling peptides to proteins and the effect of the three moieties on the immunogenicity of the conjugates. *J. Immunol. Methods* 120:133-143.

Pelmenschikov V, Siegbahn PEM (2002). Catalytic mechanism of matrix metalloproteinases: Two-layered ONIOM study. *Inorg. Chem.* 41:5659-5666.

Petersen AL, Binderup T, Rasmussen P, Henriksen JR, Elema DR, Kjær A, Andresen TL (2011). ^{64}Cu loaded liposomes as positron emission tomography imaging agents. *Biomaterials* 32:2334-2341.

Petersen AL, Binderup T, Jølck RI, Rasmussen P, Henriksen JR, Pfeifer AK, Kjær A, Andresen TL (2012). Positron emission tomography evaluation of somatostatin receptor targeted ^{64}Cu-TATE-liposomes in a human neuroendocrine carcinoma mouse model. *J. Controlled Release* 160:254-263.

Petersen AL, Hansen AE, Gabizon A, Andresen TL (2012). Liposome imaging agents in personalized medicine. *Adv. Drug Delivery Rev.* 64:1417-1435.

Phelps ME, Hoffman EJ, Mullani NA, Ter-Pogossian MM (1975). Application of annihilation coincidence detection to transaxial reconstruction tomography. *J. Nucl. Med.* 16:210-224.

Phillips WT (1999). Delivery of gamma-imaging agents by liposomes. *Adv. Drug Delivery Rev.* 37:13-32.

Phillips WT, Goins BA, Bao A (2009). Radioactive liposomes. *Wiley Interdiscipl. Rev. Nanomed. Nanobiotechnol.* 1:69-83.
Pierschbacher MD, Ruoslahti E (1984). Cell attachment activity of fibronectin can be dublicated by small synthetic fragments of the molecule. *Nature* 309:30-33.

Pradayrol L, Jörnvall H, Mutt V, Ribet A (1980). N-terminally extended somatostatin: The primary structure of somatostatin-28. *FEBS Lett.* 109:55-58.

Reubi JC, Schär J-C, Waser B, Wenger S, Heppeler A, Schmitt JS, Mäcke HR (2000). Affinity profiles for human somatostatin receptor subtypes SST1-SST5 of somatostatin radiotracers selected for scintigraphic and radiotherapeutic use. *Eur. J. Nucl. Med.* 27:273-282.

Richard A, Bourel-Bonnet L (2005). Internalization of a peptide into multilamellar vesicles assisted by the formation of an α-oxo oxime bond. *Chem. Eur. J.* 11:7315-7321.

Richardson VJ, Jeyasingh K, Jewkes RF, Ryman BE, Tattersall MHN (1977). Properties of [^{99m}Tc]Technetium-labelled liposomes in normal and tumour-bearing rates. *Biochem. Soc. Trans.* 5:290-291.

Romberg B, Hennink WE, Storm G (2008). Sheddable coatings for long-circulating nanoparticles. *Pharmacol. Res.* 49:185-198.

Roomi MW, Monterrey JC, Kalinovsky T, Rath M, Niedzwiecki A (2009). Patterns of MMP-2 and MMP-9 expression in human cancer cell lines. *Oncology Reports* 21:1323-1333.

Rose K, Zeng W, Regamey P-O, Chernushevich IV, Standing KG, Gaertner HF (1996). Natural peptides as building blocks for the synthesis of large protein-like molecules with hydrazone and oxime linkages. *Bioconjugate Chem.* 7:552-556.

Rostovtsev VV, Green LG, Fokin VV, Sharpless KB (2002). A stepwise Huisgen cycloaddition process: Copper(I)-catalyzed regioselective "ligation" of azides and terminal alkynes. *Angew. Chem. Int. Ed.* 41:2596-2599.

Rubin P, Casarett G (1966). Microcirculation of tumors Part I: Anatomy, function and necrosis. *Clin. Radiol.* 17:220-229.

Rundhaug JE (2003). Matrix metalloproteinases, angiogenesis, and cancer. *Clin. Cancer Res.* 9:551-554.

Ruoslahti E (1996). RGD and other recognition sequences for integrins. *Annu. Rev. Cell Dev. Biol.* 12:697-715.

Ruoslahti E, (2002). Specialization of tumor vasculature. *Nat. Rev. Cancer* 2:83-90.

Ruoslahti E, Bhatia SN, Sailor MJ (2010). Targeting of drugs and nanoparticles to tumors. *J. Cell Biol.* 188:759-768.

Saiki I, Murata J, Matsuno K, Ogawa R, Nishi N, Tokura S, Azuma I (1990). Anti-metastatic and anti-invasive effects of polymeric Arg-Gly-Asp (RGD) peptide, poly(RGD), and its analogs. *Jpn. J. Cancer Res.* 81:660-667.

Salminen E, Hogg A, Binns D, Frydenberg M, Hicks R (2002). Investigations with FDG-PET scanning in prostate cancer show limited value for clinical practice. *Acta Oncol.* 41:425-429.

Sapra P, Allen TM (2003). Ligand-targeted liposomal anticancer drugs. *Prog. Lipid Res.* 42:439-462.

Sarkar N, Banerjee J, Hanson AJ, Elegbede AI, Rosendaht T, Krueger AB, Banerjee AL, Tobwala S, Wang R, Lu X, Mallik S, Srivastava DK (2008). Matrix metalloproteinase-assisted triggered release of liposomal contents. *Bioconjugate Chem.* 19:57-64.

Sarkar NR, Rosendahl T, Krueger AB, Banerjee AL, Benton K, Mallik S, Srivastava DK (2004). "Uncorking" of liposomes by matrix metalloproteinase-9. *Chem. Commun.* 8:999-1001.

Saul JM, Annapragada A, Natarajan JV, Bellamkonda RV (2003). Controlled targeting of liposomal doxorubicin via the folate receptor in vitro. *J. Controlled Release* 92:49-67.

Schnell O, Krebs B, Wagner E, Romagna A, Beer AJ, Grau SJ, Thon N, Goetz C, Kretzschmar HA, Tonn J-C, Goldbrunner RH (2008). Expression of integrin $\alpha_v\beta_5$ in gliomas correlates with tumor grade and is not restriced to tumor vasculature. *Brain Pathology* 18:378-386.

Schroeder A, Kost J, Barenholz Y (2009). Ultrasound, liposomes, and drug delivery: Principles for using ultrasound to control the release of drugs from liposomes. *Chem. Phys. Lipids* 162:1-16.

Schultz MK, Parameswarappa SG, Pigge FC (2010). Synthesis of a DOTA-biotin conjugate for radionuclide chelation via Cu-free click chemistry. *Org. Lett.* 12:2398-2401.

Senior J, Gregoriadis G (1982). Is half-life of circulating liposomes determined by changes in the permeability? *FEBS Lett.* 145:109-114.

Seo JW, Qin S, Mahakian LM, Watson KD, Kheirolomoom A, Ferrara KW (2011). Positron emission tomography imaging of the stability of Cu-64 labeled dipalmitoyl and distearoyl lipids in liposomes. *J. Controlled Release* 151:28-34.

Sharpless WD, Wu P, Hansen TV, Lindberg JG (2005). Just click it: Undergraduate procedures for the copper(I)-catalyzed formation of 1,2,3-triazoles from azides and terminal acetylenes. *J. Chem. Educ.* 82:1833-1836.

Shea KJ, Kim J-S (1992). Influence of strain on chemical reactivity. Relative reactivity of torsionally strained double bonds in 1,3-dipolar cycloadditions. *J. Am. Chem. Soc.* 114:4846-4855.

Shen L-P. Pictet RL, Rutter WJ (1982). Human somatostatin I: Sequence of the cDNA. *Proc. Natl. Acad. Sci. U.S.A.* 79:4575-4579.

Shimada K, Kamps JAAM, Regts J, Ikeda K, Shiozawa T, Hirota S, Scherphof GL (1997). Biodistribution of liposomes containing synthetic galactose-terminated diacylglycerol-poly(ethyleneglycol)s. *Biochim. Biophys. Acta* 1326:329-341.

Shin J, Shum P, Thompson DH (2003). Acid-triggered release via dePEGylation of DOPE liposomes containing acid-labile vinyl ether PEG lipids. *J. Controlled Release* 91:187-200.

Sridhar M, Narsaiah C, Raveendra J, Reddy GK, Reddy MKK, Ramanaiah BC (2011). Efficient microwave-assisted synthesis of oximes from acetohydroxamic acid and carbonyl compounds using $BF_3 \cdot OEt_2$ as the catalyst. *Tetrahedron Lett.* 52:4701-4704.

Terada T, Iwai M, Kawakami S, Yamashita F, Hashida M (2006). Novel PEG-matrix metalloproteinase-2 cleavable peptide-lipid containing galactosylated liposomes for hepatocellular carcinoma-selective targeting. *J. Controlled Release* 111:333-342.

Torchilin VP, Goldmacher VS, Smirnov VN (1978). Comparative studies on covalent and noncovalent immobilization of protein molecules on the surface of liposomes. *Biochem. Biophys. Res. Commun.* 85:983-990.

Torchilin VP, Klibanov AL, Huang L, O'Donnell S, Nossiff ND, Khaw BA (1992). Targeted accumulation of polyethylene glycol coated immunoliposomes in infarcted rabbit myocardium. *FASEB J.* 6:2716-2719.

Torchilin VP, Omelyanenko VG, Papisov MI, Bogdanov AA, Trubetskoy VS, Herron H`JN, Gentry CA (1994). Poly(ethylene glycol) on the liposome surface: On the mechanism of polymer-coated liposome longevity. *Biochim. Biophys. Acta* 1195:11-20.

Tornøe CW, Christensen C, Meldal M (2002). Peptidotriazoles on solid phase: [1,2,3]-triazoles by regiospecific copper(I)-catalyzed 1,3-dipolar cycloadditions of terminal alkynes to azides. *J. Org. Chem.* 67:3057-3064.

Tornøe CW, Meldal M (2001). Peptidotriazoles: Copper(I)-catalyzed 1,3-dipolar cycloadditions on solid-phase. In: Peptides 2001, Proc. Am. Pept. Symp.; American Peptide Society and Kluwer Academic Publishers, San Diego, pp 263-264.

Troutman TS, Barton JK, Romanowski M (2008). Biodegradable plasmon resonant nanoshells. *Adv. Mater.* 20:2604-2608.

Tsuji A, Toshikawa T, Nishide K, Minami H, Kimura M, Nakashima E, Terasaki T, Miyamoto E, Nightingale CH, Yamana T (1983). Physiologically based pharmacokinetic model for β-lactam antibiotics I: Tissue distribution and elimination in rats. *J. Pharm. Sci*. 72:1239-1252.

Uster PS, Deamer DW (1985). pH-dependent fusion of liposomes using titratable polycations. *Biochemistry* 24:1-8.

Veber DF, Saperstein R, Nutt RF, Freidinger RM, Nramdy SF, Curley P, Perlow DS, Paleveda WJ, Colton CD, Zacchei AG, Tocco DJ, Hoff DR, Vandlen RL, Gerich JE, Hall L, Mandarino L, Cordes EH, Anderson PS, Hirschmann R (1984). A super active cyclic hexapeptide analog of somatostatin. *Life Science* 34:1371-1378.

Villar AV, Goñi FM, Alonso A (2001). Diacylglycerol effects on phosphatidylinositol-specific phospholipase C activity and vesicle fusion. *FEBS Lett.* 494:117-120.

Volante M, Rosas R, Allìa E, Granata R, Baragli A, Muccioli G, Papotti M (2008). Somatostatin, cortistatin and their receptors in tumours. *Mol. Cell. Endocrinol.* 286:219-229.

Weitman SD, Lark RH, Coney LR, Fort DW, Frasca V, Zurawski VR, Kamen BA (1992). Distribution of the folate receptor GP38 in normal and malignant cell lines and tissues. *Cancer Res.* 52:3396-3401.

Weitman SD, Weinberg AG, Coney LR, Zurawski VR, Jennings DS, Kamen BA (1992). Cellular localization of the folate receptor: Potential role in drug toxicity and folate homeostasis. *Cancer Res.* 52:6708-6711.

Wheeler JJ, Palmer L, Ossanlou M, MacLachlan I, Graham RW, Zhang YP, Hope MJ, Scherrer P, Cullis PR (1999). Stabilized plasmid-lipid particles: Construction and characterization. *Gene Therapy* 6:271-281.

Widmaier EP, Raff H, Strang KT. Vander, Sherman, Luciano. Human Physiology: The Mechanisms of Body Function. McGraw Hill, New York, 9th edition, 2004.

Williams HA, Robinson S, Julyan P, Zweit J, Hastings D (2005). A comparison of PET imaging characteristics of various copper radioisotopes. *Eur. J. Nucl. Med. Mol. Imaging* 32:1473-1480.

Woodle MC, Lasic DD (1992) Sterically stabilized liposomes. *Biochim. Biophys. Acta* 1113:171-199.
www.iarc.fr.

Xiong J-P, Stehle T, Zhang R, Joachimiak A, Frech M, Goodman SL, Arnaout MA (2002). Crystal structure of the extracellular segment of integrin $\alpha_v\beta_3$ in complex with an arg-gly-asp ligang. *Science* 296 151-155.

Xu H, Deng Y, Chen D, Hong W, Lu Y, Dong X (2008). Esterase-catalyzed dePEGylation of pH-sensitive vesicles modified with cleavable PEG-lipid derivatives. *J. Controlled Release* 130:238-245.
Yagi N, Ogawa Y, Kodaka M, Okada T, Tomohiro T, Konakahara T, Okuno H (2000). Preparation of functional liposomes with peptide ligands and their binding to cell membranes. *Lipids* 35:673-679.

Ye Y, Bloch S, Xu B, Achilefu S (2006). Design, synthesis, and evaluation of near infrared fluorescent multimeric RGD peptides for targeting tumors. *J. Med. Chem.* 49:2268-2275.

Yuan F, Dellian M, Fukumura D, Leunig M, Berk DA, Torchilin VP, Jain RK (1995). Vascular permeability in a human tumor xenograft: Moleculer size dependence and cutoff size. *Cancer Res.* 55:3752-3756.

Zabner J, Fasbender AJ, Moninger T, Poellinger KA, Welsh MJ (1995). Cellular and molecular barriers to gene transfer by a cationic lipid. *J. Biol. Chem.* 270:18997-19007.

Zalipsky S (1993). Synthesis of an end-group functionalized polythylene glycol-lipid conjugate for preparation of polymer-grafted liposomes. *Bioconjugate Chem.* 4:296-299.

Zhu J, Xue J, Guo Z, Zhang L, Marchant RE (2007). Biomimetic glycoliposomes as nanocarriers for targeting P-selectin in activated platelets. *Bioconjugate Chem*. 18:1366-1369.

Zignani M, Drummond DC, Meyer O, Hong K, Leroux J-C (2000). *In vitro* characterization of a novel polymeric-based pH-sensitive liposome system. *Biochim. Biophys. Acta* 1463:383-394.

Appendix I

Publications

Article I

Feldborg LN, Jølck RI, Andresen TL (2012). Quantitative evaluation of bioorthogonal chemistries for surface functionalization of nanoparticles. *Bioconjugate Chem.* 23:2444-2450.

Article II

Jølck RI, Feldborg LN, Andersen S, Moghimi SM, Andresen TL (2011). Engineering liposomes and nanoparticles for biological targeting. *Adv. Biochem. Engin./Biotechnol.* 125:251-280.

Article III

Henriksen JR, Feldborg LN, Andresen TL, Duelund L, Ipsen JH (2010). Understanding detergent effects on lipid membranes: A model study of lysolipids. *Biophys. J.* 98:2199-2205.

Article I

Paper published in Bioconjugate Chemistry 2012.

This paper was prepared in collaboration with Rasmus I. Jølck and Thomas L. Andresen. Jølck was responsible for the synthesis and characterization of the different functional peptides, while Feldborg planned and performed the conjugation reactions and treated the data. Feldborg wrote the paper in collaboration with Jølck and Andresen.

This paper is a part of Chapter two.

Bioconjugate Chemistry

pubs.acs.org/bc December 2012 Volume 23, Number 12

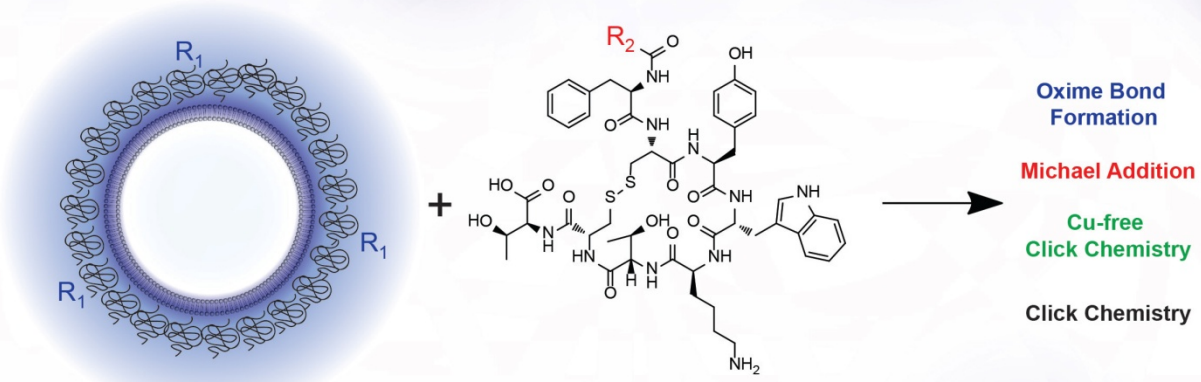

R¹= alkyne, cyclooctyne, azide, thiol, maleimide or aldehyde

R² = alkyne, azide, thiol, maleimide or hydroxylamine

ACS Publications
MOST TRUSTED. MOST CITED. MOST READ.
www.acs.org

Bioconjugate Chemistry

Article

pubs.acs.org/bc

Quantitative Evaluation of Bioorthogonal Chemistries for Surface Functionalization of Nanoparticles

Lise N. Feldborg,[†] Rasmus I. Jølck,[†] and Thomas L. Andresen*

DTU Nanotech, Department of Micro- and Nanotechnology, Technical University of Denmark, Building 423 2800 Lyngby, Denmark

Supporting Information

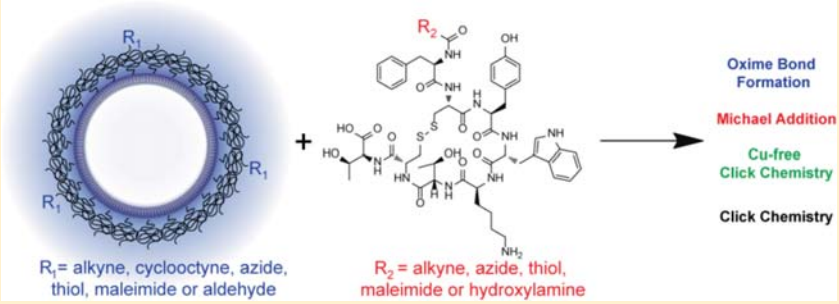

ABSTRACT: We present here a highly efficient and chemoselective liposome functionalization method based on oxime bond formation between a hydroxylamine and an aldehyde-modified lipid component. We have conducted a systematic and quantitative comparison of this new approach with other state-of-the-art conjugation reactions in the field. Targeted liposomes that recognize overexpressed receptors or antigens on diseased cells have great potential in therapeutic and diagnostic applications. However, chemical modifications of nanoparticle surfaces by postfunctionalization approaches are less effective than in solution and often not high-yielding. In addition, the conjugation efficiency is often challenging to characterize and therefore not addressed in many reports. We present here an investigation of PEGylated liposomes functionalized with a neuroendocrine tumor targeting peptide (TATE), synthesized with a variety of functionalities that have been used for surface conjugation of nanoparticles. The reaction kinetics and overall yield were quantified by HPLC. Reactions were conducted in solution as well as by postfunctionalization of liposomes in order to study the effects of steric hindrance and possible affinity between the peptide and the liposome surface. These studies demonstrate the importance of choosing the correct chemistry in order to obtain a quantitative surface functionalization of liposomes.

INTRODUCTION

Functional nanomaterials have attracted considerable attention due to their highly interesting properties in relation to diagnostic,[1−3] sensor,[4,5] imaging,[6,7] vaccine,[8] and drug delivery applications.[9,10] Within the drug delivery field, liposomes have particularly advantageous properties.[11] However, despite positive results obtained by exploiting the EPR-effect,[12] numerous methods to improve drug bioavailability in the diseased tissue, while maintaining stable liposomes during circulation, is currently being investigated. By coating the liposome surfaces with targeting ligands such as antibodies,[13,14] peptides,[15] proteins,[16] polysaccharides,[17] lectins,[18] and vitamin analogues,[19,20] which are recognized by antigens or receptors selectively, or overexpressed in, e.g., tumor tissue, increased drug accumulation in tumors can be achieved. Numerous bioconjugation methods have been established to surface-modify liposomes with targeting ligands to enhance tissue specificity. To ensure correct orientation of the targeting ligand, bioorthogonal and site-specific surface reactions are required. By the incorporation of unnatural amino acids in peptide or protein sequences,[21] introduction of unnatural functional groups such as maleimides for Michael addition, azides for copper(I)-catalyzed Huisgen 1,3-dipolar cycloaddition[22−24] (CuAAC) or Staudinger ligation using triphosphines,[25,26] controlled display of surface ligands can be obtained. Unfortunately, ligand conjugation to the surface of nanoparticles can suffer from low reproducibility and highly varying yields; e.g., we have previously found that it can be very difficult to control the Michael addition of a somatostatin receptor targeting peptide (TATE) to a lipid moiety, even though the maleimide-based Michael addition is one of the most utilized conjugation chemistries for peptides and proteins.[27,28] As a consequence hereof, we have conducted a systematic study on a variety of generally applied conjugation reactions using HPLC as a method to follow and quantify the reactions both in solution and by direct conjugation to the liposomal surface. Reactions conducted directly on liposome surfaces are likely not to show the same reaction kinetics as ones preformed in

Received: September 8, 2012
Revised: October 24, 2012
Published: November 16, 2012

solution, and the yield of functionalization will not necessarily be quantitative and has to be determined case by case.

In this study, we furthermore introduce a novel highly selective and bioorthogonal conjugation reaction relevant for the surface functionalization of liposomes. We show a fast and quantitative coupling of a hydroxylamine functionalized peptide to an aldehyde-modified liposome, a strategy for coating liposomes, which to our knowledge has not previously been reported. In addition, we show a large dependency on the relative position of the conjugation functionalities. A knowledge which we believe is highly useful when designing new functionalized liposomal systems or other functional nanomaterials.

EXPERIMENTAL PROCEDURES

Synthesis of Functionalized TATE Peptides. The functionalized TATE peptides **1a−e** were synthesized manually by using a Wang Resin preloaded with NH_2-Thr(*t*Bu)-OH by standard Fmoc methodology. Each coupling was performed by activating the Fmoc protected amino acid with *O*-(7-azabenzotriazol-1-yl)-*N*,*N*,*N*′,*N*′-tetramethyluronium hexafluorophosphate (HATU) in the presence of 2,4,6-collidine in DMF. Cleavage of the Fmoc group was carried out using piperidine in DMF. Completion of each coupling and deprotection step was monitored by the Kaiser test. Removal of the acetamidomethyl (Acm) protection groups on the two cysteines and simultaneous disulfide bond formation was achieved by addition of $Tl(CF_3COO)_3$ in DMF. The resin containing the cyclized peptide was extensively washed with DMF and subsequently divided into five solid-phase peptide synthesis (SPPS) reaction vials in which the N-terminal was acylated with the desired functionality, cleaved from the solid support, and purified by HPLC. Full experimental details and peptide characterization are available as Supporting Information.

Synthesis of Functionalized DSPE-PEG_{2000} Phospholipids. Functionalized DSPE-PEG_{2000} phospholipids **2a−d** were synthesized in a single step from DSPE-PEG_{2000}-NH_2 by acylation of the amino group with the desired functionality in the presence of either HATU or EDC·HCl. Phospholipid **3** was synthesized in a single step from DSPE-PEG_{2000}-PDP by reduction by dithiothreitol (DTT). Full experimental details and lipid characterization are available as Supporting Information.

Liposome Formulation. Lipids were dissolved in CH_3Cl/MeOH (9:1) and mixed in the ratio 95:4:1 DSPC/DSPE-PEG_{2000}/DSPE-PEG_{2000}-R (R being the different functional groups illustrated in Schemes 2 and 3). The solvent was removed under a stream of nitrogen and the films placed under vacuum overnight to remove remaining traces of organic solvent. The obtained films were hydrated in a Hepes buffer, (10 mM Hepes, pH 6.5, 145 mM NaCl) at 65 °C for 1 h; followed by 10 freeze−thaw cycles and extrusion at 65 °C through a 100 nm polycarbonate filter using an Avanti Polar Lipids mini-extruder. The size distribution of the liposomes was analyzed using dynamic light scattering, as well as their zeta potential using a Brookhaven Zeta PALS analyzer. All sizes were 100−120 nm and all zeta potentials were slightly negative (approximately −5 mV).

Conjugation in Solution. DSPE-PEG_{2000} functionalized lipid (0.2 mM, 0.55 mL, 1.1 equiv.) was dissolved in MeOH and mixed with the corresponding functionalized TATE in MeOH (0.2 mM, 0.50 mL, 1.0 equiv.). The reaction was stirred at room temperature and aliquots (50 μL) were removed at the indicated times and analyzed by analytical HPLC. A linear gradient was used from 100% A (aqueous solution containing 5% MeCN and 0.1% TFA) to 100% B (MeCN containing 0.1% TFA) over 15 min with a flow rate of 1 mL/min and AUC for the free TATE was measured relative to AUC for the coupled product at 280 nm. For the reaction between the maleimide and thiol functionalities Et_3N (50 mM, 6.0 μL, 3.0 equiv.) was added to facilitate the coupling, while for the copper catalyzed click reactions $CuSO_4{\cdot}5H_2O$ (1.0 M, 2.5 μL, 25 equiv.) and sodium ascorbate (1.0 M, 5.0 μL, 50 equiv.) were added. Before injecting the aliquots from the copper catalyzed click reactions onto the analytical HPLC column 20 μL of a 10% NH_4OH solution was added to ensure the copper ions were in solution and not interfering with the HPLC signals.[29]

Conjugation by Post-Functionalization of Liposomes. Preformed functionalized liposomes ((25 mM, 0.50 mL, 1.1 equiv.) - normalized according to a 45:55 distribution ratio between the inner- and outer liposomal membrane) were mixed with the corresponding TATE peptide (4.2 mM, 15 μL, 1.0 equiv.) dissolved in MeOH. The reactions were shaken (not stirred; to avoid foaming) at room temperature and aliquots (40 μL) removed for analysis by analytical HPLC. A linear gradient was used from 100% A (aqueous solution containing 5% MeCN and 0.1% TFA) to 100% B (MeCN containing 0.1% TFA) over 15 min with a flow rate of 1 mL/min. The AUC for the free TATE was calculated relative to the AUC of the phospholipid coupled product at 280 nm to monitor the conjugation efficiency. For the copper catalyzed click reactions $CuSO_4{\cdot}5H_2O$ (1.0 M, 1.6 μL, 25 equiv.) and sodium ascorbate (1.0 M, 3.1 μL, 50 equiv.) were added. As for the conjugations done in solution 20 μL of a 10% NH_4OH solution was added to the copper catalyzed click aliquots prior to HPLC analysis.

RESULTS AND DISCUSSION

Synthesis and Characterization. The model peptides **1a−1e** for somatostatin receptor targeting[30] were prepared using a SPPS strategy as shown in Scheme 1.[31] The N-terminal functionalized TATE peptides **1a−e** were synthesized by SPPS on H-Thr(*t*Bu)-OH preloaded Wang Resin. Acylation of the N-terminal of the peptide was achieved by activating the Fmoc-protected amino acid with HATU to ensure high conversion with minimum epimerization. After assembly of the resin immobilized octapeptide, H-D-Phe-Cys(Acm)-Tyr(*t*Bu)-D-Trp-(Boc)-Lys(Boc)-Thr(*t*Bu)-Cys(Acm)-Thr(*t*Bu)-resin, the peptide was treated with $Tl(CF_3COO)_3$, which in a single step removed the two Acm-protection groups present on the cysteine residues and formed the intramolecular disulfide bond. The reaction was followed by cleavage of a small amount of peptide from the resin with TFA and analyzing the crude peptide by MALDI-TOF MS. Complete Acm-removal and disulfide formation were observed after 75 min with no sign of dimerization. After extensive washing of the resin, the N-terminal was acylated with the desired carboxylic acid functionalized linker derivatives and cleaved from the solid support by treatment with a mixture of TFA/H_2O/TIS (95:2.5:2.5) to give the desired functionalized TATE peptides **1a−e**. Final purification of the peptides was accomplished by HPLC and the obtained products **1a−e** characterized by MALDI-TOF MS (Table 1). In order to formulate liposomes exposing the appropriate chemical functionalities at the distal end of the PEG-corona, PEGylated phospholipids with the desired functionalities were synthesized from either DSPE-

dx.doi.org/10.1021/bc3005057 | *Bioconjugate Chem.* 2012, 23, 2444−2450

Scheme 1. Synthesis of the TATE-Derivatives 1a−1e

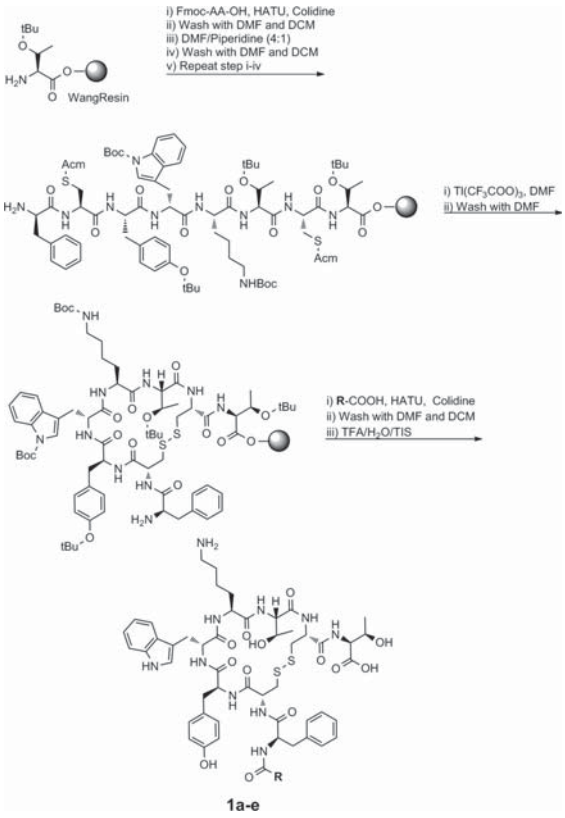

Table 1. Chemical Structure of R-COOH Used for Synthesis of TATE Derivatives 1a−1e and Corresponding Characterization by MALDI TOF MS

Compound #	R_1	MS (M+Na)$^+$ (cald.)	MS (M+Na)$^+$ (found)
1a	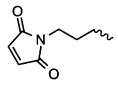	1236.35	1236.39
1b		1159.33	1159.57
1c	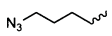	1196.33	1196.60
1d		1129.31	1129.47
1e		1144.25	1144.41

PEG_{2000}-NH_2 or DSPE-PEG_{2000}-PDP as illustrated in Schemes 2 and 3. PEGylated phospholipids exposing a terminal alkyne, a cyclic alkyne, an aldehyde, or an azide functionality at the distal end of the polymer (**2a−d**) were synthesized by acylating DSPE-PEG_{2000}-NH_2 with 4-pentynoic acid, 1-fluorocyclooct-2-ynecarboxylic acid, 4-carboxybenzaldehyde, or 5-azidopentanoic acid, respectively. 1-Fluorocyclooct-2-ynecarboxylic acid was synthesized as described elsewhere.[32] DSPE-PEG_{2000}-SH (**3**) was synthesized in a single step from DSPE-PEG_{2000}-PDP by reduction of the pyridyldithiopropionate (PDP) group by DTT applying standard conditions[33] which resulted in the desired free thiol (Scheme 3). The DSPE-PEG_{2000}-maleimide (**4**) functionalized phospholipid was purchased from Avanti Polar Lipids, Inc., Alabama.

Scheme 2. Synthesis of the DSPE-PEG_{2000}-NH_2 Modified Phospholipids 2a−d

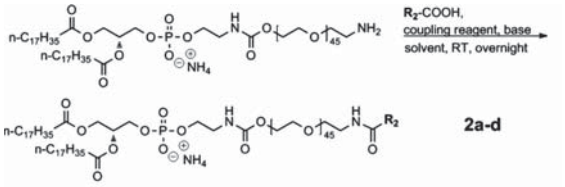

Compound #	R_2	Coupling reagent	Base	Solvent
2a		EDC·HCl	DMAP	CH_2Cl_2
2b		HATU	Et_3N	DMF
2c	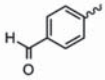	HATU	Et_3N	DMF
2d		HATU	Et_3N	DMF

Scheme 3. Synthesis of the DSPE-PEG_{2000}-SH (3) Functionalized Phospholipid

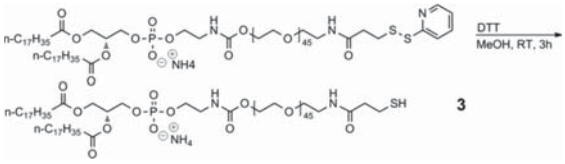

In order to evaluate the efficiency of the different coupling strategies and make a valid comparison, a standardized protocol was used to minimize the influence of other parameters. Functionalized liposomes composed of DSPC/DSPE-PEG_{2000}/DSPE-PEG_{2000}-R (95:4:1) (R = alkyne (**2a**), cycloalkyne (**2b**), aldehyde (**2c**), azide (**2d**), thiol (**3**), or maleimide (**4**)) were prepared by the method described by Bangham and co-workers.[34] The lipid components were dissolved in a mixture of $CHCl_3$/MeOH (9:1), and the solvent was removed to form a transparent lipid film. The lipid film was hydrated in HEPES-buffer (pH 6.5) at 65 °C and extruded through 100 nm polycarbonate filters to form liposomes in the 100 nm range. The liposomes were characterized by dynamic light scattering (DLS), and the ζ-potentials were measured to ensure that liposomes were formed. All liposomes had a diameter of approximately 100 nm and slightly negative ζ-potential due to the presence of the DSPE-PEG_{2000} lipids. Postfunctionalization was carried out by adding the required components for the individual reactions (e.g., $CuSO_4 \cdot 5H_2O$ and sodium ascorbate for the CuAAC reaction), followed by addition of the required functionalized TATE peptide **1a−e** (1 equiv peptide to 1.1 equiv of the functionalized lipid component) in MeOH. Postfunctionalization reactions were carried out at room temperature and carefully mixed using a plate shaker.

dx.doi.org/10.1021/bc3005057 | *Bioconjugate Chem.* 2012, 23, 2444−2450

For the conjugation reactions in solution, functionalized phospholipids (1.1 equiv) and functionalized TATE peptides (1 equiv) were dissolved in methanol, mixed with the required additives to facilitate reaction, as described in the Experimental Procedures, and stirred at room temperature. Triplicates of all reactions were carried out to ensure reproducibility and elucidate the heterogeneity of liposomal postfunctionalization. The amount of functionalized TATE added in the two conjugation approaches was carefully controlled by measuring the concentration of the peptide stock solution by UV−vis, thus ensuring exactly the same peptide concentration in all reactions. To ensure the same total concentration of phospholipids in all reactions, phosphorus content measurement was carried out by ICP-AES. All reactions were monitored for 24 h by HPLC using UV-detection (λ = 280 nm), and up to 72 h in selected cases, by removing small aliquots from the reaction vial, and the conjugation efficiency was calculated based on the area under the curve (AUC) for the free peptide and the DSPE-PEG_{2000}-TATE conjugate, respectively (Figure 1). MALDI-TOF MS was used to verify that an excess of the functionalized phospholipids reagent existed in all reactions that did not go to completion within 72 h.

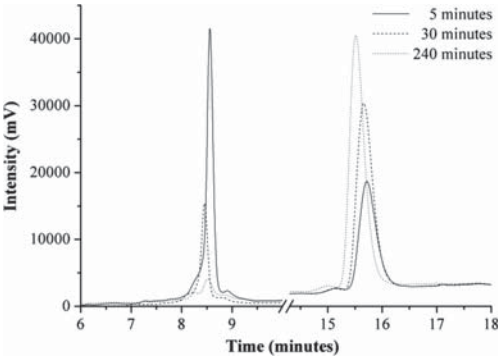

Figure 1. Example of the monitoring of a conjugation reaction by HPLC over time at 280 nm. The decreasing peak at 8.5 min belongs to the free TATE-maleimide (**1a**), while the peak increasing at 15.6 min is the product from the Michael addition between TATE-maleimide (**1a**) and DSPE-PEG_{2000}-SH (**3**).

Conjugation of TATE and DSPE-PEG_{2000} by Oxime Formation. This method, which has not previously been reported for the surface functionalization of liposomes, is chemoselective and bioorthogonal to functional groups in most natural occurring ligands and could serve as an excellent alternative to existing liposome postfunctionalization methods.[35] TATE-hydroxylamine (**1e**) and DSPE-PEG_{2000}-benzaldehyde (**2c**) were conjugated, both in solution and on the liposome surface, by simply mixing the two components without any additives. Oxime bond formation in solution was found to be quantitative within one hour, whereas eight hours of incubation was needed once performed directly on the liposome surface (Figure 2). Both procedures resulted in complete conversion to the phospholipid coupled TATE within 24 h under mild conditions.

Oxime bond formation is known to be accelerated by the presence of aniline,[36] acetic acid,[37] or Lewis acids.[38] In order to verify this, acetic acid (0.1% v/v) was added to a liposome batch containing TATE-hydroxylamine (**1e**). Under these

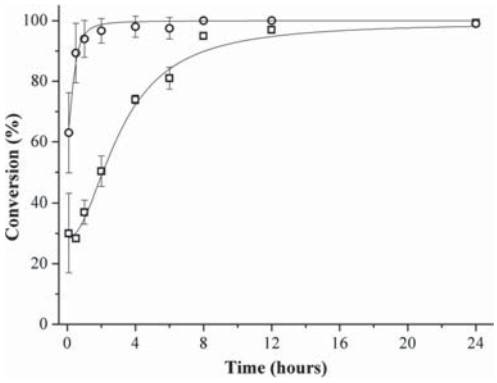

Figure 2. Conjugation of DSPE-PEG_{2000} and TATE by oxime bond formation. Reactions carried out in solution and directly on the liposome surface. TATE-hydroxylamine (**1e**) + DSPE-PEG_{2000}-benzaldehyde (**2c**) in solution (○), TATE-hydroxylamine (**1e**) + DSPE-PEG_{2000}-benzaldehyde (**2c**) on liposomes (□). All values are means ± SEM (n = 3).

conditions, the conjugation yield reached 78% within 5 min. Without the presence of the catalyst, 30% conversion was observed within the same time frame. The oxime bond formation is a reversible process; however, HPLC and MALDI TOF MS did not show any reversible formation of the starting materials within one week in aqueous medium, which supports the reporting of oxime bonds to be more hydrolytically stable than, e.g., its analogous hydrazine bond at physiologically relevant pH.[39] The position of these two functional groups is not interchangeable, as placing the aldehyde functionality on TATE will induce the risk of intramolecular imine formation.

Conjugation of TATE and DSPE-PEG_{2000} by CuAAC. An often applied procedure for nanoparticle functionalization is the CuAAC reaction—commonly referred to as the Click Reaction.[22−24] Conjugation of TATE and DSPE-PEG_{2000} by the CuAAC reaction was carried out using sodium ascorbate to generate Cu^{I} from $CuSO_4 \cdot 5H_2O$ in situ. Reactions were carried out with the azide present on the TATE peptide, the alkyne at the PEG terminal of DSPE-PEG_{2000}, and vice versa. The relative position of the functional moieties was found to have no significant effect on the reaction efficacy under the solution conditions, as both orientations result in approximately 98% yield after 12 h (Figure 3). A different result was obtained when monitoring the postfunctionalization reaction on the liposome surface. The cycloaddition between the azide-functionalized TATE (**1c**) and the alkyne-modified phospholipid (**2a**) resulted in about 75% yield after 2 h, while the opposite position having the azide functionality present on the liposomes and the alkyne at the N-terminal of the peptides leveled out at 43% (Figure 3).

Functionalization of azide-modified liposomes by the CuAAC reaction has not previously been reported elsewhere to our knowledge. Functionalization of liposomes by the CuAAC reaction has consistently been carried out with alkyne-modified liposomes and azide-functionalized ligands; thus, these reports have not observed the clear negative trend observed here with the azide-functionalized liposomes. Furthermore, removing the copper fully from the final product to avoid copper induced cytotoxicity can be challenging, which

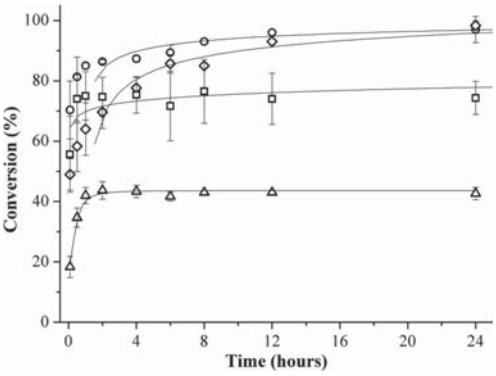

Figure 3. Conjugation of DSPE-PEG$_{2000}$ and TATE by the CuAAC reaction. Reactions carried out in solution and directly on the liposome surface. TATE-azide (**1c**) + DSPE-PEG$_{2000}$-alkyne (**2a**) in solution (○), TATE-azide (**1c**) + DSPE-PEG$_{2000}$-alkyne (**2a**) on liposomes (□), TATE-alkyne (**1d**) + DSPE-PEG$_{2000}$-azide (**2d**) in solution (◊), TATE-alkyne (**1d**) + DSPE-PEG$_{2000}$-azide (**2d**) on liposomes (Δ). All values are means ± SEM (n = 3).

to some degree reduces the usability of this reaction for biological purposes.

Conjugation of TATE and DSPE-PEG$_{2000}$ by Cu-Free Click Chemistry. A method to avoid addition of toxic copper salts as catalyst in the triazole formation is to use strained or electron-deficient alkynes.[40,41] This strategy was studied using the DSPE-PEG$_{2000}$-cyclooctyne (**2b**) and azide-functionalized TATE (**1c**). In solution, the conjugation was remarkably slow, yet highly reliable and reproducible with no form of decomposition or side product formation. As the reaction was terminated after 50 days, a product yield of 86% was obtained without reaching a plateau. Applying the post-functionalization protocol resulted in a remarkably faster initial reaction (Figure 4), and a level of 84% yield was reached after 72 h.

Interestingly, triazole formation was significantly faster when performed on liposome surfaces compared to the reaction in solution. This is presumably due to favorable interactions between the liposome surface and TATE-azide (**1c**). As TATE-azide (**1c**) is not highly soluble in the buffer, it prefers to bind to the PEG layer, bringing it closer to the reaction sites on the surface, which leads to a faster reaction. Choosing a more reactive cyclooctyne could not only increase the reaction rate in solution, but also increase the risk of side product formation.[42,43] However, a relatively long synthetic procedure to obtain the cyclooctyne moiety limits the use of this type of copper-free click reaction. Furthermore, it has been shown that thiols can add spontaneously to cyclooctynes limiting the bioorthogonality, as some degree of nonspecific reactions can occur.[44]

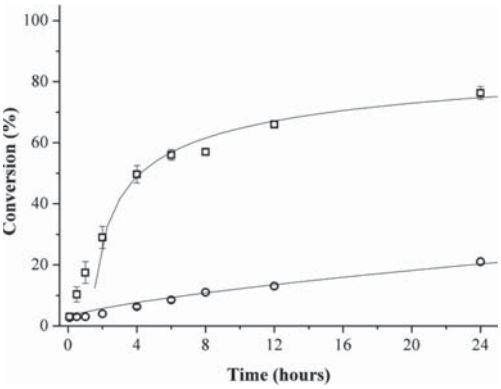

Figure 4. Conjugation of DSPE-PEG$_{2000}$ and TATE by strain-promoted Click reaction. Reactions were carried out in solution and directly on the liposome surface. TATE-azide (**1c**) + DSPE-PEG$_{2000}$-cyclooctyne (**2b**) in solution (○), TATE-azide (**1c**) + DSPE-PEG$_{2000}$-cyclooctyne (**2b**) on liposomes (□). All values are means ± SEM (n = 3).

Conjugation of TATE and DSPE-PEG$_{2000}$ by Michael Addition. The final approach tested to conjugate TATE and DSPE-PEG$_{2000}$ was using the Michael addition procedure. In general, the Michael addition proceeded rapidly within the first four hours until reaching a plateau, and reactions carried out in solution were slightly faster compared to the liposomal counterpart. The orientation of the maleimide and the thiol was found to have a decisive impact on the conjugation efficiency. Michael addition in solution between DSPE-PEG$_{2000}$-SH (**3**) and TATE-maleimide (**1a**) resulted in 97% conversion, whereas when performed on the liposome surface, 92% conversion was observed. The opposite orientation of functionalities expressed in the form of DSPE-PEG$_{2000}$-maleimide (**4**) and TATE-thiol (**1b**) only resulted in 53% product formation when performed in solution and 40% for the postfunctionalization of liposomes (Figure 5), which was surprising. The origin for this observation is not clear, however; multiple factors could have caused this drop in conversion. Hydrolysis of the maleimide moiety to the nonreactive maleamic acid at pH > 8.5 has been reported in the literature,[45] but at pH 6.5 where our reactions are carried out, this should be minimized.[46,47] This was confirmed by MALDI-TOF MS where intact DSPE-PEG$_{2000}$-maleimide as well as unreacted TATE-SH was observed. However, a minor amount of methoxy-substituted maleimide was also observed by MALDI-TOF MS indicating that the oxa-Michael addition is a competing side

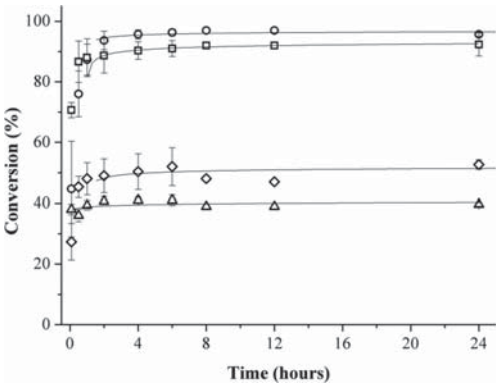

Figure 5. Conjugation of DSPE-PEG$_{2000}$ and TATE by Michael addition. Reactions carried out in solution and directly on the liposome surface. TATE-maleimide (**1a**) + DSPE-PEG$_{2000}$-SH (**3**) in solution (○), TATE-maleimide (**1a**) + DSPE-PEG$_{2000}$-SH (**3**) on liposomes (□), TATE-thiol (**1b**) + DSPE-PEG$_{2000}$-maleimide (**4**) in solution (◊), TATE-thiol (**1b**) + DSPE-PEG$_{2000}$-maleimide (**4**) on liposomes (Δ). All values are means ± SEM (n = 3).

reaction.[48] As poor conversion was observed for the reaction carried out in solution as well as on the surface, we speculated that the TATE-thiol (**1b**) peptide was the limiting factor in this reaction. TATE-thiol (**1b**) is highly prone to oxidation resulting in nonreactive TATE-dimers; however, dimerization was not observed by HPLC or by MALDI-TOF MS. As a positive control of the reactivity of the commercial DSPE-PEG_{2000}-maleimide (**4**), a test reaction using 2-mercaptoethanol was conducted. Using this small and highly reactive thiol, complete product formation was observed within two hours as confirmed by MALDI-TOF MS, confirming excellent reactivity of DSPE-PEG_{2000}-maleimide (**4**). Hence, the reason for the low coupling efficiency between DSPE-PEG_{2000}-maleimide (**4**) and TATE-SH (**1b**) is not clear.

CONCLUSION

In conclusion, a novel highly effective method to functionalize liposomes by postfunctionalization as well as under solution conditions has been introduced in the form of an oxime bond formation between an aldehyde and a hydroxylamine. This conjugation is chemoselective and bioorthogonal to functional groups in most naturally occurring relevant ligands, and based on our investigations, it could serve as an excellent alternative to existing liposome postfunctionalization methods.

In addition, a systematic study has been conducted to elucidate the optimal postfunctionalization chemistry with focus on the relative position of the reactive functionalities. In general, the reactions carried out directly on the surface of the functionalized liposomes were slower than the solution-phase counterpart, except for the strain-promoted Click reaction, which surprisingly showed the opposite trend. Despite of possible heterogeneities of liposomal formulations, surface conjugation reactions were, in general, highly reproducible. The relative position of the reactive functionalities was found to have a significant impact on the degree of conversion for the Michael addition and the CuAAC reaction. The Michael addition was found to be most effective when the nucleophilic thiol was present at the distal end of the PEG polymer compared to the N-terminal of TATE. A similar observation was observed for the CuAAC reaction. The relative positions of the azide and the alkyne did not influence the degree of conversion in solution; however, once performed on the liposome surface it had a decisive impact. Having the alkyne functionality present at the liposome surface resulted in 75% conversion, whereas the azide functionalized liposomes only resulted in 43% product formation.

The findings described above will be useful for future postfunctionalization designs and clearly illustrate that care should be taken to select the most appropriate chemistry for the desired chemical manipulation. Furthermore, it is also evident that postfunctionalized nanoparticles in general should always be analyzed in order to ensure the desired composition of the nanoparticle constructs.

ASSOCIATED CONTENT

Supporting Information

Detailed description of the synthetic approach to compounds **1a–e**, **2a–d**, **3** and their characterization (^{1}H NMR, FT-IR, HPLC, and MALDI-TOF MS). This material is available free of charge via the Internet at http://pubs.acs.org.

AUTHOR INFORMATION

Corresponding Author

*E-mail: Thomas.andresen@nanotech.dtu.dk.

Author Contributions

†Authors contributed equally.

Notes

The authors declare no competing financial interest.

ACKNOWLEDGMENTS

The Danish Strategic Research Council (NABIIT) grant 2106-07-0033 and 2106-08-0081 is gratefully acknowledged for funding.

ABBREVIATIONS

EPR, enhanced permeability and retention effect; CuAAC, copper catalyzed azide–alkyne cycloaddition; TATE, [Tyr^3,Thr^8]-octreotate; DSPC, 1,2-distearoyl-*sn*-glycero-3-phosphocholine; DSPE, 1,2-distearoyl-*sn*-glycero-3-phosphoethanolamine; HPLC, high-performance liquid chromatography; SPPS, solid-phase peptide synthesis; MALDI TOF MS, matrix-assisted laser desorption/ionization time-of-flight mass spectroscopy; DLS, dynamic light scattering; ICP-AES, inductively coupled plasma atomic emission spectroscopy.

REFERENCES

(1) Petersen, A. L., Hansen, A. E., Gabizon, A., and Andresen, T. L. (2012) Liposome imaging agents in personalized medicine. *Adv. Drug Delivery Rev. 64*, 1417–1435.

(2) Phillips, M. A., Gran, M. L., and Peppas, N. A. (2010) Targeted nanodelivery of drugs and diagnostics. *Nano Today 5*, 143–159.

(3) Petersen, A. L., Binderup, T., Jølck, R. I., Rasmussen, P., Henriksen, J. R., Pfeifer, A. K., Kjaer, A., and Andresen, T. L. (2012) Positron emission tomography evaluation of somatostatin receptor targeted 64Cu-TATE-liposomes in a human neuroendocrine carcinoma mouse model. *J. Controlled Release 160*, 254–263.

(4) Pavlov, V., Xiao, Y., Shlyahovsky, B., and Willner, I. (2004) Aptamer-functionalized Au nanoparticles for the amplified optical detection of thrombin. *J. Am. Chem. Soc. 126*, 11768–11769.

(5) Liu, J., and Lu, Y. (2006) Preparation of aptamer-linked gold nanoparticle purple aggregates for colorimetric sensing of analytes. *Nat. Protoc. 1*, 246–252.

(6) Taylor, K. M. L., Kim, J. S., Rieter, W. J., An, H., Lin, W., and Lin, W. (2008) Mesoporous silica nanospheres as highly efficient MRI contrast agents. *J. Am. Chem. Soc. 130*, 2154–2155.

(7) Sun, I. C., Eun, D. K., Koo, H., Ko, C. Y., Kim, H. S., Yi, D. K., Choi, K., Kwon, I. C., Kim, K., and Ahn, C. H. (2011) Tumor-targeting gold particles for dual computed tomography/optical cancer imaging. *Angew. Chem., Int. Ed. 50*, 9348–9351.

(8) Muhs, A., Hickman, D. T., Pihlgren, M., Chuard, N., Giriens, V., Meerschman, C., van der Auwera, I., van Leuven, F., Sugawara, M., Weingertner, M. C., Bechinger, B., Greferath, R., Kolonko, N., Nagel-Steger, L., Reisner, D., Brady, R. O., Pfeifer, A., and Nicolau, C. (2007) Liposomal vaccines with conformation-specific amyloid peptide antigens define immune response and efficacy in APP transgenic mice. *Proc. Natl. Acad. Sci. U.S.A. 104*, 9810–9815.

(9) Davis, M. E., Chen, Z. G., and Shin, D. M. (2008) Nanoparticle therapeutics: An emerging treatment modality for cancer. *Nat. Rev. Drug Discovery 7*, 771–782.

(10) Petros, R. A., and DeSimone, J. M. (2010) Strategies in the design of nanoparticles for therapeutic applications. *Nat. Rev. Drug Discovery 9*, 615–627.

(11) Gregoriadis, G., Wills, E. J., Swain, C. P., and Tavill, A. S. (1974) Drug-carrier potential of liposomes in cancer chemotherapy. *Lancet 1*, 1313–1316.

(12) Maeda, H., Wu, J., Sawa, T., Matsumura, Y., and Hori, K. (2000) Tumor vascular permeability and the EPR effect in macromolecular therapeutics. A review. *J. Controlled Release 65*, 271−284.
(13) Koning, G. A., Gorter, A., Scherphof, G. L., and Kamps, J. A. (1999) Antiproliferative effect of immunoliposomes containing 5-fluorodeoxyuridine dipalmitate on colon cancer cells. *Br. J. Cancer 80*, 1718−1725.
(14) Koning, G. A., Morselt, H. W., Gorter, A., Allen, T. M., Zalipsky, S., Scherphof, G. L., and Kamps, J. A. (2003) Interaction of differently designed immunoliposomes with colon cancer cells and Kupffer cells. An in vitro comparison. *Pharm. Res. 20*, 1249−1257.
(15) Nardin, A., Lefebvre, M. L., Labroquère, K., Faure, O., and Abastado., J. P. (2006) Liposomal muramyl tripeptide phosphatidylethanolamine: Targeting and activating macrophages for adjuvant treatment of osteosarcoma. *Curr. Cancer Drug Targets 6*, 123−133.
(16) Chiu, S. J., Liu, S., Perrotti, D., Marcucci, G., and Lee, R. J. (2006) Efficient delivery of a Bcl-2-specific antisense oligodeoxyribonucleotide (G3139) via transferrin receptor-targeted liposomes. *J. Controlled Release 112*, 199−207.
(17) Zhu, J., Xue, J., Guo, Z., Zhang, L., and Marchant, R. E. (2007) Biomimetic glycoliposomes as nanocarries for targeting P-selectin on activated platelets. *Bioconjugate Chem. 18*, 1366−1369.
(18) Matsui, M., Shimizu, Y., Kodera, Y., Kondo, E., Ikehara, Y., and Nakanishi, H. (2010) Targeted delivery of oligomannose-coated liposome to the omental micrometastasis by peritoneal macrophages from patients with gastric cancer. *Cancer Sci. 101*, 1670−1677.
(19) Lee, R. J., and Low, P. S. (1994) Delivery of liposomes into cultured KB cells via folate receptor-mediated endocytosis. *J. Biol. Chem. 269*, 3198−3204.
(20) Sudimack, J., and Lee, R. J. (2000) Targeted drug delivery via the folate receptor. *Adv. Drug Delivery Rev. 41*, 147−162.
(21) O'Donnell, M. J., Zhou, C., and Scott, W. L. (1996) Solid-phase unnatural peptide synthesis. *J. Am. Chem. Soc. 118*, 6070−6071.
(22) Tornøe, C. W., Christensen, C., and Meldal, M. (2002) Peptidotriazoles on solid phase: [1,2,3]-triazoles by regiospecific copper(I)-catalyzed 1,3-dipolar cycloadditions of terminal alkynes to azides. *J. Org. Chem. 67*, 3057−3064.
(23) Meldal, M., and Tornøe, C. W. (2008) Cu-catalyzed azide-alkyne cycloaddition. *Chem. Rev. 108*, 2952−3015.
(24) Rostovtsev, V. V., Green, L. G., Fokin, V. V., and Sharpless, K. B. (2002) A stepwise huisgen cycloaddition process: Copper(I)-catalyzed regioselective "ligation" of azides and terminal alkynes. *Angew. Chem., Int. Ed. 41*, 2596−2599.
(25) Staudinger, H., and Meyer, J. (1919) New organic compounds of phosphorus. III. phosphinemethylene derivatives and phosphinimines. *Helv. Chim. Acta 2*, 635−646.
(26) Saxon, E., and Bertozzi, C. R. (2000) Cell surface engineering by a modified Staudinger reaction. *Science 287*, 2007−2010.
(27) Reubi, J. C., and Maecke, H. R. (2008) Peptide-based probes for cancer imaging. *J. Nucl. Med. 49*, 1735−1738.
(28) Jølck, R. I., Feldborg, L. N., Andersen, S., Moghimi, S. M., and Andresen, T. L. (2011) Engineering liposomes and nanoparticles for biological targeting. *Adv. Biochem. Eng. Biotechnol. 125*, 251−280.
(29) Sharpless, W. D., Wu, P., Hansen, T. V., and Lindberg, J. G. (2005) Just click it: Undergraduate procedures for the copper(I)-catalyzed formation of 1,2,3-triazoles from azides and terminal acetylenes. *J. Chem. Educ. 82*, 1833−1836.
(30) Bauer, W., Briner, U., Doepfner, W., Haller, R., Huguenin, R., Marbach, P., Petcher, T. J., and Pless, J. (1982) SMS 201−995: A very potent and selective octapeptide analog of somatostatin with prolonged action. *Life Sci. 31*, 1133−1140.
(31) Merrifield, R. B. (1963) Solid phase peptide synthesis. I. The synthesis of a tetrapeptide. *J. Am. Chem. Soc. 85*, 2149−2154.
(32) Schultz, M. K., Parameswarappa, S. G., and Pigge, F. C. (2010) Synthesis of a DOTA-biotin conjugate for radionuclide chelation via Cu-free click chemistry. *Org. Lett. 12*, 2398−2401.
(33) Cleland, W. W. (1964) Dithiothreitol, a new protective reagent for SH groups. *Biochemistry 3*, 480−482.
(34) Bangham, A. D., and Horne, R. W. (1964) Negative staining of phospholipids and their structural modification by surface-active agents as observed in the electron microscope. *J. Mol. Biol. 8*, 660−668.
(35) Richard, A., and Bourel-Bonnet, L. (2005) Internalization of a peptide into multilamellar vesicles assisted by the formation of an alpha-oxo oxime bond. *Chem.—Eur. J. 11*, 7315−7321.
(36) Dirksen, A., and Dawson, P. E. (2008) Rapid oxime and hydrazone ligations with aromatic aldehydes for biomolecular labeling. *Bioconjugate Chem. 19*, 2543−2548.
(37) Gustafsson, M., Olsson, R., and Andersson, C.-M. (2001) General combinatorial synthesis of tertiary amines on solid support. A novel conditional release strategy based on traceless linking at nitrogen. *Tetrahedron Lett. 42*, 133−136.
(38) Sridhar, M., Narsaiah, C., Raveendra, J., Reddy, G. K., Reddy, M., Reddy, M. K. K., and Ramanaiah, B. C. (2011) Efficient microwave-assisted synthesis of oximes from acetohydroxamic acid and carbonyl compounds using $BF_3{\cdot}OEt_2$ as the catalyst. *Tetrahedron Lett. 52*, 4701−4704.
(39) Rose, K., Zeng, W., Regamey, P. O., Chernushevich, I. V., Standing, K. G., and Gaertner, H. F. (1996) Natural peptides as building blocks for the synthesis of large protein-like molecules with hydrazone and oxime linkages. *Bioconjugate Chem. 7*, 552−556.
(40) Agard, N. J., Prescher, J. A., and Bertozzi, C. R. (2004) A strain-promoted [3 + 2] azide-alkyne cycloaddition for covalent modification of biomolecules in living systems. *J. Am. Chem. Soc. 126*, 15046−15047.
(41) Li, Z., Seo, T. S., and Ju, J. (2004) 1,3-dipolar cycloaddition of azides with electron-deficient alkynes under mild condition in water. *Tetrahedron Lett. 45*, 3143−3146.
(42) Chenoweth, K., Chenoweth, D., and Goddard, W. A., III. (2009) Cyclooctyne-based reagents for uncatalyzed click chemistry: A computational survey. *Org. Biomol. Chem. 7*, 5255−5258.
(43) Codelli, J. A., Baskin, J. M., Agard, N. J., and Bertozzi, C. R. (2008) Second-generation difluorinated cyclooctynes for copper-free click chemistry. *J. Am. Chem. Soc. 130*, 11486−11493.
(44) Fairbanks, B. D., Sims, E. A., Anseth, K. S., and Bowman, C. N. (2010) Reaction rates and mechanisms for radical, photoinitated addition of thiols to alkynes, and implications for thiol-yne photopolymerizations and click reactions. *Macromolecules 43*, 4113−4119.
(45) Gregory, J. D. (1955) The stability of N-ethylmaleimide and its reaction with sulfhydryl groups. *J. Am. Chem. Soc. 77*, 3922−3923.
(46) Barradas, R. G., Fletcher, S., and Porter, J. D. (1976) The hydrolysis of maleimide in alkaline solution. *Can. J. Chem. 54*, 1400−1404.
(47) Matsui, S., and Aida, H. (1978) Hydrolysis of some N-alkylmaleimides. *J. Chem. Soc., Perkin Trans. 2*, 1277−1280.
(48) Finnegan, R. A., and Mueller, W. H. (1965) Base-catalyzed addition and solvolysis reactions of N-phenyl-maleimide in methanol. *J. Pharm. Sci. 54*, 1257−1260.

Article II

Paper published in Advances in Biochemical Engineering/Biotechnology 2011.

This paper was prepared in collaboration with Rasmus I. Jølck, Simon Andersen, S. Moein Moghimi and Thomas L. Andresen. Jølck wrote the Introduction and the Surface Functionalization of Liposomes section. Future Directions and Conclusion was writing in collaboration between Jølck and Andresen. Feldborg covered the section in Targeting Strategies, and Andersen wrote the section on Membrane Anchors. Moghimi and Andresen both contributed to the idea and content of the review.

Parts of this paper is presented in Chapter one and two.

Adv Biochem Engin/Biotechnol (2011) 125: 251-280
DOI: 10.1007/10_2010_92

Published Online: 4 November 2010

Engineering Liposomes and Nanoparticles for Biological Targeting

Rasmus I. Jølck, Lise N. Feldborg, Simon Andersen, S. Moein Moghimi and Thomas L. Andresen

Abstract Our ability to engineer nanomaterials for biological and medical applications is continuously increasing, and nanomaterial designs are becoming more and more complex. One very good example of this is the drug delivery field where nanoparticle systems can be used to deliver drugs specifically to diseased tissue. In the early days, the design of the nanoparticles was relatively simple, but today we can surface functionalize and manipulate material properties to target diseased tissue and build highly complex drug release mechanisms into our designs. One of the most promising strategies in drug delivery is to use ligands that target overexpressed or selectively expressed receptors on the surface of diseased cells. To utilize this approach, it is necessary to control the chemistry involved in surface functionalization of nanoparticles and construct highly specific functionalities that can be used as attachment points for a diverse range of targeting ligands such as antibodies, peptides, carbohydrates and vitamins. In this review we provide an overview and a critical evaluation of the many strategies that have been developed for surface functionalization of nanoparticles and furthermore provide an overview of how these methods have been used in drug delivery systems.

Keywords Biological targeting · Drug delivery · Functionalization · Liposome · Nanoparticle

Abbreviations

CAC	Critical aggregation concentration
ConA	Concanavalin A
DCC	*N,N′*-dicyclohexylcarbodiimide
DOPE	1,2-Dioleoyl-*sn*-glycero-3-phosphoethanolamine

R. I. Jølck, L. N. Feldborg, S. Andersen and T. L. Andresen (✉)
Department of Micro- and Nanotechnology, DTU Nanotech, Technical University of Denmark, Frederiksborgvej 399, 4000 Roskilde, Denmark
e-mail: thomas.andresen@nanotech.dtu.dk

S. M. Moghimi
Department of Pharmaceutics and Analytical Chemistry, Centre for Pharmaceutical Nanotechnology and Nanotoxicology, University of Copenhagen, Universitetsparken 2, 2100 Copenhagen Ø, Denmark

DOPS	1,2-Dioleoyl-*sn*-glycero-3-phospho-L-serine
DPPE	1,2-Dipalmitoyl-*sn*-glycero-3-phosphoethanolamine
DSPC	1,2-Distearoyl-*sn*-glycero-3-phosphocholine
DSPE	1,2-Distearoyl-*sn*-glycero-3-phosphoethanolamine
DTT	Dithiothreitol
EDC	1-Ethyl-3-(3-dimethylaminopropyl)carbodiimide
ELAM	Endothelial-leukocyte adhesion molecule-1
EPR	Enhanced permeation and retention
GPI	Glycophosphatidylinositol
HER2	Human epidermal growth factor receceptor 2
ICAM-1	Intercellular adhesion molecule 1
IgG	Immunoglobulin G
LAMP	Lysosome-associated membrane protein
MAb	Monoclonal antibodies
MESNA	Mercaptoethanesulfonate
mon2C5	Monoclonal antinucleosome antibody 2C5
mon2G4	Monoclonal antimyosin antibody 2G4
NBD	7-Nitro-1,2,3-benzoxadiazole
NHS	*N*-hydroxysuccinimide
PDP	*N*-(3′-(pyridyldithio)propionoyl
PE	Phosphatidylethanolamine
PEG	Poly(ethylene glycol)
PL	Phospholipids
PLA2	Phosholipase A2
*p*NP	*p*-Nitrophenylcarbonyl
QCM	Quartz crystal microbalance
RES	Reticuloendothelial system
SPPS	Solid phase peptide synthesis
TFA	Trifluoroacetic acid
TfR	Transferrin receptor
VCAM-1	Vascular cell adhesion molecule 1
VEGF	Vascular endothelial growth factor
VIP	Vasoactive intestinal peptide
WGA	Wheat germ agglutinin

Contents

1 Introduction

The pharmaceutical industry has successfully developed numerous drugs for the treatment of cancer, but it remains one of the world's most devastating diseases with more than 10 million new incidences every year [105]. One of the major obstacles to current treatments is inadequate delivery of the therapeutics to the tumor site, which leads to severe side effects [8]. There is therefore increasing demand for delivery systems that transport the drug specifically to the diseased tissue and improve the therapeutic index of the encapsulated drug. Nanoparticle systems have been investigated as drug delivery systems for several decades, and strategies are becoming increasingly complex to fulfill the growing requirement for treating diseases. The nanoparticle drug delivery systems offer new treatment regimes for a large variety of different diseases; however, due to the relatively high costs of many of the utilized materials, they have mainly found applications for treatment of cancer. Of the many classes of nanocarrier systems that are currently under investigation, liposomes remain one of the most successful. Liposomes were first proposed as drug delivery vehicles by Gregoriadis et al. [54] in 1974. Early liposomal formulations suffered from rapid clearance by phagocytic cells of the reticuloendothelial system (RES). This issue was solved by coating the liposomes with polymers, particularly poly(ethylene glycol) (PEG), which suppress protein absorption and opsonization of the liposomes [139]. These *Stealth*® or *sterically stabilized* liposomes were found to accumulate in tumors and inflammatory tissue by passive diffusion because of the leaky vasculature and the lack of an effective lymphatic drainage present in such tissues [82, 87]. This phenomenon is commonly referred to as the enhanced permeation and retention effect (EPR effect). Despite the enhanced accumulation in cancerous or inflammatory tissue as a result of the EPR effect, there is strong motivation for improving the accumulation by

coating the outer liposomal membrane with ligands targeted towards overexpressed or selectively expressed receptors on diseased cells. *Active targeting* with ligands, such as peptides, carbohydrates, glycoproteins, antibodies or fragments thereof, has been utilized to selectively deliver drugs to the desired site of action by increasing the nanocarrier accumulation. Targeted liposomes/nanoparticles are superior compared to drug immunoconjugates since only few targeting ligands are needed to deliver several thousands drug molecules. Furthermore, liposomes are highly biocompatible and can protect encapsulated drugs from premature degradation in the blood stream. However, surface functionalization of liposomes or nanoparticles with targeting ligands are not trivial even though multiple reports have already utilized the targeting strategy. One of the largely overlooked problems when attaching targeting ligands is that reactions that normally work well in solution may proceed very slowly on a surface, and care should be taken to select the chemistry that is suitable for the desired synthetic manipulation. In particular, in many studies there is no evaluation of the success of the functionalization, which is highly problematic as many of the utilized chemistries are far from quantitative.

The aim of this review is to summarize the recent advances in the field of nanoparticle functionalization. The focus is on surface functionalization of liposomes, but the discussed chemistry is equally relevant for other nanoparticle constructs. We will discuss the many new and highly specific conjugation methods that have been developed in recent years to functionalize liposomes and give examples of how different classes of targeting ligands have been attached to liposomes and used to target diseased tissue. We will furthermore briefly discuss the membrane anchors that are employed, which is an overlooked problem in many studies.

2 Surface Functionalization of Liposomes

Three methods are commonly used to functionalize liposomes with targeting ligands. Small targeting ligands, such as vitamins [44, 77, 117], saccharides [25, 33, 122, 149] and small peptides [37, 39], are often covalently attached to a hydrophobic anchor (e.g., a lipid) in organic solvent and purified. The functionalized lipid can thereafter be mixed with natural lipids and hydrated to form liposomes. This approach is only possible when working with smaller ligands and is particularly useful when the ligand comes in relatively large quantities (due to the purification step). A major advantage of the approach is the complete control of the amount of ligands per liposome since the initially added amount can be varied in a controlled manner. However, approximately 50% of the added functionalized lipids will be oriented towards the interior of the liposome, thus, not interacting with the outer environment.

Another way to introduce specific ligands at the outer liposomal membrane is the *post-insertion* approach [62], which is useful for expensive ligands. In this

approach the ligands are typically covalently coupled to preformed lipid–PEG micelles (e.g., DSPE–PEG), which have functionality in the distal end of the PEG that allows coupling to the ligand. Alternatively, synthesized and purified ligand–lipid moieties made by the strategy discussed above can also be used. Succeeding, incubation of the micelles with preformed liposomes allows the DSPE–PEG–ligand conjugates to transfer from the micelles into the outer liposomal membrane in a temperature- and time-dependent manner, if the process is thermodynamically favored. This approach has been used to functionalize liposomes with antibodies [6, 13, 36, 61, 62, 100], peptides [95, 114, 135] and proteins [24]. A major advantage of this approach is that the loading of the liposomes is decoupled from the insertion of the ligands, which allows for optimization of both parameters. Targeting liposomes prepared by the *post-insertion* approach have been shown to have the same in vitro drug leakage rates, cell association profiles and therapeutic efficacies compared to liposomes made by other approaches [6, 61, 95]. However, the amount of ligands inserted into the liposome membrane must be quantified when using this approach.

Functionalization of liposomes with targeting ligands can also be carried out by *post-functionalization*, e.g., performing the conjugation directly on the preformed liposomes with anchors exposing specific functionalities in their respective head groups. This method is primarily used with larger and complex ligands, such as proteins and antibodies or fragments thereof. One should realize that the reactions often do not go to completion, and the degree of functionality should always be quantified. A large number of different anchors, e.g., fatty acids, phospholipids and sterols, have been used. The effect and the properties of these anchors will be discussed in the end of this review.

Ideally, surface coupling reactions should be simple, fast, efficient, reproducible and result in bonds that are non-toxic and non-immunogenic. Furthermore, reaction conditions for surface functionalization should be mild in order to retain the biological activity of the targeting ligands. A wide range of coupling methods has successfully been developed during the last 25 years, resulting in a broad variety of possible methods to functionalize liposomes. Early coupling methods are generally characterized by unspecific surface functionalization resulting in moderate yields, whereas the modern approaches enable site-specific functionalization in high yields. Each coupling reaction used to covalently attach ligands to the liposome surface will be described separately in order to highlight the advantages and disadvantages of the various methods. To limit the scope of this review, only surface functionalization of liposomes is discussed; however, the surface chemistry applies for the majority of other nanoparticle-based drug delivery systems.

2.1 Coupling of Ligands to Amine-Modified Liposomes

One of the earliest developed methods to covalently couple ligands to the liposome surface is based on amine functionalized liposomes. Torchilin et al. [124, 125]

described the use of two homobifunctional crosslinkers (Fig. 1a), glutaraldehyde (**1**) and dimethyl suberimidate (**2**) (Fig. 2), for amine–amine crosslinking. Addition of either **1** or **2** to DPPE-containing liposomes resulted in up to 70% imine or amidine formation, respectively, at the liposome surface. Incubation of these liposomes with rabbit anticanine cardiac myosin antibodies at 4°C in aqueous buffer resulted in 60% conversion [125] without loss of the binding capacity of the antigen.

The major advantage of this surface functionalization approach is the fact that it is based on naturally occurring lipids, which can be used without prior derivatization. However, the use of homobifunctional crosslinkers can result in uncontrollable homopolymerization of ligands or liposomes during the crosslinking reaction, which can lead to liposome aggregation. Furthermore, since multiple amine functionalities are usually present in antibodies, a random attachment can be

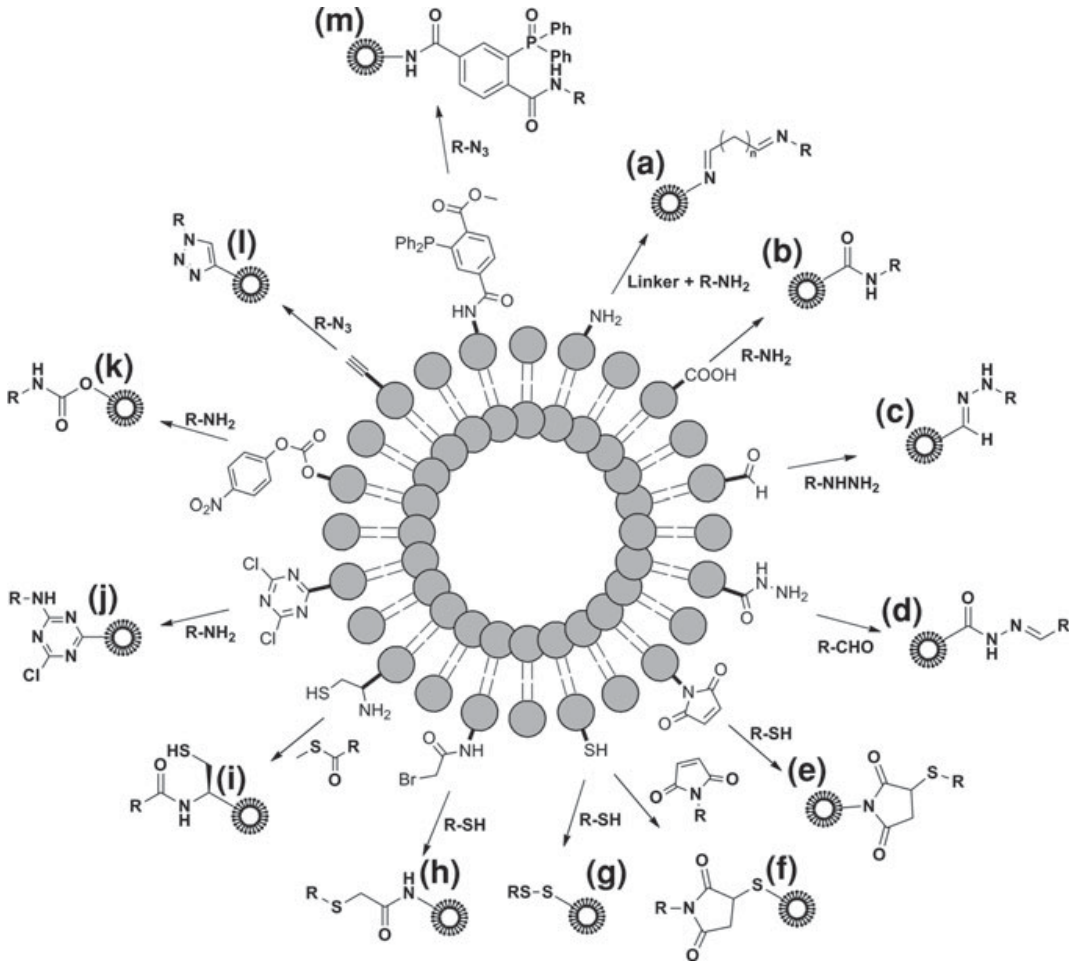

Fig. 1 Schematic illustration of the various coupling methods that have been developed in order to post-functionalize liposomes. **a** Amine functionalization, **b** carboxylic acid functionalization, **c** aldehyde functionalization, **d** hydrazine functionalization, **e** maleimide functionalization, **f** thiol functionalization, **g** thiol functionalization (disulfide bond formation), **h** bromoacetyl functionalization, **i** cysteine functionalization, **j** cyanur functionalization, **k***p*-nitrophenylcarbonyl functionalization, **l** alkyne functionalization, **m** triphosphine functionalization

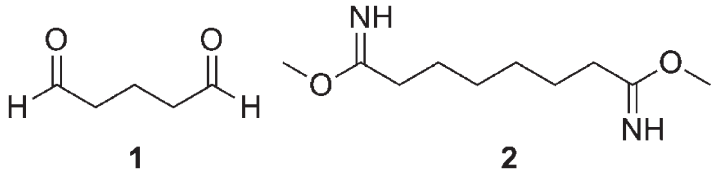

Fig. 2 Chemical structure of glutaraldehyde (**1**) and dimethyl suberimidate (**2**) utilized for amine–amine crosslinking by Torchilin et al. [124, 125]

expected. This may interfere with the binding of the antibody to its receptor and thus alter the binding affinity.

2.2 Coupling of Ligands to Carboxylic Acid-Modified Liposomes

Covalent coupling of ligands to carboxylic acid-modified liposomes (Fig. 1b) is a widely used approach to functionalize liposomes [14, 16, 63, 74, 86, 99, 143]. The method was first introduced by Kung and Redemann [74], who introduced the carboxylic acid functionality by reacting PE-lipids with a wide range of anhydrides in presence of triethylamine. Liposomes, exposing the carboxylic acid functionality, were activated in situ by the addition of water soluble 1-ethyl-3-(3-dimethylaminopropyl) carbodiimide (EDC). The activated ester was found to react readily with primary amines present on mouse IgG resulting in a stable amide bond. The achieved coupling efficiencies ranged from 1 to 58%, depending on the length of the spacer between the liposome surface and the carboxylic acid functionality.

The effect of the spacer becomes negligible when the ligand is introduced at the PEG terminus, as described by Maruyama et al. [86], who prepared monoclonal IgG 273-34A-modified liposomes by the above-described approach. These immunoliposomes were found to have prolonged circulation times and a higher degree of target cell recognition compared to liposomes exposing antibodies directly on the liposome surface.

The major advantage of using carboxylic acid-modified liposomes for surface modification purposes is that no prior ligand modification is required, thus reducing the risk of denaturation. On the other hand, since multiple amine functionalities are present in antibodies, a random attachment can be expected, which could alter the binding affinity towards the targeted receptor.

2.3 Coupling of Ligands to Aldehyde-Modified Liposomes

Coupling of hydrazino-derivatized ligands to aldehyde functionalized liposomes by hydrazone formation (Fig. 1c) has been described by Bonnet et al. [20], who

introduced the aldehyde functionalized ether lipid di-*O*-hexadecyl-*rac*-glyceraldehyde into the liposomal membrane. Incubation with a hydrazino-derivatized dodecapeptide from the cytoplasmic domain of lysosome-associated membrane protein (LAMP) in aqueous buffer resulted in quantitative conversion within 5 h.

The method described by Bonnet et al. [20] offers an effective approach to conjugate synthetic peptides prepared by solid-phase peptide synthesis (SPPS) to liposomes. The hydrazino functionality is easily introduced to the synthetic peptide on resin by the use of *N*,*N*,*N*-tri(*tert*-butyloxycarbonyl)-hydrazino acetic acid, which is fully compatible with SPPS synthesis [18, 19]. Furthermore, hydrazone formation occurs spontaneously without the need of a catalyst. Thus, this method is one of the most effective for the functionalization of liposomes with targeting ligands when it is possible to introduce a hydrazino group into the ligand. However, this is unfortunately problematic for antibodies and other complex ligands.

2.4 Coupling of Ligands to Hydrazide-Modified Liposomes

A more widely adapted approach, compared to the one described above, is to invert the position of the functional groups, i.e., introducing the aldehyde to the ligand and the hydrazine functionality to the liposome surface (Fig. 1d) [26, 56, 57, 72, 91, 145, 146]. Initially, the hydrazine functionality was introduced by incorporation of lauric acid hydrazide [26] into the liposome membrane (it should be noted that this is a poor anchor). Later, a method to introduce the hydrazine functionality to the distal end of the PEG chain of DSPE–PEG has been described by Zalipsky [145]. Having the hydrazine functionality exposed on the liposomal membranes offers a unique advantage for coupling of antibodies to the liposomal membrane. Mild oxidation of the carbohydrate groups on the constant region of the heavy chain of the immuoglobulin with either galactose oxidase [26] or sodium periodate [26, 56, 57, 72, 91] results in the formation of an aldehyde, which can be chemoselectively attached to the hydrazine-functionalized liposomes through hydrazone bond formation. By utilizing the carbohydrate groups from the Fc region, the antibodies are correctly oriented once attached onto the surface of the liposomes, because only the Fc region is involved in the coupling reaction, leaving the antigen-binding site available for receptor interactions. Comparative studies have indicated that this method results in low coupling efficiencies (17%) [56], yet positive in vitro results have been obtained using this methodology with liposomes targeted towards rat colon carcinoma CC531 cells [72].

2.5 Coupling of Ligands to Maleimide-Modified Liposomes

The most often used approach to functionalize liposomes with targeting ligands is based on the formation of a thioether bond between maleimide-functionalized liposomes and thiol-derivatized ligands [13, 29, 34, 40, 42, 49, 64, 70, 85, 98, 101,

119] by Michael Addition (Fig. 1e). For direct surface functionalization, *N*-(4-(*p*-Maleimidophenyl)butyryl)-phosphatidylethanolamine has been used as the functionalized anchor, whereas DSPE–PEG–maleimide is used for attachment on the distal end of the PEG polymer. Garnier et al. [49] recently used this approach to covalently attach the Annexin-A5 protein, known to target membranes containing negatively charged phospholipids, to DSPE–PEG–maleimide functionalized liposomes. A mutant of the natural Annexin-A5 protein (35 kDa), exposing a cysteine residue at a highly accessible loop on the concave face of the protein, was developed. Addition of this protein to liposomes exposing the maleimide functionality in HBS buffer at pH 6.3 for 4 h resulted in a coupling efficiency of approximately 80%. The Annexin-A5-functionalized liposomes were found to bind to solid supported lipid membranes composed of DOPC/DOPS in a Ca^{2+} depending manner, as monitored by quartz crystal microbalance (QCM). Michael addition of thiolated OX26 MAb Fab′ fragments to DSPE–PEG–maleimide functionalized liposomes has recently been described by Béduneau et al. [13]. Despite optimizing the coupling conditions, the coupling yield was constantly approximately 25%. However, it is noteworthy to mention that quantitative coupling efficiencies have been reported with small thiolated pentameric cRGD peptides using a similar coupling protocol [64].

An interesting study performed by Fleiner et al. [40] concerning the influence of the spacer length between the liposome surface and the reactive maleimido group and its polarity revealed that longer polar spacers resulted in higher coupling efficiencies. Surprisingly, comparison of the reactivity of liposome functionalized with either *m*- or *p*-maleimido benzoic acid esters revealed that the less reactive (less electrophilic) *m*-maleimido benzoic acid ester resulted in a higher coupling efficiency (46 ± 7%) compared to the more electrophilic *p*-maleimido benzoic acid analogue (30 ± 5%). This could be explained by the increasing susceptibility to competing nucleophiles, such as water, of the maleimide group with higher electrophilicity.

Surface conjugation to maleimide-functionalized liposomes is a straightforward and reliable method to attach ligands without prior activation or addition of catalysts to promote the reaction. The reaction proceeds at ambient temperature, close to neutral pH and within a short period of time. Conjugation of smaller ligands often results in quantitative yields, whereas more moderate yields can be expected for larger molecules. Despite the popularity of this conjugation method, maleimide derivatives have been shown to be immunogenic [17, 106].

2.6 Coupling of Ligands to Thiol-Modified Liposomes

Thiol-functionalized liposomes have often been used for the attachment of ligands to the outer liposomal membrane. Normally, the reactive thiol is introduced to the membrane as the disulfide protected derivate *N*-(3′-(pyridyldithio)propionoylamino–PEG–DSPE (DSPE–PEG–PDP), which is activated in situ by reduction with

dithiothreitol (DTT), as described by Allen et al. [5]. Attachment of maleimide-derivatized antibodies (Fig. 1f) was achieved by overnight incubation in yields ranging from 13 to 88%, depending on the liposome composition and amount of maleimide-derivatized antibodies added. Quantitative conjugation yields with maleimide-derivatized My10 antibodies have been reported when the reactive thiol is introduced at the distal end of longer PEG chains than the ones otherwise present in the liposome [92].

Surface conjugation to thiol-modified liposomes can also be achieved by disulfide formation (Fig. 1g). This approach was adopted by Muñoz et al. [96], who introduced the hepatitis A VP3 (101–121) peptide to DSPE–PEG–PDP containing liposomes. Overnight incubation in borate buffer at pH 8 resulted in approximately 50% conjugation yield. A disadvantage of this approach is that free thiols may react among themselves to produce intermolecular disulfide bonds, leading to crosslinking of the reactive ligands or liposomes.

2.7 Coupling of Ligands to Bromoacetyl-Modified Liposomes

Conjugation of cysteine-containing peptides to bromoacetyl-modified liposomes (Fig. 1h) has been described by Frisch et al. [42]. The bromoacetyl functionality was introduced by acylation of DPPE with 2-[2-[2-[(2-bromoacetyl)amino]ethoxy]ethoxy]ethoxy acetic acid (**3**) (Fig. 3) in the presence of *N,N′*-dicyclohexylcarbodiimide (DCC). An octapeptide derivatized from the C-terminal of the histone H_3 peptide was added to liposomes, exposing the bromoacetyl functionality at pH 9.0 resulting in quantitative conversion within 1 h. At lower pH, the reaction was found to be less pronounced. This phenomenon was utilized by Schelté et al. [119], who formulated liposomes exposing both the maleimide- and the bromoacetyl functionality at the outer membrane. This study showed that important kinetic discrimination can be achieved between the maleimide and bromoacetyl functionalities when the reactions with thiols are performed at pH 6.5. Reaction with cysteine-containing peptides was found to be three orders of magnitude faster with the maleimide functionality than with the bromoacetyl derivative, resulting in a high degree of chemoselectivity. These findings enabled the coupling of two different cysteine peptides sequentially. The first coupling was carried out on the maleimide derivative at pH 6.5, followed by a coupling to the bromoacetyl derivative at pH 9.0 under experimental conditions, which were found

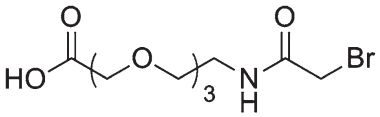

3

Fig. 3 Chemical structure of 2-[2-[2-[(2-bromoacetyl)amino]ethoxy]ethoxy]ethoxy acetic acid (**3**) used to introduce the acetyl bromo functionality to DPPE, as described by Frisch et al. [42]

not to alter the integrity of the liposomes. Furthermore, neither the bromoacetyl nor the maleimide functionality was found to react with other nucleophiles such as α- and ε-amino groups or imidazole, which could also be present in peptides.

2.8 Coupling of Ligands to Cysteine-Modified Liposomes

Conjugation of recombinant proteins to the liposome surfaces through native chemical ligation (Fig. 1i) has recently been described by Reulen et al. [109]. Native chemical ligation was first reported by Dawson et al. [32] as a unique method to ligate two unprotected peptide fragments and form an amide bond, thereby facilitating the synthesis of large proteins. Native chemical ligation is a chemoselective reaction, which occurs spontaneously between a thioester and an N-terminal cysteine under aqueous conditions at neutral pH, which makes it ideally suited for liposome conjugation purposes. Reulen et al. [109] introduced the cysteine functionality to the distal end of DSPE–PEG–NH_2 by reacting it with succinimidyl-activated trityl-protected cysteine, followed by deprotection of the trityl protection groups with dilute trifluoroacetic acid (TFA). The C-terminal of the collagen-binding protein domain (CNA35) from the bacterial adhesion protein of *Staphylococcus aureus* was modified with sodium 2-mercaptoethanesulfonate (**4**) (MESNA) (Fig. 4) to form a thioester suitable for native chemical ligation. Cysteine-functionalized liposomes were incubated with MESNA-CNA35 protein in HBS buffer at pH 8 for 48 h in the presence of thiophenol, benzyl mercaptan or MESNA to catalyze the reaction. In the presence of either thiophenol or benzyl mercaptan, approximately 30% conversion was observed, whereas only 10% conversion was achieved with MESNA. However, the poorly water soluble and toxic thiophenol and benzyl mercaptan were found to accumulate in the phospholipid bilayer, making them difficult to remove after ligation. This was not the case with the water-soluble MESNA, which was easily removed by centrifugation. The CNA35-functionalized liposomes were tested in a collagen-binding assay and were found to have a 150-fold increase in affinity compared to the free protein.

Surface conjugation through native chemical ligation is an attractive method to directly conjugate thioester-modified ligands to the liposome surface. The method enables site-specific conjugation, since only a single site in the ligand is available for conjugation. The low coupling yield is an obstacle that needs to be addressed.

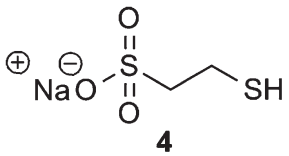

4

Fig. 4 Chemical structure of sodium 2-mercaptoethanesulfonate (**4**) (MESNA) used to catalyze the native chemical ligation on the liposome surface, as described by Reulen et al. [109]

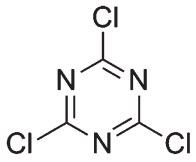

5

Fig. 5 Chemical structure of cyanur chloride (**5**) used to introduce the cyanur functionality into liposomes by acylation of DPPE–PEG–OH, as described by Brendas et al. [21]

2.9 Coupling of Ligands to Cyanur-Modified Liposomes

A method for attaching antibodies directly to the PEG terminus of liposomes without prior derivatization has been described by Brendas et al. [21]. Introduction of the cyanur functionality to the PEG terminus of DPPE–PEG–OH was achieved under basic conditions by adding cyanuric chloride (**5**) (Fig. 5). Anti E-selectin monoclonal antibodies were coupled to cyanuric-modified liposomes (Fig. 1j) at pH 8.8 by nucleophilic substitution resulting in immunoliposomes having a high degree of in vitro binding to Chinese hamster ovary cells expressing E-selectins receptors. The nucleophilic substitution between the anti-E-selectin monoclonal antibodies and the cyanur-modified liposomes was found to be very sensitive towards the pH of the buffer. No surface functionalization was observed at neutral pH, whereas a more alkaline environment resulted in hydrolytic degradation of the cyanuric chloride.

This methodology offers a straightforward approach for attaching antibodies to the PEG terminus of liposomes without previous derivatization. However, cyanuric chloride is known to react with a wide range of nucleophilic functionalities, such as alcohols, amines and thiols, which means that a random attachment of the antibodies can be expected. This may interfere with the binding of the antibody to its receptor, thus altering the binding affinity. In addition to this, cyanuric chloride is regarded as a sensory respiratory irritant [113], but has not shown any sign of acute, chronic or genotoxicity [140].

2.10 Coupling of Ligands to p-Nitrophenylcarbonyl-Modified Liposomes

An additional method to directly conjugate antibodies to the PEG terminus of liposomes without prior derivatization has been described by Torchilin et al. [128]. The amphiphilic derivate *p*-nitrophenylcarbonyl–PEG–1,2-dioleoyl-*sn*-glycero-3-phosphoethanolamine (*p*NP–PEG–DOPE), which was obtained in a single step from DOPE and bis(*p*-nitrophenylcarbonyl)-PEG, forms stable and non-toxic carbamate bonds with ligands containing primary amines (Fig. 1k). However, one drawback is the utilization of the bis-functionalized bis(*p*-nitrophenylcarbonyl)-PEG, which may result in dimerization, although this side product is easily

separated from the product. Torchilin et al. demonstrated this approach with several proteins, such as concanavalin A (ConA), wheat germ agglutinin (WGA), avidin, monoclonal antimyosin antibody 2G4 (mon2G4) and monoclonal antinucleosome antibody 2C5 (mon2C5), and observed almost quantitative surface functionalization yields at pH 8.0. Despite the fact that this method does not enable site-specific conjugation, the specific activities of the surface bound proteins were retained after conjugation.

2.11 Coupling of Ligands to Alkyne-Modified Liposomes

One of the more elegant coupling methods to functionalize liposomes is based on the work of Meldal and co-workers [129, 130] and Sharpless and co-workers [111], who reported the use of Cu(I) to catalyze the azide/alkyne Huisgen 1,3-dipolar cycloaddition, commonly referred to as the click reaction. This reaction offers unique flexibility because of the high level of orthogonality to other chemical functionalities and generally proceeds rapidly in high yields. This approach to functionalize liposomes was first described by Hassane et al. [58], who introduced the alkyne functionality to the liposome surface by incorporating the synthetic ether lipid *N*-[2-(2-(2-(2-(2,3-bis(hexadecyloxy)propoxy)ethoxy)ethoxy)-ethoxy)ethyl]hex-5-ynamide (**6**) (Fig. 6) into the liposomal membrane (Fig. 1l). Addition of an azido-modified mannose ligand in the presence of $CuSO_4$ and sodium ascorbate to generate Cu(I) in situ resulted in approximately 25% yield within 24 h. However, by adding the water-soluble Cu(I)-stabilizing ligand bathophenanthroline disulfonic acid [78] to the reaction mixture, complete conversion was observed within 6 h. These reaction conditions did not alter the size of the liposomes or provoke leakage from liposomes loaded with self-quenching concentrations of 5,6-carboxyfluoroscein. Furthermore, the mannose residue was found to be readily accessible to concanavalin A, which upon addition to the liposomes caused instant aggregation.

The click reaction approach has also been adopted by Cavalli et al. [23], who introduced the alkyne functionality by derivatization of DOPE with proliolic acid. Full conversion was in this case achieved within 20 h with a small azido-NBD derivative without the use of bathophenanthroline disulfonic acid.

The Cu(I) catalyzed azide/alkyne Huisgen 1,3-dipolar cycloaddition is a very powerful conjugation reaction for surface modification of liposomes. The

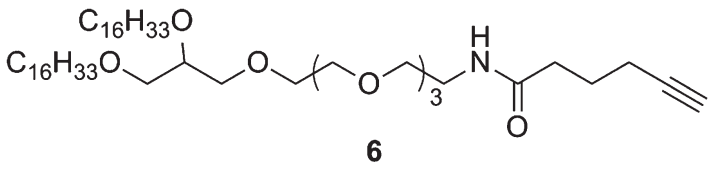

6

Fig. 6 Chemical structure of *N*-[2-(2-(2-(2-(2,3-bis(hexadecyloxy)propoxy)ethoxy)ethoxy)-ethoxy)ethyl]hex-5-ynamide (**6**) used to introduce the alkyne functionality into the liposome membrane as described by Hassane et al. [58]

unreactive nature of both alkynes and azides towards the other functionalities present in biomolecules makes site-specific conjugation possible. Furthermore, the formed triazole ring is both thermal and hydrolytically stable, and the reaction can occur efficiently in aqueous media at room temperature. However, the mandatory use of copper catalyst represents a limitation. Copper is considered toxic and complete removal prior to in vitro or in vivo use is necessary. In addition to this, unsaturated phospholipids are known to be oxidized by copper ions in the presence of oxygen [46, 75], which could cause degradation of the liposomal membrane. Alternative methods to promote triazole formation between azides and alkynes, without Cu(I), have been described recently. Strain-promoted [3] or electron-deficient alkynes [79] have been reported to react with azides in absence of Cu(I), but these methods have not yet been applied to the liposome field.

2.12 Coupling of Ligands to Triphosphine-Modified Liposomes

The latest member of the wide range of possible surface conjugation reactions described is based on the Staudinger ligation [118], in which an azide and a triphosphine selectively react to form an amide bond (Fig. 1m). This approach was adopted by Zhang et al. [148], who introduced the triphosphine functionality by acylation of DPPE with 3-diphenylphosphino-4-methoxycarbonylbenzoic acid (**7**) (Fig. 7). Triphosphine-functionalized liposomes were incubated with an unprotected lactosyl derivate carrying an ethyl spacer functionalized with an azide group in PBS buffer, which resulted in 80% surface functionalization within 6 h. The surface conjugation reaction was not found to alter the size or provoke leakage of the liposomes. The surface-conjugated lactose residues were shown to be easily accessible to β-galactose-binding lectin, which, upon addition, caused aggregation of the liposomes.

The methodology described by Zhang et al. [148] offers an efficient and chemoselective conjugation method for liposome surface functionalization. The reaction benefits from being performed under mild conditions without the need of a catalyst. Furthermore, methods to engineer bacteria and yeast enabling them to incorporate azido functionalities into proteins have been developed [53]. This enables direct attachment to the triphosphine-functionalized liposome without prior derivatization of the protein.

3 Targeting Strategies: Active Targeting of Tumor Vasculature and Tumor Cells

Ligand-modified liposomes can be designed to target receptors expressed by cells in the tumor vasculature or on the tumor cells. When targeting tumor cells directly,

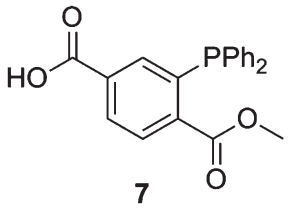

7

Fig. 7 Chemical structure of 3-diphenylphosphino-4-methoxycarbonylbenzoic acid (**7**) used to introduce the triphosphine functionality into liposomes by acylation of DPPE as described by Zhang et al. [148]

a number of obstacles have to be overcome as the drug delivery system has to cross the vasculature and travel through the interstitium in the tumor tissue before being able to deliver the drug at the desired site of action. Vascular targeting is generally considered to be advantageous over tumor cell targeting as endothelial cells are genetically stable and the risk of developing drug resistance is minimized [1]. Proliferating endothelial cells in solid tumors share similar characteristics in a variety of tumor types and a number of these can be utilized. In addition, endothelial cells lining the blood vessels in tumors are more accessible for binding by circulating drug delivery systems that are administered intravenously [1]. A strategy that targets both the tumor vasculature and the tumor cells has been envisioned as more effective than targeting the two tissues individually, and Koning et al. have provided proof-of-principle for this hypothesis [73]. These strategies have been investigated using a range of targeting molecules including antibodies, peptides, carbohydrates and vitamin analogs, and an overview of these different targeting moieties is discussed below.

3.1 Immunoliposomes

Antibodies represent one of the most versatile ligands that can be attached to liposomes. However, the antibody functionalization of liposomes is generally challenging, where region specificity and degree of conversion are the main problems, even though a number of good methods exist. One of the main reasons for this is that antibodies can only be attached to liposomes by *post-functionalization*, i.e., the lipsomes are formed prior to attachment, and the chemistry therefore has to work well in aqueous buffer. Early attempts to attach these molecules for the specific targeting of diseased tissue were originally communicated in the 1970s [136] where antibodies were coupled to the surface of non-PEGylated liposomes. Today, it is commonly known that non-PEGylated (or non-polymer) liposomes have little treatment benefit because of fast clearance from the blood stream. Coupling of the targeting ligands to the distal end of PEG is therefore the method-of-choice today to maximize liposome accumulation at the target site [56, 116]. Antibodies can be attached as whole monoclonal antibodies or as a fragment thereof (Fig. 8). Full antibodies have stability advantages over small

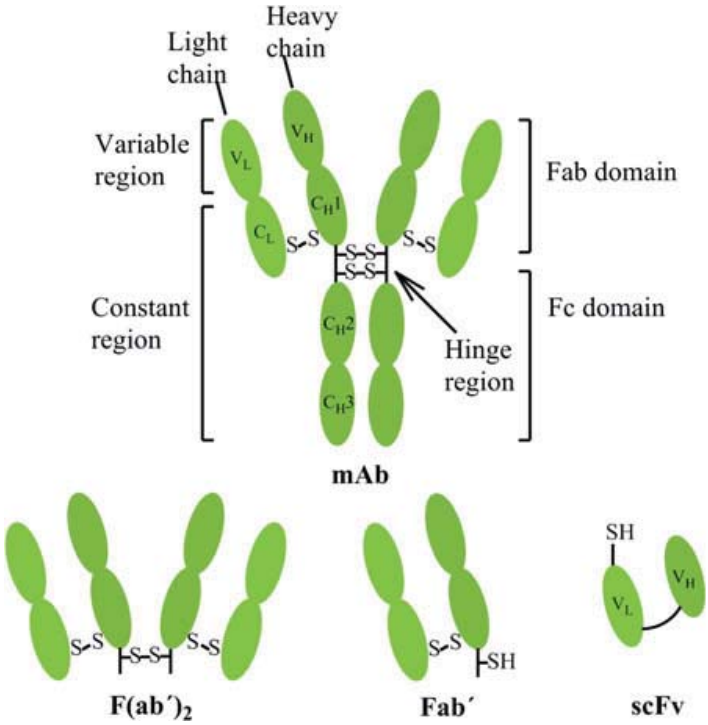

Fig. 8 Schematic representation of various antibody constructs: Monoclonal antibody (mAb); $F(ab')_2$ generated by pepsin digestion of the Fc domain of mAb; Fab′ from reduction of the disulfide bond in the hinge region of $F(ab')_2$; scFv of recombinant V_L and V_H regions linked by a short peptide sequence

fragments such as Fab′ and scFv, but can trigger complement [94] and induce antibody-dependent cell-mediated cytotoxicity [115]. Furthermore, the Fc fragment is known to accelerate clearance of the immunoliposome by uptake of circulating liver and spleen macrophages possibly through opsonization, and thus decreases the circulation time of the liposomes [5]. By attaching fragments of the antibody such as Fab′ or Fv, this undesired clearance can be minimized [12].

The most commonly used antibody-targeting moieties belong to the immunoglobulins of the IgG class [126], which have been coupled to the distal end of PEG using a hydrazido-PEG–DSPE construct [57]. The oligosaccharide moiety of the antibody molecule was oxidized using sodium periodate, creating an aldehyde functionality that reacts with the hydrazido-group on the PEG–DSPE to form a stable hydrazone linkage. Immunoglobulins consist of 82–96% polypeptide and 4–18% carbohydrates [10, 11], and the carbohydrate moieties are mainly situated on the heavy chain in the Fc portion of the antibody. As this region is not involved in the binding to the receptor, a modification in this part should not influence antigen-binding efficacy [52]. However, one potential problem with the oxidation of the carbohydrates is the risk of oxidizing amino acids situated in the antigen-binding Fab′ region. Amino acids most prone to oxidation with sodium periodate are cysteine, methionine, tryptophan, tyrosine and histidine, as well as serine and threonine if they occur as terminal residues [28].

Antibodies against the human epidermal growth factor receptor 2 (HER2) have been widely used in combination with liposomal drug delivery systems. This antigen is frequently overexpressed on various types of cancer cells and is only weakly expressed in normal tissues. One of the first studies of investigating Fab′

and scFv targeting of HER2 was reported by [85]. They utilized PEGylated liposomes that were functionalized with a maleimide functionality in the distal end of PEG. Fab′ was conjugated to the liposomes through a thioether linkage using the free thiol group in the Fab′ hinge region at pH above 7 to deprotonate the thiol. This site is located distant from the antigen-binding site and should not interfere with its function. The thioether bond formed between Fab′ and the maleimide functionalized liposome was stable and not prone to reduction in a reductive environment, e.g., serum [84]. ScFv fragments contain immunoglobulin heavy- and light-chain variables linked by a $[\text{-}(\text{Gly})_4\text{-Ser-}]_3$ motif. At the C-terminal end of the recombinantly produced scFv, a cysteine can be introduced that can be exploited in the covalent attachment to maleimide-activated PEG–DSPE. Two internal disulfide bonds are present in the scFv fragment; however, these have proven to be rather stable to reduction [4]. An analogous approach has been developed with the use of a PDP–PEG–DSPE liposome composition. After reduction with DTT, the liposome was incubated with an anti-HER2 maleimidophenylbutyrate functionalized Fab′ fragment, resulting in the immunoliposome [47]. For targeting the transferrin receptor (TfR), its antibodies or Fab′ fragments have been coupled to maleimide-modified PEG–DSPE liposomes. The TfR expression is elevated in many types of cancerous tissues and correlates with the proliferation rate and aggressiveness of the cancer. Hence, the TfR is a valuable potential target for drug delivery in cancer therapy [13, 141].

For the targeting of endothelial cells in malignant tissues, different forms of adhesion molecules such as endothelial-leukocyte adhesion molecule-1 (ELAM), intercellular adhesion molecule 1 (ICAM-1) and vascular cell adhesion molecule 1 (VCAM-1) have been applied. These have been coupled to DOPE-*N*-dodecanoyl lipids by the use of EDC/*N*-hydroxysuccinimide (NHS) chemistry [55]. However, as there are several amine groups in anti-ELAM and anti-ICAM, this strategy leads to a non-specific crosslinking between the liposome and the antibody. This can be avoided by applying the maleimide method described above where the antibody is coupled via a thioether bond to the surface of PEGylated liposomes. However, an additional step is required to introduce a thiol functionality on the cell adhesion molecule. This is readily done using *N*-succinimidyl-*S*-acetylthioacetate [35]. Related to this strategy, immunoliposomes have been prepared using maleimide–DPPE through a reaction with thiolated $F(ab')_2$ fragments of the monoclonal antibody GAH [131]. GAH recognizes surface molecules especially in stomach cancer, and a PEGylated immunoliposome formulation using GAH targeting has been shown to have better efficacy than non-targeting liposomes in Phase I clinical trials [59, 88].

A significant number of monoclonal antibodies have been identified and can be engineered as Fab′ or scFv fragments as well as chimeric or humanized antibodies. Highly effective and reproducible methods of coupling whole antibodies or their fragments to the surface of plain liposomes or PEGylated liposomes exist, and in general immunoliposomes show an enhanced recognition of target cells, as well as a better internalization and intracellular drug delivery over non-targeted liposomes [71, 102].

3.2 Folate-Modified Liposomes

Liposomes functionalized with the vitamin, folic acid, have attracted much attention as the folate receptor is highly overexpressed in a number of cancers, and it can retain its high affinity binding to the folate receptors even after being covalently linked to a variety of macromolecules [144]. The vitamin is internalized to a large extent in proliferating cells as folic acid is essential in the biosynthesis of nucleotides; consequently, cancerous cells overexpress the folate receptor as the fast-dividing malignant cells are in great need of this nutrient. Normally, the folate receptor is expressed at the apical side of epithelial cells and is not accessible to blood-borne drugs. However, when the epithelial cells become malignant, the membrane loses its polarity and the folate receptor can be located at the basal surface of the membrane as well, taking up therapeutics from the plasma [81]. There is no evidence that normal healthy cells are expressing the folate receptor to a significant extent, and healthy tissue should therefore not be affected by the delivery of folate-targeted drugs [103, 138]. The first report of using folate-targeted liposome to transport drugs into tumor cells was published in the 1990s by Lee and Low [76]. They conjugated the NHS-ester of folic acid to the distal end of a NH_2-PEGylated liposomes forming a stable amide bond. Gabizon et al. applied a similar approach simply using a DCC-mediated coupling procedure linking the terminal free γ-carboxylic acid on folate and the free PEG amine functionality [44]. Folate contains both an α- and γ-carboxylic acid moiety, but as the gamma position has a higher reactivity, this is the main coupling product observed [68]. After endocytotic uptake [9] of the liposome complex by the folate receptor-expressing cell, release of the liposome content has been accomplished taking advantage of the endosomal acidic environment, either by introducing pH-sensitive fusogenic peptides to promote uptake into the endosome [134] or adding pH-sensitive lipids to the liposome to increase liposome permeability and accelerate unloading of the content in the acidic endosome [112]. The folate molecule can form dimers, trimers and even higher self-assembling constructs. An increasing level of folate attached to the liposome surface was found not to increase the level of folate–liposome-complex binding to the folate receptor, as this receptor can only bind one folate and will not respond to multiple folates [27, 107]. One of the advantages with folate targeting is that the lipid–PEG–folate conjugates can be synthesized in organic solvent and purified. This allows for a precise control of the amount of targeting ligands that are present in the liposome, and there is no need for *post-functionalization*.

3.3 Saccharides

A large number of mammalian cells express sugar-binding proteins known as lectins. These have been found to be overexpressed on malignant cells and are believed to be involved in metastasis formation [31, 43]; they can thus serve as a

target for drug delivery systems. Liposomes functionalized with carbohydrates are biodegradable, low in toxicity and have a protein-shielding ability that makes them able to minimize liposome clearance from circulation. For instance, monosialoganglioside have been shown to enhance the circulation time similar to that observed for PEGylated liposomes [8, 90]. A number of different carbohydrates have been conjugated to the surface of liposomes. Hassane et al. [58] used click chemistry to couple an unprotected α-D-mannosyl derivative carrying a PEG spacer functionalized terminally with a reactive azide moiety. However, selective protection of the mannose alcohol groups is naturally required during functionalization with the PEG chain to avoid multiple substitutions [58]. Surface functionalization of liposomes using lactose, galactose and a diverse array of polysaccharides as the carbohydrate components have been synthesized using Staudinger ligation [148], thioglycoside-mediated attachment [147] and EDC couplings between the headgroup amine on the lipid, and an activated NHS-ester of the saccharide moiety [123, 142]. The employed methods have both involved *post-functionalization* and complete synthesis of the targeting lipid–ligand conjugate in organic solvent, allowing isolation of the target compound. The latter method is possible with all carbohydrate targeting ligands and should be the method-of-choice.

3.4 Peptides

The use of peptide-targeted liposomes as therapeutics has become highly interesting with the increasing knowledge of specific peptide sequences of proteins involved in cell–cell interactions as well as the improvements in synthesis or expression of synthetic peptides that closely resemble the human ones. For attachment of peptide moieties to the liposome surface, the typically reactive amino acids used are lysine, serine, cysteine, histidine, arginine, aspartic acid, glutamic acid, threonine, tyrosine, the N-terminal amino group and C-terminal carboxylic acid. The primarily used method is to react one of these reactive functionalities with an activated PEG component situated on the surface of the liposome. As lysine is one of the most prevalent amino acids in proteins, this has been a favored linking site; however, upon reaction of a nucleophilic amine group with an electrophilic activated PEG, multiple substitutions are often observed due to the the presence of multiple lysines in the peptide. Amine linkage to PEG has been achieved in multiple ways including the use of PEG dichlorotriazine [2] and PEG tresylate [41]. Many PEG conjugates have furthermore been synthesized using activated carbonate derivatives, such as succinimidyl carbonate, trichlorophenyl carbonate and *p*-nitrophenyl carbonate [93, 132]. Liposomes have been modified with cell-penetrating peptides such as TAT using a *p*-nitrophenyl carbonate-functionalized PEG under slightly basic conditions to form the non-toxic carbamate linkage. TAT and other cell-penetrating peptides such as penetratin and synthetic polyarginines have been conjugated to the surfaces of liposomes to improve liposome uptake by cells [127]. In general, lower reactivity of the

carbonate reagents provides higher selectivity; however, carbonate linkage with several amino acids such as lysine, histidine and tyrosine have been observed [110]. When a highly selective conjugation is required, a PEG–propionaldehyde can be prepared. This functionality will, if pH is controlled, react selectively with the N-terminal α-amine because of the lower p*K*a value of this amine compared to other possible nucleophiles in the sequence [69]. Another possibility is to make the activated ester of PEG carboxylic acids, such as NHS–PEG, which will react with primary amines to form stable amides. This method has been applied for the modification of liposomes with the vasoactive intestinal peptide (VIP) to target VIP receptors in breast cancer [30]. The receptor for this 28-amino acid neuropeptide is found to be overexpressed and homogenously distributed in all parts of the breast tumor and thus serves as a potential tumor-targeting functionality [108]. Other active targeting carriers are based on delivery systems that mimic local bioadhesion. Integrins and in particular the $\alpha_5\beta_1$ integrin have attracted much attention as this and its ligand, fibronectin, are found to be upregulated in blood vessels in tumor biopsies. There is strong evidence that peptides that mimic the cell adhesion domain of fibronectin and contain the peptide sequence RGD (arginine-glycine-aspartic acid) are potent inhibitors of tumor-growth, tumor metastasis and tumor-induced angiogenesis [89]. The RGD sequence has been prepared as a cyclic constrained 5-mer modified with a C-terminal thioacetyl group for linkage to the liposome. Deprotection of the acetyl group and incubation with a maleimide-PEGylated functionalized liposome resulted in a thioester linkage between the peptide and liposome [120]. A similar approach was used for the attachment of the linear ATWLPPR (alanine-threonine-tryptophan-leucine-proline-proline-arginine) sequence, found to have affinity for the vascular endothelial growth factor receptor (VEGF), a receptor overexpressed in the surface of angiogenic endothelial cells [15]. Utilization of cysteine residues is the main approach for site-specific modification due to high specificity and ease of modification of a sequence that lacks a cysteine residue. In addition, few free cysteines are present on the surface of proteins compared to, e.g., lysine. An additional synthetic peptide sequence often applied in blocking cancer cell adhesion is YIGSR (tyrosine-isoleucine-glycine-serine-arginine)—a sequence shown to be important in laminin receptor binding. Conjugation of the peptide moiety to the liposomal surface can be achieved by mild periodate oxidation of the threonine residue in the hexapeptide TYIGSR, leading to a reactive glyoxylyl functionality in the N-terminal end of the peptide followed by attachment to a hydrazide functionalized PEG lipid [146]. The oxidation of carbohydrate residues or N-terminal serine or threonine creates the possibility for site-directed PEGylation using hydrazides. The glyoxylyl functionality formed by the oxidation of N-terminal serine or threonine reacts site-specifically with PEG-hydrazide derivatives [45], and the PEGylated peptide can be purified before use. A similar site-specific N-terminal modification of peptides has been described by Geoghegan and Stroh [50]. In general, the peptides discussed above can be achieved in several ways and can both be inserted by *post-functionalization* and by synthetic procedures in organic solvent. The former is an advantage for larger peptides (>30

amino acids) that are relatively expensive as the purification step utilized in the latter procedure results in loss of compound. However, a synthetic approach that involves purification should always be employed when possible to remove side products and reagents. A number of reports furthermore utilize SPPS of lipopeptide conjugates, and this is a highly efficient method for smaller peptides [66].

4 Membrane Anchors

In relation to liposomes and other self-organized materials, an important consideration when choosing the chemical structure of the targeting conjugate is that membrane affinity for the specific lipid membrane has to be sufficiently high to secure stability during blood circulation and binding to the target receptor. The easiest strategy is of course to choose the same lipid anchor for the targeting conjugate as the majority of the lipids used in the formulation; however, this may not always be possible, and for large hydrophilic targeting conjugates it may not always be sufficient. Depending on the targeting conjugate and the concentration used, the packing parameter of the molecule should also be considered [83]. The flexibility of the functional group as well as the crowding from other molecules on the membrane surface will influence the conformation of the anchored group, e.g., brush-like versus mushroom-like structures of PEG [48]. Two of the most important factors in choosing an anchoring molecule are the critical aggregation concentration (CAC) of the targeting conjugate and how compatible it is with the lipid membrane in terms of membrane thickness and fluidity, e.g., saturated versus unsaturated hydrocarbon chains. It should be noted that using poly-unsaturated hydrocarbon chains might induce a stability challenge, since these are prone to oxidation [133]. A simple example of the importance of fluidity is that rhodamine-labeled DOPE in a DSPC liposome membrane migrates in cell culture to the cell membrane, whereas rhodamine-labeled DSPC remains bound to the liposomes. It is therefore highly important to evaluate the physico-chemical properties of the targeting conjugate and measure the formulation stability with appropriate biophysical methods.

A large variety of lipids has been used to anchor different targeting ligand conjugates in liposomal membranes. Among the most widely used are phospholipids (PL) [137], cholesterol [22], ether lipids [38], acyl chains [60], glycophosphatidylinositol (GPI) [121] and molecular rods [51]. Each anchor type has several subtypes where small modifications can have a significant influence on how well the anchor of the functionalized group associates with the membrane. The choice of anchor depends on the physico-chemical properties of the conjugated group.

Phospholipids are the most widely used anchors since most liposome-based drug delivery systems are composed of commercially available PLs. PE and PE–PEG–NH_2 are the most utilized when synthesizing targeting moieties by

standard chemistry in organic solvent. The linkage chemistry of choice is often activated carbonates, and "click" chemistry is utilized more and more often due to the high level of functional group orthogonality. However, hydrazines should also be considered for reaction with aldehydes as this chemistry works very well and is highly orthogonal to other chemistries. For *post-functionalization*, Michael addition to maleimides with thiols is by far the most often used approach as this chemistry is fully compatible with the aqueous environment. "Click" chemistry can also be considered, but it is more difficult to achieve high coupling efficiency between sterically hindered moieties in comparison to the maleimide chemistries. A special case of PLs is the sphingolipids, which have three major subclasses: (1) ceramides, (2) sphingomyelins and (3) glycosphingolipids, where the latter is mainly used to anchor large proteins. One drawback of using glycerophospholipids as anchors is that enzymes that hydrolyze the lipids giving free fatty acid and lysophospholipids can be overexpressed in diseased tissue, e.g., phosholipase A2 (PLA2) [7, 65]. The enzyme hydrolysis will eventually disrupt the lipid membrane, and the liposome thereby loses its targeting capacity. To circumvent problems with enzymatic hydrolysis or chemical degradation of the ester bonds (which are the weakest chemical bond in the usual phospholipid conjugates), ether lipids can be used. The chemistry of conjugation is the same as for the normal diacyl-glycerophospholipids, but the cost of manufacturing represents a limitation.

Cholesterol and derivatives like thio-cholesterol are also among the frequently used anchors for functional groups on the surface of liposomes. Like PLs, cholesterols are widely used in liposomal drug delivery systems and are also highly present in natural membranes, making cholesterol anchors highly compatible with most membranes. Cholesterol is typically coupled to a functional group via an ester bond, carbamate ester or ether bond using the same type of chemistry as for PLs. Cholesterol will usually serve as a strong anchoring molecule to relatively large targeting conjugates with a low CAC value.

Acyl chains are also commonly used as anchors due to the easy coupling to primary amines and alcohols. The stability of the amide bond makes this approach suitable for solid phase synthesis and usually involves only one acyl chain, but in some cases it involves two or three [80].

The use of only one acyl chain has been seen in multiple studies, but does not generally serve as a sufficient anchor in vivo (or even in vitro) as the water solubility is too high and fast migration to, e.g., cell membranes will be observed. If mono-acylation is used, particular attention should always be given to verifying the anchoring stability.

Molecular rods are a relatively new form of anchors for lipid membranes with functional groups attached to each end. They are designed to fit into membranes spanning the entire bilayer, unlike most other lipid anchors, and can be synthesized with various lengths and desired rigidity needed for the individual target membrane [97]. The principle of lipids spanning the entire membrane is known from archaebacterial membranes, and mimics of the natural occurring lipids have been synthesized [104]. Both molecular rods and tetraether lipids have the advantage of

spanning the entire membrane, making it several orders of magnitude more stable compared to conventional lipids.

5 Future Directions and Conclusion

The chemistry for functionalizing liposomes with targeting ligands is diverse and has been developed over the last 3 decades. Even so, a number of challenges remain as there is a growing need for reactions that are highly regioselective and efficient. "Click" chemistry is a very good example of the type of chemistry that is required as it provides a very high degree of orthogonality to naturally occurring functional groups. However, the reaction suffers from use of copper as catalyst, and it is not a highly efficient reaction on the surface of liposomes. Another important requirement is that the reactions should be relatively cost efficient where the most important factor is that it proceeds in high yield. Lastly, for *post-functionalization*, the reactions should ideally not give any need for successive purification. Good examples of reactions that fulfill this requirement are the Michael addition to maleimides with thiol-containing ligands and hydrazine condensation with aldehydes that do not require purification if all ligands react. Another important step forward will furthermore be to develop chemistries that are easily evaluated for efficiency as it is not always a trivial task to evaluate reaction progression depending on the ligand being used. This can be envisaged in a number of ways, and it is certain that the coming years will provide much better functionalization chemistries giving high coupling efficiencies, high regio-selectivity and methods for fast evaluation of reaction progression. This is not only for use in drug delivery applications, but also to meet the growing needs in the development of new diagnostic tools where nanoparticles are in increasing demand.

Acknowledgments Financial support was kindly provided by the Technical University of Denmark and the Danish Strategic Research Council (ref. 2106-07-0033 and 09-065746/DSF).

References

1. Abu Lila AS, Ishida T, Kiwada H (2009) Recent advances in tumor vasculature targeting using liposomal drug delivery systems. Expert Opion Drug Deliv 6:1297–1309
2. Abuchowski A, McCoy JR, Palczuk NC et al (1977) Effect of covalent attachment of polyethylene glycol on immunogenicity and circulating life of bovine liver catalase. J Biol Chem 252:3582–3586
3. Agard NJ, Prescher JA, Bertozzi CR (2004) A strainpromoted [3 + 2] azide–alkyne cycloaddition for covalent modification of biomolecules in living systems. J Am Chem Soc 126:15046–15047
4. Albrecht H, Burke PA, Natarajan A et al (2004) Production of soluble ScFvs with C-terminal-free thiol for site-specific conjugation or stable dimeric ScFvs on demand. Bioconjug Chem 15:16–26

5. Allen TM, Brandeis E, Hansen CB et al (1995) A new strategy for attachment of antibodies to sterically stabilized liposomes resulting in efficient targeting to cancer cells. Biochim Biophys Acta 1237:99–108
6. Allen TM, Sapra P, Moase E (2002) Use of the post-insertion method for formation of ligand-coupled liposomes. Cell Mol Biol Lett 7:889–894
7. Andresen TL, Davidsen J, Begtrup M et al (2004) Enzymatic release of antitumor ether lipids by specific phospholipase A2 activation of liposome-forming prodrugs. J Med Chem 47:1694–1703
8. Andresen TL, Jensen SS, Jørgensen K (2005) Advanced strategies in liposomal cancer therapy: problems and prospects of active and tumor specific drug release. Prog Lipid Res 44: 68–97
9. Antony AC (1992) The biological chemistry of folate receptors. Blod 79:2807–2820
10. Baenziger JU, Kornfeld S (1974) Structure of the carbohydrate units of IgA1 immunoglobulin. I. Composition, glycopeptide isolation, and structure of the asparagine-linked oligosaccharide units. J Biol Chem 249:7260–7269
11. Baenziger JU, Kornfeld S (1974) Structure of the carbohydrate units of IgA1 immunoglobufin. II. Structure of the *O*-glycosidically linked oligosaccharide units. J Biol Chem 249:7270–7281
12. Baxter LT, Zhu H, Mackensen DG et al (1994) Physiologically based pharmacokinetic model for specific and nonspecific monoclonal antibodies and fragments in normal tissues and human tumor xenografts in nude mice. Cancer Res 54:1517–1528
13. Béduneau A, Saulnier P, Hindré F et al (2007) Design of targeted lipid nanocapsules by conjugation of whole antibodies and antibody Fab′ fragments. Biomaterials 28:4978–4990
14. Bendas G, Rothe U, Scherphof GL et al (2003) The influence of repeated injections on pharmacokinetics and biodistribution of different types of sterically stabilized immunoliposomes. Biochim Biophys Acta 1609:64–70
15. Binétruy-Tournaire R, Demangel C, Malavaud B et al (2000) Identification of a peptide blocking vascular endothelial growth factor (VEGF)-mediated angiogenesis. EMBO J 19:1525–1533
16. Blume G, Cevc G, Crommelin MDJA et al (1993) Specific targeting with poly(ethylene glycol)-modified liposomes: coupling of homing devices to the ends of the polymeric chains combines effective target binding with long circulation times. Biochim Biophys Acta 1149:180–184
17. Boeckler C, Frisch B, Muller S et al (1995) Immunogenicity of new heterobifunctional cross-linking reagents used in the conjugation of synthetic peptides to liposomes. J Immunol Methods 191:1–10
18. Bonnet D, Ollivier N, Gras-Masse H et al (2001) Chemoselective acylation of fully deprotected hydrazine acetyl peptides. Application to the synthesis of lipopeptides. J Org Chem 66:443–446
19. Bonnet D, Grandjean C, Rousselot-Pailley P et al (2003) Solid-phase functionalization of peptides by an alpha-hydrazinoacetyl group. J Org Chem 68:7033–7040
20. Bonnet L, Pécheur E, Grandjean C et al (2005) Anchorage of synthetic peptides onto liposomes via hydrazone and α-oxo hydrazone bonds. Preliminary functional investigations. Bioconjug Chem 16:450–457
21. Brendas G, Krause A, Bakowsky U et al (1999) Targetability of novel immunoliposomes prepared by a new antibody conjugation technique. Int J Pharm 181:79–93
22. Carrion C, Domingo JC, de Madariaga MA (2001) Preparation of long-circulating immunoliposomes using PEG-cholesterol conjugates: effect of the spacer arm between PEG and cholesterol on liposomal characteristics. Chem Phys Lipids 113:97–110
23. Cavalli S, Tipton AR, Overhand M et al (2006) The chemical modification of liposome surfaces via a copper-mediated [3 + 2] azide–alkyne cycloaddition monitored by a colorimetric assay. Chem Commun 3193–3195

24. Chiu S, Liu S, Perrotti D et al (2006) Efficient delivery of a Bcl-2-specific antisense oligodeoxyribonucleotide (G3139) via transferrin receptor-targeted liposomes. J Control Release 112:199–207
25. Chono S, Tanino T, Seki T et al (2007) Uptake characteristics of liposomes by rat alveolar macrophages: influence of particle size and surface mannose modification. J Pharm Pharmacol 59:75–80
26. Chua M, Fan S, Karush F (1984) Attachment of immunoglobulin to liposomal membrane via protein carbohydrate. Biochim Biophys Acta 800:291–300
27. Ciuchi F, Di Nicola G, Franz H et al (1994) Self-recognition and self-assembly of folic acid salts: columnar liquid crystalline polymorphism and the column growth process. J Am Chem Soc 116:7064–7071
28. Clamp JR, Hough L (1965) The periodate oxidation of amino acids with reference to studies on glycoproteins. Biochem J 94:17–24
29. Crosasso P, Brusa P, Dosio F et al (1997) Antitumoral activity of liposomes and immunoliposomes containing 5-fluorouridine prodrugs. J Pharm Sci 86:832–839
30. Dagar S, Sekosan M, Lee BS et al (2001) VIP receptors as molecular targets of breast cancer: implications for targeted imaging and drug delivery. J Control Release 74:129–134
31. Damodaran D, Jeyakani J, Chauhan A et al (2008) CancerLectinDB: a database of lectins relevant to cancer. Glycoconj J 25:191–198
32. Dawson PE, Muir TW, Clark-Lewis I et al (1994) Synthesis of proteins by native chemical ligation. Science 266:776–779
33. DeFrees SA, Phillips L, Guo L et al (1996) Sialyl Lewis × liposomes as a multivalent ligand and inhibitor of E-Selectin Mediated Cellular Adhesion. J Am Chem Soc 118:6101–6104
34. Derksen JTP, Moselt HWM, Scherphof GL (1988) Uptake and processing of immunoglobulin-coated liposomes by subpopulations of rat liver macrophages. Biochim Biophys Acta 971:127–136
35. Duncan RJS, Weston PD, Wrigglesworth R (1983) A new reagent which may be used to introduce sulfhydryl groups into proteins, and its use in the preparation of conjugates for immunoassay. Anal Biochem 132:68–73
36. ElBayoumi TA, Torchilin VP (2008) Tumor-specific anti-nucleosome antibody improves therapeutic efficacy of doxorubicin-loaded long-circulating liposomes against primary and metastatic tumor in mice. Mol Pharm 6:246–254
37. Elegbede AI, Banerjee J, Hanson AJ et al (2008) Mechanistic studies of the triggered release of liposomal contents by matrix metalloproteinase-9. J Am Chem Soc 130:10639–10642
38. Espuelas S, Haller P, Schuber F et al (2003) Synthesis of an amphiphilic tetraantennary mannosyl conjugate and incorporation into liposome carriers. Bioorg Med Chem Lett 13:2257–2560
39. Espuelas S, Roth A, Thumann C et al (2005) Effect of synthetic lipopeptides formulated in liposomes on the maturation of human dendritic cells. Mol Immunol 42:721–729
40. Fleiner M, Benzinger P, Fichert T et al (2001) Studies on protein–liposome coupling using novel thiol-reactive coupling lipids: influence of spacer length and polarity. Bioconjug Chem 12:470–475
41. Francis GE, Fisher D, Delgado C et al (1998) PEGylation of cytokines and other therapeutic protein and peptides: the importance of biological optimization of coupling techniques. Int J Hematol 68:1–18
42. Frisch B, Boeckler C, Schuber F (1996) Synthesis of short polyoxyethylene-based heterobifunctional cross-linking reagents. Application to the coupling of peptides to liposomes. Bioconjug Chem 7:180–186
43. Gabius H-J (1987) Endogenous lectins in tumors and the immune system. Cancer Invest 5:39-46
44. Gabizon A, Horowitz AT, Goren D et al (1999) Targeting folate receptor with folate linked to extremities of poly(ethylene glycol)-grafted liposomes: in vitro studies. Bioconjug Chem 10:289–298

45. Gaertner HF, Offord RE (1996) Site-specific attachment of functionalized poly(ethylene glycol) to the amino terminus of proteins. Bioconjug Chem 7:38–44
46. Gal S, Pinchuk I, Lichtenberg D (2003) Peroxidation of liposomal palmitoyllinoleoylphosphatidylcholine (PLPC), effects of surface charge on the oxidizability and on the potency of antioxidants. Chem Phys Lipids 126:95–110
47. Gao J, Zhong W, He J et al (2009) Tumor-targeted PE38KDEL delivery via PEGylated anti-HER2 immunoliposomes. Int J Pharm 374:145–152
48. Garbuzenko O, Barenholz Y, Priev A (2005) Effect of grafted PEG on liposome size and on compressibility and packing of lipid bilayer. Chem Phys Lipids 135:117–129
49. Garnier B, Bouter A, Gounou C et al (2009) Annexin A5-functionalized liposomes for targeting phosphatidylserine-exposing membranes. Bioconjug Chem 20:2114–2122
50. Geoghegan KF, Stroh JG (1992) Site-directed conjugation of nonpeptide groups to peptides and proteins via periodate oxidation of 2-amino alcohol. Application to modification at N-terminal serine. Bioconjug Chem 3:138–146
51. Ghebremariam B, Sidorov V, Matile S (1999) Direct evidence for the importance of hydrophobic mismatch for cell membrane recognition. Tetrahedron Lett 40:1445–1448
52. Ghose TI, Blair AH, Kulkarni PN (1983) Preparation of antibody-linked cytotoxic agents. Methods Enzymol 93:280–333
53. Graaf AJ, Kooijman M, Hennink WE et al (2009) Nonnatual amino acids for site-specific protein conjugation. Bioconjug Chem 20:1281–1295
54. Gregoriadis G, Wills EJ, Swain CP, Tavill AS (1974) Drug-carrier potential of liposomes in cancer chemotherapy. Lancet 1: 1313–1316
55. Gunawan RC, Auguste DT (2010) The role of antibody synergy and membrane fluidity in the vascular targeting of immunoliposomes. Biomaterials 31:900–907
56. Hansen CB, Kao CY, Moase EH et al (1995) Attachment of antibodies to sterically stabilized liposomes: evaluation, comparison and optimization of coupling procedures. Biochim Biophys Acta 1239:133–144
57. Harding JA, Engbers CM, Newman MS et al (1997) Immunogenicity and pharmacokinetic attributes of poly(ethylene glycol)-grafted immunoliposomes. Biochim Biophys Acta 1327:181–192
58. Hassane FS, Frisch B, Schuber F (2006) Targeted liposomes: convenient coupling of ligands to preformed vesicles using "Click Chemistry". Bioconj Chem 17:849–854
59. Hosokawa S, Tagawa T, Niki H et al (2003) Efficacy of immunoliposomes on cancer models in a cell-surface antigen-density-dependent manner. Br J Cancer 89:1545–1551
60. Huang A, Huang L, Kennel SJ (1980) Monoclonal antibody covalently coupled with fatty acid. J Biol Chem 255:8015–8018
61. Iden DL, Allen TM (2001) In vitro and in vivo comparison of immunoliposomes made by conventional coupling techniques with those made by a new post-insertion approach. Biochim Biophys Acta 1513:207–216
62. Ishida T, Iden DL, Allen TM (1999) A combinatorial approach to producing sterically stabilized (Stealth) immunoliposomal drugs. FEBS Lett 460:129–133
63. Ishida O, Maruyama K, Tanahashi H et al (2001) Liposomes bearing polyethyleneglycol-coupled transferrin with intracellular targeting property to the solid tumors in vivo. Pharm Res 18:1042–1048
64. Janssen APCA, Schiffelers RM, Hagen TLM et al (2003) Peptide-targeted PEG-liposomes in anti-angiogenic therapy. Int J Pharm 2541:55–58
65. Jensen SS, Andresen TL, Davidsen J et al (2004) Secretory phospholipase A(2) as a tumor-specific trigger for targeted delivery of a novel class of liposomal prodrug anticancer etherlipids. Mol Cancer Ther 3:1451–1458
66. Jolck RI, Berg RH, Andresen TL (2010) Solid-phase synthesis of PEGylated lipopeptides using click chemistry. Bioconjugate Chem 21:807–810
67. Kamps JA, Scherphof GL (1998) Receptor versus non-receptor mediated clearance of liposomes. Adv Drug Deliv Rev 32:81–97

68. Kim S-L, Jeong H-J, Kim E-M et al (2007) Folate receptor targeted imaging using poly(ethylene glycol)-folate: in vitro and in vivo studies. J Korean Med Sci 22:405–411
69. Kinstler OB, Gabriel NE, Farrar CE et al (1999) N-terminally chemically modified protein compositions and methods. US Patent 5:985:265
70. Kirpotin D, Park JW, Hong K et al (1997) Sterically stabilized anti-HER2 immunoliposomes: design and targeting to human breast cancer cells in vitro. Biochemistry 36:66–75
71. Kirpotin DB, Drummond DC, Shao Y et al (2006) Antibody targeting of long-circulating lipidic nanoparticles does not increase tumor localization but does increase internalization in animal models. Cancer Res 66:6732–40
72. Koning GA, Morselt HWM, Velinova MJ et al (1999) Selective transfer of a lipophilic prodrug of 5-fluorodeoxyuridine from immunoliposomes to colon cancer cells. Biochim Biophys Acta 1420:153–167
73. Koning GA, Fretz MM, Woroniecka U et al (2004) Targeting liposomes to tumor endothelial cells for neutron capture therapy. Appl Radiat Isot 61:963–967
74. Kung VT, Redemann CT (1986) Synthesis of carboxyacyl derivatives of posphatidylethanolamine and use as an efficient method for conjugation of protein to liposomes. Biochim Biophys Acta 862:435–439
75. Lee C, Barnett J, Reaven PD (1998) Liposomes enriched in oleic acid are less susceptible to oxidation and have less proinflammatory activity when exposed to oxidizing conditions. J Lipid Res 39:1239–1247
76. Lee RJ, Low PS (1994) Delivery of liposomes into cultured KB cells via folate-mediated endocytosis. J Biol Chem 269:3198–3204
77. Lee RJ, Low PS (1995) Folate-mediated tumor cell targeting of liposome-entrapped doxorubicin in vitro. Biochim Biophys Acta 1233:134–144
78. Lewis WG, Magallon FG, Fokin VV et al (2004) Discovery and characterization of catalysts for azide–alkyne cycloaddition by fluorescence quenching. J Am Chem Soc 126:9152–9153
79. Li Z, Seo TS, Ju J (2004) 1,3-Dipolar cycloaddition of azides with electron-deficient alkynes under mild condition in water. Tetrahedron Lett 45:3143–3146
80. Liang MT, Davies NM, Toth I (2005) Encapsulation of lipopeptides within liposomes: effect of number of lipid chains, chain length and method of liposome preparation. Int J Pharm 301:247–254
81. Lu Y, Low PS (2002) Folate-mediated delivery of macromolecular anticancer therapeutic agents. Adv Drug Deliv Rev 54:675–693
82. Maeda H, Wu J, Sawa T et al (2000) Tumor vascular permeability and the EPR effect in macromolecular therapeutics: a review. J Control Release 65:271–284
83. Marsh D (1996) Intrinsic curvature in normal and inverted lipid structures and in membranes. Biophys J 70:2248–2255
84. Martin FJ, Hubbell W, Papahadjopoulos D (1981) Immunospecific targeting of liposomes to cells: a novel and efficient method for covalent attachment of Fab′ fragments via disulfide bonds. Biochemistry 20:4229–4238
85. Martin FJ, Papahadjopoulos D (1982) Irreversible coupling of immunoglobulin fragments to preformed vesicles. J Biol Chem 257:286–288
86. Maruyama K, Takizawa T, Yuda T et al (1995) Targetability of novel immunoliposomes modified with amphipathic poly(ethylene glycol)s conjugated at their distal terminals to monoclonal antibodies. Biochim Biophys Acta 1234:74–80
87. Maruyama K, Ishida O, Takizawa et al (1999) Possibility of active targeting to tumor tissues with liposomes. Adv Drug Deliv Rev 40:89–102
88. Matsumura Y, Gotoh M, Muro K et al (2004) Phase I and pharmacokinetic study of MCC-465, a doxorubicin (DXR) encapsulated in PEG immunoliposome, in patients with metastatic stomach cancer. Ann Oncol 15:517–525
89. Meerovitch K, Bergeron F, Leblond L et al (2003) A novel RGD antagonist that targets both alphavbeta3 and alpha5beta1 induces apoptosis of angiogenic endothelial cells on type I collagen. Vasc Pharmacol 40:77–89

90. Mehvar R (2003) Recent trends in the use of polysaccharides for improved delivery of therapeutic agents: pharmacokinetic and pharmacodynamic perspectives. Curr Pharm Biotechnol 4:283–302
91. Menezes DEL, Pilarski LM, Allen TM (1998) In vitro and in vivo targeting of immunoliposomal doxorubicin to human B-cell lymphoma. Cancer Res 58:3320–3330
92. Mercadal M, Domigo JC, Petriz J et al (1999) A novel strategy afford high-yield coupling of antibody to extremities of liposomal surface-grafted PEG chains. Biochim Biophys Acta 1418:232–238
93. Miron T, Wilchek M (1993) A simplified method for the preparation of succinimidyl carbonate polyethylene glycol for coupling to proteins. Bioconjug Chem 4:568–569
94. Moghimi SM, Andersen AJ, Hashemi SH et al (2010) Complement activation cascade triggered by PEG-PL engineered nanomedicines and carbon nanotubes: The challenges ahead. J Control Release. doi:10.1016/j.jconrel.2010.04.003
95. Moreira JN, Ishida T, Gaspar R et al (2002) Use of the post-insertion technique to insert peptide ligands into pre-formed stealth liposomes with retention of binding activity and cytotoxicity. Pharm Res 19:265–269
96. Muñoz M, Garcia M, Reig F et al (1998) Physico-chemical characterization of liposomes with covalently attached hepatitis A VP3(101–121) synthetic peptide. Analyst 123:2223–2228
97. Müller P, Nikolaus J, Schiller S et al (2009) Molecular rods with oligospiroketal backbones as anchors in biological membranes. Angew Chem Int Ed. doi:10.1002/anie.200901133
98. Nässander UK, Steerenberg PA, Jong WHD et al (1995) Design of immunoliposomes directed against human ovarian carcinoma. Biochim Biophys Acta 1235:126–139
99. Ogawa Y, Kawahara H, Yagi N et al (1999) Synthesis of a novel lipopeptide with α-melanocyte-stimulating hormone peptide ligand and its effect on liposome stability. Lipids 34:387–394
100. Pan X, Wu G, Yang W et al (2007) Synthesis of cetuximab-immunoliposomes via a cholesterol-based membrane anchor for targeting of EGFR. Bioconjug Chem 18:101–108
101. Park JW, Kirpotin DB, Hong K et al (2001) Tumor targeting using anti-her2 immunoliposomes. J Control Release 74:95–113
102. Park JW, Hong KL, Kirpotin DB et al (2002) Anti-HER2 immunoliposomes: enhanced efficacy attributable to targeted delivery. Clin Cancer Res 8:1172–1181
103. Patrick TA, Kranz DM, van Dyke TA et al (1997) Folate receptors as potential therapeutic targets in choroid plexus tumors of SV40 transgenic mice. J Neurooncol 32:111–123
104. Patwardhan AP, Thompson DH (2000) Novel flexible and rigid tetraether cyclic and macrocyclic bisphosphocholines: synthesis and monolayer properties. Langmuir 16:10340–10350
105. Peer D, Karp JM, Hong S et al (2007) Nanocarriers as an emerging platform for cancer therapy. Nat Nanotechnol 2:751–760
106. Peeters JM, Hazendonk TG, Beuvery EC et al (1989) Comparison of four bifunctional reagents for coupling peptides to proteins and the effect of the three moieties on the immunogenicity of the conjugates. J Immunol Methods 120:133–143
107. Reddy JA, Abburi C, Hofland H et al (2002) Folate targeted cationic liposome-mediated gene transfer into disseminated peritoneal tumors. Gene Ther 9:1542–1550
108. Reubi JC (1995) In vitro identification of VIP receptors in human tumors. J Nucl Med 36:1846–1853
109. Reulen SWA, Brusselaars WWT, Langereis S et al (2007) Protein-liposome conjugates using cysteine-lipids and native chemical ligation. Bioconjug Chem 18:590–596
110. Roberts MJ, Bentley MD, Harris JM (2002) Chemistry for peptide and protein PEGylation. Adv Drug Deliv Rev 54:459–476
111. Rostovtsev VV, Green LG, Fokin VV et al (2002) A stepwise Huisgen cycloaddition process: copper(I)-catalyzed regioselective "ligation" of azides and terminal alkynes. Angew Chem Int Ed 41:2596–2599

112. Rui Y, Wang S, Low PS et al (1998) Diplasmenylcholine-folate liposomes: an efficient vehicle for intracellular drug delivery. J Am Chem Soc 120:11213–11218
113. Rydzynski K, Jedrychowski R (1994). Sensory irritating properties of cyanuric chloride as revealed with plethysmographic method. Int J Occup Med Environ Health 7:149–154
114. Santos AO, Silva LCG, Bimbo LM et al (2010) Design of peptide-targeted liposomes containing nucleic acids. Biochim Biophys Acta 1798:433–441
115. Sapra P, Allen TM (2003) Ligand-targeted liposomal anticancer drugs. Prog Lipid Res 42:439-462
116. Sapra P, Tyagi P, Allen TM (2005) Ligand-targeted liposomes for cancer treatment. Curr Drug Deliv 2:369–381
117. Saul JM, Annapragada A, Natarajan JV et al (2003) Controlled targeting of liposomal doxorubicin via the folate receptor in vitro. J. Control Release 92:49–67
118. Saxon E, Bertozzi CR (2000) Cell surface engineering by a modified Staudinger reaction. Science 287:2007–2010
119. Schelté P, Boeckler C, Frish B et al (2000) Differential reactivity of maleimide and bromoacetyl functions with thiols: application to the preparation of liposomal diepitope constructs. bioconjugate Chem 11:118–123
120. Schiffelers RM, Koning GA, ten Hagen TLM et al (2003) Anti-tumor efficacy of tumor vasculature-targeted liposomal doxorubicin. J Control Release 93:115–122
121. Schroeder R, London E, Brown D (1994) Interactions between saturated acyl chains confer detergent resistance on lipids and glycosylphosphatidylinositol (GPI)-anchored proteins: GPI-anchored proteins in liposomes and cells show similar behavior. PNAS 91: 12130–12134
122. Shimada K, Kamps JAAM, Regts J et al (1997) Biodistribution of liposomes containing synthetic galactose-terminated diacylglyceryl-poly(ethyleneglycol)s. Biochim Biophys Acta 1326:329–341
123. Song CK, Jung SH, Kim D-D et al (2009) Disaccharide-modified liposomes and their in vitro intracellular uptake. Int J Pharm 380:161–169
124. Torchilin VP, Goldmacher VS, Smirnov VN (1978) Comparative studies on covalent and noncovalent immobilization of protein molecules on the surface of liposomes. Biochem Biophys Res Commun 85:983–990
125. Torchilin VP, Khaw BA, Smirnov VN et al (1979) Preservation of antimyosin antibody activity after covalent coupling to liposomes. Biochem Biophys Res Commun 89:1114–1119
126. Torchilin VP (1985) Liposomes as targetable drug carriers. Crit Rev Ther Drug Carrier Syst 2:65–115
127. Torchilin VP (2008) TAT peptide-mediated intracellular delivery of pharmaceutical nanocarriers. Adv Drug Deliv Rev 60:548–558
128. Torchilin VP, Levchenko TS, Lukyanov AN et al (2001) *p*-Nitrophenylcarbonyl-PEG-PE-liposomes: fast and simple attachment of specific ligands, including monoclonal antibodies, to distal ends of PEG chains via *p*-nitrophenylcarbonyl groups. Biochim Biophys Acta 1511:397–411
129. Tornøe CW, Meldal M (2001) Peptidotriazoles: copper(I)-catalyzed 1,3-dipolar cycloadditions on solid-phase. In: Peptides 2001, Proc Am Pept Symp; American Peptide Society and Kluwer Academic Publishers, San Diego, pp 263–264
130. Tornøe CW, Christensen C, Meldal M (2002) Peptidotriazoles on solid phase: [1,2,3]-triazoles by regiospecific copper(I)-catalyzed 1,3-dipolar cycloadditions of terminal alkynes to azides. J Org Chem 67:3057–3064
131. Traut RR, Bollen A, Sun TT et al (1973) Methyl 4-mercaptobutyrimidate as a cleavable cross-linking reagent and its application to the *Escherichia coli* 30s ribosome. Biochemistry 12:3266–3273
132. Veronese FM, Largajolli R, Boccu E et al (1985) Activation of monomethoxy poly(ethylene glycol) by phenylchloroformate and modification of ribonuclease and superoxide dismutase. Appl Biochem Biotechnol 11:141–152

133. Vikbjerg AF, Andresen TL, Jørgensen K et al (2007) Oxidative stability of liposomes composed of docosahexaenoic acid-containing phospholipids. J Am Oil Soc 84:631-637
134. Vogel K, Wang S, Lee RJ et al (1996) Peptide-mediated release of folate-targeted liposome contents from endosomal compartments. J Am Chem Soc 118:1581–1586
135. Wang M, Löwik DWPM, Miller AD et al (2009) Targeting the urokinase plasminogen activator receptor with synthetic self-assembly nanoparticles. Bioconjug Chem 20:32–40
136. Weinstein JN, Blumenthal R, Sharrow SO et al (1978) Antibody-mediated targeting of liposomes. Binding to lymphocytes does not ensure incorporation of vesicle contents into the cells. Biochim Biophys Acta 509:272–288
137. Weissig V, Lasch J, Klibanov AL et al (1986) A new hydrophobic anchor for the attachment of proteins to liposomal membranes. FEBS 202:86–90
138. Weitman SD, Weinberg AG, Coney LR et al (1992) Cellular localization of the folate receptor: potential role in drug toxicity and folate homeostasis. Cancer Res 52:6708–6711
139. Woodle MC, Lasic DD (1992) Sterically stabilized liposomes. Biochim Biophys Acta 1113:171–199
140. Wyszynska K, Przybojewska B, Spiechowicz E et al (1994) Cyanuric chloride has no genotoxic and mutagenic properties in bacteria and bone marrow cells. Int J Occup Med Environ Health 7:281–289
141. Xu L, Tang W, Huang C-C et al (2001) Systemic p53 gene therapy of cancer with immunolipoplexes targeted by anti-Transferrin receptor scFv. Mol Med 7:723–734
142. Xu Z, Jayaseharan JS, Marchant RE (2002) Synthesis and characterization of oligomaltose-grafted lipids with application to liposomes. J Colloid Interface Sci 252:57–65
143. Yagi N, Ogawa Y, Kodaka M et al (2000) Preparation of functional liposomes with peptide ligands and their binding to cell membranes. Lipids 35:673–680
144. Yamada A, Taniguchi Y, Kawano K et al (2008) Design of folate-linked liposomal Doxorubicin to its antitumor effect in mice. Clin Cancer Res 14:8161–8168
145. Zalipsky S (1993) Synthesis of an end-group functionalized polyethylene glycol-lipid conjugate for preparation of polymer-grafted liposomes. Bioconjug Chem 4:296–299
146. Zalipsky S, Puntambekar B, Boulikas P et al (1995) Peptide attachment to extremities of liposomal surface grafted PEG chains: Preparation of the long-circulating form of laminin pentapeptide, YIGSR. Bioconjug Chem 6:705–706
147. Zalipsky S, Mullah N, Dibble A (1999) New chemoenzymatic approach to glyco-lipopolymers: practical preparation of functionally active galactose-poly(ethylene glycol)-distearoylphosphatidic acid (Gal-PEG-DSPA) conjugate. Chem Commun 7:653–654
148. Zhang H, Ma Y, Sun X-L (2009) Chemically-selective surface glyco-functionalization of liposomes through Staudinger ligation. Chem Commun 21:3032–3034
149. Zhu J, Xue J, Guo Z et al (2007) Biomimetic glycoliposomes as nanocarriers for targeting P-Selectin on activated platelets. Bioconjugate Chem 18:1366–1369

Article III

Paper published in Biophysical Journal 2010

This paper was prepared in collaboration with Jonas R. Henriksen, Thomas L. Andresen, Lars Duelund and John H. Ipsen. Henriksen planned the experiments and analyzed all data. Feldborg performed the final isothermal titration calorimetric studies and Duelund the initial isothermal titration calorimetric studies. Henriksen wrote the article in collaboration with Andresen and Ipsen.

This paper is not included in the thesis, as my experimental work constituted a minor part to the overall topic of this paper.

Understanding Detergent Effects on Lipid Membranes: A Model Study of Lysolipids

Jonas R. Henriksen,[†] Thomas L. Andresen,[†] Lise N. Feldborg,[†] Lars Duelund,[‡] and John H. Ipsen[‡*]
[†]DTU-Nanotech, The Technical University of Denmark, Roskilde, Denmark; and [‡]MEMPHYS-Center of Biomembrane Physics, Department of Physics and Chemistry, University of Southern Denmark, Odense, Denmark

ABSTRACT Lysolipids and fatty acids are the natural products formed by the hydrolysis of phospholipids. Lysolipids and fatty acids form micelles in solution and acts as detergents in the presence of lipid membranes. In this study, we investigate the detergent strength of a homologous series of lyso-phosphatidylcholine lipids (LPCs) on 1-palmitoyl-2-oleyl-*sn*-glycerol-3-phosphatidylcholine (POPC) lipid membranes by use of isothermal titration calorimetry and vesicle fluctuation analysis. The membrane partition coefficient (K) and critical micelle concentration (*cmc*) are determined by isothermal titration calorimetry and found to obey an inverse proportionality relation ($cmc \cdot K \sim 0.05$–0.3). The partition coefficient and critical micelle concentration are used for the analysis of the effect of LPCs on the membrane bending rigidity. The dependency of the bending rigidity on LPC membrane coverage has been analyzed in terms of a phenomenological model based on continuum elastic theory, which yields information about the curvature-inducing properties of the LPC molecule. The results reveal: 1), an increase in the partition coefficient with increasing LPC acyl-chain length; and 2), that the degree of acyl-chain mismatch between LPC and POPC determines the magnitude of the membrane mechanical perturbation per LPC molecule in the membrane. Finally, the three-stage model describing detergent membrane interaction has been extended by a parameter D_{MCI}, which governs the membrane curvature stability in the detergent concentration range below the *cmc*-value of the LPC molecule.

INTRODUCTION

The effect of detergents and surfactants on fluid interfaces is a well-explored field in colloidal chemistry. A classical experiment is to demonstrate the dramatic decrease of the surface tension, γ, of an aqueous interface in the presence of detergents described by the Gibbs adsorption relation. For a freely suspended lipid membrane, the interfacial tension is vanishing, and the mesoscopic and macroscopic conformational properties are determined by the bending elasticity governed by the Helfrich (1) energy functional:

$$\mathcal{H}_{\text{bend}} = \gamma A + \frac{\kappa}{2}\int_{A} dA(2H - 2H_0)^2. \qquad (1)$$

The membrane is characterized by the area, A, the mean curvature, H, and the resistance to bending is governed by the bending rigidity, κ. The spontaneous curvature, H_0, reflects the preferred mean curvature of the membrane, caused by asymmetry arising from 1), differences in the lipid composition of the two membrane leaflets; or 2), differences in solvent composition to which the two membrane leaflets are exposed. The main distinction between the amphiphile constituting the membrane and the detergent is that the latter can partition into both the membrane and the solvent. The effect of detergentlike molecules on κ has only been subjected to minor investigations, e.g., the emulsifying effect of cosurfactants in microemulsions (2). However, it is well established that lipid bilayer membranes are mechanically destabilized by the presence of detergents (3,4). A classical model of surfactant destabilization of lipid membranes is the three-stage model (5), in which 1), surfactants partition into the membrane at low concentrations; 2), mixed micelles coexist with bilayer membranes enriched in detergent above a threshold concentration; and 3), above a second threshold in the detergent concentration, only micelles persist. A more quantitative extension of the three-stage model is based on the partitioning properties of monomeric surfactants in membranes and micelles (6), where the first threshold composition of the membrane (defining the onset of membrane solubilization) can be approximated by the product of the membrane partition coefficient, K, and the critical micelle concentration, *cmc*. In this study, we show that although these models are able to describe important properties of surfactant lipid systems, they cannot account for the capacity of surfactants to destabilize membranes mechanically. An increased understanding of the interaction between detergentlike compounds and membranes has many applications in membrane biophysics, e.g., the effect of bile salts (7) and antimicrobial peptides (8) on biomembranes, isolation of membrane proteins (9), identification of insoluble membrane fragments (rafts) (10) and furthermore in the development of tumor target drug delivery systems (11). So far, few studies have been focused on the partitioning of lysolipids into membranes (12). Lysolipids have been shown to increase the ion permeability (13), cause changes in the bilayer hydration properties (14), modify membrane channel function (15), and reduce the lysis tension (16).

Submitted September 9, 2009, and accepted for publication January 15, 2010.

*Correspondence: ipsen@memphys.sdu.dk

Editor: Reinhard Lipowsky.

0006-3495/10/05/2199/7 $2.00

doi: 10.1016/j.bpj.2010.01.037

In this study, we investigate the surfactant properties of a homologous series of Lyso-phosphatidylcholine lipids (LPCX, where $X = 12, 14, 16$ represents the number of hydrocarbons along the saturated acyl-chain) on 1-palmitoyl-2-oleyl-*sn*-glycero-3-phosphatidylcholine (POPC) membranes. The interaction of LPCs and POPC lipid membranes is quantified by isothermal titration calorimetry (ITC) and vesicle fluctuation analysis (VFA) to determine the partition coefficient (K) and the membrane bending rigidity (κ), respectively. The critical micelle concentration of each lysolipid was, in addition, determined by ITC. The study is conducted in the dilute, excess water regime at 25°C, which is far above the main phase transition of POPC. The information obtained from the membrane partitioning and destabilizing capacity of the LPCs allows us to make a detailed analysis of the effect of the LPCs on the membrane stability. The results are interpreted in terms of a phenomenological model, and we propose a simple criterion for the membrane destabilizing potency of a surfactant.

MATERIALS AND METHODS

Experimental

Materials

1-Palmitoyl-2-oleyl-*sn*-glycerol-3-phosphatidylcholine (POPC; purity >98%), 1-dodecanoyl-2-hydroxy-*sn*-glycero-3-phosphocholine (LPC12), 1-tetradecanoyl-2-hydroxy-*sn*-glycero-3-phosphocholine (LPC14), and 1-hexadecanoyl-2-hydroxy-*sn*-glycero-3-phosphocholine (LPC16) were obtained from Avanti Polar Lipids (Alabaster, AL). Organic solvents and sugars were obtained from Sigma-Aldrich (St. Louis, MO). All materials were used without further purification.

Giant unilamellar vesicle preparation

Twenty microliters of POPC lipid in chloroform (0.2 mM) was deposited on platinum wire electrodes using a Hamilton syringe. The solvent was subsequently evaporated overnight in a vacuum chamber. Giant unilamellar vesicles (GUVs) were formed by electroformation (17,18) in a 75 mOsm sucrose solution containing LPCs at the desired concentration. All GUV preparations were conducted at 25°C. The vesicles were then resuspended in a 75 mOsm glucose solution containing LPCs at the desired concentration and subsequently thermostated in an observation chamber. Solution osmolarities were regulated using a freezing-point osmometer (Model 3D3; Advanced Instruments, Norwood, MA) and MilliQ water was used throughout the preparation (Millipore, Bedford, MA).

Large unilamellar vesicle preparation

One-hundred-nanometer large unilamellar vesicles (LUVs) were prepared from POPC lipid films, which were rehydrated in a 75 mOsm glucose solution for 60 min followed by extrusion with an Avanti Polar Lipids mini-extruder. The size distribution of the LUVs was checked by dynamic light scattering (Zetasizer Nano; Malvern Instruments, Malvern, UK) and the effective lipid concentration was determined by ICP-AES (Vista AX; Varian, Palo Alto, CA).

Data analysis

Isothermal titration calorimetry

Isothermal titration calorimetry (ITC) measurements were performed on an iTC200 (Microcal, Northampton, MA) with a cell volume of 204 μL. Small aliquots of 100 nm POPC LUVs were injected into a 75 mM glucose solution containing LPC. Data analysis was performed using custom-made software, which includes an improved baseline estimation and fitting of the partition model described below to the data by χ^2-minimization. The baseline is determined by linear regression of the heat transfer data from the last 20% of the time interval between two injections. The obtained regression lines are then interpolated by line segments. The measured standard deviation of data from the regression line is used to estimate the errors σ_i on the integrated heat transfer ΔQ_i for each injection. In Fig. 1 *a*, the full heat transfer curve is shown.

The data is interpreted in terms of a simple partition model,

$$\frac{C_p}{C_L} = KC_f, \quad K = \frac{1}{C_w}\exp\left(-\Delta G_w^{mem}/RT\right), \qquad (2)$$

where C_p is the concentration of lysolipids partitioned into the membrane, C_L is the total lipid concentration, C_f is the free lysolipid concentration in bulk solution, K is the partition coefficient, $C_w = 55.5$ M is the molar concentration of water, and ΔG_w^{mem} is the free energy of partitioning. The amount of lysolipid is conserved during the titration experiment and is given by the ITC cell concentration $C_0 = C_p + C_f$. Enforcing this constraint on the lysolipid

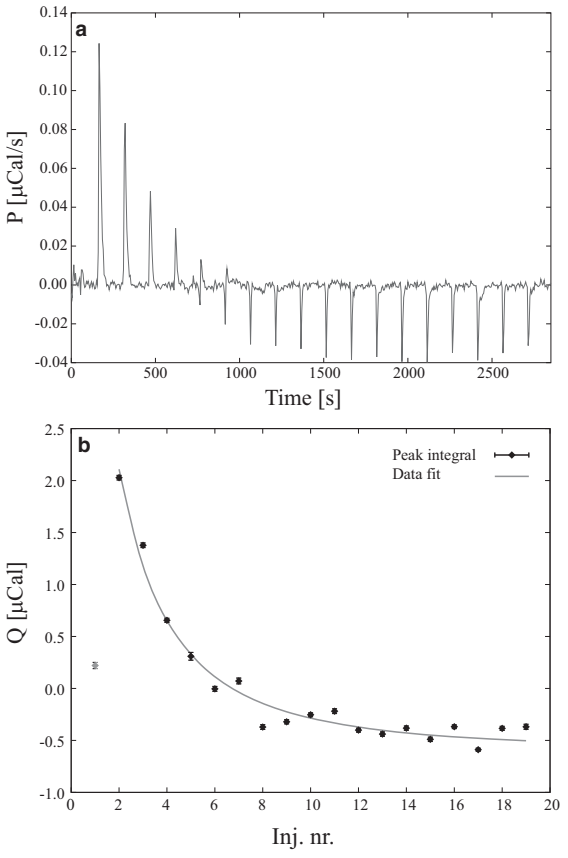

FIGURE 1 Isothermal titration calorimetry injecting POPC LUVs into LPC12 at 25°C. (*a*) Heat-spikes from 2 μL 65.4 mM POPC LUVs injected into a 200 μM LPC12 solution containing 75-mM glucose. (*b*) Peak integrals of the heat-spikes shown in panel *a* as a function of injection number. The peak integrals are fitted using Eqs. 3–5 yielding the partition coefficient, K, the molar enthalpy of partitioning, ΔH_w^{mem}, and the heat of dilution, q_{dil}, as fitting parameters.

concentration, in combination with Eq. 2, yields an expression for the amount of partitioned lysolipid $C_p = KC_LC_0/(1 + KC_L)$. According to Heerklotz and Seelig (6), the cumulant heat, Q_i, is assumed proportional to the amount of compound partitioned into the membrane plus a contribution from heat of dilution. The heat of i^{th} injection is thus modeled as

$$\begin{aligned}\Delta Q_i &= \Delta H_w^{mem} V_{cell} \Delta C_p^i + q_{dil},\\ \Delta C_p^i &= \frac{KC_L^i C_0^i}{1 + KC_L^i} - \frac{KC_L^{i-1} C_0^{i-1}}{1 + KC_L^{i-1}},\end{aligned} \tag{3}$$

where C_0^i and C_L^i are the lysolipid and lipid concentration in the cell after the i^{th} injection, respectively, V_{cell} is the ITC cell volume, ΔH_w^{mem} is the molar enthalpy of partitioning, and q_{dil} is the heat of dilution, which is assumed to be constant. According to Tellinghuisen (19), if instant mixing upon injection is assumed, the lysolipid and lipid concentrations are given by

$$\begin{aligned}C_0^i &= C_0\left(1 - \exp\left(\frac{-V_{add}^i}{V_{cell}}\right)\right),\\ C_L^i &= C_L \exp\left(\frac{-V_{add}^i}{V_{cell}}\right),\end{aligned} \tag{4}$$

where

$$V_{add}^i = \sum_0^i V_i$$

is the cumulant volume injected into the cell upon the i^{th} injection. As C_0, C_L, V_{cell}, and V_i are given by the experimental setup, the remaining unknown parameters K, ΔH_w^{mem}, and q_{dil}, are determined as fitting variables by minimization of

$$\chi^2\left(K, \Delta H_w^{mem}, q_{dil}\right) = \sum_i \left(\frac{\Delta Q_i^{exp} - \Delta Q_i}{\sigma_i}\right)^2, \tag{5}$$

where ΔQ_i^{exp} is the experimentally measured heat from each injection (shown in Fig. 2 *b*) and ΔQ_i is given by Eq. 3. The experimental error associated with the heat of injection, σ_i, is estimated from the ITC thermogram as described previously. The results are compiled in Table 1 and are averages of 3–6 independent ITC experiments.

Bending rigidity measurements

Large unilamellar vesicles were cultivated by electroformation of POPC films hydrated in a 75 mM sucrose solution containing LPC. Suspending the vesicles in a 75 mM glucose solution ensures both improved phase contrast and sedimentation of the GUVs at the bottom of the observation chamber. Preparation of GUVs with the partitioning agent present in the hydration solution ensures that 1), the LPCs are distributed evenly between the two monolayer leaflets of the bilayer; and 2), the lysolipid reservoir is large and the concentration can therefore be considered as constant. The free (bulk) concentration of lysolipid in the GUV sample can, as a consequence, be estimated by the LPC concentration in the hydration solution because only a small fraction of lysolipid has partitioned into the lipid membrane ($K \simeq 10^2 - 10^4\ M^{-1}$ and $C_L^{GUV} \simeq 10^{-7}$ M, which results in $C_p/C_0 \simeq KC_L < 10^{-3}$). In a temperature-controlled chamber (25°C), undulating vesicles are visualized using phase contrast microscopy (Axiovert S100; Carl Zeiss, Oberkochen, Germany). The chamber is sealed to prevent evaporation from the solution and possible changes of concentrations during the experiment. For each measurement, a set of 4000–6000 GUV contours is collected as described in earlier work (20). Each estimate of the bending rigidity is an average obtained from measurements of ~20 individual vesicles. The data analysis for determination of κ is performed by custom-made software (20). In general, the VFA technique is well suited for measuring the bending rigidity of membranes perturbed by partitioning agents, because the measuring principle is noninvasive and the measuring chamber prevents evaporation.

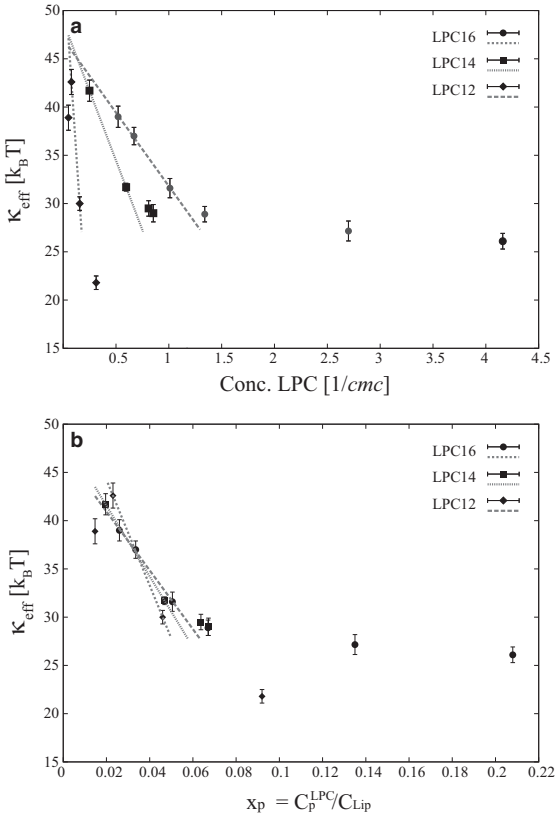

FIGURE 2 Plot of the effective bending rigidity as a function of (*a*) the LPC bulk concentration given in units of the LPC *cmc*-value and (*b*) the LPC membrane molar fraction, x_p, given by $x_p \simeq C_p^{LPC}/C_{Lip} = KC_{LPC}$ for $C_{LPC} < cmc$. Lines representing the fit of Eq. 7 are shown in panel *a* and guidelines emphasizing the differences in LPC influence on κ_{eff} as a function of x_b are shown in panel *b*.

RESULTS AND DISCUSSION

ITC

The titration of POPC LUVs into LPC solutions were all performed at LPC concentrations at which demicellization is

TABLE 1 Parameter values derived from ITC and VFA at 25° C

	LPC12	LPC14	LPC16
K [M^{-1}]	460 ± 50	1750 ± 94	12500 ± 3900
ΔG_w^{mem}[kJ/mol]	−25.1 ± 0.3	−28.1 ± 0.1	−33.3 ± 0.7
ΔH_w^{mem}[kJ/mol]	1.3 ± 0.1	−3.0 ± 0.1	−3.0 ± 0.5
cmc [μM]	640 ± 10	45 ± 2	4*
$K \cdot cmc$	0.29 ± 0.03	0.080 ± 0.006	0.050 ± 0.003
D_{MCI}	2.9	0.6	0.3
λ[Å]	1.8	1.6	1.5

Compilation of the thermodynamic data obtained by ITC at 25°C and mechanical stability parameters assessed by VFA.
*The *cmc*-value of LPC16 was adopted from the literature (12,21), which we verified by fluorescence anisotropy measurements.

neglectable, and partitioning of monomeric LPC into the membrane is thus assumed to be the main contribution of the heat transfer. The *cmc*-values for LPC12 and LPC14 were determined by ITC (data not shown) and the *cmc* of LPC16 was adopted from literature (12,21). Fig. 1 *a* shows heat-spikes from injecting POPC LUVs into LPC12. The heat per injections and the best fit of Eq. 5 to the data is given in Fig. 1 *b*. The obtained values for the partition coefficients and molar enthalpies of partitioning of LPCs into the membrane are given in Table 1. The partition coefficient increases strongly with LPC acyl-chain length with an approximative linear relationship between the free energy of partitioning and the chain length,

$$\Delta G_{\mathrm{w}}^{\mathrm{mem}}/RT = -\ln(55.5\ \mathrm{M}\cdot K) \simeq -0.14 - 0.83X,$$

in agreement with earlier reports (12). The free energy of LPC monomer partitioning into micelles similarly exhibits a linear relationship with X,

$$\Delta G_{\mathrm{w}}^{\mathrm{mic}}/RT = -\ln\,(55.5\ \mathrm{M}/cmc) \simeq 3.83 - 1.27X.$$

For the three different LPCs, $K\cdot cmc \sim 0.05 - 0.3$, showing that the free energy of transferring a monomer from micelle to membrane ($\Delta G_{\mathrm{mic}}^{\mathrm{mem}} = -RT\ \ln(K\cdot cmc) > 0$) is positive and that the process does not occur spontaneously. In work of Heerklotz and Seelig (6), the product, $K\cdot cmc$, was suggested as a measure of a surfactant's capacity to solubilize a membrane. In their classification of surfactants, $K\cdot cmc \leq 1$ ($\Delta G_{\mathrm{mic}}^{\mathrm{mem}} \geq 0$) infers a strong detergent whereas $K\cdot cmc \geq 1$ ($\Delta G_{\mathrm{mic}}^{\mathrm{mem}} \leq 0$) is a weak detergent. By this definition of detergent strength, the LPCs investigated in this study are all strong detergents and follow the sequence: LPC16 > LPC14 > LPC12.

Bending rigidity

The measurements of membrane bending rigidity were performed over a wide range of LPC concentrations at 25°C. In the case of LPC16, GUVs could be studied at concentrations ranging from zero to values above the *cmc* value of LPC16. For LPC12, GUV formation was only possible in a limited concentration-range below *cmc*, whereas for studies of LPC14 the GUVs lost their optical contrast near the *cmc*-value of LPC14. The overall trend is a dramatic decrease in the observed bending rigidity with increasing LPC concentrations, except at the lowest LPC concentrations where minor increases in the bending rigidity are observed (Fig. 2).

In Fig. 2 the bending rigidity is plotted as a function of 1), the bulk/free LPC concentration scaled with respect to the LPC *cmc*-value; and 2), as a function of the LPC membrane molar fraction $x_{\mathrm{p}} \simeq C_{\mathrm{p}}/C_{\mathrm{lip}}$. The magnitude of the LPCs' effect on the membrane bending rigidity depends on whether it is measured relative to the bulk or membrane concentration which is evident in Fig. 2. The decrease in κ, when measured as a function of x_{p} or the *cmc*-scaled bulk concentration, is more pronounced as the acyl-chain length of the lysolipids is reduced. Despite the larger partition coefficient of LPC16, the effect on κ per LPC molecule in the membrane is less than for its shorter homologs. For LPC16, a saturation of κ is observed at high concentrations (Fig. 2 *a*), which correlates with the formation of micelles above the *cmc*-value. Above *cmc*, the LPC16 monomer concentration in the solution is approximately constant and no further partitioning of LPC monomers into the membrane occurs. Below *cmc*, the monomer concentration in the solution is well approximated by total lysolipid concentration. From Fig. 2 *b*, it is evident that the LPC molecules reduce the effective bending rigidity in a common range of x_{p}; however, there are differences in the degree of the perturbation caused by the individual LPC molecules depending on acyl-chain length. This effect is evident by the change in κ_{eff} as a function of x_{p}, as indicated by the slope of the guidelines shown in Fig. 2 *b*.

Phenomenological model

The dramatic reduction in the effective bending rigidity at low lysolipid concentration can be interpreted in terms of a simple phenomenological model, which includes the local effect of the LPCs on the membrane mean curvature. The Helfrich (1) free energy (see also Eq. 1), for the case $H_0 = 0$, is extended by adding a free energy contribution arising from the lateral distribution of lysolipids,

$$\begin{aligned}\mathcal{H}_{\mathrm{int}} &= \kappa_0\lambda\int dA(\rho_+ - \rho_-)2H \\ &\quad + k_{\mathrm{B}}T\int dA\big(\rho_- ln\big(a_{\mathrm{lyso}}\rho_-\big) + \rho_+\ln\big(a_{\mathrm{lyso}}\rho_+\big)\big),\end{aligned} \tag{6}$$

where $\rho_\pm$ is the local lateral density of lysolipids in the upper and lower monolayer leaflets and a_{lyso} is the cross-sectional area per lysolipid in the membrane. The bending rigidity of the detergent free lipid membrane is given by κ_0. In a first approximation, a_{lyso} can be set equal to $a_{\mathrm{lipid}} = 70$ Å^2 (22). The second term in Eq. 6 represents the gas approximation of the free energy for the lateral distribution of lysolipids in the membrane monolayers, while the first term models the coupling between the local lysolipid density difference ($\rho_+ - \rho_-$) and the mean curvature (H). The coupling strength of ($\rho_+ - \rho_-$) and H is governed by the parameter λ, which has dimension of length. The term $\lambda/2\ (\rho_+ - \rho_-)$ can be identified as the local spontaneous curvature. Stability analysis of the total free energy, $\mathcal{H} = \mathcal{H}_{\mathrm{int}} + \mathcal{H}_{\mathrm{int}}$, show that the coupling term ($\mathcal{H}_{\mathrm{int}}$) in general leads to a reduction of the effective bending rigidity of the membrane (23,24),

$$\frac{\kappa_{\mathrm{eff}} - \kappa_0}{\kappa_0} = -4\lambda^2\rho_0\frac{\kappa_0}{k_{\mathrm{B}}T} = -\frac{4\lambda^2}{a_{\mathrm{lipid}}}\frac{\kappa_0}{k_{\mathrm{B}}T}(Kcmc)\frac{c_{\mathrm{f}}}{cmc}, \tag{7}$$

where ρ_0 is the average lateral density of lysolipid in the membrane. A fit of Eq. 7 to the data shown in Fig. 2 *a* provides an estimate of λ for each of the three lysolipids, which are given in Table 1. The data shown in Fig. 2 and the predictions of the phenomenological model (Eq. 7),

$$\kappa_{\text{eff}} \rightarrow 0 \quad \text{for} \quad \frac{4\lambda^2}{a_{\text{lipid}}}\frac{\kappa_0}{k_{\text{B}}T}(Kcmc)\frac{c_{\text{f}}}{cmc} > 1,$$

suggest an extension of Heerklotz and Seelig's (6) measure of detergent potency by introducing a membrane curvature instability (MCI) parameter:

$$D_{\text{MCI}} = \frac{4\lambda^2}{a_{\text{lipid}}}\frac{\kappa_0}{k_{\text{B}}T}(Kcmc). \tag{8}$$

In this study, the fit of Eq. 7 to the data shown in Fig. 2 *a* yield equal values of κ_0 for all three LPCs, while $K\cdot cmc$ and λ decreases with the LPC acyl-chain length leading to significant changes in D_{MCI} (see Table 1). In general, both the extent of partitioning and the local membrane perturbing effect is important for the overall mechanical stability of the membrane subject to the partitioning agents. Both of these effects are incorporated into the parameter D_{MCI}. Within the framework of the presented phenomenological model, the detergent strength is thus defined as strong when $D_{\text{MCI}} > 1$ and weak for $D_{\text{MCI}} < 1$. The value $D_{\text{MCI}} < 1$ corresponds to the classical model of membrane destabilization (5). According to this, micelles and membranes may coexist at concentration levels above *cmc*, and even the smallest lipid-uptake by the micelles will eventually lead to the disappearance of the bilayer membranes with increasing surfactant concentration. In the case $D_{\text{MCI}} < 1$, the phase-line separating the region of mixed micelles and of intact membranes is given by $C_{\text{D}}^{\text{sat}} = (1 + KC_{\text{L}})cmc$, where $C_{\text{D}}^{\text{sat}}$ is the detergent concentration at which the membrane is saturated (6,25). For the case $D_{\text{MCI}} > 1$, the vesicles collapse at a concentration $C_{\text{D}}^{\text{MCI}}$ below *cmc* of the surfactant due to membrane curvature stress. Above this concentration, lipid-surfactant aggregates are characterized by a higher curvature ($1/R$) and a considerable increase in the partition coefficient of $\sim\exp(\kappa/k_{\text{B}}T\ \lambda/R\ \rho a_{\text{lyso}})$ is expected (due to the first term of Eq. 6). The structure of these lipid-surfactant aggregates will depend on the particular system, but tubular membranes of high curvature or tubular micelles are obvious candidates and have been observed in some lipid surfactant systems (26). Furthermore, for $D_{\text{MCI}} > 1$, the phase-line separating the region of intact membranes and the collapsed state is given by $C_{\text{D}}^{\text{MCI}} = (1 + KC_{\text{L}})cmc/D_{\text{MCI}}$, where $C_{\text{D}}^{\text{MCI}}$ is the detergent concentration at which the membrane collapses. The parameter D_{MCI} can be determined via the previous equation if $K\cdot cmc$ and the phase line has been determined experimentally, e.g., by ITC. According to this definition of detergent strength, only LPC12 is a strong detergent and the LPCs investigated follow the sequence: LPC12 > LPC14 > LPC16.

Interpretation of λ

The incorporation of LPCs into lipid bilayers is expected to organize with their polar PC-headgroups close to the bilayer interface and their hydrocarbon chain buried into the hydrophobic core of the membrane, as shown in Fig. 3. A single lysolipid in one of the monolayers will perturb the packing properties of the surrounding lipids in a radius characterized by the lateral correlation length ξ (27). For temperatures well above the main phase transition of the lipid membrane, this correlation length is short, at $\xi \simeq$ 1–2 nm. A possible calculation procedure is to consider a membrane square patch (length of 2ξ with zero tension) with a lysolipid incorporated into one of the monolayers and calculate λ by (28)

$$\kappa_0\frac{\lambda}{a_{\text{lyso}}} = \int_{-\delta}^{\delta}\Pi(z)z\,dz, \tag{9}$$

where $\Pi(z)$ is the lateral pressure profile through the membrane of thickness 2δ. This can be done by self-consistent field theory (29,30), molecular dynamics, or coarse-grained simulations of the membrane.

A simpler approach is to make a rough estimate of λ from dimensional analysis by assuming that the lateral effects from a local membrane perturbation, e.g., insertion of a lysolipid, vanish over the length ξ. A simple packing consideration leads to

$$\lambda \simeq \frac{a_{\text{lyso}}}{l}\left(1 + \frac{\Delta n}{\overline{n}_{\text{Lip}}}\right)\frac{1}{N_\xi}, \tag{10}$$

where $\overline{n}_{\text{Lip}} = (n_{sn1} + n_{sn2})/2$ is the average lipid hydrocarbon chain length and $\Delta n = \overline{n}_{\text{Lip}} - X$ is a measure of the chain length difference between lipid and lysolipid. Here $2l$ corresponds to the hydrophobic thickness of the lipid bilayer and N_ξ is the number of lipids within a lateral coherence patch. Assuming $a_{\text{lyso}} = 70$ Å^2, $l_{\text{max}} = 1$ nm, $\overline{n}_{\text{Lip}} = 17$, and $N_\xi = 7$ leads to λ(LPC16) = 1.1 Å, λ(LPC14) = 1.2 Å,

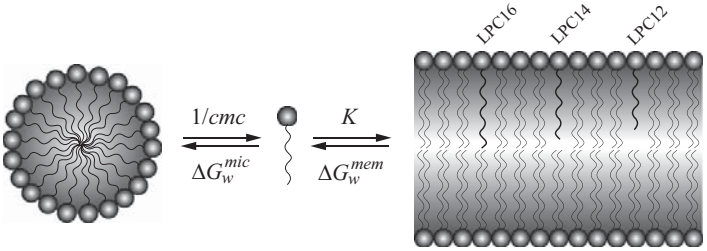

FIGURE 3 Illustration of the LPC equilibria in the presence of a lipid membrane. The partitioning of LPC is given by the partition coefficient, K, and the free energy of partitioning, $\Delta G_{\text{w}}^{\text{mem}}$. The micelle formation equilibrium is described by the *cmc*-value and the free energy of transferring a detergent monomer from bulk to micelle, $\Delta G_{\text{w}}^{\text{mic}}$. The incorporation of LPC molecules in the membrane bilayer is illustrated, showing increased degree of acyl-chain mismatch going from LPC16 to LPC12.

and λ(LPC12) = 1.3 Å, which is a reasonable estimate of the size and trend of λ when compared to the values in Table 1.

Comparison with antimicrobial peptides

The above results have strong similarity with findings on the membrane perturbation of antimicrobial peptides. Antimicrobial peptides are typically small helical peptides that partition into the bilayer leaflets and perturb the membrane by inducing curvature stress. Membrane softening and destabilizing behavior has also been observed with this class of peptides. Gramicidin (31) and Magainin (20,23) are specific examples where a saturation in the bending rigidity is observed with increasing bulk concentration. However, there are no indications of aggregation in the bulk solution to explain this behavior and interaction and aggregation of peptides in the membrane must thus be taken into account. For Gramicidin, the *trans*-membrane dimerization, and for Magainin, the transient membrane pore formation, serve to couple peptides between the monolayers. Consequently, the membrane destabilization parameter, D_{MCI}, must be modified so that *cmc* is replaced by the bulk concentration at which some aggregation of peptides in the membrane takes place. It is interesting to note that the lytic activity of amphiphatic peptides has been observed to increase with both the peptide partitioning into the membrane and the hydrophobic moment, a measure of the capability of a peptide to perturb a bilayer interface (32). Indications of bilayer softening in the presence of cationic surfactants can be inferred from observations of extensive swelling of the lamella phase (33,34). Because high salt concentration (100 mM NaCl) excludes long-ranged electrostatic repulsion as a possible mechanism, the Helfrich (1) steric entropic repulsion due to reduced membrane bending rigidity is the most plausible explanation. Furthermore, deuterium nuclear-magnetic-resonance studies (35) suggest that lipid bilayers are softened by a range of antimicrobial peptides.

CONCLUSIONS

In this article, the interaction of LPC molecules with POPC lipid membranes was investigated using ITC and VFA techniques. The obtained results for the membrane partition properties of the LPCs and the influence on the membrane bending rigidity revealed significant differences in the action of LPCs on the membrane, depending on the LPC acyl-chain length. The longest acyl-chain LPC16 (displaying the smallest acyl-chain mismatch to POPC) gave the weakest perturbation per LPC molecule associated with the membrane, while the LPC12, with the shortest acyl-chain (displaying the largest acyl-chain mismatch) displayed the largest perturbation. Furthermore, GUVs were formed well above the *cmc* of LPC16, whereas studies of LPC12 were only possible at concentrations $C_{\mathrm{D}}^{\mathrm{MCI}} < 0.4 \cdot cmc$(LPC14)— i.e., well below the *cmc*-value. These results point to the conclusion that some detergents are strong in the sense that they mechanically destabilize the membrane through curvature stress, resulting in curvature-induced instability of the GUV, and others are strong detergents in the sense that they form micelles in which the membrane can dissolve. In extension of the three-stage model, a parameter D_{MCI} was proposed that captures the curvature instability induced by a detergent. The MCI parameter revealed that LPC12 is a strong ($D_{\mathrm{MCI}} > 1$) and LPC14 and LPC16 are weak ($D_{\mathrm{MCI}} < 1$) detergents of POPC membranes. From phenomenological modeling, we found that the parameter D_{MCI} can be expressed by the bending rigidity, $cmc \cdot K$, and the local mean curvature coupling-parameter λ, which is related to the packing properties of LPCs in the bilayer. The criterion of a strong detergent by the model of Heerklotz and Seelig (6) ($K \cdot cmc < 1$) is not always sufficient, and the introduction of the D_{MCI} parameter may provide an alternative determination of detergent strength.

The MEMPHYS-Centre for Biomembrane Physics is supported by the Danish National Research Foundation. J.R.H. was supported by the Danish Medical Research Council (grant No. 271-08-0146) and the Danish Council for Strategic Research, Nanoscience and Technology, Biotechnology and IT (NABIIT) (grant No. 2106-07-0033). L.N.F. was supported by the Danish Council for Strategic Research, NABIIT (grant No. 2106-08-0081).

REFERENCES

1. Helfrich, W. 1973. Elastic properties of lipid bilayers: theory and possible experiments. *Naturforsch Z.* 28:693–703.
2. de Gennes, P. G., and C. Taupin. 1982. Microemulsions and the flexibility of oil/water interfaces. *J. Phys. Chem.* 86:2294–2304.
3. Koynova, R., and B. Tenchov. 2001. Interaction of surfactants and fatty acids with lipids. *Curr. Opin. Colloid Interface Sci.* 6:277–286.
4. Alonso, A., and F. Goni. (Guest editors.). 2000. Detergents in biomembranes studies. *Biochim. Biophys. Acta.* 1508:1–19. (Special issue).
5. Helenius, A., and K. Simons. 1975. Solubilization of membranes by detergents. *Biochim. Biophys. Acta.* 415:29–79.
6. Heerklotz, H., and J. Seelig. 2000. Correlation of membrane/water partition coefficients of detergents with the critical micelle concentration. *Biophys. J.* 78:2435–2440.
7. O'Connor, C. J., R. G. Wallace, …, J. Sunamoto. 1985. Bile salt damage of egg phosphatidylcholine liposomes. *Biochim. Biophys. Acta.* 817:95–102.
8. Bechinger, B., and K. Lohner. 2006. Detergent-like actions of linear amphipathic cationic antimicrobial peptides. *Biochim. Biophys. Acta.* 1758:1529–1539.
9. le Maire, M., P. Champeil, and J. V. Møller. 2000. Interaction of membrane proteins and lipids with solubilizing detergents. *Biochim. Biophys. Acta.* 1508:86–111.
10. Simons, K., and E. Ikonen. 1997. Functional rafts in cell membranes. *Nature.* 387:569–572.
11. Andresen, T. L., S. S. Jensen, and K. Jørgensen. 2005. Advanced strategies in liposomal cancer therapy: problems and prospects of active and tumor specific drug release. *Prog. Lipid Res.* 44:68–97.
12. Høyrup, P., J. Davidsen, and K. Jørgensen. 2001. Lipid membrane partitioning of lysolipids and fatty acids: effect of membrane phase structure and detergent chain lengths. *J. Phys. Chem. B.* 105: 2649–2657.
13. Mills, J., and D. Needham. 2006. Lysolipid incorporation in dipalmitoylphosphatidylcholine bilayer membranes enhances the ion

permeability and drug release rates at the membrane phase transition. *Biochim. Biophys. Acta.* 1716:77–96.

14. Marsh, D. 1989. Water adsorption isotherms and hydration forces for lysolipids and diacyl phospholipids. *Biophys. J.* 55:1093–1100.
15. Lundbaek, J. A., and O. S. Andersen. 1994. Lysophospholipids modulate channel function by altering the mechanical properties of lipid bilayers. *J. Gen. Physiol.* 104:645–673.
16. Zhelev, D. V. 1998. Material property characteristics for lipid bilayers containing lysolipid. *Biophys. J.* 75:321–330.
17. Angelova, M. I., and D. S. Dimitrov. 1986. Liposome electroformation. *Faraday Discuss. Chem. Soc.* 81:303–311.
18. Angelova, M. I., S. Soleau, …, P. Bothorel. 1992. Preparation of giant vesicles by external AC electric fields. Kinetics and applications. *Prog. Colloid Polym. Sci.* 89:127–131.
19. Tellinghuisen, J. 2007. Calibration in isothermal titration calorimetry: heat and cell volume from heat of dilution of NaCl(aq). *Anal. Biochem.* 360:47–55.
20. Henriksen, J., A. C. Rowat, and J. H. Ipsen. 2004. Vesicle fluctuation analysis of the effects of sterols on membrane bending rigidity. *Eur. Biophys. J.* 33:732–741.
21. Marsh, D. 1990. Handbook of Lipid Bilayers. CRC Press, Boca Raton, FL.
22. Nagle, J. F., and S. Tristram-Nagle. 2000. Structure of lipid bilayers. *Biochim. Biophys. Acta.* 1469:159–195.
23. Bouvrais, H., P. Méléard, …, J. H. Ipsen. 2008. Softening of POPC membranes by magainin. *Biophys. Chem.* 137:7–12.
24. Leibler, S. 1986. Curvature instability in membranes. *J. Phys. (Fr.).* 47:507–516.
25. Heerklotz, H., and J. Seelig. 2001. Detergent-like action of the antibiotic peptide surfactin on lipid membranes. *Biophys. J.* 81:1547–1554.
26. Almgren, M. 2000. Mixed micelles and other structures in the solubilization of bilayer lipid membranes by surfactants. *Biochim. Biophys. Acta.* 1508:146–163.
27. Ipsen, J. H., K. Jørgensen, and O. G. Mouritsen. 1990. Density fluctuations in saturated phospholipid bilayers increase as the acyl-chain length decreases. *Biophys. J.* 58:1099–1107.
28. Helfrich, W. 1981. Physics of defects. *In* Les Houches Session XXV. R. Balian, M. Kléman, and J.-P. Poirier, editors. North-Holland, Amsterdam, The Netherlands.
29. Zemel, A., A. Ben-Shaul, and S. May. 2004. Membrane perturbation induced by interfacially adsorbed peptides. *Biophys. J.* 86:3607–3619.
30. Kik, R. A., J. M. Kleijn, and F. A. M. Leermakers. 2005. Bending moduli and spontaneous curvature of the monolayer in a surfactant bilayer. *J. Phys. Chem. B.* 109:14251–14256.
31. Gerbeaud, C. 1998. Effect of the insertion of proteins and peptides upon membrane mechanical properties and the morphological changes of giant vesicles [Effect de l'insertion de protéines et de peptides membranaires sur les propriétés mécaniques et les changements morphologiques de vésicules géantes]. PhD thesis, L'Université Bordeaux I, Bordeaux, France.
32. Castano, S., B. Desbat, …, J. Dufourcq. 1999. Structure, orientation and affinity for interfaces and lipids of ideally amphipathic lytic $L_iK_{j(i=2j)}$ peptides. *Biochim. Biophys. Acta.* 1416:176–194.
33. Gustafsson, J., G. Oradd, …, M. Almgren. 1997. A defective swelling lamellar phase. *Langmuir.* 13:852–860.
34. Gustafsson, J., G. Oradd, and M. Almgren. 1997. Disintegration of the lecithin lamellar phase by cationic surfactants. *Langmuir.* 13: 6956–6963.
35. Otten, D., M. F. Brown, and K. Beyer. 2000. Softening of membrane bilayers by detergents elucidated by deuterium NMR spectroscopy. *J. Chem. Phys. B.* 104:12119–12129.

Appendix II

Materials and methods for Chapter 2

Materials

1,2-Distearoyl-*sn*-glycero-3-phosphocholine (DSPC), 1,2-distearoyl-*sn*-glycero-3-phosphoethanolamine-(polyethylene glycol)$_{2000}$ (DSPE-PEG$_{2000}$), 1,2-distearoyl-*sn*-glycero-3-phosphoethanolamine-N-[amino(polyethylene glycol)$_{2000}$] (DSPE-PEG$_{2000}$-NH$_2$), 1,2-distearoyl-*sn*-glycero-3-phosphoethanolamine-N-[maleimide(polyethylene glycol)$_{2000}$] (DSPE-PEG$_{2000}$-Mal), and 1,2-distearoyl-*sn*-glycero-3-phosphoethanolamine-N-[PDP(polyethylene glycol)$_{2000}$] (DSPE-PEG$_{2000}$-PDP) were purchased from Avanti Polar Lipids Inc. (Alabaster, USA). Dithiothreitol (DTT), 5-azidopentanoic acid, 4-formyl benzoic acid, 4-pentynoic acid, N-(3-dimethylaminopropyl)-N′-ethylcarbodiimide hydrochloride (EDC·HCl), thallium(III) trifluoroacetate, trifluoroacetic acid (TFA), and triisopropylsilane (TIS) were purchased from Sigma Aldrich (Schnelldorf, Germany). The coupling reagent *O*-(7-Azabenzotriazol-1-yl)-*N,N,N′,N′*-tetramethyluronium hexafluorophosphate (HATU), Wang Resin and all Fmoc protected amino acids used for the solid phase peptide synthesis were purchased from GL Biochem (Shanghai, China). All chemicals and reagents were of analytical grade and used without further purification.

Instrumentation

FT-IR was recorded on a Perkin Elmer Spectrum 100 FT-IR Spectrometer. Dynamic light scattering and zeta-potential measurements were performed on a Brookhaven Instruments Corporation Zeta PALS zeta potential analyzer. Analytical reversed-phase high-performance liquid chromatography (RP-HPLC) was carried out on a Shimadzu LC-2010

analytical HPLC by employing a Waters XTerra® C_8 5 µm (4.6 x 150 mm) column. Semi-preparative HPLC was performed on a Waters Semi-preparative HPLC equipped with a Waters 600 Pump & Controller and a Waters 2489 UV/Visible Detector using a a Waters XTerra® C_8 5µm (19 x 150 mm) column. HPLC Eluent A consisted of a 5% MeCN aqueous solution with 0.1% TFA; HPLC Eluent B consisted of 0.1% TFA in MeCN. HPLC analysis was monitored using dual channel UV detection at 254 nm and 280 nm. Pre-packed Strata C_8 solid phase extraction (SPE) (55 µm, 70 Å) Giga Tubes from Phenomenex (Torrance, USA) were used for the purification of functionalized phospholipids. Mass spectra were recorded using a Bruker Daltonics Reflex IV MALDI-TOF Spectrometer using 2,5-dihydroxybenzoic acid (DHB) spiked with sodium trifluoroacetate in MeOH as matrix. NMR spectra were recorded either on a Bruker Avance DPS 250 MHz or a Varian Mercury 300 MHz Spectrometer using the solvent peak as an internal reference.

Synthesis of functionalized TATE peptides

General SPPS protocol: The linear TATE octapeptide NH_2-D-Phe-Cys(Acm)-Tyr(*t*Bu)-D-Trp(Boc)-Lys(Boc)-Thr(*t*Bu)-Cys(Acm)-Thr(*t*Bu)-Resin was synthesized manually by SPPS on a Wang Resin preloaded with NH_2-Thr(*t*Bu)-OH (0.50 g, 0.50 mmol/g) by standard Fmoc methodology. Each coupling was performed by 4.0 equiv. Fmoc protected amino acid, 3.95 equiv. HATU and 8.0 equiv. 2,4,6-collidine in DMF (5.0 mL). Cleavage of the Fmoc group was carried out using piperidine in DMF (1:4) for 2 x 5 minutes. Completion of each coupling and deprotection step were monitored by the Kaiser test. Removal of the Acm protection groups on the two cysteines and simultaneous disulfide bond formation was achieved by addition of $Tl(CF_3COO)_3$ (0.27 g, 0.50 mmol, 2.0 equiv.) in DMF (5.0 mL) for 75 min.. The resin containing the cyclized peptide was extensively washed with DMF (10 × 5.0 mL) and subsequently divided into five SPPS reaction vials (5 × 0.10 g) in which the N-terminal was acylated with the desired functionality as described below.

TATE-maleimide (1a). 4-Maleimidobutyric acid (38 mg, 0.20 mmol, 4.0 equiv.), HATU (75 mg, 0.198 mmol, 3.95 equiv.) and 2,4,6-colidine (53 uL, 0.40 mmol, 8.0 equiv.) in DMF (2.0 mL) were added to the resin immobilized cyclic octapeptide for 2 hours at room temperature followed by washing with DMF (4 × 5.0 mL). The peptide was cleaved from the solid support by addition of TFA/H_2O/TIS (95:2.5:2.5) for 2 hours. Final

purification was achieved by semi-preparative HPLC employing a Waters Xterra® C_8 5µm (19 x 150 mm) column. Eluent: (A) 5% CH_3CN + 0.1% TFA in H_2O, (B) 0.1% TFA in CH_3CN. Gradient profile; linear gradient from 0% B to 100% B over 15 min. Flow rate; 15 mL/min. Maleimido-TATE (1a) was isolated as a homogenous peak with retention time of 7.99 min. The solvent was removed *in vacuo* and the product lyophilized from a mixture of water and acetonitrile to give a white fluffy powder (27 mg, 45%). The purity of the product was monitored by analytical HPLC, using the same gradient profile and solvent mixtures as above, but with a Waters XTerra® C_8 5µm (4.6 x 150 mm) column, flow rate 1 mL/min. Purity >98%. MALDI-TOF MS (m/z) (DHB+Na): Calcd. For $C_{57}H_{71}N_{11}O_{15}S_2$ $(M+Na)^+$ 1236.45. Found: 1236.39.

TATE-SH (1b). 3-(tritylthio)-propionoic acid (70 mg, 0.20 mmol, 4.0 equiv.), HATU (75 mg, 0.198 mmol, 3.95 equiv.) and 2,4,6-colidine (53 µL, 0.40 mmol, 8.0 equiv.) in DMF (2.0 mL) were added to the resin immobilized cyclic octapeptide for 2 hours at room temperature followed by washing with DMF (4 × 5.0 mL). The peptide was cleaved from the solid support by addition of TFA/H_2O/TIS (95:2.5:2.5) for 2 hours. Final purification was achieved by semi-preparative HPLC employing a Waters Xterra® C_8 5µm (19 x 150 mm) column. Eluent: (A) 5% CH_3CN + 0.1% TFA in H_2O, (B) 0.1% TFA in CH_3CN. Gradient profile; linear gradient from 0% B to 40% B over 15 min. Flow rate; 15 mL/min. TATE-thiol (1b) was isolated as a homogenous peak with retention time of 13.83 min. The solvent was removed *in vacuo* and the product lyophilized from a mixture of water and acetonitrile to give a white fluffy powder (2.8 mg, 6.0%). The purity of the product was monitored by analytical HPLC using the same gradient profile and solvent mixtures as above, but with a Waters XTerra® C_8 5µm (4.6 x 150 mm) column, flow rate 1 mL/min. Purity >98%. MALDI-TOF MS (m/z) (DHB+Na): Calcd. For $C_{52}H_{68}N_{10}O_{13}S_3$ $(M+Na)^+$ 1159.33. Found: 1159.57.

TATE-azide (1c). 5-azidopentonoic acid (29 mg, 0.20 mmol, 4.0 equiv.), HATU (75 mg, 0.198 mmol, 3.95 equiv.) and 2,4,6-colidine (53 µL, 0.40 mmol, 8.0 equiv.) in DMF (2.0 mL) were added to the resin immobilized cyclic octapeptide for 2 hours at room temperature followed by washing with DMF (4 × 5.0 mL). The peptide was cleaved from the solid support by addition of TFA/H_2O/TIS (95:2.5:2.5) for 2 hours. Final purification was achieved by semi-preparative HPLC employing a Waters Xterra® C_8 5µm (19 x 150 mm) column. Eluent: (A) 5% CH_3CN + 0.1% TFA in H_2O, (B) 0.1% TFA in CH_3CN.

Gradient profile; linear gradient from 0% B to 40% B over 15 min. Flow rate; 15 mL/min. TATE-azide (16b) was isolated as a homogenous peak with retention time of 16.22 min. The solvent was removed *in vacuo* and the product lyophilized from a mixture of water and acetonitrile to give a white fluffy powder (9.6 mg, 17%). The purity of the product was monitored by analytical HPLC using the same gradient profile and solvent mixtures as above but with a Waters XTerra® C_8 5μm (4.6 x 150 mm) column, flow rate 1 mL/min. Purity >98%. MALDI-TOF MS (m/z) (DHB+Na): Calcd. For $C_{54}H_{71}N_{13}O_{13}S_2$ $(M+Na)^+$ 1196.33. Found: 1236.39.

TATE-alkyne (1d). 4-pentynoic acid (20 mg, 0.20 mmol, 4.0 equiv.), HATU (75 mg, 0.198 mmol, 3.95 equiv.) and 2,4,6-colidine (53 μL, 0.40 mmol, 8.0 equiv.) in DMF (2.0 mL) were added to the resin immobilized cyclic octapeptide for 2 hours at room temperature followed by washing with DMF (4 × 5.0 mL). The peptide was cleaved from the solid support by addition of TFA/H_2O/TIS (95:2.5:2.5) for 2 hours. Final purification was achieved by semi-preparative HPLC employing a Waters Xterra® C_8 5μm (19 x 150 mm) column. Eluent: (A) 5% CH_3CN + 0.1% TFA in H_2O, (B) 0.1% TFA in CH_3CN. Gradient profile; linear gradient from 0% B to 30% B over 15 min. Flow rate; 15 mL/min. TATE-alkyne (16c) was isolated as a homogenous peak with retention time of 18.32 min. The solvent was removed *in vacuo* and the product lyophilized from a mixture of water and acetonitrile to give a white fluffy powder (7.2 mg, 13%). The purity of the product was monitored by analytical HPLC using the same gradient profile and solvent mixtures as above, but with a Waters XTerra® C_8 5μm (4.6 x 150 mm) column, flow rate 1 mL/min. Purity >98%. MALDI-TOF MS (m/z) (DHB+Na): Calcd. For $C_{54}H_{68}N_{10}O_{13}S_2$ $(M+Na)^+$ 1151.29. Found: 1151.51.

TATE-hydroxylamine (1e). Bis-Boc-amino-oxyacetic acid (47 mg, 0.15 mmol, 3 equiv.), HATU (56 mg, 0.146 mmol, 2.95 equiv.) and 2,4,6-colidine (41 μL, 0.30 mmol, 6.0 equiv.) in DMF (2.0 mL) were added to the resin immobilized cyclic octapeptide for 2 hours at room temperature, followed by washing with DMF (4 × 5.0 mL). The peptide was cleaved from the solid support by addition of TFA/H_2O/TIS (95:2.5:2.5) for 2 hours. Final purification was achieved by semi-preparative HPLC employing a Waters Xterra® C_8 5μm (19 x 150 mm) column. Eluent: (A) 5% CH_3CN + 0.1% TFA in H_2O, (B) 0.1% TFA in CH_3CN. Gradient profile; linear gradient from 0% B to 30% B over 15 min. Flow rate; 15 mL/min. TATE-hydroxylamine (16d) was isolated as a homogenous peak with

retention time of 14.17 min. The solvent was removed *in vacuo* and the product lyophilized from a mixture of water and acetonitrile to give a white fluffy powder (15 mg, 27%). The purity of the product was monitored by analytical HPLC using the same gradient profile and solvent mixtures as above, but with a Waters XTerra® C_8 5µm (4.6 x 150 mm) column, flow rate 1 mL/min. Purity >98%. MALDI-TOF MS (m/z) (DHB+Na): Calcd. For $C_{51}H_{67}N_{11}O_{14}S_2$ $(M+Na)^+$ 1144.25. Found: 1144.41.

Synthesis of functionalized DSPE-PEG$_{2000}$ phospholipids

DSPE-PEG$_{2000}$-alkyne (2a). DSPE-PEG$_{2000}$-NH_2 (40 mg, 14 µmol, 1.0 equiv.) was dissolved in dry CH_2Cl_2 (5.0 mL) in a pre-dried flask under a nitrogen atmosphere. A mixture of 4-pentynoic acid (6.4 mg, 66 µmol, 4.7 equiv.) , EDC·HCl (12.2 mg, 64 µmol, 4.6 equiv.) and DMAP (16.2 mg, 0.13 mmol, 9.3 equiv.) in dry CH_2Cl_2 (1.0 mL) were added and the reaction stirred overnight under nitrogen at room temperature. The solvent was removed *in vacuo* and the product purified on a Strata-C_8 SPE column using a 10% stepwise gradient from 0-100% MeOH in water. Fractions with the desired compound was combined, reduced *in vacuo* and lyophilized from a mixture of water and acetonitrile to give the title compound as a white powder (25 mg, 61%). ^{1}H-NMR (250MHz, $CDCl_3$): δ 8.20 (bs, 1H), 6.57 (bs, 1H), 5.87 (bs, 1H), 5.27-5.18 (m, 1H), 4.36 (dd, *J* = 11.7, 3.4Hz, 1H), 4.25-3.90 (m, 7H), 3.64 (bs, 164H), 2.35-2.25 (m, 8H), 2.02 (t, *J* = 2.5Hz, 2H), 1.67-1.51 (m, 4H), 1.25 (bs, 56H), 0.88 (t, *J* = 6.6Hz). MALDI-TOF MS (m/z) (DHB+Na): 2807.1 ± n×44.0. IR (KBr): ν(cm^{-1}) 3435.9, 2918.3, 2851.4, 1697.5, 1112.9.

DSPE-PEG$_{2000}$-cyclooctyne (2b). DSPE-PEG$_{2000}$-NH_2 (75 mg, 27 µmol, 1.0 equiv.) was dissolved in dry DMF (3.0 mL) in a pre-dried flask under a nitrogen atmosphere. A mixture of 1-fluorocyclooct-2-ynecarboxylic acid (Schultz, 2010) (9.2 mg, 54 µmol, 2.0 equiv.), Et_3N (7.5 µL, 54 µmol, 2 equiv.) and HATU (20 mg, 53 µmol, 1.96 equiv.) in dry DMF (3.0 mL) were added and the reaction stirred overnight under nitrogen at room temperature. The solvent was removed *in vacuo* and the product purified on a Strata-C_8 SPE column using a 10% stepwise gradient from 0-100% MeOH in water. Fractions with the desired compound was combined, reduced *in vacuo* and lyophilized from a mixture of water and acetonitrile to give the title compound as a white powder (56 mg, 71%). ^{1}H-NMR (250MHz, $CDCl_3$): δ 6.89 (bs, 1H), 5.83 (bs, 1H), 5.25-5.19 (m, 1H) , 4.40-4.04 (m, 10H), 3.95-3.89 (m, 2H), 3.64 (bs, 164H), 3.53-3.33 (m, 6H), 2.37-2.29 (m, 6H), 1.67-1.55 (m, 6H), 1.25 (bs, 56H), 0.88 (t, *J* = 6.6 Hz, 6H). MALDI-TOF MS (m/z)

(DHB+Na): 2968.3 ± n×44.0. IR (KBr): ν(cm^{-1}) 3445.3, 2918.2, 2851.4, 1741.6, 1648.9, 1104.6.

DSPE-PEG_{2000}-benzaldehyde (2c). DSPE-PEG_{2000}-NH_2 (100 mg, 36 μmol, 1.0 equiv.) was dissolved in dry DMF (1.0 mL) in a pre-dried flask under a nitrogen atmosphere. A mixture of 4-formyl benzoic acid (22 mg, 0.14 mmol, 4.0 equiv.), Et_3N (40 μL, 0.29 mmol, 8 equiv.) and HATU (54 mg, 0.14 mmol, 3.95 equiv.), in dry DMF (0.40 mL) were added and the reaction was stirred under nitrogen over night at room temperature. The solvent was removed *in vacuo* and the product purified on a Strata-C_8 SPE column using a 10% stepwise gradient from 50-100% MeOH in water. Fractions with the desired compound was combined, reduced *in vacuo* and lyophilized from a mixture of water and acetonitrile to give the title compound as a white powder (62 mg, 59%). ^{1}H-NMR (300MHz, $CDCl_3$): δ 10.08 (s, 1H), 8.01 (d, *J* = 8.4Hz, 2H), 7.94 (d, *J* = 8.4Hz, 2H), 6.00 (bs, 1H), 5.21 (bs, 1H), 4.37-3.31 (m, 1H), 4.22-4.03 (m, 10H), 3.89-3.85 (m, 2H), 3.64 (bs, 164H), 3.51-3.39 (m, 4H), 2.37-2.29 (m, 6H), 1.67-1.55 (m, 6H), 1.25 (bs, 56H), 0.88 (t, *J* = 6.6 Hz, 6H). MALDI-TOF MS (m/z) (DHB+Na): 2904.6 ± n×44.0. IR (*neat*): ν(cm^{-1}) 2917.0, 2850.8, 1744.5, 1702.1, 1466.5, 1343.5, 1102.5.

DSPE-PEG_{2000}-azide (2d). DSPE-PEG_{2000}-NH_2 (100 mg, 36 μmol, 1.0 equiv.) was dissolved in dry DMF (1.0 mL) in a pre-dried flask. A mixture of 5-azidopentanoic acid (21 mg, 0.14 mmol, 4.0 equiv.), Et_3N (40 μL, 0.29 mmol, 8.0 equiv.) and HATU (54 mg, 0.14 mmol, 3.95 equiv.) in dry DMF (0.50 mL) were added and the reaction stirred overnight under nitrogen at room temperature. The solvent was removed *in vacuo* and the product purified on a Strata-C_8 SPE column using a 10% stepwise gradient from 50-100% MeOH in water. Fractions with the desired compound was combined, reduced *in vacuo* and lyophilized from a mixture of water and acetonitrile to give the title compound as a white powder (79 mg, 79%). ^{1}H-NMR (300MHz, $CDCl_3$): δ 6.37 (bs, 1H), 5.20 (bs, 1H), 5.83 (bs, 1H), 4.38-4.32 (m, 1H) , 4.23-3.99 (m, 8H), 3.89-3.84 (m, 4H), 3.64 (bs, 164H), 3.54-3.27 (m, 4H), 2.33-2.16 (m, 8H), 1.75-1.55 (m, 8H), 1.25 (bs, 58H), 0.88 (t, *J* = 6.6 Hz, 6H). MALDI-TOF MS (m/z) (DHB+Na): 2898.4 ± n×44.0. IR (*neat*): ν(cm^{-1}) 2917.2, 2851.0, 2097.7, 1739.3, 1343.2, 1102.3.

DSPE-PEG_{2000}-SH (3). DTT (10 mg, 66 μmol, 3.9 equiv.) was added to a pre-dried flask under a nitrogen atmosphere containing DSPE-PEG_{2000}-PDP (50 mg, 17 μmol, 1.0 equiv.)

in dry MeOH (1.0 mL). The reaction was stirred under nitrogen over night at room temperature after which the solvent was removed and the product purified on a Strata-C_8 SPE column, using a 10% stepwise gradient from 50-100% MeOH in water. Fractions with the desired compound were combined, reduced *in vacuo and* lyophilized from a mixture of water and acetonitrile to give a white fluffy powder (34 mg, 71%). ^{1}H-NMR (300MHz, $CDCl_3$): δ 6.99 (bs, 1H), 6.59 (bs, 1H), 5.20 (bs, 1H), 4.39-4.34 (m, 1H) , 4.23-4.13 (m, 4H), 4.08-3.99 (m, 4H), 3.89-3.85 (m, 2H), 3.64 (bs, 166H), 3.57-3.38 (m, 4H), 2.81 (dt, J = 8.3, 6.8 Hz, 2H), 2.51 (t, J = 6.8 Hz, 2H), 2.33-2.26 (m, 4H), 2.07 (s, 1H), 1.67-1.56 (m, 6H), 1.25 (bs, 56H), 0.88 (t, J = 6.6 Hz, 6H). MALDI-TOF MS (m/z) (DHB+Na): 2904.4 ± n×44.0. IR (*neat*): ν(cm^{-1}) 2917.1, 2850.9, 1739.0, 1466.6, 1343.0, 1101.6.

Appendix III

Materials and methods for Chapter 3

Materials

1,2-Distearoyl-*sn*-glycero-3-phosphocholine (DSPC), 1,2-distearoyl-*sn*-glycero-3-phosphoethanolamine-(polyethylene glycol)$_{2000}$ (DSPE-PEG$_{2000}$), 1,2-distearoyl-*sn*-glycero-3-phosphoethanolamine-N-[amino(polyethylene glycol)$_{2000}$] (DSPE-PEG$_{2000}$-NH_2), 1,2-distearoyl-*sn*-glycero-3-phosphoethanolamine-N-(7-nitro-2-1,3-benzoxadiazol-4-yl) (DSPE-NBD), cholesterol were purchased from Avanti Polar Lipids Inc. (Alabaster, USA). 5-azidopentanoic acid, trifluoroacetic acid (TFA), and triisopropylsilane (TIS) were purchased from Sigma Aldrich (Schnelldorf, Germany). 1,4,7,10-tetra-azacyclododecane-1,4,7,10-tetraacetic acid (DOTA) was purchased from Macrocyclics (Dallas, USA). The coupling reagent *O*-(7-Azabenzotriazol-1-yl)-*N,N,N′,N′*-tetramethyluronium hexafluorophosphate (HATU), 2-chlorotrityl chloride Resin and all Fmoc protected amino acids used for the solid phase peptide synthesis were purchased from GL Biochem (Shanghai, China). Amicon Ultra-15 centrifugal filter units were purchased from Millipore (Denmark). TLC-plates Silica gel 60 F254 (ref. no. 1.05549.001) were purchased from Merck (Darmstadt, Germany). All chemicals and reagents were of analytical grade and used without further purification.

Instrumentation

Dynamic light scattering and zeta-potential measurements were performed on a Brookhaven Instruments Corporation Zeta PALS zeta potential analyzer. FT-IR was recorded on a Perkin Elmer Spectrum 100 FT-IR Spectrometer. UV spectra were

recorded using a Shimadzu UV-visible Spectrophotometer. Analytical reversed-phase high-performance liquid chromatography (RP-HPLC) was carried out on a Shimadzu LC-2010 analytical HPLC by employing a Waters XTerra® C_{18} 5 μm (4.6 x 150 mm) column or a Waters XTerra® C_8 5 μm (4.6 x 150 mm) column. Semi-preparative HPLC was performed on a Waters Semi-preparative HPLC equipped with a Waters 600 Pump & Controller and a Waters 2489 UV/Visible Detector using a a Waters XTerra® C_{18} 5μm (19 x 150 mm) column or a Waters XTerra® C_8 5μm (19 x 150 mm) column. HPLC Eluent A consisted of a 5% MeCN aqueous solution with 0.1% TFA; HPLC Eluent B consisted of 0.1% TFA in MeCN. HPLC analysis was monitored using dual channel UV detection at 206 nm and 254 nm. Pre-packed Strata C_8 solid phase extraction (SPE) (55 μm, 70 Å) Giga Tubes from Phenomenex (Torrance, USA) were used for the purification of functionalized phospholipids. Mass spectra were recorded using a Bruker Daltonics Reflex IV MALDI-TOF Spectrometer using 2,5-dihydroxybenzoic acid (DHB) spiked with sodium trifluoroacetate in MeOH as matrix. Flow cytometry was carried out on a Gallios flow cytometer (Beckman Coulter, Denmark). NBD-fluorescent cells were measured by the blue laser (488 nm) for excitation and fluorescence emission was measured in FL2 (band pass filter 525 ± 10 nm). Confocal imaging was performed on a Leica TCS SP5 AOBS with a 63x water-immersed objective (Leica Microsystems, Germany).

DSPE-PEG$_{2000}$-azide (2d). DSPE-PEG$_{2000}$-NH_2 (200 mg, 72 μmol, 1.0 equiv.) was dissolved in dry DMF (2.0 mL) in a pre-dried flask. A mixture of 5-azidopentanoic acid (41 mg, 0.29 mmol, 4.0 equiv.), Et_3N (80 μL, 0.57 mmol, 8.0 equiv.) and HATU (108 mg, 0.28 mmol, 3.95 equiv.) in dry DMF (0.50 mL) were added and the reaction stirred overnight under nitrogen at room temperature. The solvent was removed *in vacuo* and the product purified on a Strata-C_8 SPE column using a 10% stepwise gradient from 50-100% methanol in water. Fractions with the desired compound was combined, reduced *in vacuo* and lyophilized from a mixture of water and acetonitrile to give the title compound as a white powder (185 mg, 88%). MALDI-TOF MS (m/z) (DHB+Na): 2898.4 ± n×44.0. IR (*neat*): ν(cm^{-1}) 2914, 2885, 2850, 2097, 1739, 1343, 1100.

cRGDfPropargyl (5). The linear RGDfPropargyl pentapeptide NH_2-Asp(O*t*Bu)-$_D$-Phe-Propargyl-Arg(Pbf)-Gly-Resin was synthesized manually by SPPS on a 2-chlorotrityl chloride Resin (0.40 g, 0.20 mmol/g) by standard Fmoc methodology. Fmoc

quantification was used to determine the precise loading (λ = 290 nm, ε = 5253 $M^{-1}cm^{-1}$). Each coupling was performed by 4.0 equiv. Fmoc protected amino acid, 3.95 equiv. HATU (119 mg, 0.31 mmol, 3.95 equiv.) and 8.0 equiv. 2,4,6-collidine (83 µL, 0.64 mmol, 8.0 equiv.) in DMF (4.0 mL). Cleavage of the Fmoc group was carried out using piperidine in DMF (1:4) for 2 x 2 minutes. Completion of each coupling and deprotection step were monitored by the Kaiser test. The peptide was cleaved from the solid support by addition of AcOH:TFE:CH_2Cl_2 (10:20:70) for 2 x 20 minutes. Cyclization was performed in solution (15 mL DMF) between the N-terminal of the aspartic acid and the free carboxylic acid on glycine using diphenyl phosphoryl azide (257 mg, 0.80 mmol, 3.0 equiv.) and sodium hydrogencarbonate (336 mg, 4.0 mmol, 15 equiv.). The reaction was moitored by MALDI-TOF MS and was complete within 3 hours. The cyclized peptide was extracted using ethyl acetate, the organic phase combined and washed with a saturated solution of ammonium chloride, followed by brine and dried over anhydrous magnesium sulphate. Solvent was removed *in vacuo* and the crude peptide dissolved in TFA:H_2O:TIS (95:2.5:2.5). Deprotection was complete within 24 hours. The TFA mixture was removed *in vacuo* and the crude peptide re-dissolved in acetonitrile:water (1:3) and purified by semi-preparative HPLC employing a Waters Xterra® C_{18} 5µm (19 x 150 mm) column. Eluent: (A) 5% CH_3CN + 0.1% TFA in H_2O, (B) 0.1% TFA in CH_3CN. Gradient profile; linear gradient from 0% B to 100% B over 20 min. Flow rate; 14 mL/min. cRGDfPropargyl was isolated as a homogenous peak with retention time of 7 min. The solvent was removed *in vacuo* and the product lyophilized from a mixture of water and acetonitrile to give a white fluffy powder (31 mg, 69%). The purity of the product was monitored by analytical HPLC, using the same gradient profile and solvent mixtures as above, but with a Waters XTerra® C_{18} 5µm (4.6 x 150 mm) column, flow rate 1 mL/min. Purity >98%. MALDI-TOF MS (m/z) (DHB+Na): Calcd. For $C_{26}H_{34}N_8O_7$ $(M+Na)^+$ 570.25. Found: 570.43.

cGRDfPropargyl (6). The linear GRDfPropargyl pentapeptide NH_2-Asp(O*t*Bu)-$_D$-Phe-Propargyl-Gly-Arg(Pbf)-Resin was synthesized manually by SPPS on a 2-chlorotrityl chloride Resin (0.40 g, 0.40 mmol/g) by standard Fmoc methodology. Fmoc quantification was used to determine the precise loading (λ = 290 nm, ε = 5253 $M^{-1}cm^{-1}$). Each coupling was performed by 4.0 equiv. Fmoc protected amino acid, 3.95 equiv. HATU (239 mg, 0.63 mmol, 3.95 equiv.) and 8.0 equiv. 2,4,6-collidine (167 µL, 1.3

mmol, 8.0 equiv.) in DMF (4.0 mL). Cleavage of the Fmoc group was carried out using piperidine in DMF (1:4) for 2 x 2 minutes. Completion of each coupling and deprotection step were monitored by the Kaiser test. The peptide was cleaved from the solid support by addition of AcOH:TFE:CH_2Cl_2 (10:20:70) for 2 x 20 minutes. Cyclization was performed in solution (15 mL DMF) between the N-terminal of the aspartic acid and the free carboxylic acid on arginine using diphenyl phosphoryl azide (129 mg, 0.47 mmol, 3.0 equiv.) and sodium hydrogencarbonate (197 mg, 2.3 mmol, 15 equiv.). The reaction was moitored by MALDI-TOF MS and was complete within 24 hours. The cyclized peptide was extracted using ethyl acetate, the organic phase combined and washed with a saturated solution of ammonium chloride, followed by brine and dried over anhydrous magnesium sulphate. Solvent was removed *in vacuo* and the crude peptide dissolved in TFA:H_2O:TIS (95:2.5:2.5). Deprotection was complete within 24 hours. The peptide in TFA was precipitated into icecold diethyl ether, solid collected by centrifugation, resuspended in water and acetonitrile from which it was lyophilized giving a white fluffy powder (28 mg, 62%). The purity of the product was monitored by analytical HPLC, using the same gradient profile, solvent mixtures, column, and flow rate as above (cRGDfPropargyl (5)). Purity >98%. MALDI-TOF MS (m/z) (DHB+Na): Calcd. For $C_{26}H_{34}N_8O_7$ $(M+Na)^+$ 570.25. Found: 570.59.

DSPE-PEG_{2000}-cRGD (7). cRGDfPropargyl (5) (19 mg, 34 μmol, 2.0 equiv.) and DSPE-PEG_{2000}-N_3 (2d) (47 mg, 16 μmol, 1.0 equiv.) were dissolved in methanol (1.0 mL). Copper(II) sulphate pentahydrate (8.0 mg, 32 μmol, 2.0 equiv.) and sodium ascorbate (13 mg, 65 μmol, 4.0 equiv.) were dissolved in water (1.0 mL) and added to the above mixture. The reaction was stirred overnight. The solution was extracted with chloroform, the organic phases combined, washed with water and dried over anhydrous sodium sulphate. The solvent was removed *in vacuo* and the product purified by semi-preparative HPLC employing a Waters Xterra® C_8 5μm (19 x 150 mm) column. Eluent: (A) 5% CH_3CN + 0.1% TFA in H_2O, (B) 0.1% TFA in CH_3CN. Gradient profile; linear gradient from 50% B to 100% B over 20 min. Flow rate; 14 mL/min. DSPE-PEG_{2000}-cRGD (7) was isolated as a homogenous peak with retention time of 10 min. The solvent was removed *in vacuo* and the product lyophilized from a mixture of water and acetonitrile to give a white fluffy powder (29 mg, 52%). The purity of the product was monitored by analytical HPLC, using the same gradient profile and solvent mixtures as above, but with

a Waters XTerra® C_8 5µm (4.6 x 150 mm) column, flow rate 1 mL/min. Purity >98%. MALDI-TOF MS (m/z) (DHB+Na): 3468.9 ± n×44.0.

DSPE-PEG$_{2000}$-cGRD (8). cGRDfPropargyl (6) (4.7 mg, 8.2 µmol, 2.0 equiv.) and DSPE-PEG$_{2000}$-N_3 (2d) (12 mg, 4.1 µmol, 1.0 equiv.) were dissolved in methanol (1.0 mL). Copper(II) sulphate pentahydrate (2.0 mg, 8.2 µmol, 2.0 equiv.) and sodium ascorbate (3.2 mg, 16 µmol, 4.0 equiv.) were dissolved in water (1 mL) and added to the above mixture. The reaction was stirred overnight. The solution was extracted with chloroform, the organic phases combined, washed with water and dried over anhydrous sodium sulphate. The solvent was removed *in vacuo* and the product purified by semi-preparative HPLC employing a Waters Xterra® C_8 5µm (19 x 150 mm) column. Eluent: (A) 5% CH_3CN + 0.1% TFA in H_2O, (B) 0.1% TFA in CH_3CN. Gradient profile; linear gradient from 50% B to 100% B over 20 min. Flow rate; 14 mL/min. DSPE-PEG$_{2000}$-cGRD (8) was isolated as a homogenous peak with retention time of 10 min. The solvent was removed *in vacuo* and the product lyophilized from a mixture of water and acetonitrile to give a white fluffy powder (7.6 mg, 53%). The purity of the product was monitored by analytical HPLC, using the same gradient profile and solvent mixtures as above, but with a Waters XTerra® C_8 5µm (4.6 x 150 mm) column, flow rate 1 mL/min. Purity >98%. MALDI-TOF MS (m/z) (DHB+Na): 3469.0 ± n×44.0.

Liposomes for *in vitro* applications. Small unilamellar vesicles were prepared as described by Bangham *et al.* Lipids were dissolved in methanol:chloroform (1:9) and mixed in the desired ratios. For functionalized liposomes this ratio was DSPC:DSPE-NBD:DSPE-PEG$_{2000}$:DSPE-PEG$_{2000}$-R (R being either cRGD or cGRD) (94.5:0.5:4:1) and for control PEG-liposomes the ratio was DSPC:DSPE-NBD:DSPE-PEG$_{2000}$ (94.5:0.5:5). The organic solvent was removed under a gentle strem of nitrogen and fully removed *in vacuo* overnight. The lipid film were hydrated in a phosphate buffered saline (PBS) at 65 °C for 1 hour, followed by freeze-thaw cycles and extrusion at 65 °C through 100 nm polycarbonate filters using an Avanti Polar Lipids mini-extruder. The small unilamellar liposomes were analyzed by dynamic light scattering and zeta potential measurements (Zeta PALS, Brookhaven Instruments).

Liposomes for *in vivo* applications. Small unilamellar vesicles were prepared as described by Bangham *et al.* Lipids were dissolved in methanol:chloroform (1:9) and mixed in the desired ratios. For functionalized liposomes this ratio was DSPC:cholesterol:DSPE-PEG_{2000}:DSPE-PEG_{2000}-R (R being either cRGD or cGRD) (55:40:4:1) and for control PEG-liposomes the ratio was DSPC:cholesterol:DSPE-PEG_{2000} (55:40:5). The organic solvent was removed under a gentle stream of nitrogen and fully removed *in vacuo* overnight generating a lipid film. The lipid film were hydrated in an aqueous HEPES buffer (10 mM, 150 mM NaCl, pH 7.4), containing DOTA (C_{DOTA} = 10 mM) adjusted to pH 7.4 and 375 mOsm/l using NaOH and/or HCl. The lipid film was hydrated at 65 °C for 1 hour, followed by extrusion at 65 °C through 100 nm polycarbonate filters using an Avanti Polar Lipids mini-extruder. Un-encapsulated DOTA were removed by filtration through Amicon Ultra-15 centrifugal filter units exchanging the external buffer with a HEPES buffer (10 mM, 150 mM NaCl, pH 7.4, 295 mOsm/l). The formed liposomes were characterized by DLS and zeta potential measurements (Zeta PALS, Brookhaven Instruments).

Flow cytometry. The internalization of cRGD-, cGRD-, and PEG-liposomes were analyzed using flow cytometry (Gallios, Beckman Coulter). The human glioblastoma U87MG cells were grown in RPMI 1640 medium supplemented with 10% fetal bovine serum (Sigma-Aldrich) and 100 UI/mL penicillin and streptomycin (Lonza). Cells were incubated in a 5% CO_2 humidified incubator at 37 °C. The day before used the cells were plated in 12-well dishes (50,000 cells per well). The medium was replaced with fresh and liposomes were added. The cells were incubated 5 hours at 37 °C. The cells were washed with PBS, trypsinized and placed into a FACS tube containing 3 mL of PBS using 1 mL of medium. The cells were centrifuged for 3 min at 850 rpm, supernatant removed and the cells resuspended in 300-500 µL PBS. The NBD-fluorescent cells were measured with a blue laser (488 nm) for excitation and emission was measured in FL2 with a band pass filter of 525 ± 10 nm. 10,000 events were collected for each sample and non-treated cells were used as reference and the gates adjusted from those.

Inhibition study. The human glioblastoma U87MG cells were grown in RPMI 1640 medium supplemented with 10% fetal bovine serum (Sigma-Aldrich) and 100 UI/mL penicillin and streptomycin (Lonza). Cells were incubated in a 5% CO_2 humidified

incubator at 37 °C. The cells were plated in 12-well dishes and used when 50,000 cells per well were present. The medium was replaced with fresh and free peptide dissolved in 20% DMSO in PBS in concentrations ranging from 2.3 mM to 2.3 μM was added (20 μL per 1 mL media). The cells were incubated 15 minutes at 37 °C, before the addition of liposomes. The cells were incubated with the liposomes for 5 hours at 37 °C. Then washed with PBS, trypsinized and placed into a FACS tube containing 3 mL of PBS using 1 mL of medium. The cells were centrifuged for 3 min at 850 rpm, supernatant removed and the cells resuspended in 300-500 μL PBS. The NBD-fluorescent cells were measured using flow cytometry (Gallios, Beckman Coulter) with a blue laser (488 nm) for excitation and emission was measured in FL2 with a band pass filter of 525 ± 10 nm. 10,000 events were collected for each sample and non-treated cells were used as reference and the gates adjusted from those.

Confocal microscopy. The internalization of cRGD-, cGRD-, and PEG-liposomes were analyzed using confocal microscopy (Leica Microsystems). The human glioblastoma U87MG cells were grown in RPMI 1640 medium supplemented with 10% fetal bovine serum (Sigma-Aldrich) and 100 UI/mL penicillin and streptomycin (Lonza). Cells were incubated in a 5% CO_2 humidified incubator at 37 °C. The day before used the cells were plated in 24-well plates (20,000 cells per well) ontop of small glasslides. The medium was replaced with fresh and liposomes were added. The cells were incubated 24 hours at 37 °C. The cells were washed with PBS, heparin containing PBS and two times with PBS again. They were fixated in 4% paraformaldehyde in PBS for 3 minutes, followed by washing with PBS. The plate was allowed to dry, before being mounted on a microscope slide using Vectashield® HardSet Mounting Medium. The imaging was performed with a Leica confocal microscope using an excitation wavelength of $\lambda = 476$ nm and an emission bandwidth range of 485-600 nm.

^{64}Cu-liposomes. ^{64}Cu was produced on a PETtrace cyclotron (GE Healthcare) equipped with a beamline [Petersen, 2011]. Radioactive $^{64}CuCl_2$ was evaporated to dryness from aqueous hydrochloric acid and the DOTA containing liposomes were added. The mixture was incubated at 50-55 °C for 1 hour, before the loading efficiency was measured. This was done by separating un-encapsulated ^{64}Cu-DOTA from ^{64}Cu-liposomes by size exclusion chromatography (SEC) using a Sephadex G-25 column (1 x 25 cm) eluted with

a HEPES buffer (10 mM, 150 mM NaCl, pH 7.4). The fraction of un-encapsulated free ^{64}Cu i the liposome containing solution was quantified by radio-thin layer chromatography (radio-TLC) eluting the plates in 10% ammonium acetate:methanol (50:50). The retention factor of ^{64}Cu-DOTA was 0.3-0.4, while ^{64}Cu stayed at the baseline. The loading efficiencies were < 95%.

Animal xenograft model. Seven weeks old female NMRI nude mice purchased from Tarconic (Borup, Denmark) were inoculated in the right and left flank with 10E+07 U87MG cells (LGC standards, Boras, Sweden) in a 1:1 mixture with matrixgel™ (BD Biosciences, Albertslund, Denmark). Tumors were allowed to grow for 4 weeks. The mice were divided in 3 groups; cRGD-liposomes (n = 4), cGRD-liposomes (n = 4) and untargeted control PEG-liposomes (n = 6). The animal experiments were approved by the Animal Research Committee of the Danish Ministry of Justice.

Acquisition protocol for *in vivo* studies. ^{64}Cu-liposome suspensions were administered intravenous (i.v.) for biodistribution imaging and quantification. The ^{64}Cu-liposome formulations was intravenously injected in a lateral tail vein of anesthetized mice at a volume of 200 μL and a lipid concentration of 20 mg/kg. The average administered activity dose levels were 9.63 ± 0.60 MBq animal^{-1}. The PET/CT scans were acquired on a dedicated small animal system (MicroPET Focus 120 & MicroCAT® II, Siemens Medical Solutions, Malvern, PA, USA) at 1h, 18h and 45h post injection (p.i.) with PET acquisition times of 10, 15 & 30 min. respectively. PET data were reconstructed with the 2-dimentional ordered-subset expectation maximization (OSEM2D) reconstruction algorithm. PET and CT images were analyzed as fused images using the Inveon software (Siemens). CT settings were a tube voltage of 64 kVp, a tube current of 500 μA, 360 rotation steps, an exposure time of 400 ms and a voxel size of 0.089 mm. Immediately following the last PET scan the mice were euthanized and blood as well as organs of interest collected and counted in a gamma counter (Perkin Elmer Life Sciences).

Appendix IV

Materials and methods for Chapter 4

Materials

1,2-Distearoyl-*sn*-glycero-3-phosphocholine (DSPC), 1,2-distearoyl-*sn*-glycero-3-phosphoethanolamine-(polyethylene glycol)$_{2000}$ (DSPE-PEG$_{2000}$), 1,2-distearoyl-*sn*-glycero-3-phosphoethanolamine-N-[amino(polyethylene glycol)$_{2000}$] (DSPE-PEG$_{2000}$-NH$_2$), cholesterol, 1,2-dioleoyl-*sn*-glycero-3-phosphoethanolamine-N-(lissamine rhodamine B sulfonyl) (DOPE-RhoB), 1,2-dioleoyl-3-trimethylammonium-propane (DOTAP) were purchased from Avanti Polar Lipids Inc. (Alabaster, USA). Folic acid, 5-azidopentanoic acid, 4-formyl benzoic acid, trifluoroacetic acid (TFA), and triisopropylsilane (TIS) were purchased from Sigma Aldrich (Schnelldorf, Germany). The coupling reagent *O*-(7-Azabenzotriazol-1-yl)-*N,N,N′,N′*-tetramethyluronium hexafluorophosphate (HATU), TentaGEL PAP Resin was purchased from Rapp Polymere and NovoSyn TGR Resin from Novabiochem. 2-chlorotrityl chloride Resin, and all Fmoc protected amino acids used for the solid phase peptide synthesis were purchased from GL Biochem (Shanghai, China). All chemicals and reagents were of analytical grade and used without further purification.

Instrumentation

UV spectra were recorded using a Shimadzu UV-visible Spectrophotometer. Dynamic light scattering and zeta-potential measurements were performed on a Brookhaven Instruments Corporation Zeta PALS zeta potential analyzer. Analytical reversed-phase high-performance liquid chromatography (RP-HPLC) was carried out on a Shimadzu LC-

2010 analytical HPLC by employing a Waters XTerra® C_8 5 µm (4.6 x 150 mm) column or a Waters XTerra® C_{18} 5 µm (4.6 x 150 mm) column. Semi-preparative HPLC was performed on a Waters Semi-preparative HPLC equipped with a Waters 600 Pump & Controller and a Waters 2489 UV/Visible Detector using a a Waters XTerra® C_8 5µm (19 x 150 mm) column or a Waters XTerra® C_{18} 5µm (19 x 150 mm) column. HPLC Eluent A consisted of a 5% MeCN aqueous solution with 0.1% TFA; HPLC Eluent B consisted of 0.1% TFA in MeCN. HPLC analysis was monitored using dual channel UV detection at 254 nm and 280 nm. Pre-packed Strata C_8 solid phase extraction (SPE) (55 µm, 70 Å) Giga Tubes from Phenomenex (Torrance, USA) were used for the purification of functionalized phospholipids. Mass spectra were recorded using a Bruker Daltonics Reflex IV MALDI-TOF Spectrometer using 2,5-dihydroxybenzoic acid (DHB) spiked with sodium trifluoroacetate in MeOH as matrix.

DSPE-PEG$_{2000}$-benzaldehyde (2c). DSPE-PEG$_{2000}$-NH_2 (100 mg, 36 µmol, 1.0 equiv.) was dissolved in dry DMF (1.0 mL) in a pre-dried flask under a nitrogen atmosphere. A mixture of 4-formyl benzoic acid (22 mg, 0.14 mmol, 4.0 equiv.), Et_3N (40 µL, 0.29 mmol, 8.0 equiv.) and HATU (54 mg, 0.14 mmol, 3.95 equiv.), in dry DMF (0.50 mL) were added and the reaction was stirred under nitrogen over night at room temperature. The solvent was removed *in vacuo* and the product purified by semi-preparative HPLC employing a Waters Xterra® C_8 5µm (19 x 150 mm) column. Eluent: (A) 5% CH_3CN + 0.1% TFA in H_2O, (B) 0.1% TFA in CH_3CN. Gradient profile; linear gradient from 40% B to 100% B over 15 min. Flow rate; 14 mL/min. DSPE-PEG$_{2000}$-benzaldehyde (2c) was isolated as a broad peak with retention time of 12.5 min. The solvent was removed *in vacuo* and the product lyophilized from a mixture of water and acetonitrile to give a white fluffy powder (98 mg, 96%). MALDI-TOF MS (m/z) (DHB+Na): 2860.9 ± n×44.0.

DSPE-PEG$_{2000}$-azide (2d). DSPE-PEG$_{2000}$-NH_2 (200 mg, 72 µmol, 1.0 equiv.) was dissolved in dry DMF (2.0 mL) in a pre-dried flask. A mixture of 5-azidopentanoic acid (41 mg, 0.29 mmol, 4.0 equiv.), Et_3N (80 µL, 0.57 mmol, 8.0 equiv.) and HATU (108 mg, 0.28 mmol, 3.95 equiv.) in dry DMF (0.50 mL) were added and the reaction stirred overnight under nitrogen at room temperature. The solvent was removed *in vacuo* and the product purified on a Strata-C_8 SPE column using a 10% stepwise gradient from 50-100% methanol in water. Fractions with the desired compound was combined, reduced *in vacuo* and lyophilized from a mixture of water and acetonitrile to give the title compound as a

white powder (185 mg, 88%). MALDI-TOF MS (m/z) (DHB+Na): 2898.4 ± n×44.0. IR (*neat*): ν(cm^{-1}) 2914, 2885, 2850, 2097, 1739, 1343, 1100.

cRGDfPropargyl (5). The linear RGDfPropargyl pentapeptide NH_2-Asp(O*t*Bu)-$_D$-Phe-Propargyl-Arg(Pbf)-Gly-Resin was synthesized manually by SPPS on a 2-chlorotrityl chloride Resin (0.40 g, 0.20 mmol/g) by standard Fmoc methodology. Fmoc quantification was used to determine the precise loading (λ = 290 nm, ε = 5253 $M^{-1}cm^{-1}$). Each coupling was performed by 4.0 equiv. Fmoc protected amino acid, 3.95 equiv. HATU (119 mg, 0.31 mmol, 3.95 equiv.) and 8.0 equiv. 2,4,6-collidine (83 µL, 0.64 mmol, 8.0 equiv.) in DMF (4.0 mL). Cleavage of the Fmoc group was carried out using piperidine in DMF (1:4) for 2 x 2 minutes. Completion of each coupling and deprotection step were monitored by the Kaiser test. The peptide was cleaved from the solid support by addition of AcOH:TFE:CH_2Cl_2 (10:20:70) for 2 x 20 minutes. Cyclization was performed in solution (15 mL DMF) between the N-terminal of the aspartic acid and the free carboxylic acid on glycine using diphenyl phosphoryl azide (257 mg, 0.80 mmol, 3.0 equiv.) and sodium hydrogencarbonate (336 mg, 4.0 mmol, 15 equiv.). The reaction was moitored by MALDI-TOF MS and was complete within 3 hours. The cyclized peptide was extracted using ethyl acetate, the organic phase combined and washed with a saturated solution of ammonium chloride, followed by brine and dried over anhydrous magnesium sulphate. Solvent was removed *in vacuo* and the crude peptide dissolved in TFA:H_2O:TIS (95:2.5:2.5). Deprotection was complete within 24 hours. The TFA mixture was removed *in vacuo* and the crude peptide re-dissolved in acetonitrile:water (1:3) and purified by semi-preparative HPLC employing a Waters Xterra® C_{18} 5µm (19 x 150 mm) column. Eluent: (A) 5% CH_3CN + 0.1% TFA in H_2O, (B) 0.1% TFA in CH_3CN. Gradient profile; linear gradient from 0% B to 100% B over 20 min. Flow rate; 14 mL/min. cRGDfPropargyl (5) was isolated as a homogenous peak with retention time of 7 min. The solvent was removed *in vacuo* and the product lyophilized from a mixture of water and acetonitrile to give a white fluffy powder (31 mg, 69%). The purity of the product was monitored by analytical HPLC, using the same gradient profile and solvent mixtures as above, but with a Waters XTerra® C_{18} 5µm (4.6 x 150 mm) column, flow rate 1 mL/min. Purity >98%. MALDI-TOF MS (m/z) (DHB+Na): Calcd. For $C_{26}H_{34}N_8O_7$ $(M+Na)^+$ 570.25. Found: 570.43.

DSPE-PEG$_{2000}$-cRGD (7). cRGDfPropargyl (5) (19 mg, 34 µmol, 2.0 equiv.) and DSPE-PEG$_{2000}$-N$_3$ (2d) (47 mg, 16 µmol, 1.0 equiv.) were dissolved in methanol (1.0 mL). Copper(II) sulphate pentahydrate (8.0 mg, 32 µmol, 2.0 equiv.) and sodium ascorbate (13 mg, 65 µmol, 4.0 equiv.) were dissolved in water (1.0 mL) and added to the above mixture. The reaction was stirred overnight. The solution was extracted with chloroform, the organic phases combined, washed with water and dried over anhydrous sodium sulphate. The solvent was removed *in vacuo* and the product purified by semi-preparative HPLC employing a Waters Xterra® C$_8$ 5µm (19 x 150 mm) column. Eluent: (A) 5% CH$_3$CN + 0.1% TFA in H$_2$O, (B) 0.1% TFA in CH$_3$CN. Gradient profile; linear gradient from 50% B to 100% B over 20 min. Flow rate; 14 mL/min. DSPE-PEG$_{2000}$-cRGD (7) was isolated as a homogenous peak with retention time of 10 min. The solvent was removed *in vacuo* and the product lyophilized from a mixture of water and acetonitrile to give a white fluffy powder (29 mg, 52%). The purity of the product was monitored by analytical HPLC, using the same gradient profile and solvent mixtures as above, but with a Waters XTerra® C$_8$ 5µm (4.6 x 150 mm) column, flow rate 1 mL/min. Purity >98%. MALDI-TOF MS (m/z) (DHB+Na): 3468.9 ± n×44.0.

DP-MCP-PEG (9). The linear peptide dipalmitoyl-Dap-Trp(Boc)-Ile-Pro-Val-Ser(*t*Bu)-Leu-Arg(Pbf)-Ser(*t*Bu)-Gly-Glu(O*t*Bu)-Glu(O*t*Bu)-Glu(O*t*Bu)-Glu(O*t*Bu)-PEG$_{2000}$-Resin was synthesized manually by SPPS on a TentaGEL PAP Resin (0.89 g, 0.34 mmol/g) by standard Fmoc methodology. Each coupling was performed by 4.0 equiv. Fmoc protected amino acid, 3.95 equiv. HATU (451 mg, 1.19 mmol, 3.95 equiv.) and 8.0 equiv. 2,4,6-collidine (320 µL, 2.4 mmol, 8.0 equiv.) in DMF (9.0 mL). Cleavage of the Fmoc group was carried out using piperidine in DMF (1:4) for 2 x 2 minutes. Completion of each coupling and deprotection step were monitored by the Kaiser test. The peptide was cleaved from the solid support by addition of TFA:H$_2$0:TIS (95:2.5:2.5) for 3 hours. The TFA mixture was removed *in vacuo* and the crude peptide re-dissolved in dimethyl sulfoxide:water (1:1) and purified by semi-preparative HPLC employing a Waters Xterra® C$_8$ 5µm (19 x 150 mm) column. Eluent: (A) 5% CH$_3$CN + 0.1% TFA in H$_2$O, (B) 0.1% TFA in CH$_3$CN. Gradient profile; linear gradient from 20% B to 100% B over 15 min. Flow rate; 14 mL/min. DP-MCP-PEG (9) was isolated as a broad peak with retention time of 10.3 min. The solvent was removed *in vacuo* and the product lyophilized from a mixture of water and acetonitrile to give a white fluffy powder (328 mg, 26%). The purity of the product was monitored by analytical HPLC, using the same gradient

profile and solvent mixtures as above, but with a Waters XTerra® C_8 5µm (4.6 x 150 mm) column, flow rate 1 mL/min. Purity >95%. MALDI-TOF MS (m/z) (DHB+Na): 4119.2 ± n×44.0.

DSPE-PEG$_{2000}$-Folate (10). DSPE-PEG$_{2000}$-NH_2 (10 mg, 3.6 µmol, 1.0 equiv.) was dissolved in dry DMF (0.50 mL) in a pre-dried flask. A mixture of folic acid (3.2 mg, 7.2 µmol, 2.0 equiv.), Et_3N (1.0 µL, 7.2 µmol, 2.0 equiv.) and HATU (1.4 mg, 3.6 µmol, 1.01 equiv.) in dry DMF (0.50 mL) were added and the reaction stirred overnight under nitrogen at room temperature. The solvent was removed *in vacuo* and the product purified purified by semi-preparative HPLC employing a Waters Xterra® C_8 5µm (19 x 150 mm) column. Eluent: (A) 5% CH_3CN + 0.1% TFA in H_2O, (B) 0.1% TFA in CH_3CN. Gradient profile; linear gradient from 50% B to 100% B over 20 min. Flow rate; 14 mL/min. DSPE-PEG$_{2000}$-Folate (10) was isolated as a broad peak with retention time of 14.2 min. The solvent was removed *in vacuo* and the product lyophilized from a mixture of water and acetonitrile to give a yellow powder (3.1 mg, 27%). The purity of the product was monitored by analytical HPLC, using the same gradient profile and solvent mixtures as above, but with a Waters XTerra® C_8 5µm (4.6 x 150 mm) column, flow rate 1 mL/min. Purity >89%. MALDI-TOF MS (m/z) (DHB+Na): 3230.2 ± n×44.0.

Octaarginine-hydroxylamine (11). The linear peptide Bis-Boc-amino-oxyacetic acid-[Arg(Pbf)]$_8$-Resin was synthesized manually by SPPS on a NovaSyn tentagel (0.72 g, 0.25 mmol/g) by standard Fmoc methodology. Each coupling was performed by 4.0 equiv. Fmoc protected amino acid, 3.95 equiv. HATU (267 mg, 0.71 mmol, 3.95 equiv.) and 8.0 equiv. 2,4,6-collidine (186 µL, 1.4 mmol, 8.0 equiv.) in DMF (8.0 mL). Cleavage of the Fmoc group was carried out using piperidine in DMF (1:4) for 2 x 2 minutes. Completion of each coupling and deprotection step were monitored by the Kaiser test. The peptide was cleaved from the solid support by addition of TFA:H_20:TIS (95:2.5:2.5) for 4 hours. The solvent was removed *in vacuo* and the product purified purified by semi-preparative HPLC employing a Knauer Eurospher 100 C_{18} 5µm (20 x 250 mm) column. Eluent: (A) 5% CH_3CN + 0.1% TFA in H_2O, (B) 0.1% TFA in CH_3CN. Gradient profile; linear gradient from 0% B to 50% B over 15 min. Flow rate; 14 mL/min. Octaarginine-hydroxylamine (10) was isolated as a homogenous peak with retention time of 7 min. The solvent was removed *in vacuo* and the product lyophilized from a mixture of water and

acetonitrile to give a white powder (65 mg, 27%). MALDI-TOF MS (m/z) (DHB+Na): Calcd. For $C_{50}H_{102}N_{34}O_{10}$ $(M+Na)^+$ 1338.85. Found: 1339.43.

DSPE-PEG$_{2000}$-Octaarginine (12). DSPE-PEG2000-aldehyde (2c) (94 mg, 33 µmol, 1.0 equiv.) was dissolved in methanol (3.0 mL) and mixed with Octaarginine-hydroxylamine (10) (64 mg, 48 µmol, 1.4 equiv.) dissolved in water (3.0 mL). The reaction was stirred overnight. The product was purified directly from the methanol:water mixture by semi-preparative HPLC employing a Waters Xterra® C_8 5µm (19 x 150 mm) column. Eluent: (A) 5% CH_3CN + 0.1% TFA in H_2O, (B) 0.1% TFA in CH_3CN. Gradient profile; linear gradient from 0% B to 100% B over 15 min. Flow rate; 14 mL/min. DSPE-PEG$_{2000}$-Octaarginine (12) was isolated as a broad peak with retention time of 11 min. The solvent was removed *in vacuo* and the product lyophilized from a mixture of water and acetonitrile to give a white sticky powder (95 mg, 69%). The purity of the product was monitored by analytical HPLC, using the same gradient profile and solvent mixtures as above, but with a Waters XTerra® C_8 5µm (4.6 x 150 mm) column, flow rate 1 mL/min. Purity >98%. MALDI-TOF MS (m/z) (DHB+Na): 4181 ± n×44.0.

Preparation of liposomes for uptake studies. Small unilamellar vesicles were prepared as described by Bangham *et al.* Lipids were dissolved in methanol:chloroform (1:9) and mixed in the desired ratio. Generally, the liposomes consisted of DSPC, DOPE-RhoB, cholesterol and total of 5% DSPE-PEG$_{2000}$ lipid - either as pure DSPE-PEG$_{2000}$ phospholipid or as a mixture with functionalized DSPE-PEG$_{2000}$ phospholipid. DOTAP was excluded or used in an amount of 7.5%. Hence, liposomes composed without DOTAP would have the formulation of DSPC/DOPE-RhoB/cholesterol/DSPE-PEG$_{2000}$ (54.5:0.5:40:5), while liposomes containing DOTAP would be of the formulation DSPC/DOPE-RhoB/cholesterol/DSPE-PEG$_{2000}$/DOTAP (47:0.5:40:5:7.5). The organic solvent was removed under a gentle strem of nitrogen and fully removed *in vacuo* overnight. The lipid films were hydrated in a HEPES/sucrose buffer (10 mM HEPES, 10%w/v sucrose, pH 7.4) at at 65 °C for 1 hour, followed by freeze-thaw cycles and extrusion at 65 °C through 100 nm polycarbonate filters using an Avanti Polar Lipids mini-extruder. The small unilamellar liposomes were analyzed by dynamic light scattering and zeta potential measurements (Zeta PALS, Brookhaven Instruments).

Preparation of Oxaliplation loaded liposomes. Small unilamellar vesicles were prepared as described by Bangham *et al.* Lipids were dissolved in methanol:chloroform (1:9) and mixed in the desired ratio. The ratio of phospholipids were identical with the formulations described above only excluding the fluorescence DOPE-RhoB phospholipid. The organic solvent was removed under a gentle strem of nitrogen and fully removed *in vacuo* overnight. The lipid films were hydrated in a HEPES/sucrose buffer (10 mM HEPES, 10%w/v sucrose, pH 7.4) containing oxaliplatin (~15 mg/mL) at 70 °C for 1 hour followed by freeze-thaw cycles and extrusion at 70 °C through 100 nm polycarbonate filters using an Avanti Polar Lipids mini-extruder. To remove un-encapsulated oxaliplatin from the outside of the liposomes, they were transferred to dialysis cassettes (Slide-A-lyzer Dialysis Cassette, Thermo Scientific, USA, MWCO 10 kDa) and dialyzed 3 days, exchanging the external oxaliplatin containing buffer with a HEPES/sucrose buffer. The encapsulation efficiency of oxaliplatin and leakiness of the liposomes were measured by ICP-AES.

Flow cytometry. The internalization of fluorescent liposomes was analyzed using flow cytometry (Gallios, Beckman Coulter). The human glioblastoma U87MG were grown in RPMI 1640 medium, the human fibrosarcoma HT1080 were grown in DMEM medium, and the human nasopharyngeal epidermal carcinoma cell line KB were grown in RPMI 1640 medium depleted of folic acid. All medium were supplemented with 10% fetal bovine serum (Sigma-Aldrich) and 100 UI/mL penicillin and streptomycin (Lonza). Cells were incubated in a 5% CO_2 humidified incubator at 37 °C. The day before used the cells were plated in 12-well dishes (50,000 cells per well). The medium was replaced with fresh and liposomes were added. The cells were incubated 2 hours for KB and HT1080 cells and 5 hours for U87MG and HT1080 cells at 37 °C. The cells were washed with PBS, trypsinized and placed into a FACS tube containing 3 mL of PBS using 1 mL of medium. The cells were centrifuged for 3 min at 850 rpm, supernatant removed and the cells resuspended in 300-500 µL PBS. The RhoB-fluorescent cells were measured with a blue laser (488 nm) for excitation and emission was measured in FL2 with a band pass filter of 575 ± 10 nm. 10,000 events were collected for each sample and non-treated cells were used as reference and the gates adjusted from those.

Inhibition study. The human nasopharyngeal epidermal carcinoma cell line KB were grown in RPMI 1640 medium depleted of folic acid. The media was supplemented with 10% fetal bovine serum (Sigma-Aldrich) and 100 UI/mL penicillin and streptomycin (Lonza). Cells were incubated in a 5% CO_2 humidified incubator at 37 °C. The day before used the cells were plated in 12-well dishes (50,000 cells per well). The medium was replaced with fresh and free peptide dissolved in 20% DMSO in PBS in concentrations ranging from 10 mM to 0.1 μM was added (20 μL per 1 mL media). The cells were incubated 15 minutes at 37 °C, before the addition of liposomes. The cells were incubated with the liposomes for 2 hours at 37 °C. Then washed with PBS, trypsinized and placed into a FACS tube containing 3 mL of PBS using 1 mL of medium. The cells were centrifuged for 3 min at 850 rpm, supernatant removed and the cells resuspended in 300-500 μL PBS. The RhoB-fluorescent cells were measured using flow cytometry (Gallios, Beckman Coulter) with a blue laser (488 nm) for excitation and emission was measured in FL2 with a band pass filter of 575 ± 10 nm. 10,000 events were collected for each sample and non-treated cells were used as reference and the gates adjusted from those.

Confocal microscopy. The internalization of fluorescent liposomes were analyzed using confocal microscopy (Leica Microsystems). The human glioblastoma U87MG were grown in RPMI 1640 medium; the human fibrosarcoma HT1080 were grown in DMEM medium, and the human nasopharyngeal epidermal carcinoma cell line KB were grown in RPMI 1640 medium depleted of folic acid. All medium were supplemented with 10% fetal bovine serum (Sigma-Aldrich) and 100 UI/mL penicillin and streptomycin (Lonza). Cells were incubated in a 5% CO_2 humidified incubator at 37 °C. The day before used the cells were plated in 24-well plates (20,000 cells per well) ontop of small glasslides. The medium was replaced with fresh and liposomes were added. The cells were incubated 24 hours at 37 °C. The cells were washed with PBS, heparin containing PBS and two times with PBS again. They were fixated in 4% paraformaldehyde in PBS for 3 minutes, followed by washing with PBS. The plate was allowed to dry, before being mounted on a microscope slide using Vectashield® HardSet Mounting Medium. The imaging was performed with a Leica confocal microscope using an excitation wavelength of $\lambda = 561$ nm and an emission bandwidth range of 568-711 nm.

Cytotoxicity assay. The cytotoxicity of oxaliplatin loaded liposomes was evaluated using a colorimetric method for determining the number of viable cells. Cells were seeded in 96-wells (3,000 cells per well) the day before use. Oxaliplatin loaded liposomes were added in concentrations from 0.3 μM to 50 μM and the cells incubated 24 hours before replacement of the oxaliplatin containing medium with fresh. The cells were incubated another 72 hours, before replacement of the medium with a MTS (3-(4,5-dimethylthiazol-2-yl)-5-(3-carboxymethoxyphenyl)-2-(4-sulfophenyl)-2H-tetrazolium salt) / PMS (phenazine methosulphate) containing medium. The plates were incubated 2 hours before the absorbance of the formazan product was measured at λ = 490 nm using a micro plate reader (Perkin Elmer).

Incubation with Thermolysin. DP-MCP-PEG containing liposomes (20 μL) were diluted into 20 μL HBS-1 buffer (100 mM NaCl, 50 mM HEPES, 1 mM $CaCl_2$, 2 μM $ZnCl_2$, pH 7.4). Thermolysin stock (0.4 mg/mL) (5 μL) was added and the mixture incubated overnight at 37 °C. The following day zeta potential was measured using 40 μL of the incubated mixture and 1460 μL HEPES/sucrose buffer (10 mM HEPES, 10%w/v sucrose, pH 7.4). The last 5 μL was mixed with matrix (DHB, Na) for MALDI-TOF MS analysis.